

UNIVERSIDADE FEDERAL DE MINAS GERAIS
PROGRAMA DE PÓS-GRADUAÇÃO EM SANEAMENTO,
MEIO AMBIENTE E RECURSOS HÍDRICOS

EVALUATION OF *ESCHERICHIA COLI*
INACTIVATION AND SUNLIGHT PENETRATION
IN A SHALLOW MATURATION POND:
HYDRODYNAMICS AND DISINFECTION

Daniel Filipe Cristelo Dias

Belo Horizonte

2016

**EVALUATION OF *ESCHERICHIA COLI* INACTIVATION
AND SUNLIGHT PENETRATION IN A SHALLOW
MATURATION POND: HYDRODYNAMICS AND
DISINFECTION**

Daniel Filipe Cristelo Dias

**EVALUATION OF *ESCHERICHIA COLI*
INACTIVATION AND SUNLIGHT PENETRATION IN A
SHALLOW MATURATION POND: HYDRODYNAMICS
AND DISINFECTION**

PhD Thesis submitted to the Post-Graduate Programme in Sanitation, Environment and Water Resources, Federal University of Minas Gerais, for obtaining a Doctorate degree in Sanitation, Environment and Water Resources.
Area of focus: Sanitation

Research line: Wastewater treatment

Supervisor: Marcos von Sperling

Belo Horizonte
Engineering Faculty of UFMG
2016

D541e

Dias, Daniel Filipe Cristelo.

Evaluation of *Escherichia coli* inactivation and sunlight penetration in a shallow maturation pond [manuscrito] /: hydrodynamics and disinfection
Daniel Filipe Cristelo Dias. - 2016.

xv, 256 f., enc.: il.

Orientador: Marcos von Sperling .

Tese (doutorado) - Universidade Federal de Minas Gerais,
Escola de Engenharia.

Anexos: f. 224-256.

Bibliografia: f. 209-223.

1. Engenharia sanitária - Teses. 2. Saneamento - Teses. 3. *Escherichia coli* - Teses. 4. Águas residuais - Purificação - Tratamento biológico - Teses. I. Von Sperling, Marcos. II. Universidade Federal de Minas Gerais. Escola de Engenharia. III. Título.

CDU: 628(043)

ACKNOWLEDGMENT

There are so many people who I would like to thank that helped me get to this moment in time, but of course it is hard to remember everybody, so I hope I do not forget everyone, and if I forgot you, I owe you a beer!

Firstly, special thanks to my Dad and Mom whom without their guidance and belief I would not be where I am and I would still probably be in high school (not a joke!). My beautiful sister who has wowed everyone and has become a much better and loving person than me. My girlfriend, Andreia, who is a lot to me and much more intelligent than me, if it were not for you I would have not started my PhD degree, and I would have quitted a long time ago. Thank you for putting up with my mini crisis when I really needed your help and thank you for choosing this “maluco”.

Special thanks to my PhD advisor, Prof. Marcos von Sperling, who gambled on me knowing that I came from a different background (not knowing a thing about sanitation!). You're enthusiasm for research and going beyond is contagious and I am glad to have past the last four years of my life getting to know you, and for that you have my deepest gratitude and respect. Eduardo von Sperling, thank you for talking sense into me when I was ready to jump ship.

Now, let's see if I can remember everyone to thank here in Brazil: Júlio, Ricardo, Ronan (for putting me up when I arrived in Brazil and for being the greatest of friends), Fernando, Thiago, Bernardo, Cynthia, Gabriel (for being my first friends at the university), Cíntia, Calebe, Leandro, Izabela, Lara, Lorena (without your support in the field and lab, none of this would have been possible), Jessyca, Iacy, Jorge, Higor, Deborah, Debora, Lucas, Laurita, Diogo, Elias, Lariza, Rodrigo, Nicole (for the good times in the study room and when we were out gallivanting), Matt and Wendy (USA), and if I forgot anyone, please fill in here_____. Sorry for that! Thank you so much to Sr. Raimundo and Suzane, without them none of this would have been possible.

A special thank you to Bill & Melinda Gates Foundation for funding the project “Stimulating local innovation on sanitation for the urban poor in Sub-Saharan Africa and South-East Asia” under the coordination of UNESCO-IHE, Institute for Water Education, Delft, the Netherlands. Without them, none of this would have been possible.

RESUMO

Lagoas de maturação podem ser usadas como pós-tratamento de reatores aeróbios e anaeróbios. São unidades de pós-tratamento de águas residuárias bastante usadas nos países em desenvolvimento como o Brasil, devido à sua robustez e baixo custo de implantação e operação, bem como por serem eficazes na remoção de patógenos e de nitrogênio. Para esta pesquisa, foi proposto utilizar uma área total necessária para o tratamento completo dos esgotos por um sistema natural, utilizando 1,5 m²/hab., e mantendo alta eficiência na remoção dos principais constituintes. A fim de reduzir a área necessária, foi proposto usar, após um reator anaeróbio de manta de lodo e fluxo ascendente (UASB), uma lagoa sem chicanas seguida por outra com chicanas e com profundidade rasa (44 cm). Um filtro de pedra com três granulometrias decrescentes também foi incorporado no sistema após as lagoas em série para remover a matéria orgânica particulada remanescente vinda das lagoas. O sistema foi projetado para tratar esgoto de 250 habitantes. Este trabalho teve como objetivo avaliar o desempenho do novo sistema de tratamento, com especial foco na remoção de coliformes e os mecanismos associados à radiação ultravioleta (UV). Os resultados do período de monitoramento para todo o sistema são muito positivos em termos de eficiência de remoção de DBO e DQO, com eficiências médias de 92,6% e 79,4%, respectivamente, e excelente eficiência de remoção de *E. coli* (6,1 unidades log). A radiação solar foi medida na superfície e a diversos níveis dentro da segunda lagoa para determinar as profundidades de extinção. As radiações nas faixas UV-A e UV-B só atingiram um máximo de 10 cm e a radiação fotossinteticamente ativa (PAR) penetrou até 30 cm. Modelos para estimar a atenuação de PAR também foram estimados correlacionando-se com a turbidez. A caracterização de perfis de inativação de *E. coli* segundo a profundidade foram realizados em testes por batelada em frascos de quartzo inseridos em distintos níveis dentro da lagoa para dois períodos do dia (manhã e tarde). A taxa de inativação de *E. coli* diminuiu com o aumento da profundidade, e nas profundidades maiores, a inativação no turno da manhã foi maior. A inativação no escuro mostrou ter pouca influência global, mas tanto a reparação como o decaimento ocorreram. Um modelo simplificado de decréscimo dos coeficientes de inativação com a profundidade foi incorporado ao modelo de fluxo disperso, e proporcionou ótimos ajustes com os dados de *E. coli* efluente monitorados em ambas as lagoas. As doses aplicadas e recebidas de UV e PAR também foram estimadas em relação ao coeficiente de inativação. Chicanas verticais foram inseridas na segunda lagoa para aumentar a inativação de *E. coli*, e os resultados indicaram que melhorias foram alcançadas com esta modificação.

ABSTRACT

Maturation ponds can be used as post-treatment of anaerobic and aerobic reactors. They are widely used post-treatment units for treating wastewater in developing countries like Brazil because of their robustness and low implementation and operation costs, as well as being effective in removing pathogens and nitrogen. For this research, a natural wastewater treatment line was proposed to treat raw sewage, using a total area of 1.5 m²/inhab., while maintaining high removal efficiencies for the major constituents. In order to reduce the required area, an upflow anaerobic sludge blanket (UASB) reactor, a pond without baffles followed by another shallow pond (44 cm) with baffles was proposed. A rock filter with three decreasing grain sizes was also incorporated into the system after the ponds in series to remove the remaining particulate organic matter from the ponds. The system was designed to treat sewage of 250 inhabitants. This study aimed to evaluate the performance of the new treatment line, with special attention on the removal of coliforms and mechanisms associated with ultraviolet (UV) radiation. The results of the monitoring period for the whole system were very positive for BOD and COD removal, with average removal efficiencies of 92.6% and 79.4%, respectively, and excellent *E. coli* removal efficiency (6.1 log units). Solar radiation was measured at the surface and various levels within the second pond to determine extinction depths. UV-A and UV-B waves only reached a maximum of 10 cm and photosynthetically active radiation (PAR) penetrated up to 30 cm. Models to estimate PAR attenuation were also estimated and correlated with turbidity. *E. coli* inactivation profiles regarding depth were performed in batch tests using quartz tubes inserted at different levels within the pond for two different periods of the day (morning and afternoon). The *E. coli* inactivation rate decreased with increasing depth, and at deeper depths, inactivation in the morning was greater. Dark inactivation showed to have little overall influence, but both repair and the decay occurred. A simple model for the decrease of the inactivation coefficient with depth was incorporated into the dispersed flow model, and allowed very good fittings with the effluent *E. coli* concentrations monitored at both ponds. The applied and received doses of UV and PAR were estimated regarding the inactivation coefficient. Vertical baffles were inserted in the second pond to increase *E. coli* inactivation, and results indicated that improvements were achieved with this modification.

TABLE OF CONTENTS

RESUMO	II
ABSTRACT	III
TABLE OF CONTENTS	IV
LIST OF FIGURES	VII
LIST OF TABLES	XII
ACRONYMS.....	XIV
1. INTRODUCTION.....	1
2. HYPOTHESES	5
3. OBJECTIVES	6
3.1. <i>General objective</i>	6
3.2. <i>Specific objectives</i>	6
4. LITERATURE REVIEW.....	7
4.1. <i>Maturation ponds and Escherichia coli disinfection</i>	7
4.2. <i>Electromagnetic spectrum: what are waves?</i>	8
4.2.1. Visible light or photosynthetically active radiation (PAR)	9
4.2.2. Ultraviolet spectrum	10
4.3. <i>Disinfection mechanisms in ponds</i>	14
4.3.1. Temperature	16
4.3.2. Sedimentation and attachment.....	17
4.3.3. Dissolved oxygen and pH levels	19
4.3.4. Sunlight-mediated disinfection (in combination with DO and pH) and dark disinfection/repair	21
4.3.5. Predation, starvation and competition (biological disinfection)	30
4.3.6. Algal toxins	33
4.3.7. Hydrodynamic factors influencing bacterial disinfection in ponds	35
4.3.8. Summary of disinfection mechanisms affecting <i>E. coli</i>	38
4.4. <i>Pond arrangement, depth and HRT for E. coli disinfection</i>	43
4.5. <i>Baffles to increase E. coli disinfection</i>	47
4.6. <i>Discharging the final effluent into waterbodies: concerns</i>	51
4.7. <i>Quantifying bacterial disinfection in waste stabilisation ponds</i>	52
4.8. <i>Solar irradiance attenuation rate with depth in ponds</i>	71
4.9. <i>Solar irradiance dose</i>	72
4.10. <i>Research gaps that were drivers for the current research</i>	73
5. MATERIAL AND METHODS	74
5.1. <i>Location of the experimental apparatus and climate characteristics</i>	74
5.2. <i>Experimental apparatus</i>	75
5.3. <i>Sampling points and methods for routine monitoring of the treatment system</i>	81
5.3.1. Sampling methods and analysis	81
5.3.2. Sampling points.....	82
5.3.3. Core sampler	83
5.4. <i>Solar radiation measurement</i>	84
5.4.1. Measuring principal.....	84
5.4.2. Total solar irradiance (TSI) at ground level	84
5.4.3. Depth profiling of solar irradiance in a shallow maturation pond.....	86
5.4.4. Cleaning and upkeep of the sensors	90
5.4.5. Attenuation coefficients (K_d) estimated and modelled with turbidity and \log_{10} of turbidity for predicting irradiance attenuation.	90
5.5. <i>Escherichia coli disinfection in a shallow maturation pond</i>	91
5.5.1. <i>E. coli</i> disinfection rate at different depths in a shallow maturation pond	91
5.5.2. Vessels (isolated environments) used to conduct the experiments.....	92

5.5.3.	Submerging and sampling of the vessels in the pond.....	94
5.6.	<i>Research phases and monitoring routine</i>	101
5.6.1.	1 st Phase.....	102
5.6.2.	2 nd Phase.....	105
5.7.	<i>Data analysis</i>	107
6.	RESULTS AND DISCUSSION.....	108
6.1.	<i>Overall evaluation of the treatment system</i>	108
6.1.1.	Flow, hydraulic retention time (HRT) and depth.....	110
6.1.2.	Biochemical oxygen demand (BOD).....	111
6.1.3.	Chemical Oxygen Demand (COD).....	113
6.1.4.	COD/BOD ratio in the raw sewage.....	115
6.1.5.	Suspended Solids and Turbidity.....	115
6.1.6.	Total Kjeldahl Nitrogen (TKN) and Ammonia Nitrogen (Ammonia-N).....	117
6.1.7.	Total coliforms and <i>E. coli</i>	119
6.1.8.	Environmental data.....	121
6.1.9.	Comparison of the final effluent with the previous treatment line setup.....	123
6.1.10.	Compliance with discharge goals and irrigation reuse.....	125
6.2.	<i>Solar Radiation</i>	128
6.2.1.	Overall total surface solar irradiance.....	128
6.2.2.	Seasonal variation of total solar irradiance.....	131
6.2.3.	Depth profiling of solar radiation.....	137
6.2.4.	Modelling attenuation coefficients for sunlight penetration.....	156
6.3.	<i>E. coli disinfection throughout the depth in a shallow maturation pond</i>	165
6.3.1.	Disinfection coefficient (K_b).....	166
6.3.2.	Dark disinfection or repair coefficient (K_d).....	170
6.3.3.	Log units removed at different depths and time periods associated with environmental parameters.....	172
6.3.4.	Nonparametric variance analysis of K_b , K_d , log unit values and environmental parameters between depths and periods (Kruskal-Wallis).....	178
6.3.5.	Applied and received UV and PAR doses.....	182
6.3.6.	Modelling <i>E. coli</i> disinfection coefficient (K_b).....	184
6.3.7.	Modelling <i>E. coli</i> disinfection based on two different approaches and applied in the dispersed flow regime.....	193
6.3.8.	Vertical hydrodynamic profiling and comparison between the two hydraulic phases (without and with vertical baffles).....	201
7.	CONCLUSIONS.....	205
8.	RECOMMENDATIONS.....	208
9.	REFERENCES.....	209
	APPENDIX I.....	224
	APPENDIX II.....	225
	APPENDIX III.....	227
	APPENDIX IV.....	229
	APPENDIX V.....	231
	APPENDIX VI.....	233
	APPENDIX VII.....	236
	APPENDIX VIII.....	238
	APPENDIX IX.....	241
	APPENDIX X.....	243
	APPENDIX XI.....	245
	APPENDIX XII.....	247

APPENDIX XIII	248
APPENDIX XIV.....	251
APPENDIX XV	253
APPENDIX XVI.....	255

LIST OF FIGURES

FIGURE 1.1 – WASTEWATER TREATMENT TECHNOLOGIES APPLIED IN LATIN AMERICAN COUNTRIES. (ADAPTED: NOYOLA <i>ET AL.</i> 2012).	1
FIGURE 4.1 - EXAMPLE OF A SINUSOIDAL WAVE (WITH A WAVELENGTH λ).....	8
FIGURE 4.2 - VISIBLE LIGHT AND ULTRAVIOLET LIGHT SPECTRUMS (SOURCE: RYER, 1997).	10
FIGURE 4.3 - ULTRAVIOLET RADIATION FROM A NATURAL SOURCE (SUN). UV-C IS BLOCKED BY THE ATMOSPHERE (BLUE).	11
FIGURE 4.4 - LEVELS OF OZONE AT VARIOUS ALTITUDES AND BLOCKING OF DIFFERENT BANDS OF ULTRAVIOLET RADIATION. DU – DOBSON UNIT (MEASURE THE TOTAL COLUMN OF THE OZONE). (SOURCE: HTTP://WWW.SCHOOLPHYSICS.CO.UK/AGE14-16/WAVE%20PROPERTIES/TEXT/OZONE_LAYER/INDEX.HTML ; HTTPS://ESPO.NASA.GOV/SOLVEII/IMPLEMENT.HTML).	13
FIGURE 4.5 - IDENTIFICATION OF GERMICIDAL PORTION OF THE UV RADIATION SPECTRUM. SOURCE: HTTPS://REDSQUAREPOOLS.FILES.WORDPRESS.COM/2011/02/SCIENCEUV-CSPECTRUM.JPG	13
FIGURE 4.6 – <i>E. COLI</i> DISTRIBUTION IN FUNCTION OF TEMPERATURE VARIATION ALONG THE DEPTH OF A WSP. TEMPERATURE DECREASES AS DEPTH INCREASES, THEREFORE INDUCING STRATIFICATION BECAUSE OF THE DIFFERENCES IN TEMPERATURE AT THE TOP (LIGHT BLUE) AND BOTTOM (DARK BLUE) OF THE WSP, THEREFORE INFLUENCING DISINFECTION MECHANISMS.	17
FIGURE 4.7 - SEDIMENTATION AND ATTACHMENT OF <i>E. COLI</i> IN A PRIMARY WASTE STABILISATION POND. PLACEMENT OF INLET STRUCTURE LOCATED AT THE BOTTOM TO PROMOTE FASTER SEDIMENTATION AND OUTLET STRUCTURE LOCATED AT THE TOP.	19
FIGURE 4.8 - pH AND DO CONCENTRATION EFFECT ON <i>E. COLI</i> DISINFECTION DURING DAY AND NIGHT TIME IN A WASTE STABILISATION POND.	21
FIGURE 4.9 - DIRECT PHOTOBIOLOGICAL DAMAGE CAUSED TO <i>E. COLI</i> THROUGH UV-B.	24
FIGURE 4.10 - INDIRECT INTERNAL PHOTOOXIDATIVE DAMAGE TO <i>E. COLI</i> (ENDOGENOUS DAMAGE) CAUSED INDIRECTLY BY UV-A AND UV-B.	25
FIGURE 4.11 - INDIRECT INTERNAL PHOTOOXIDATIVE DAMAGE TO <i>E. COLI</i> (EXOGENOUS DAMAGE) CAUSED INDIRECTLY BY UV AND PAR.	27
FIGURE 4.12 - PREDATION OF <i>E. COLI</i> BY HIGHER ORDER ORGANISMS IN THE PRESENCE AND ABSENCE OF NUTRIENTS.	33
FIGURE 4.13 - ALGAE PROTECTING AND INACTIVATING <i>E. COLI</i> : E.G.: SUNLIGHT-MEDIATED PROTECTION WITH SHADING (INLET) AND ALGAL TOXINS INACTIVATING <i>E. COLI</i> (OUTLET).....	35
FIGURE 4.14 – SCHEMATIC REPRESENTATION OF THE VARIOUS DISINFECTION MECHANISMS FOR <i>E. COLI</i> DISINFECTION IN WASTE STABILISATION PONDS.....	42
FIGURE 4.15 - STANDALONE TREATMENT SYSTEM COMPRISED OF A FACULTATIVE POND (VON SPERLING 2007)...	43
FIGURE 4.16 - TREATMENT SYSTEM COMPRISED OF AN ANAEROBIC AND FACULTATIVE POND IN SERIES (VON SPERLING 2007).	44
FIGURE 4.17 - TREATMENT SYSTEM COMPRISED OF AN ANAEROBIC, FACULTATIVE AND MATURATION PONDS IN SERIES (VON SPERLING 2007).	44
FIGURE 4.18 - UASB REACTOR FOLLOWED MATURATION PONDS IN SERIES (VON SPERLING 2007).....	45
FIGURE 4.19 - ROCK FILTER DESIGNS FROM THE STATE OF ILLINOIS (SOURCE: MIDDLEBROOKS, 1988).	52
FIGURE 4.20 - FORMULAS FOR CALCULATION OF THE EFFLUENT COLIFORM CONCENTRATION (N) FOR PONDS (SOURCE: VON SPERLING (2007)).	54
FIGURE 5.1 - OVERVIEW OF WASTE WATER TREATMENT PLANT (A) AND EXPERIMENTAL PLANT (CePTS) (B)...	75
FIGURE 5.2 - POND 2 RENOVATION. (A) DESLUDGING AND REMOVAL OF THE EXISTING GEOMEMBRANE CANVAS (POND 2); (B) PLACEMENT OF NEW GEOMEMBRANE CANVAS (POND 2); (C) PILLARS CONSTRUCTED AT EACH END; (D) BAFFLES 90% THE LENGTH OF THE POND ARE ANCHORED TO THE PILLARS.....	76
FIGURE 5.3 - (A) METAL PLATE AND RUBBER FIXING BAFFLE TO THE PILLAR; (B) THREE DIFFERENT HEIGHTS FOR BOLTING THE CABLE OF THE BAFFLE; (C) CABLE CROSSING BREADTH OF THE POND TO AVOID SAGGING CAUSED BY THE WEIGHT OF THE BAFFLES AND LINTELS TO MINIMISE WATER PASSING UNDERNEATH THE BAFFLES; (D) ORDINARY DUSTBIN TO ROUND OFF THE EDGE OF THE BAFFLE NOT FIXED TO THE PILLARS.....	77

FIGURE 5.4 - RENOVATION OF POND 3. (A) COMPACTING THE BOTTOM AND EMBANKMENTS; (B) GROF WITH DECREASING GRAIN SIZE FROM THE INLET TO THE OUTLET.....	78
FIGURE 5.5 – THE EXPERIMENTAL WASTEWATER TREATMENT LINE SETUP.	79
FIGURE 5.6 – (A) UNITS FROM THE TREATMENT LINE. UASB REACTOR; (B) POND 1 WITHOUT BAFFLES; (C) AND POND 2 WITH BAFFLES; (D) GRADED ROCK FILTER (GROF) WITH DECREASING GRAIN SIZE.	80
FIGURE 5.7 - SAMPLING POINTS IN THE TREATMENT LINE AND FLOW DIRECTION.	82
FIGURE 5.8 - CORE SAMPLER, SAMPLING DEPTHS AND OPERATING PRINCIPLE.....	83
FIGURE 5.9 - POURING THE EFFLUENT FROM THE CORE SAMPLER INTO BEAKER AND RECIPIENT AFTER SAMPLING.	84
FIGURE 5.10 - METEOROLOGICAL STATION INSTALLED AT CePTS FOR ONSITE MONITORING OF VARIOUS ENVIRONMENTAL PARAMETERS.....	85
FIGURE 5.11 - (A) UV-A, UV-B AND PAR SENSORS, DATA LOGGER AND LEVELLING PLATE FROM SKYE INSTRUMENTS®; (B) CONCRETE BASE WITH HELICAL RIDGE RODS AND BOLTS FOR HEIGHT ADJUSTMENT.	87
FIGURE 5.12 - (A) DOWNLOADING SOLAR IRRADIANCE DATA FROM THE DATALOGGER ON TO A COMPUTER; (B) SKYELYNX COMMS® SOFTWARE.	87
FIGURE 5.13 - UV-A, UV-B AND PAR SENSORS PLACED AT P_2B_3 AT 0.05 M IN DEPTH FOR CONTINUOUS MONITORING OVER ONE WEEK.	89
FIGURE 5.14 - LEVEL CHANGING AND HEIGHTS OF UV-A, UV-B AND PAR SENSORS FOR MONITORING IN THE POND.	89
FIGURE 5.15 - (A) CLEAN SENSORS BEFORE PLACED IN THE POND; (B) ALGAL AND BIOFILM ACCUMULATION AFTER THREE DAYS IN THE POND AT 0.05 M.	90
FIGURE 5.16 - SPECTRUM TRANSMITTANCE OF VESSELS USED (SOURCE: ACTQUARTZO®).....	92
FIGURE 5.17 - (A) VESSELS FOR CONDUCTING EXPERIMENTS FOR <i>E. COLI</i> DISINFECTION IN ISOLATED ENVIRONMENTS. INDIVIDUAL TEST TUBE WITH TEFLON LID; (B) TEN TEST TUBES.	93
FIGURE 5.18 - FLOWSHEET OF THE STEPS FOR THE EXPERIMENT IN THE SHALLOW MATURATION POND WITH VESSELS EXPOSED TO SOLAR RADIATION FOR FOUR HOURS. THE VESSELS WERE SUSPENDED IN POND 2 EITHER AT P_2B_2 (END OF BAFFLE 1) OR P_2B_3 (END OF BAFFLE 2).	96
FIGURE 5.19 - (A) STAND AND NET PLANE USED FOR HANGING THE VESSELS AND; (B) HOLES FOR ADJUSTING THE VERTICAL HEIGHT OF THE HORIZONTAL NET PLANE.....	97
FIGURE 5.20 – (A) TEST TUBES AND ELASTIC BANDS; (B) ELASTIC BANDS WRAPPED AROUND THE TEST TUBES AND SUSPENDED AT DIFFERENT LEVELS AND THE NET PLANE AT A CONSTANT LEVEL; (C) ALL TEST TUBES SUSPENDED ON THE SAME NET PLANE WITH THE SAME HEIGHT ADJUSTMENTS BEFORE SUBMERGING IN P_2B ; (D) THE APPARATUS (TEST TUBES AND STAND) SUBMERGED IN P_2B , PROFILING 0.10 M DISINFECTION.	98
FIGURE 5.21 - (A) VESSEL AND ALUMINIUM FOIL USED FOR DARK CONTROL TESTS; (B) ATTACHING THE CONTAINER TO THE PVC POLE; (C) THE CONTAINER COVERED WITH THE ALUMINIUM SHEET AND ATTACHED TO THE PVC POLE; (D) THE PVC POLE AND THE DARK CONTROL VESSEL SUBMERGED IN P_2B	99
FIGURE 5.22 – DEPTH PROFILING UP TO 0.30 M WITH THREE DIFFERENT 0.10 M PROFILES EVALUATED FOR DETERMINING <i>E. COLI</i> DISINFECTION BECAUSE OF THE EFFECT OF DIFFERENT WAVELENGTHS IN P_2B	100
FIGURE 5.23 - SOLAR SENSORS PLACED IN THE POND AT THE THREE DIFFERENT DEPTHS, ACCOMPANIED BY THE SUSPENDED TEST TUBES IN THE POND AT THE SAME HEIGHTS AS SENSORS (SENSORS LENSES WERE PLACED AT THE SAME LEVEL AS THE BOTTOM OF THE TEST TUBES).	104
FIGURE 5.24 - (A) ANATOMY OF THE "VERTICAL BAFFLES" AND; (B) BASKETS WITH CRUSHED STONE TO WEIGHT DOWN THE BAFFLES. PLASTIC HOLDERS TO LOWER THE BAFFLES INTO THE POND AND MAKE THEM VISIBLE.	106
FIGURE 5.25 - (A) POSITIONING OF THE “VERTICAL BAFFLES”; (B) AND PLACEMENT OF THE “VERTICAL BAFFLES” IN THE FIRST CHANNEL OF THE SECOND POND (BETWEEN THE INLET AND P_2B_2); (C) AND A CROSS-SECTION OF THE SECOND POND ILLUSTRATING A FRONT VIEW OF THE SECOND “VERTICAL BAFFLE” IN POSITION.	107
FIGURE 6.1 - BOX-PLOT AND COLUMN GRAPH OF TOTAL BOD CONCENTRATIONS AND MEDIAN REMOVAL EFFICIENCIES IN THE TREATMENT LINE FOR EACH UNIT AND OVERALL (RS = RAW DOMESTIC SEWAGE; P_1 = POND 1; P_2B_4 = POND 2; GROF = GRADED ROCK FILTER).....	112

FIGURE 6.2 - COLUMN GRAPHS OF PARTICULATE AND FILTERED BOD MEDIAN REMOVAL EFFICIENCIES IN THE TREATMENT LINE FOR EACH UNIT AND OVERALL (RS = RAW DOMESTIC SEWAGE; P_1 = POND 1; P_2B_4 = POND 2; GROF = GRADED ROCK FILTER).	113
FIGURE 6.3 - BOX-PLOT AND COLUMN GRAPH OF TOTAL COD CONCENTRATIONS AND MEDIAN REMOVAL EFFICIENCIES IN THE TREATMENT LINE FOR EACH UNIT AND OVERALL (RS = RAW DOMESTIC SEWAGE; P_1 = POND 1; P_2B_4 = POND 2; GROF = GRADED ROCK FILTER).	114
FIGURE 6.4 - COLUMN GRAPHS OF PARTICULATE AND FILTERED COD MEDIAN REMOVAL EFFICIENCIES IN THE TREATMENT LINE FOR EACH UNIT AND OVERALL (RS = RAW DOMESTIC SEWAGE; P_1 = POND 1; P_2B_4 = POND 2; GROF = GRADED ROCK FILTER).	114
FIGURE 6.5 - BOX-PLOT AND COLUMN GRAPHS OF TSS AND TURBIDITY CONCENTRATIONS (TOP GRAPHS) AND MEDIAN REMOVAL EFFICIENCIES (BOTTOM GRAPHS) FOR EACH UNIT AND OVERALL (RS = RAW DOMESTIC SEWAGE; P_1 = POND 1; P_2B_4 = POND 2; GROF = GRADED ROCK FILTER).	116
FIGURE 6.6 - COLUMN GRAPHS OF FSS AND VSS MEDIAN REMOVAL EFFICIENCIES FOR EACH UNIT AND OVERALL (RS = RAW DOMESTIC SEWAGE; P_1 = POND 1; P_2B_4 = POND 2; GROF = GRADED ROCK FILTER).	117
FIGURE 6.7 - BOX-PLOT AND COLUMN GRAPHS OF TKN AND AMMONIA-N CONCENTRATIONS (TOP GRAPHS) AND MEDIAN REMOVAL EFFICIENCIES (BOTTOM GRAPHS) FOR EACH UNIT AND OVERALL (RS = RAW SEWAGE; P_1 = POND 1; P_2B_4 = POND 2; GROF = GRADED ROCK FILTER).	118
FIGURE 6.8 - BOX-PLOT AND COLUMN GRAPHS OF TOTAL COLIFORM CONCENTRATION AND MEDIAN REMOVAL EFFICIENCIES FOR EACH UNIT AND OVERALL (RS = RAW DOMESTIC SEWAGE; P_1 = POND 1; P_2B_4 = POND 2; GROF = GRADED ROCK FILTER).	119
FIGURE 6.9 - BOX-PLOT AND COLUMN GRAPHS OF <i>E. COLI</i> CONCENTRATION AND MEDIAN REMOVAL EFFICIENCIES FOR EACH UNIT AND OVERALL (RS = RAW DOMESTIC SEWAGE; P_1 = POND 1; P_2B_4 = POND 2; GROF = GRADED ROCK FILTER).	121
FIGURE 6.10 - COLUMN GRAPHS OF DISSOLVED OXYGEN AND pH CONCENTRATION IN RS AND EACH TREATMENT UNIT (RS = RAW DOMESTIC SEWAGE; P_1 = POND 1; P_2B_4 = POND 2; GROF = GRADED ROCK FILTER).	122
FIGURE 6.11 - COLUMN GRAPHS OF TEMPERATURE AND ORP VALUES IN RS AND EACH TREATMENT (RS = RAW DOMESTIC SEWAGE; P_1 = POND 1; P_2B_4 = POND 2; GROF = GRADED ROCK FILTER).	123
FIGURE 6.12 - EXAMPLES OF OPTIONS FOR THE REDUCTION OF VIRAL, BACTERIAL AND PROTOZOAN PATHOGENS BY DIFFERENT COMBINATIONS OF HEALTH PROTECTION MEASURES THAT ACHIEVE THE HEALTH-BASED TARGET OF $\leq 10^{-6}$ DALY PER PERSON PER YEAR (SOURCE: WHO, 2006).	126
FIGURE 6.13 - BOX-PLOT OF TOTAL SOLAR IRRADIANCE FOR THE OVERALL MONITORING PERIOD CONDENSED INTO ONE DAY (JULY 2014 – NOVEMBER 2015).	130
FIGURE 6.14 - BOX-PLOT OF SOLAR IRRADIANCE FOR THE DRY AND COOL SEASON DURING THE MONITORING PERIOD CONDENSED INTO ONE DAY (JULY 2014 – NOVEMBER 2015).	132
FIGURE 6.15 - BOX-PLOT OF SOLAR IRRADIANCE FOR THE WARM AND WET SEASON DURING THE MONITORING PERIOD CONDENSED INTO ONE DAY (JULY 2014 – NOVEMBER 2015).	134
FIGURE 6.16 – COMPARISON BETWEEN MEDIAN AND MEAN TOTAL SOLAR IRRADIANCE OF THE DRY AND COLD (APRIL TO SEPTEMBER) AND WARM AND WET (OCTOBER TO MARCH) SEASONS.	136
FIGURE 6.17 – COMPARISON BETWEEN MAXIMUM TOTAL SOLAR IRRADIANCE OF THE DRY AND COLD (APRIL TO SEPTEMBER) AND WARM AND WET (OCTOBER TO MARCH) SEASONS.	136
FIGURE 6.18 – COMPARISON BETWEEN MINIMUM TOTAL SOLAR IRRADIANCE OF THE DRY AND COLD (APRIL TO SEPTEMBER) AND WARM AND WET (OCTOBER TO MARCH) SEASONS.	137
FIGURE 6.19 – (A) ARITHMETIC MEAN AND (B) MEDIAN OF PAR AND UV SOLAR IRRADIANCE AT A DEPTH OF 5 CM IN THE 2 ND POND CONDENSED INTO ONE DAY.	140
FIGURE 6.20 – ARITHMETIC MEAN FOR COLD AND DRY (A) AND WET AND WARM (B) FOR PAR AND UV SOLAR IRRADIANCE AT 5 CM IN DEPTH IN THE 2 ND POND CONDENSED INTO ONE DAY.	142
FIGURE 6.21 – ARITHMETIC MEAN (A) AND MEDIAN (B) OF PAR AND UV SOLAR IRRADIANCE AT A DEPTH OF 10 CM IN 2 ND POND CONDENSED INTO ONE DAY.	145
FIGURE 6.22 – ARITHMETIC MEAN FOR COLD AND DRY (A) AND WET AND WARM (B) FOR PAR AND UV SOLAR IRRADIANCE AT 10 CM IN DEPTH IN THE 2 ND POND CONDENSED INTO ONE DAY.	147

FIGURE 6.23 – ARITHMETIC MEAN (A) AND MEDIAN (B) OF PAR SOLAR IRRADIANCE AT 15 CM, 20 CM AND 30 CM IN DEPTH IN THE 2 ND POND CONDENSED INTO ONE DAY.	149
FIGURE 6.24 – ARITHMETIC MEAN FOR COLD AND DRY (A) AND WET AND WARM (B) FOR PAR AT 20 CM AND 30 CM IN DEPTH IN THE 2 ND POND CONDENSED INTO ONE DAY.	151
FIGURE 6.25 – MEAN ATTENUATION PERCENTAGES BETWEEN 10 CM AND 5 CM FOR UV-A AND UV-B OVER ONE DAY.	153
FIGURE 6.26 – MEAN ATTENUATION PERCENTAGES BETWEEN 10CM/5CM, 20CM/10CM, 30CM/20CM, 30CM/10CM AND 30CM/5 CM FOR PAR OVER ONE DAY.....	153
FIGURE 6.27 – SUMMARY OF UV-A, UV-B AND PAR MEDIAN IRRADIANCE IN RELATION TO DEPTH AND TIME...	155
FIGURE 6.28 - PLOTTED MEAN VALUES OF TURBIDITY FOR THE DIFFERENT DEPTH PROFILES AT EACH TIME INTERVAL.	157
FIGURE 6.29 - K_A UV-A vs NTU (A); K_A UV-B vs NTU (B); K_A PAR vs NTU (C) CONSIDERING SHILTON (2005) PERCENTAGES FOR ESTIMATING SURFACE IRRADIANCE; AND K_A VALUES FOR UV-A, UV-B AND PAR (D).	158
FIGURE 6.30 - OBSERVED AND ESTIMATED IRRADIANCE FOR EQUATION 6.1 (A); OBSERVED AND ESTIMATED IRRADIANCE FOR EQUATION 6.2 (B) AND; OBSERVED AND ESTIMATED IRRADIANCE FOR EQUATION 6.3 (C). ALL GRAPHS SHOW THE 45° LINE OF THEORETICAL PERFECT FITTING.	160
FIGURE 6.31 - K_A UV-A vs NTU (A); K_A UV-B vs NTU (B); K_A PAR vs NTU (C) CONSIDERING SMARTS PREDICTION FOR SURFACE IRRADIANCE; AND K_A VALUES FOR UV-A, UV-B AND PAR (D).	162
FIGURE 6.32 - OBSERVED AND ESTIMATED IRRADIANCE FOR EQUATION 6.4 (A); OBSERVED AND ESTIMATED IRRADIANCE FOR EQUATION 6.5 (B) AND; OBSERVED AND ESTIMATED IRRADIANCE FOR EQUATION 6.6 (C). ALL GRAPHS SHOW THE 45° LINE OF THEORETICAL PERFECT FITTING.	164
FIGURE 6.33 – SUMMARY OF OVERALL MEAN K_B VALUES (H^{-1}) FOR THE MORNING AND AFTERNOON PERIOD AT 10 CM = 0 - 10 CM, 20 CM = 10 - 20 CM AND 30 CM = 20 - 30 CM PROFILES IN THE 2 ND MATURATION POND.	169
FIGURE 6.34 – SUMMARY OF MEAN K_B VALUES (H^{-1}) STANDARDISED FOR A TEMPERATURE OF 20 °C DURING THE MORNING AND AFTERNOON PERIOD AT 10 CM = 0 - 10 CM, 20 CM = 10 - 20 CM AND 30 CM = 20 - 30 CM PROFILES IN THE 2 ND MATURATION POND.....	169
FIGURE 6.35 – SUMMARY OF MEAN K_D VALUES DURING THE MORNING AND AFTERNOON PERIOD AT 10 CM = 0 - 10 CM, 20 CM = 10 - 20 CM AND 30 CM = 20 - 30 CM PROFILES IN THE 2 ND MATURATION POND.....	171
FIGURE 6.36 – SUMMARY OF MEAN $K_{D20°C}$ VALUES STANDARDISED FOR A TEMPERATURE OF 20 °C DURING THE MORNING AND AFTERNOON PERIOD AT 10 CM = 0 - 10 CM, 20 CM = 10 - 20 CM AND 30 CM = 20 - 30 CM PROFILES IN THE 2 ND MATURATION POND.....	171
FIGURE 6.37 – <i>E. COLI</i> LOG UNITS REMOVED: 10 CM = 0 – 10 CM VS. 20 CM = 10 – 20 CM VS. 30 CM = 20 – 30 CM (MORNING AND AFTERNOON) OVER 4 HOURS OF EXPOSURE.	173
FIGURE 6.38 - BOX PLOT OF DO CONCENTRATIONS AT DIFFERENT DEPTHS AND DURING DIFFERENT PERIODS OF THE DAY (MORNING AND AFTERNOON) MEASURED IN THE TEST TUBES.	174
FIGURE 6.39 - DO CONCENTRATIONS VS REMOVAL EFFICIENCIES (LOG UNITS).	175
FIGURE 6.40 - BOX PLOT OF pH VALUES AT DIFFERENT DEPTHS AND DURING DIFFERENT PERIODS OF THE DAY (MORNING AND AFTERNOON) MEASURED IN THE TEST TUBES.	176
FIGURE 6.41 - pH VALUE VS REMOVAL EFFICIENCIES (LOG UNITS).	176
FIGURE 6.42 - BOX PLOT OF TEMPERATURE VALUES AT DIFFERENTS DEPTHS AND DURING DIFFERENT PERIODS OF THE DAY (MORNING AND AFTERNOON) MEASURED IN THE TEST TUBES.	177
FIGURE 6.43 - TEMPERATURE VALUES VS REMOVAL EFFICIENCIES (LOG UNITS).	177
FIGURE 6.44 – MEAN K_B VALUES DURING THE MORNING (BLUE LINE) AND AFTERNOON (RED LINE) FOR THE DIFFERENT DEPTH PROFILES AND DISINFECTION RATE EQUATIONS CONSIDERING ONLY DEPTH.	185
FIGURE 6.45 – MEAN K_D VALUES DURING THE MORNING (BLUE LINE) AND AFTERNOON (RED LINE) FOR THE DIFFERENT DEPTH PROFILES AND DISINFECTION RATE EQUATIONS CONSIDERING ONLY DEPTH.	186
FIGURE 6.46 - OBSERVED K_B VALUES VS ESTIMATED K_B VALUES CONSIDERING MAYO (1995) EQUATION. EQUATION 6.16 – CD = 0.097.	188
FIGURE 6.47 - OBSERVED K_B VALUES VS ESTIMATED K_B VALUES CONSIDERING SARIKAYA AND SAATÇI (1987) EQUATION. EQUATION 6.18 – CD = 0.04.	189

FIGURE 6.48 - OBSERVED K_B VALUES VS ESTIMATED K_B VALUES CONSIDERING OUALI <i>ET AL.</i> (2014) EQUATION. EQUATION 6.20 – CD = 0.31.....	190
FIGURE 6.49 - OBSERVED K_B VALUES VS ESTIMATED K_B VALUES CONSIDERING OUALI <i>ET AL.</i> (2014) EQUATION. EQUATION 6.21 – CD = 0.32.....	191
FIGURE 6.50 - OBSERVED K_B VALUES VS ESTIMATED K_B VALUES CONSIDERING OUALI <i>ET AL.</i> (2014) EQUATION. EQUATION 6.23 – CD = 0.55.....	192
FIGURE 6.51 - ESTIMATED <i>E. COLI</i> CONCENTRATION VS POND HEIGHT IN THE FIRST POND [BLACK VERTICAL LINE DEMONSTRATES THE GEOMETRIC MEAN CONCENTRATION OF <i>E. COLI</i> IN THE 30 CM LIQUID COLUMN ($1.80 \times 10^{+06}$ MPN/100 mL)]......	200
FIGURE 6.52 - ESTIMATED <i>E. COLI</i> CONCENTRATION VS POND HEIGHT IN THE SECOND POND [BLACK VERTICAL LINE DEMONSTRATES THE GEOMETRIC MEAN CONCENTRATION OF <i>E. COLI</i> IN THE 30 CM LIQUID COLUMN ($3.31 \times 10^{+04}$ MPN/100 mL)]......	200
FIGURE 6.53 - PLOTTED MEAN VALUES OF TURBIDITY FOR THE DIFFERENT DEPTH PROFILES AT EACH TIME INTERVAL.	202

LIST OF TABLES

TABLE 4.1 - UV LIGHT SPECTRUM. (SOURCE: ISO-21348).	11
TABLE 4.2 - APPROPRIATE CHARACTERISTICS OF INDICATOR ORGANISMS (SOURCE: SHILTON, 2005).	14
TABLE 4.3 - FACTORS BELIEVED TO CAUSE OR INFLUENCE DISINFECTION IN WSPs (ADAPTED: SHILTON, 2005)...	15
TABLE 4.4 - SUMMARY OF DISINFECTION MECHANISMS, DISINFECTION ROUTES AND CHARACTERISTICS.	38
TABLE 4.5 - CHARACTERISTICS OF THE THREE MAIN MECHANISMS OF SUNLIGHT DISINFECTION PROMOTING DISINFECTION IN WSP'S (ADAPTED: SHILTON, 2005). *PROPOSED INCLUSION DUE TO RECENT RESEARCH).	41
TABLE 4.6 - RANGES OF VARIABLE VALUES USED FOR CALCULATING EQUATION 4.33. SOURCE: CURTIS, MARA AND SILVA (1992B).	66
TABLE 4.7 - ANNUAL RANGE OF MEAN MONTHLY IRRADIANCES FROM VARIOUS LOCATIONS. SOURCE: CURTIS, MARA AND SILVA (1992B).	66
TABLE 4.8 - SUMMARY OF K_B MODELS, PARAMETER AND CONSTANTS REVIEWED.	70
TABLE 5.1 - PHYSICAL AND OPERATIONAL CHARACTERISTICS OF POND AND FILTER UNITS.	81
TABLE 5.2 - MONITORING PROGRAMME FOR UV-A, UV-B AND PAR AT DIFFERENT DEPTHS OVER A TIME FRAME.	88
TABLE 5.3 - 1 ST PHASE AND 2 ND PHASE: MEASUREMENT AND ANALYSIS OF PARAMETERS AND SAMPLE FREQUENCY IN THE TREATMENT SYSTEM.	102
TABLE 5.4 – MONITORING PROGRAMME USED FOR <i>E. COLI</i> DISINFECTION DURING THE 1 ST PHASE.	104
TABLE 6.1 - MEAN/MEDIAN (STANDARD DEVIATION) CONCENTRATIONS FOR RAW SEWAGE AND EFFLUENTS ALONG THE TREATMENT LINE.	109
TABLE 6.2 – MEAN/MEDIAN (STANDARD DEVIATION) VALUES FOR ENVIRONMENTAL VARIABLES FOR RAW SEWAGE AND THE EFFLUENTS FROM EACH UNIT ALONG THE TREATMENT LINE, INCLUDING INTERMEDIATE SAMPLE POINTS FROM THE 2 ND POND.	109
TABLE 6.3 – MEDIAN REMOVAL EFFICIENCIES IN EACH TREATMENT UNIT AND IN THE OVERALL TREATMENT SYSTEM, AS WELL AS IN THE INTERMEDIATE (P_2B_2 AND P_2B_3) POINTS IN THE 2 ND POND.	110
TABLE 6.4 – COMPARISON BETWEEN FINAL EFFLUENT CONCENTRATIONS OF MAIN CONSTITUENTS (MEAN/MEDIAN) OF THE NEW TREATMENT LINE AND THE PREVIOUS TREATMENT LINE STUDIED BY DIAS <i>ET AL.</i> (2014).	124
TABLE 6.5 – PERCENTAGE OF STABILISATION POND EFFLUENT SAMPLES COMPLYING WITH STANDARDS FOR DISCHARGING IN WATERBODIES. OFFICIAL JOURNAL OF THE EUROPEAN COMMUNITIES No. L 135/40.....	125
TABLE 6.6 - VERIFICATION MONITORING ^A (<i>E. COLI</i> NUMBERS PER 100 mL OF TREATED WASTEWATER) FOR THE VARIOUS LEVELS OF WASTEWATER TREATMENT IN OPTIONS A–G PRESENTED IN FIGURE 6.12 (WHO, 2006).	126
TABLE 6.7 – MEAN NEPHELOMETRIC TURBIDITY UNITS (NTU) FOR EACH DEPTH (10 CM, 20 CM AND 30 CM) AND OVERALL DEPTH DURING EACH TIME FRAME.	156
TABLE 6.8 - K_A VALUES, COEFFICIENT OF DETERMINATION AND K_d UNITS FOR EQUATIONS 6.1, 6.2 AND 6.3.....	159
TABLE 6.9 - K_A VALUES, COEFFICIENT OF DETERMINATION AND K_d UNITS FOR EQUATIONS 6.4, 6.5 AND 6.6.	163
TABLE 6.10 - PERCENTAGE RATIO BETWEEN UV-A, UV-B AND PAR IRRADIANCE ESTIMATED BY SMARTS AND TOTAL SOLAR IRRADIANCE MEASURED FROM THE METEOROLOGICAL STATION.	165
TABLE 6.11 – SUMMARY OF RANGE AND (<i>MEAN</i>) VALUES FOR ENVIRONMENTAL VARIABLES DURING THE <i>E. COLI</i> DISINFECTION TEST TUBES EXPERIMENT FOR MORNING AND AFTERNOON PERIODS FOR EACH DEPTH PROFILE. OUALI <i>ET AL.</i> (2014) DO, pH AND TEMPERATURE RESULTS.	167
TABLE 6.12 - THE DIFFERENCE BETWEEN THE K_B AND THE K_d COEFFICIENTS FOR THE DIFFERENT PERIODS AND DEPTHS.	172
TABLE 6.13 - SUMMARY OF MEAN (<i>MEDIAN</i>) VALUES AND PERCENTAGES OF REMOVAL EFFICIENCIES, DO CONCENTRATIONS, pH AND TEMPERATURE VALUES FOR THE DIFFERENT DEPTH PROFILES AND PERIODS FOR THE 4 HOUR EXPERIMENT IN THE TEST TUBES.	172
TABLE 6.14 - SUMMARY OF THE MULTIPLE COMPARISON TEST (P-VALUES) FOR K_B , $K_{B20^{\circ}C}$, REMOVAL EFFICIENCY, TEMPERATURE, DO AND pH CONSIDERING A CONFIDENCE LEVEL OF 95%.	181

TABLE 6.15 - APPLIED SURFACE DOSES AND RECEIVED DOSES AT DIFFERENT DEPTHS FOR MORNING AND AFTERNOON PERIODS (4 HOURS EACH) DURING THE WHOLE MONITORING PERIOD.....	183
TABLE 6.16 – OVERALL MORNING IRRADIANCE DOSE (UV-A, UV-B AND PAR) RECEIVED AND <i>E. COLI</i> REMOVAL EFFICIENCY AND DISINFECTION COEFFICIENTS FOR DIFFERENT DEPTH PROFILES.	184
TABLE 6.17 – OVERALL AFTERNOON IRRADIANCE DOSE (UV-A, UV-B AND PAR) RECEIVED AND <i>E. COLI</i> REMOVAL EFFICIENCY AND DISINFECTION COEFFICIENTS FOR DIFFERENT DEPTH PROFILES.	184
TABLE 6.18 - DEPTH FROM THE SURFACE AND RESULTING K'_b AND K'_d IN EACH OF THE 20 VERTICAL LAYERS OF THE FIRST AND SECOND PONDS BASED ON EQUATIONS 6.27 AND 6.28, INCLUDING THE FINAL WEIGHTED MEAN FOR K'_b AND K'_d IN BOTH PONDS.	195
TABLE 6.19 - N_0 , K_B (WHOLE LIQUID COLUMN APPROACH), T AND DISPERSION NUMBER (D) (PASSOS <i>ET AL.</i> , 2015; 2016) IN THE FIRST AND SECOND POND.....	197
TABLE 6.20 - OBSERVED N VS ESTIMATED N IN THE FIRST AND SECOND POND FOR THE DISPERSED MODEL CONSIDERING A SIMPLER FORM OF ESTIMATING K_B	197
TABLE 6.21 - K_B IN EACH LAYER AND ESTIMATED N FOR EACH INDIVIDUAL LAYER IN THE FIRST AND SECOND POND FOR <i>E. COLI</i> , AS WELL AS THEIR RESPECTIVE WEIGHTED MEAN. ESTIMATED MEAN <i>E. COLI</i> CONCENTRATION FROM THE EFFLUENT OF THE FIRST POND AND SECOND POND.	198
TABLE 6.22 - OBSERVED N VS ESTIMATED N IN THE FIRST AND SECOND POND FOR THE DISPERSED MODEL USING THE DISPERSED FLOW MODEL APPLIED WITH THE MULTILAYER APPROACH.	199
TABLE 6.23 - SUMMARY OF MEAN/MEDIAN REMOVAL EFFICIENCIES (LOG UNITS) AND GEOMETRIC MEANS FOR THE TREATMENT LINE DURING THE OVERALL 1 ST AND 2 ND PHASES.	203
TABLE 6.24 - SUMMARY OF MEAN/MEDIAN REMOVAL EFFICIENCIES (LOG UNITS) AND GEOMETRIC MEANS FOR THE TREATMENT LINE DURING THE SAME PERIOD OF THE 1 ST (25/09/2014 – 23/04/2015) AND 2 ND (30/09/2015 – 19/04/2015) PHASES.	204

ACRONYMS

λ – Lambda (wave length)
Ammonia-N – Ammonia Nitrogen
B – Breadth
BOD – Biochemical Oxygen Demand
C&D – Cold and dry
CePTS – Centre of Research and Training in Sanitation
COD – Chemical Oxygen Demand
COPASA – Sanitation works company in Minas Gerais
d – Days
DESA – Department of Sanitary and Environmental Engineering
DO – Dissolved Oxygen
E. coli – *Escherichia coli*
EM – Electromagnetic
FSS – Fixed suspended solids
GRoF – Graded Rock Filter
H – Depth
HRT – Hydraulic Retention Time
K_a – Light attenuation coefficient
K_b – disinfection coefficient
K_d – Dark disinfection coefficient
L – Length
L/B – Length to breadth ratio
N – nitrogen
nm – Nanometre
PAR – Photosynthetically Active Radiation
P₁ – Pond 1
P₂B₂ – Pond 2 point 2
P₂B₃ – Pond 2 point 3
P₂B₄ – Pond 2 point 4
ROS – Reactive Oxygen Species
SI – International Units
S₀, I, I_r – Solar irradiance
t – HRT
TCB – Total Coliform Bacteria
ThCB – Thermotolerant Coliform Bacteria
TKN – Total Kjeldahl Nitrogen
TSI – Total Solar Irradiance
TSS – Total Suspended Solids
UFMG – Federal University of Minas Gerais
UV-A – Ultraviolet A
UV-B – Ultraviolet B
UV-C – Ultraviolet C
VSS – Volatile suspended solids
W&W – Wet and warm
WSP – Waste Stabilisation Pond
WWTP – Wastewater Treatment Plant

“Agitation of thought
is the beginning of wisdom.”

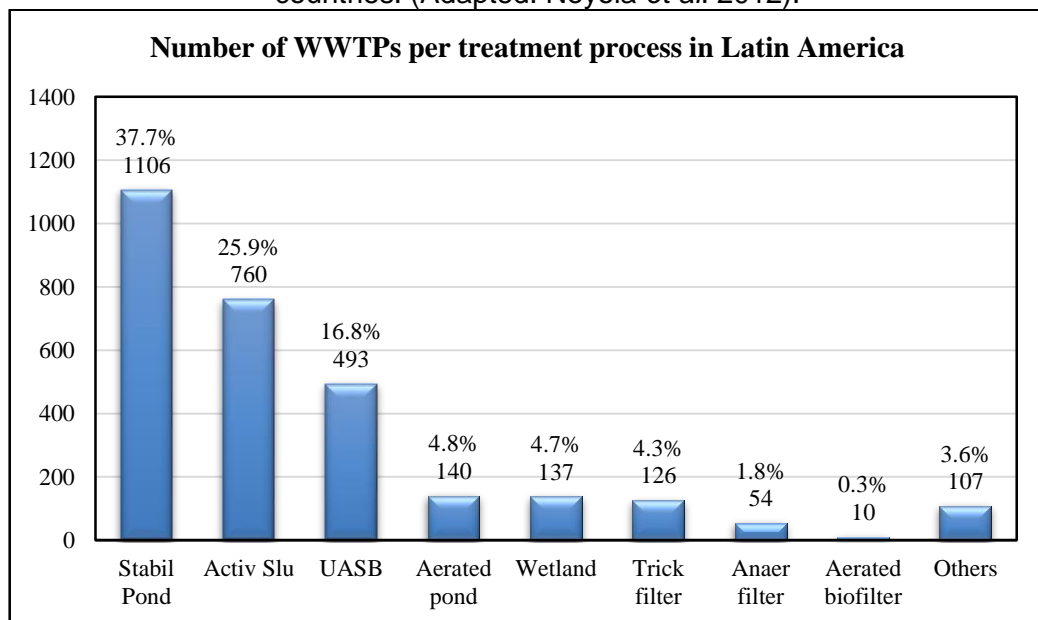
- Vitoria Woodhull

1. INTRODUCTION

Wastewater treatment has come a long way, as not so long ago (roughly 100 years) raw sewage was directly dumped into water courses or oceans. Unfortunately, this still occurs in many communities in developing countries and even in Europe. A possible solution can be the use of low-cost, low-maintenance and simple-to-implement wastewater treatment plants. Raw sewage treatment through natural systems is considered an attractive alternative in developing countries compared to more expensive and resource consuming treatment systems, such as activated sludge, aerated biofilters and biodiscs. Waste Stabilisation Ponds (WSP), a natural wastewater treatment unit, is used around the world to treat domestic sewage for millions of people.

Gloyna (1971) classified WSPs as a biological treatment unit for wastewater and ideal for regions where land is inexpensive, fluctuations in organic loadings and scarce qualified labour. In tropical climates they excel in treating wastewater because of high annual average temperatures and sunlight radiation. They are also the most common type of treatment technology in developing countries across the world and in fact are the most used technology for treating domestic sewage in Latin American countries (Figure 1.1) (Noyola *et al.*, 2012).

Figure 1.1 – Wastewater treatment technologies applied in Latin American countries. (Adapted: Noyola *et al.* 2012).



Their key factor for success is undoubtedly simplicity to build and operate (Shilton, 2005) and are well documented in literature throughout the world, especially Brazil. WSPs are usually

considered “low-tech”, but yet they are very complex units because most mechanisms are still considered a “black-box” due to the range of transformations occurring to organic matter and other constituents. Nonetheless our understanding of the mechanisms involved is increasing and possibly lead to enhancing design and usage of the system by reducing land requirements and maintaining a reliable effluent quality. Natural ponds can be divided into three main types:

- Anaerobic;
- Facultative and;
- Maturation.

Anaerobic ponds are designed to receive and treat high loads of organic matter per unit volume, while dissolved oxygen (DO) and algal biomass are virtually absent. These ponds are deeper than other types of ponds.

Facultative ponds are the most implemented type of pond for treating raw sewage in the world (Shilton, 2005). These ponds are a crossover between an anaerobic and maturation pond due to the two distinct layers that are formed within. The bottom liquid layer is anaerobic and the top liquid layer is primarily aerobic, promoting two different environments for stabilisation and disinfection of domestic sewage. They are shallower than anaerobic ponds but deeper than 1.0 m.

Maturation ponds are even shallower (less than 1.0 m) than facultative ponds and usually serve as a polishing stage following a facultative or anaerobic pond. Their primary objective is pathogenic organism removal through natural processes/mechanisms (favourable environment formed within): high levels of pH and DO concentrations; sunlight exposure; and combination of sunlight with DO and pH. Facultative and anaerobic ponds do not have this as their primary objective, requiring complementary treatment to discharge a high quality effluent in bacteriological terms (low pathogen concentration). One or more maturation ponds in series, following any primary treatment unit and can produce the desired results for low pathogen concentration. Other processes/mechanisms for bacterial disinfection present in WSPs are predation by higher order organisms, sedimentation, and toxic substances believed to be produced by algae (Awuah, 2006). Some of these mechanisms could occur more frequently in facultative and anaerobic ponds than in maturation ponds.

A simple setup can be comprised of an anaerobic pond followed by a facultative pond, therefore removing carbonaceous matter, followed by one or more maturation ponds, depending on the level of treatment required (von Sperling, 2008a). Land requirements can be reduced by implementing an upflow anaerobic sludge blanket (UASB) reactor, eliminating the need for a facultative or anaerobic pond before maturation ponds. UASB reactors are very good at removing organic matter, reaching removal efficiencies up to 70% (Dias *et al.*, 2014, 2015). Maturation ponds following a UASB reactor are also considered a polishing stage (Chernicharo, 2007), but usually the first maturation pond after the UASB reactor also offers complementary organic matter removal (von Sperling *et al.*, 2008; Dias *et al.*, 2014, 2015) apart from pathogen disinfection (Bastos *et al.*, 2011; Dias *et al.*, 2014, 2015; Godinho *et al.*, 2010; Jack *et al.*, 2009; Nelson *et al.*, 2009; Sinton *et al.*, 2002; von Sperling, Bastos and Kato, 2005; von Sperling and Mascarenhas, 2005; von Sperling and De Andrada, 2006; von Sperling *et al.*, 2010; von Sperling, 2008b). In fact, the final effluent has the potential for agricultural reuse (Santos *et al.*, 2009).

Understanding the processes involved in WSP disinfection could produce better predictions concerning effluent quality, leading to efficiency improvements while maintaining a consistent treatment quality (Davies-Colley, Donnison and Speed, 2000). A broad knowledge on pathogen removal processes/mechanisms could provide basic guidelines for design, operation and maintenance improvements of WSP. On the other hand, basic mechanisms involved in bacterial disinfection in literature are numerous and even controversial (Maynard *et al.*, 1999).

Escherichia coli (*E. coli*) disinfection in maturation ponds is more pronounced because of greater sunlight, pH and DO exposure. Sunlight penetration in WSPs is not clearly understood, as well as how it affects bacteria as depth increases. Generally, disinfection decreases with depth, usually attributed to limited sunlight penetration, but maturation ponds are characterised by high values of pH and DO. DO and pH could have a detrimental effect on bacteria in the absence of sunlight radiation. Light penetration in shallow maturation ponds is unknown and few studies have been done on this subject (Nelson *et al.*, 2009; Bolton *et al.*, 2011a). Curtis, Mara and Silva (1992b) referred: “*No one has yet made the detailed wavelength-by-wavelength study of variations in removal rates...*”, meaning that each wavelength acts differently on bacteria at different depths. Light penetration is currently unknown in shallow maturation ponds situated in a tropical climate.

Greater removal efficiencies are expected to be achieved for *E. coli* when improving hydraulics in a pond, e.g., implementing baffles and creating a flow pattern approaching plug flow. This promotes longer contact times of the liquid with the detrimental environmental conditions, favouring removal mechanisms for *E. coli*. Influencing vertical mixing, a natural occurrence in ponds, could also allow for further disinfection.

Although ponds are used throughout the world, the mechanisms involved in thermotolerant coliform bacteria (ThCB) disinfection in literature are not in agreement, as well as how these mechanisms can be enhanced. Sunlight penetration in shallow maturation ponds is not reported in literature, only deeper ponds (>2.0 m) in tropical climates (Curtis, 1994) have been investigated on this matter. Direct and indirect sunlight influence on *E. coli* disinfection throughout depth is also not reported, except that disinfection decreases as depth increases (Mayo, 1989). Understanding sunlight penetration and its influence on *E. coli* disinfection will lead to optimising the geometry of ponds, i.e. promoting longer mean hydraulic retention times (HRT) with baffles, lower water levels, and consequently resulting in less land requirement.

In this work, experiments were conducted at the Centre for Research and Training on Sanitation (CePTS) UFMG/Copasa, located at the Arrudas treatment plant, in the city of Belo Horizonte, Brazil. The ponds have been in operation for over 13 years, where different setups have been researched with success. The project proposed a new treatment line setup to save on land requirement while maintaining overall efficiency. This PhD thesis is part of a larger project funded by the Bill & Melinda Gates Foundation – Sanitation for the Urban Poor (BMGF – SaniUP), coordinated by UNESCO-IHE, the Netherlands, and involving several universities around the world. The project included a complete evaluation of the proposed treatment line - a UASB reactor, two ponds (the first pond without baffles and the second pond with baffles) in series, and a graded rock filter with decreasing grain size as the last unit in the treatment line. The PhD thesis covers the treatment line for the removal of several variables and *E. coli* disinfection in depth, considering a multitude of environmental parameters believed to influence this organism and hydrodynamics.

The term disinfection in the current document regards all types of removal, inactivation, disinfection and decay processes for the microorganisms.

2. HYPOTHESES

H1 – Sunlight attenuation coefficients in shallow maturation ponds are affected by optical conditions and seasons;

H2 – The dark disinfection and dark repair (K_d) occurs at different depths and different times of the day;

H3 – An overall *E. coli* disinfection coefficient (K_b) based on K_b and K_d estimations from different depths and considering total solar irradiance (S_0), pH and DO concentrations will produce a general kinetic die-off coefficient model for shallow maturation ponds independently of the hydraulic regime;

H4 – Photosynthetically active radiation (PAR) does not influence *E. coli* disinfection at deeper depths;

H5 – Stratification and destratification occur in shallow maturation ponds in tropical climates, consequently influencing disinfection rates in the distinct stratified layers;

H6 – Vertical baffles perpendicular to the flow placed at the bottom of the pond will destratify the liquid layer and promote further disinfection in the shallow maturation pond.

3. OBJECTIVES

3.1. General objective

The research sought out to evaluate the influence of physiochemical parameters, the hydrodynamic pattern and ultraviolet A (UV-A), ultraviolet B (UV-B) and photosynthetically active radiation (PAR) penetration in a shallow baffled maturation pond on *E. coli* disinfection.

3.2. Specific objectives

1. Evaluate the overall performance of the treatment line (UASB reactor, unbaffled maturation pond, baffled maturation pond, rock filter) in terms of the removal of the major wastewater constituents;
2. Evaluate UV-A, UV-B and PAR attenuation in the shallow maturation pond and establish a depth profile of sunlight penetration regarding *E. coli* disinfection;
3. Evaluate the time needed for *E. coli* cells to remain in the surface layer of the shallow maturation pond for disinfection;
4. Model *E. coli* disinfection coefficients (K_b) for shallow maturation ponds independently from the hydraulic regime;
5. Estimate the effect of vertical baffles on *E. coli* disinfection.

4. LITERATURE REVIEW

4.1. *Maturation ponds and Escherichia coli disinfection*

Pathogenic organism disinfection is an important objective for wastewater treatment because they can cause diseases to the population. Waste Stabilisation Ponds (WSP) are often very efficient in this area, i.e., it is their primary objective, although other types of ponds do offer complementary pathogen removal. Maturation ponds are designed as a tertiary stage in wastewater treatment and are usually referred to as polishing ponds. Bacterial disinfection mechanisms are not always in agreement in literature because of limited understanding of how they occur. The following indicators for faecal contamination are: total coliform bacteria (TCB), thermotolerant (faecal) coliform bacteria (ThCB) and *E. coli*, being the latter part of the coliform bacteria population and considered the most representative of faecal contamination (Metcalf and Eddy, 2013). Each person discharges up to 400 billion coliform bacteria per day. *E. coli* is found in warm-blooded animals and if tested positive in a sample can be considered an indicator of thermotolerant contamination and possible presence of enteric pathogens (APHA. AWWA. WEF. – Standard Methods, 2005). Maturation ponds can remove up to 99.999% of ThCB (von Sperling, 2005a), allowing compliance with guidelines for practices of unrestricted irrigation when achieving a geometric mean value of less than 1000 MPN/100 mL (WHO, 2006).

The disinfection mechanisms used to remove *E. coli* can be grouped into three categories: biological processes; physical processes; and chemical processes (Awuah, 2006). Some mechanisms are more researched than others, while some are considered more pronounced and active. Sunlight-mediated disinfection is widely recognised in academia as the main role for disinfection, but more recently research shows that it does not operate as a stand-alone mechanism (Davies-Colley, Donnison and Speed, 2000; Santos *et al.*, 2013; and Kadir and Nelson 2014). This makes sunlight-mediated disinfection difficult to quantify and understand, and in some cases contradictory. Sunlight combined with high concentrations of dissolved oxygen (DO) and pH levels further enhances disinfection, pointing out the importance of the combination of mechanisms. By understanding each mechanism and how they interact with the pond environment (including hydrodynamics) and each other could improve and further optimise pond disinfection.

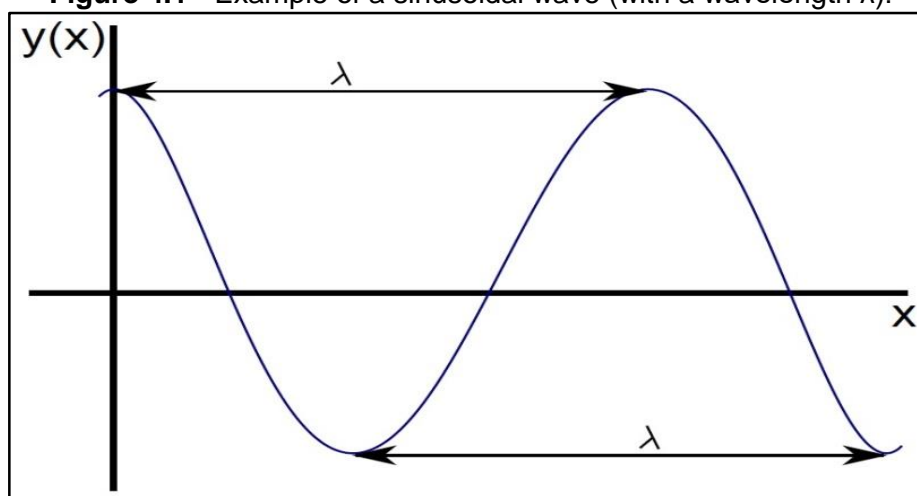
4.2. *Electromagnetic spectrum: what are waves?*

This section will show the importance of understanding which waves from the electromagnetic spectrum (EM) are of importance for sunlight-mediated disinfection.

EM radiation experimenting was first done by Frederick William Herschel in the 1800 by studying the temperature differences of colours from the visible light spectrum with the help of a thermometer. Herschel noticed that the highest temperature recorded was beyond the colour red. He had just discovered infrared, which at the time named it “heat waves”. One year later, Johann Wilhelm Ritter discovered ultraviolet (UV) radiation, which he called “oxidising ray” and shortly after changed to “chemical rays” because they could induce certain chemical reactions and behaved similar to visible light, but were not from the visible light spectrum (shorter in length).

Wavelengths travel in a wavelike shape, just like the function of the sine and cosine in mathematics, stretching when waves are longer (e.g.: radio waves, microwaves) and shrinking when shorter (e.g.: gamma rays, visible light, UV light). A sinusoidal wave is defined by the distance between two identical points in adjacent sequences of a waveform signal propagating through space, as shown in Figure 4.1. If the wave is longer, the distance will also be longer, while the opposite occurs when in the presence of shorter waves. A wavelength is designated by the letter λ (lambda) and expressed in metres according to the international system of units (SI). Infrared, visible light, ultraviolet and gamma radiation are usually represented in nanometres (nm).

Figure 4.1 - Example of a sinusoidal wave (with a wavelength λ).



Nowadays, our understanding of the EM spectrum is more advanced and most of it has been applied in science for spectroscopic interactions in order to characterise matter. For this research, only visible light or Photosynthetically Active Radiation (PAR) (400 – 700 nm) and ultraviolet (UV) light (100 – 400 nm) were addressed because of previous studies showing their disinfection properties for bacteria/pathogens in WSPs (Bolton *et al.*, 2011a; Bolton *et al.*, 2010; Curtis *et al.*, 1994; Curtis, Mara, and Silva, 1992a; Curtis, Mara, and Silva, 1992b; Davies-Colley, Donnison and Speed, 2000; Davies-Colley *et al.*, 1999; Hartley and Weiss, 1970; Holzinger and Lütz, 2006; Maïga *et al.*, 2009a; Muela *et al.*, 2002; Silverman *et al.*, 2013; Sinton *et al.*, 2002; Whitman *et al.*, 2008). On the other hand, Acher *et al.* (1997) stated that visible light and UV light above 360 nm do not produce any microbiocidal effect, but contribute to photosynthesis dependent organisms in the epilimnion layers of waterbodies.

The waves can be characterised as the following:

- **Visible light/PAR** is what the human eye can see and detect. Every type of light that can be seen is considered visible light, whether it be emitted by stars, light bulbs or fireflies.
- **Ultraviolet radiation** has as its natural source the sun. It is generally known to the public due to its ability to tan and cause sun burns, but it also produces harmful effects on microorganisms.

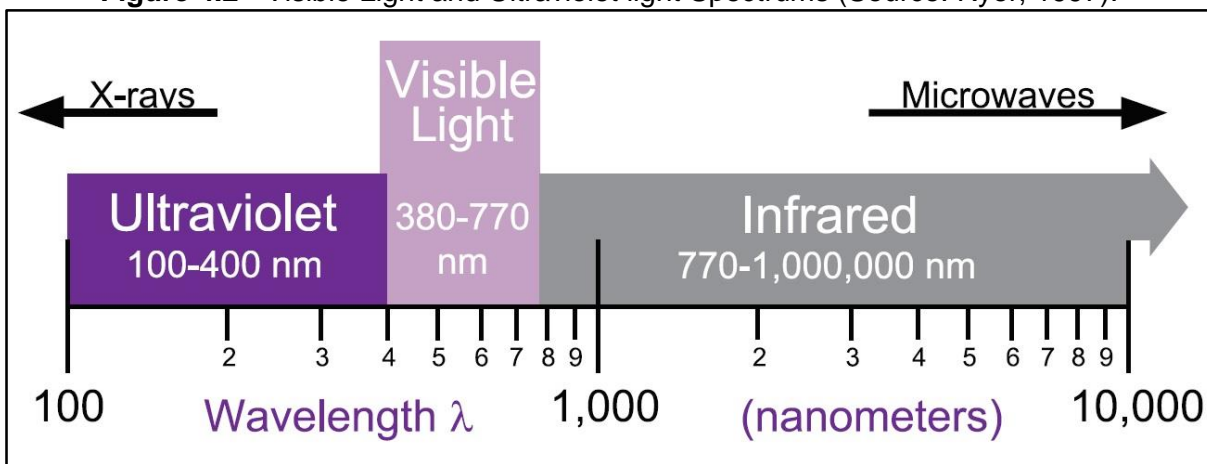
Fortunately, the ozone layer filters the majority of UV light from the short and middle wavelength (Table 4.1) and described by the International Organization for Standardisation (ISO) on determining solar irradiances (ISO-21348).

4.2.1. Visible light or photosynthetically active radiation (PAR)

PAR has a wavelength between 400 nm and 700 nm. Visible light has a wavelength from 380 nm to 770 nm, situated between ultraviolet, a shorter wave, and infrared, a longer wave (Figure 4.2), covering the whole PAR spectrum and justifying why the two spectrums are often known to be synonymous. Visible light, or just light, is defined by the International Lighting Vocabulary as “*Any radiation capable of causing a visual sensation directly*”, or simply light which is visible to the human eye and causes the sense of sight. One of the best ways to witness light is in the presence of a rainbow, where all the colours of the spectrum are perceptible.

PAR levels are usually greater during the summer months at mid-day, varying due to the time of day, season and latitude. Other factors such as cloud cover, shading, and air pollution can reduce the amount of PAR. For algae and aquatic plants, PAR measurements are important because the photosynthesis rate is directly related to how deep light penetrates in a water body. In turbid waters PAR penetrates less and consequently the rate of photosynthesis is lower. PAR can be absorbed by algal pigments and dissolved organic matter, or scattered due to other particles that are not characterised for absorbing radiation. This affects light attenuation rates causing it to attenuate faster at shallower depths.

Figure 4.2 - Visible Light and Ultraviolet light Spectrums (Source: Ryer, 1997).



4.2.2. Ultraviolet spectrum

Ultraviolet (UV), a Latin word, where ultra means “beyond” and violet is the colour of the shortest wave in the visible light spectrum, as shown in Figure 4.2. These waves are not perceptible to the human eye because they are not within our visible detection range.

Ultraviolet light has as its main contributor the sun, at least from Earth's perspective, but also black lights can imitate ultraviolet light. The wavelength ranges between 100 nm and 400 nm, being considered non-ionising radiation in the electromagnetic spectrum (WHO, 1994 and Al-Juboori, Aravinthan and Yusaf, 2010). Ionising radiation only occurs when wavelengths are < 100 nm.

UV radiation causes sunburn and damage to molecules in biological systems. In the middle wave range, UV rays cannot ionise but can act on chemical bonds and break them down, altering molecules to be abnormally reactive (Table 4.1). Sunburn is caused due to disrupting effects of

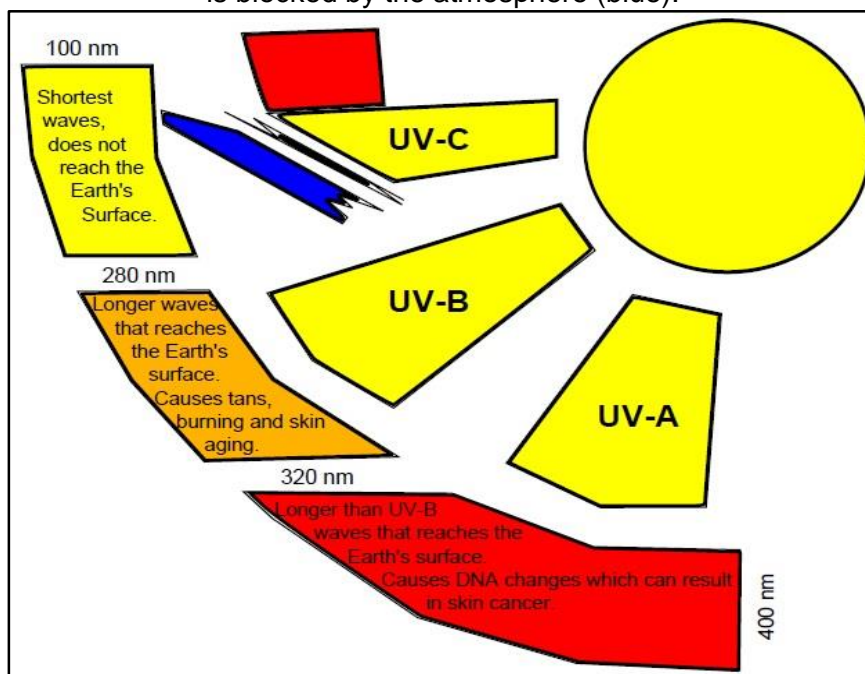
the middle UV range on skin cells and can lead to skin cancer, with a possibility to cause irreparable damage to complex molecules in cells producing thymine dimers (molecular lesions caused by thymine bases in DNA via photochemical reactions). Therefore UV is considered a very effective mutagen (Figure 4.3). There are a multiple number of different ultraviolet waves in the UV spectrum, varying from the longest wave, UV-A to the shortest, Vacuum UV (Table 4.1).

Table 4.1 - UV light spectrum. (SOURCE: ISO-21348).

<u>Name</u>	<u>Abbreviatio n</u>	<u>Wavelength(nm)</u>	<u>Alternative names/ notes</u>
<i>Ultraviolet A</i>	UV-A	400 – 315	long wave, black light
<i>Ultraviolet B</i>	UV-B	315 – 280	medium wave, germicidal
<i>Ultraviolet C</i>	UV-C	280 – 100	short wave, germicidal
<i>Near Ultraviolet</i>	N-UV	400 – 300	visible to birds, insects and fish
<i>Middle Ultraviolet</i>	M-UV	300 – 200	-
<i>Far Ultraviolet</i>	F-UV	200 – 122	-
<i>Hydrogen Lyman-alpha</i>	H Lyman- α	122 – 121	-
<i>Extreme Ultraviolet</i>	E-UV	121 – 10	-
<i>Vacuum Ultraviolet</i>	V-UV	200 – 10	-

Only UV-A, UV-B and UV-C (Table 4.1) are of concern for disinfection in wastewater due to their germicidal properties (Figure 4.3).

Figure 4.3 - Ultraviolet radiation from a natural source (sun). UV-C is blocked by the atmosphere (blue).

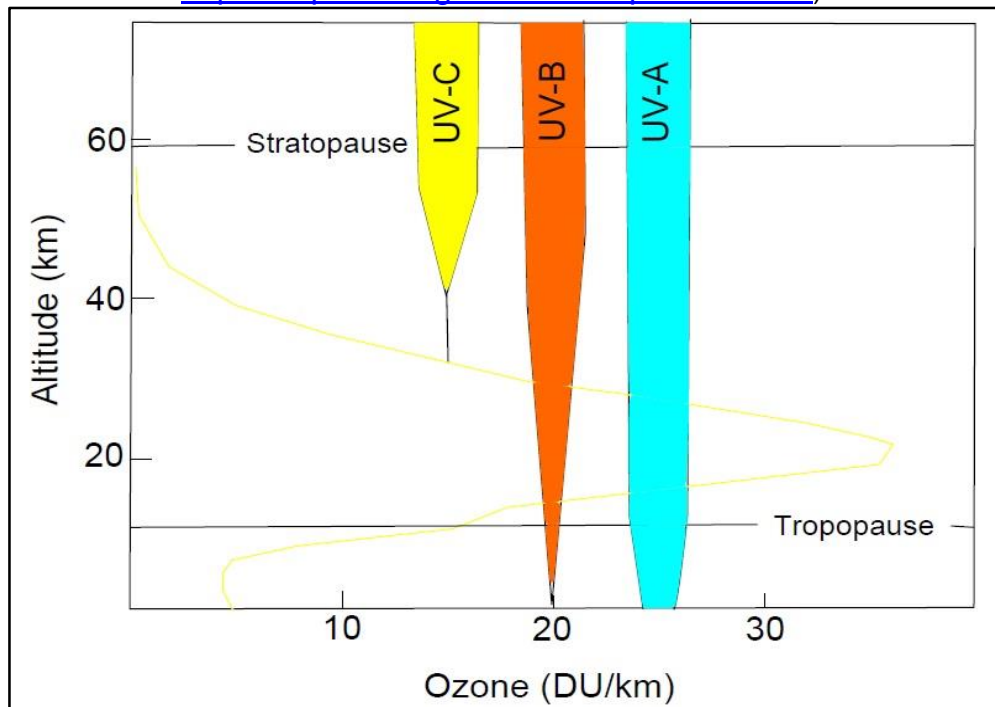


Since the discovery of the germicidal properties of UV radiation in the early 1900's, this “free source of technology” has been used for water supplies and wastewater disinfection. It has proven to be an effective way to disinfect wastewater from bacteria and viruses, while not producing or contributing for the formation of toxic by-products (Metcalf and Eddy, 2013). In developed countries UV disinfection is performed with artificial UV lamps, but in developing countries, like those in Latin America and Africa, the use of these lamps proves to be too expensive to buy and maintain, and therefore shallow WSPs are the primary route for wastewater disinfection (Noyola *et al.*, 2012). The amount of radiation that ponds receive is not controllable when compared with systems using UV lamps for disinfection, and as a consequence this can vary the disinfection efficiency when (WHO, 2002):

- Shading occurs due to cloud cover causing UV radiation levels to drop;
- Latitude can also affect UV radiation levels, where higher levels can be experienced closer to the equator;
- UV radiation varies with the time of day and year, i.e., the higher the sun is in the sky, the higher the level of UV. Outside the tropics, maximum UV levels are around midday (summer months);
- At higher altitudes the atmosphere is thinner and absorbs less UV radiation. UV radiation increases 10 to 12% for every 1000 m;
- The ozone layer absorbs some of the UV radiation that would otherwise reach Earth's surface;
- UV radiation can be reflected or scattered by different surfaces such as fresh snow (as much as 80%), dry beach sand (15%) and sea foam (25%) – the reflection ratio is commonly known as albedo.

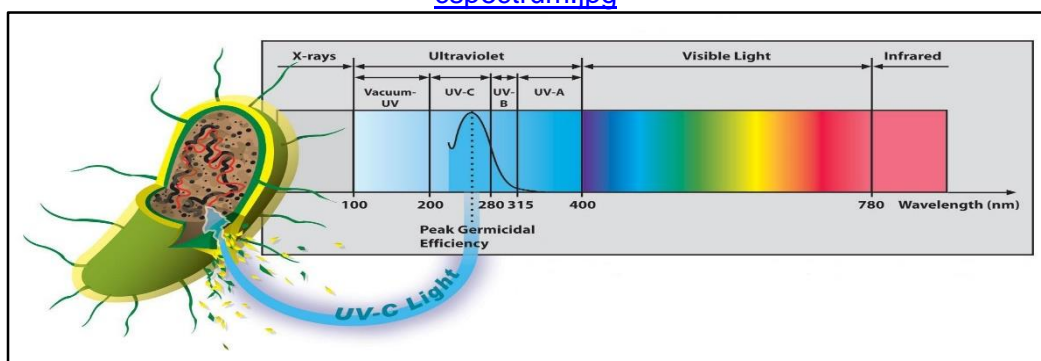
The germicidal range in the UV spectrum is considered to be between 220 and 320 nm, accounting all of the UV-C radiation range (200 to 280 nm) and all of the UV-B radiation range (280 to 315 nm). Peak germicidal efficiency occurs between 255 nm and 265 nm at around 260 nm (Figure 4.5), considered ideal for effective microbial disinfection, and found only in the form of UV-C which does not reach the Earth's surface (Figure 4.3 and Figure 4.4) (Metcalf and Eddy, 2013).

Figure 4.4 - Levels of ozone at various altitudes and blocking of different bands of ultraviolet radiation. DU – Dobson Unit (measure the total column of the ozone). (Source: http://www.schoolphysics.co.uk/age14-16/Wave%20properties/text/Ozone_layer/index.html; <https://espo.nasa.gov/solvell/implement.html>).



The UV range for sunlight-mediated disinfection is composed of UV-C, UV-B and UV-A, where the curved line represents the relative DNA absorbance (Figure 4.5). The absorbance is still quite representative in the UV-B range, showing that some absorbance occurs, although lower than in the UV-C array which is the most germicidal wavelength from the UV spectrum.

Figure 4.5 - Identification of germicidal portion of the UV radiation spectrum. SOURCE: <https://redsquarepools.files.wordpress.com/2011/02/scienceuv-cspectrum.jpg>



Developed countries use UV-C lamps for disinfection because UV-C does not reach the Earth’s surface, extinguishing half way between the Tropopause (boundary between the Troposphere

and Stratosphere) and Stratopause (centre of the atmosphere between the Stratosphere and the Mesosphere), due to the presence of air (Figure 4.4). UV-B and UV-A radiation reach Earth's surface, although UV-B reaches the surface in smaller quantities when compared to UV-A (Figure 4.4).

4.3. *Disinfection mechanisms in ponds*

Using *E. coli* as an indicator for pathogens has given rise as to doubt whether it is considered a indicator, even though it is always present at reliable levels in domestic sewage (Shilton, 2005). The amount of different types of pathogens discharged into wastewater treatment plants (WWTP) are very variable (Haas, 1986; Bitton, 1999), therefore resulting in difficulties in quantifying one specific type of pathogen. The question arises on which pathogens to test. Do these pathogens reoccur in test samples or will they be absent in future samples. It usually is not cheaper to quantify these pathogens opposed to indicator organisms. Therefore, the presence of *E. coli*, as mentioned above in subsection 4.1, is a reliable indication of faecal contamination, and consequently pathogenic bacteria, making it easy to detect in wastewater when compared to specific pathogens. Even in recent experiments, where the new trend is virus disinfection, *E. coli* seems to be a better indicator for the removal of echovirus 7 than MS2 phage (Weaver *et al.*, 2016). Table 4.2 indicates the characteristics that indicator organisms should present. Although no indicator fulfils all these criteria, *E. coli* is considered good on most of the criteria (Shilton, 2005). One important characteristic is that *E. coli* should usually live longer than most common pathogenic bacteria during natural disinfection in treatment lines (Awuah, 2006).

Table 4.2 - Appropriate characteristics of indicator organisms (Source: Shilton, 2005).

Criterion	Rationale
1 – Ubiquitous enteric organism	Always present in faecally-contaminated wastewater
2 – Always present in presence of enteric pathogens	So that presence of indicator warns of risk of disease
3 – More common than pathogens	Easier to detect/monitor
4 – More resistant than pathogens	Pathogen will not be present if no indicator is detected
5 – Does not multiply in the environment	So that contamination is not falsely indicated
6 – Easily detected by inexpensive methods	So on-going, routine monitoring is affordable
7 – Non pathogenic	No danger to laboratory personnel

Shilton (2005) presents an overview of mechanisms and factors that influence natural disinfection of bacteria, viruses, protozoan and helminth in WSPs (anaerobic, facultative and maturation), which is shown in Table 4.3 and discussed in the following subsections. The following sections will only focus on bacterial disinfection, that is coliforms and *E. coli*, as the

other microorganisms are out of the scope of this research. For a review on virus removal in wastewater treatment pond systems, consult Verbyla and Mihelcic (2015).

Table 4.3 - Factors believed to cause or influence disinfection in WSPs (Adapted: Shilton, 2005).

Factor	Likely mechanism(s)	Bacteria	Viruses	Protozoan parasites	Helminth eggs	Ponds¹
Temperature	Affects rates of removal processes	X	X	X	X	A, F, M
Sedimentation	Settlement of infectious agents (e.g. ova, cysts) or settlement of aggregated solids, including infectious agent	?	?	X	X	A, F, M
Sunlight	DNA damage by solar UV-B radiation or photo-oxidation (DO-sensitive) (different wavelengths)	X ²	X	?	-	F, M
Biological disinfection – predation, starvation and competition	Ingestion by higher order organisms (protozoans)	X	X	?	-	F, M
Algal toxins	Algal exudates are toxic to certain bacteria	?	-	-	-	F, M
Hydraulic retention time	Affects extent of removal (time of operation)	X	X	X	X	A, F, M

1 – Ponds: A – Anaerobic; F – Facultative; M – Maturation.

2 – Most of the DNA damage done to bacteria by UV-B radiation is repairable, where lethal effect is usually related by overwhelming the repair capacity.

Natural die-off is considered a disinfection mechanism (Awuah, 2006) and is possibly influenced by all the disinfection mechanisms by either enhancing natural die-off or extending survival rates. Pathogen or indicator organism disinfection is driven by a combination of mechanisms and factors, whereas temperature, pH and DO play an important role in disinfection (Liu, Hall and Champagne, 2015).

4.3.1. Temperature

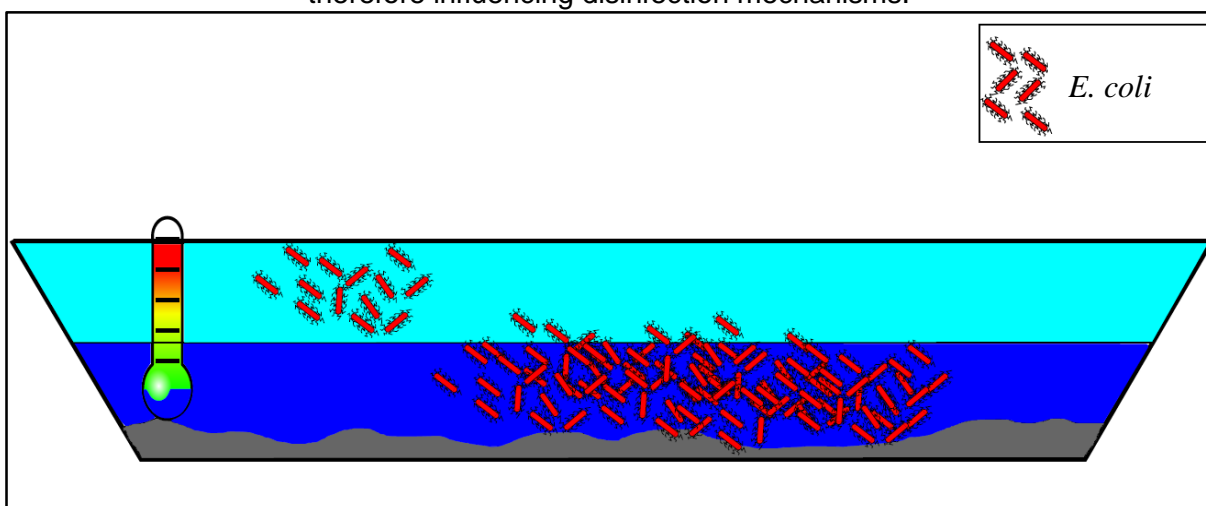
Temperature used to be considered the most important parameter influencing *E. coli* disinfection, and was solely utilised in the first design equation to estimate disinfection in ponds (Marais and Shaw, 1961; Marais, 1974). Although the equation was purposely structured to be simple, this influenced nearly a decade of researchers to consider just temperature as the key parameter when modelling *E. coli* disinfection in WSPs (Klock, 1971; Bowles et al., 1979; Ferrara and Harleman (1981)).

Later on, researchers considered that disinfection processes in WSPs were much more complex than considering just one parameter, and there had to be some sort of synergy of disinfection mechanisms. They were right and now researchers consider that physical, chemical and biological disinfection mechanisms all interact with each other, but a rise in temperature still increases disinfection (Polprasert *et al.*, 1983; Pearson *et al.*, 1987a, b; Barzily and Kott, 1991; Mara *et al.*, 1992, Mezrioui *et al.*, 1995; Pachepsky *et al.*, 2014). Blaustein *et al.* (2013) showed that *E. coli* survival rates depend on water temperature considered it to be a major factor and concluded that disinfection rates considering temperature vary from water source to water source.

Mayo and Noike (1996) considered that temperatures above 30 °C decrease heterotrophic bacteria organisms. Temperature should be considered a secondary factor as it does not cause disinfection on its own because it is only lethal to microorganisms when reaching 45 °C and provoking a thermal shock (Mills, 1992; Shilton, 2005), or when interacting with other mechanisms. Mara and Pearson (1986) exemplified this when comparing removal rates in maturation, anaerobic and facultative ponds, all operating at the same temperature. Disinfection was greater in the maturation pond, suggesting the involvement of other mechanisms. Mayo (1995) concluded that for modelling disinfection rates, temperature and solar irradiation should not be considered in the same equation, as these are redundant variables. In a more recent research temperature was found to be an important factor because it was statistically well correlated with *E. coli* concentrations (Liu, Hall and Champagne, 2015). Then again, Mayo (1995) inferred that temperature should only be included as a variable when implementing ponds in temperate climate countries because of greater temperature fluctuations.

Figure 4.6 illustrates a WSP where temperature is greater near to the surface and decreases as depth increases. Stratification can occur due to temperature differences between the top and the bottom of WSPs, therefore causing denser layers at the bottom of the pond. This causes short-circuiting in ponds and therefore reduces disinfection efficiency (Passos and von Sperling, 2015). *E. coli* counts are greater towards the bottom of the pond (Moumouni *et al.*, 2015), with cooler conditions, and decreasing in numbers near to the surface. Because of stratified conditions in ponds, other disinfection mechanisms are most likely reduced (sunlight-mediated disinfection, pH disinfection, etc.) because *E. coli* remain in the lower layers of the pond, therefore escaping these important disinfection mechanisms. Sunlight cannot penetrate very deeply into ponds due to optical conditions, and pH and dissolved oxygen levels are lower at the bottom layer of the pond compared to the top layer.

Figure 4.6 – *E. coli* distribution in function of temperature variation along the depth of a WSP. Temperature decreases as depth increases, therefore inducing stratification because of the differences in temperature at the top (light blue) and bottom (dark blue) of the WSP, therefore influencing disinfection mechanisms.



4.3.2. Sedimentation and attachment

Sedimentation has long been considered the primary route for removing organic matter and helminth eggs WSPs because they sediment due to their own weight, but in some cases helminths attach themselves to structures, whereas *E. coli* can also perform this undertaking by using ligands to attach themselves (Fletcher, 1996; Tortora *et al.*, 2003). James (1988) considered this disinfection mechanism to occur in the primary stage of any pond system, predominantly in anaerobic ponds, removing about 50% of the incoming bacteria. *E. coli* can also be removed by adsorption to settleable solids, such as particulate organic matter or algae, but removal can decrease if suspended solids in the system are low in concentration

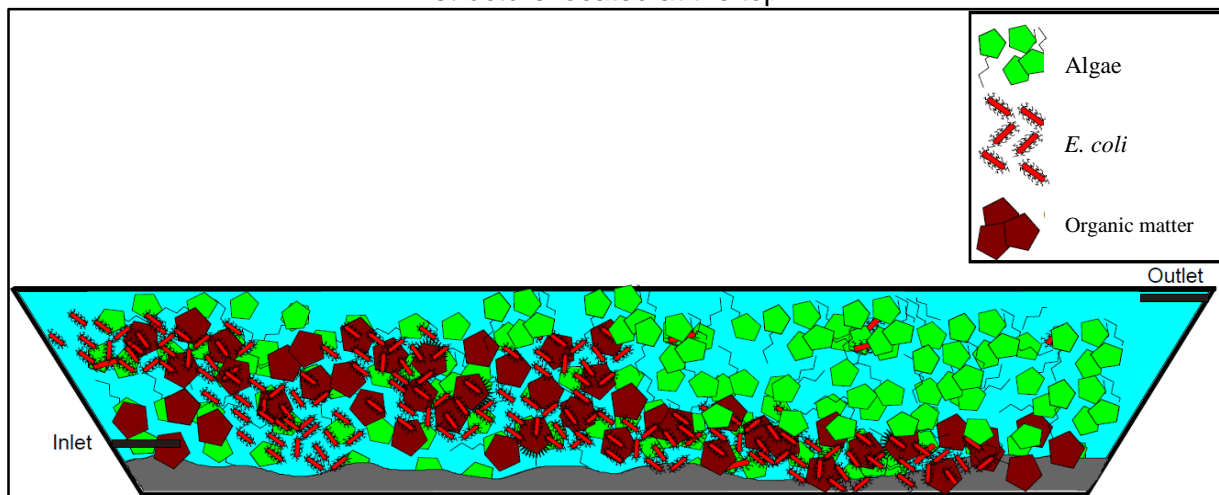
(Papadopoulos, Tsihrintzis and Zdragas, 2011). The mechanism becomes less significant in further stages of pond systems in series, and more pronounced in primary and deep ponds (anaerobic ponds) (Mayo, 1995).

E. coli is in a stable suspension state, only settling to the bottom of the pond when part of flocs (Wilkinson *et al.*, 1994). This shows that attachment and sedimentation are closely related. Gannon *et al.* (1983), Auer and Niehaus (1993) and Ansa *et al.* (2011) suggested that sedimentation is an important factor for models predicting coliform bacteria disinfection in WSPs, although the mechanism is considered more pronounced in primary and deeper ponds (Mayo, 1995). Sedimentation overtakes sunlight-mediated disinfection as the primary route for disinfection when solar exposure is limited or inexistent and as mentioned in deeper ponds (Mayo, 1989). Awuah (2006) debated on whether attachment of *E. coli* to algae could increase disinfection due to favourable conditions on the surface of ponds or protect them by “shading”. Sedimentation also depends on hydraulic retention time (HRT), where the longer HRT is, the higher the probability for solids to settle to the bottom of the pond and consequently remove *E. coli*.

Maynard *et al.* (1999) showed that sedimentation is the primary removal mechanism of cysts and eggs in WSPs. This does not mean that the eggs are inactivated, because usually helminth eggs can remain viable in the sludge at the bottom of the pond for long periods of time and mobilise due to thermal turn-over or other disruptions caused to the sludge (Feachem *et al.*, 1983; Larsen and Roepstorff, 1999; Maynard *et al.*, 1999). This is not the case for *E. coli* given that their life cycle is very short.

The attachment and sedimentation disinfection mechanism for *E. coli* in WSP is illustrated in Figure 4.7.

Figure 4.7 - Sedimentation and attachment of *E. coli* in a primary waste stabilisation pond. Placement of inlet structure located at the bottom to promote faster sedimentation and outlet structure located at the top.



E. coli attach themselves or are adsorbed by algae or particulate organic matter, settling to the bottom of the pond with the sludge. There they remain and are inactivated in a short time period when compared to cysts and eggs. A factor influencing this mechanism is the position of the inlet and outlet structures; the inlet structure should be placed closer to the bottom of the pond to promote faster sedimentation and the outlet structure near to the surface. This will be addressed in detail in section 4.3.7.2.

4.3.3. Dissolved oxygen and pH levels

High levels of dissolved oxygen (DO) occur in pond systems, especially in maturation ponds due to photosynthesis performed by algae. DO concentrations depend on the organic loading received by the pond, increasing or decreasing depending on a lower or higher load, respectively. When saturated or oversaturated with DO, high pH levels can be encountered, while lower pH values are present when DO concentrations reduce. This occurs because photosynthesis by algae removes carbon dioxide from the water, consequently increasing pH. In other words, pH values increase with decreasing organic loads as well (Mayo, 1995).

The upper levels of WSPs are known to reach high DO concentrations, above saturation, and over 30 mg/L in the summer months (Sweeney *et al.*, 2007), but high concentrations depend on a favourable climate (high solar exposure) and organic loading (due to the balance between oxygen consumption and production). At night, DO at the surface can be close to zero (Shilton, 2005). DO stratification can differ expressively in these systems due to light attenuation, with

nearly all light being absorbed in the upper layers (Haag and Hoigne 1986), reducing photosynthesis as depth increases. Passos *et al.* (2016) showed this in a maturation pond with 0.80 m deep, where DO concentrations during the day between the surface and bottom of the pond were distinctively different (a difference as high as 40 mg/L). At night, DO concentration at the surface decreased until finally equalising in concentration with the bottom, therefore occurring mixing of the two layers. This observation occurred on a daily basis and was dictated by thermal stratification and mixing.

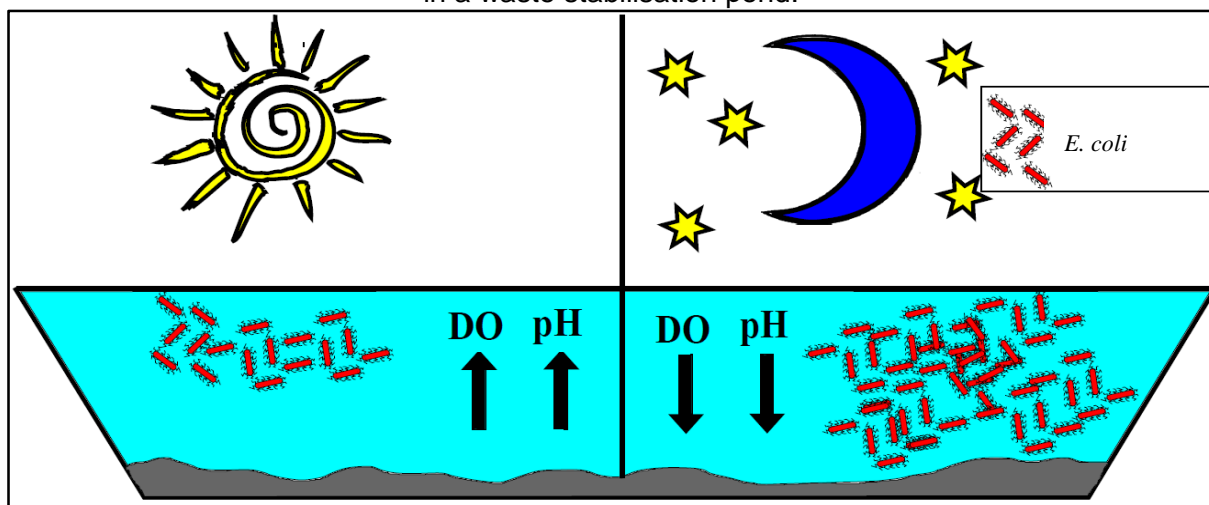
Curtis, Mara and Silva (1992b) and Maïga *et al.* (2009a) showed that supersaturated oxygen on its own in dark conditions (no light), does not produce any adverse effect on *E. coli*. Microorganisms survival is dependent on the presence of oxygen, but decreases with increasing oxygen concentration in the presence of light (Curtis, Mara and Silva (1992b)). Liu, Hall and Champagne (2015) showed that DO was not well correlated with *E. coli* disinfection but to other factors, such as sunlight penetration and intensity.

As with DO, pH also shows a strong dependence with light exposure. pH values greater than 9.3 rapidly disinfect *E. coli* (Parhad and Rao, 1974), being extremely detrimental when greater than 10 (Mendonca *et al.*, 1994 and Mayo and Noike, 1996). Significant diurnal pH changes in ponds can be observed (Bolton *et al.*, 2010), varying from 7.0 to 9.4 (Kayombo *et al.* 2002; Sweeney *et al.* 2007). Mendonca *et al.* (1994) showed that high pH values can rapidly destroy gram-negative food borne pathogens, where at pH levels of 12, *E. coli* decreased at least 8 log units within 15 s. *E. coli* viability decreased as exposure time to pH levels of 10 and 11 increased, especially at temperatures of 45°C, therefore combining high pH values and high temperatures. pH at extremely high levels affects disinfection and shows a strong dependence (Mayo, 1995). Curtis, Mara and Silva (1992b) considered two possibilities, high pH values either decrease the resistance of the organism regarding the effects of light or increases the production of toxic forms of oxygen, detrimental for bacteria. High temperatures combined with high pH values could be another reason why WSPs in tropical countries perform very well when compared to temperate countries. Smallman (1986) and Pearson *et al.* (1987b) suggested that values above 9 already produced adverse effects and high alkaline conditions appear to be more bactericidal for *E. coli* than on *V. cholerae* (Mezrioui *et al.*, 1994). Just like temperature, *E. coli* counts have been shown to be statistically correlated to pH, where pH values greater than 8 are already effective for disinfection (Liu, Hall and Champagne, 2015). Literature

presents different pH levels considered to effectively inactivate or to enhance disinfection, but there is no agreement on the starting value causing disinfection, varying from 9.0, 9.3 and 8.0.

Diurnal and nocturnal effects on *E. coli* are shown in Figure 4.8. Sunlight exposure during the day increases DO concentration and pH values due to photosynthesis by algae (not present in the image). Consequently, *E. coli* counts decrease, especially at high levels of pH. At night, photosynthesis is inexistent and oxygen consumption continues to takes place, therefore reducing DO and increasing CO₂, and consequently decreasing pH and reducing disinfection.

Figure 4.8 - pH and DO concentration effect on *E. coli* disinfection during day and night time in a waste stabilisation pond.



4.3.4. Sunlight-mediated disinfection (in combination with DO and pH) and dark disinfection/repair

Sunlight is an abundant, free and natural resource and considered a major disinfection factor for WSPs. It has long been recognised to have a detrimental effect on enteric bacteria in water bodies (Fujioka *et al.*, 1981), where the bacterial disinfection rate is considered proportional to sunlight intensity (Moeller and Calkins, 1980; Polprasert *et al.*, 1983; Whitlam and Codd, 1986; Gersberg *et al.*, 1987; Curtis *et al.*, 1992a, 1994). Disinfection is increased by a factor of five when compared to no natural sunlight conditions (Noble *et al.*, 2004), therefore causing great losses in cultivability of cells (Davies and Evison 1991). The absence of a UV-protective pigmentation, short generation time and the small size of bacteria are some factors which allows for sunlight to be effective (Garcia-Pichel 1994). Davies-Colley *et al.* (1999) considered that *E. coli* disinfection is dominated by sunlight exposure, but are complicated to inactivate because

of their complex bacterial cell structure (Kadir and Nelson, 2014). Moreover, they are metabolically active in the environment.

Sunlight-mediated damage to bacteria in WSPs is caused by three waves from the EM spectrum: Photosynthetically Active Radiation (PAR: 400 – 700 nm), commonly known as visible light; Ultraviolet-A (UV-A: 320 – 400 nm); and Ultraviolet-B (UV-B: 290 – 320 nm). UV-C is the strongest disinfectant wave, but only special UV-C lamps emit it because it is attenuated completely by the atmosphere and therefore does not reach the Earth. Sunlight attenuation (through absorption and scattering) is very strong in WSPs (Curtis *et al.*, 1994) and little advantage is achieved when depths are greater than 3 or 4 m (Crites *et al.*, 2014). This was corroborated by Caslake *et al.* (2004) who showed that bacterial disinfection rates are affected by turbidity, i.e., disinfection takes longer in water with higher turbidity. Therefore, it is essential not to overload the first pond with too many solids in order to favour the passage of sunlight (Da Costa, Gomes and Filho, 2011). On the other hand, thermal stratification in ponds provides an excellent environment for algae growth and increase their concentration in maturation ponds. By disturbing stratification, algal growth would decrease (Crites *et al.*, 2014) and therefore reduce turbidity.

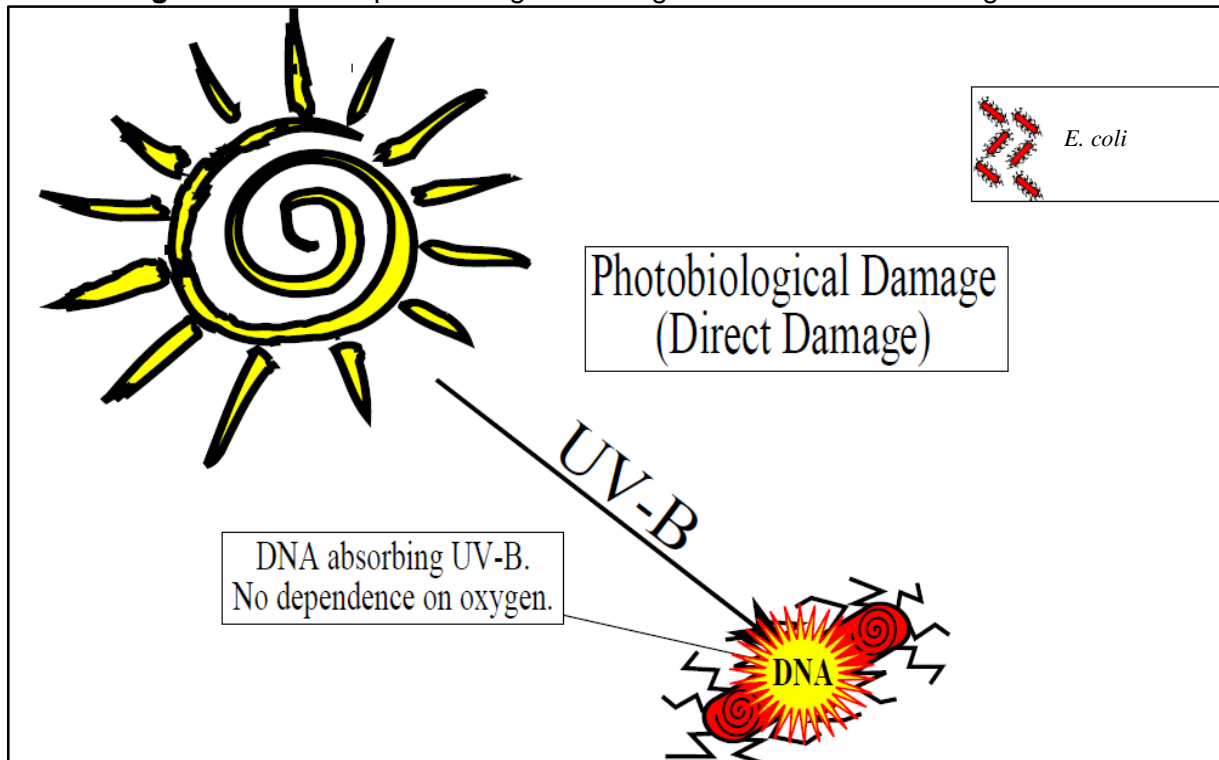
Bolton *et al.* (2011a) showed that PAR, UV-A and UV-B penetration was limited to 0.43 m, 0.15 m and 0.08 m, respectively in a facultative pond (1.5 m). Kohn and Nelson (2007) concluded that 99% of UV-B and PAR are absorbed in the first 2.5 cm and 8.0 cm, respectively. Haag and Hoigne (1986) concluded that virtually all effective light, in most water bodies, is fully attenuated before 1.0 m in depth. Balogh, Németh and Vörös (2009) confirmed that UV-B radiation is only limited to the first few centimetres in turbid water bodies, while in clear and deep water bodies it can penetrate several metres. UV-B impact not only depends on attenuation depth but also mixing processes (De Lange, 2000). Balogh, Németh and Vörös (2009) considered that different factors control UV and PAR attenuation in lakes, and this could quite be the case for WSPs. James (1988) commented that sunlight-mediated disinfection was not a major disinfection mechanism for WSP, justifying that sunlight was limited to the first 15 cm, an area that rarely has a high concentration of bacteria, but vertical mixing could expose bacteria to the upper layers. UV-B only accounts for about 0.2% of the amount of total solar radiation reaching the surface, UV-A about 5% and visible light around 50% of total solar radiation at noon (Shilton, 2005), therefore limiting penetration depths. Bolton *et al.* (2011a) suggested

turbidity as a surrogate parameter for predicting UV-A and UV-B attenuation in WSP, but no equations were presented. A simple form of determining water transparency or sunlight attenuation is using a Secchi disk, but only produces an attenuation coefficient for PAR/visible light and not UV-A and UV-B.

There are three distinct mechanisms accepted by researchers for sunlight-mediated disinfection in WSP. Simultaneous damage is caused to *E. coli* by the three mechanisms, suggesting a joint action of photosensitisation and photobiological processes (Muela *et al.* 2002). Sunlight-mediated mechanisms depend on physico-chemical conditions (pH and salinity) and DO, further enhancing disinfection depending on the mechanism (Table 4.5). Temperature on the other hand seems to only have a secondary influence by affecting DNA repair rates (Mayo, 1989). Davies-Colley, Donnison and Speed (2000) proposed the following three light-driven mechanisms occurring in WSP for bacteria/pathogen disinfection:

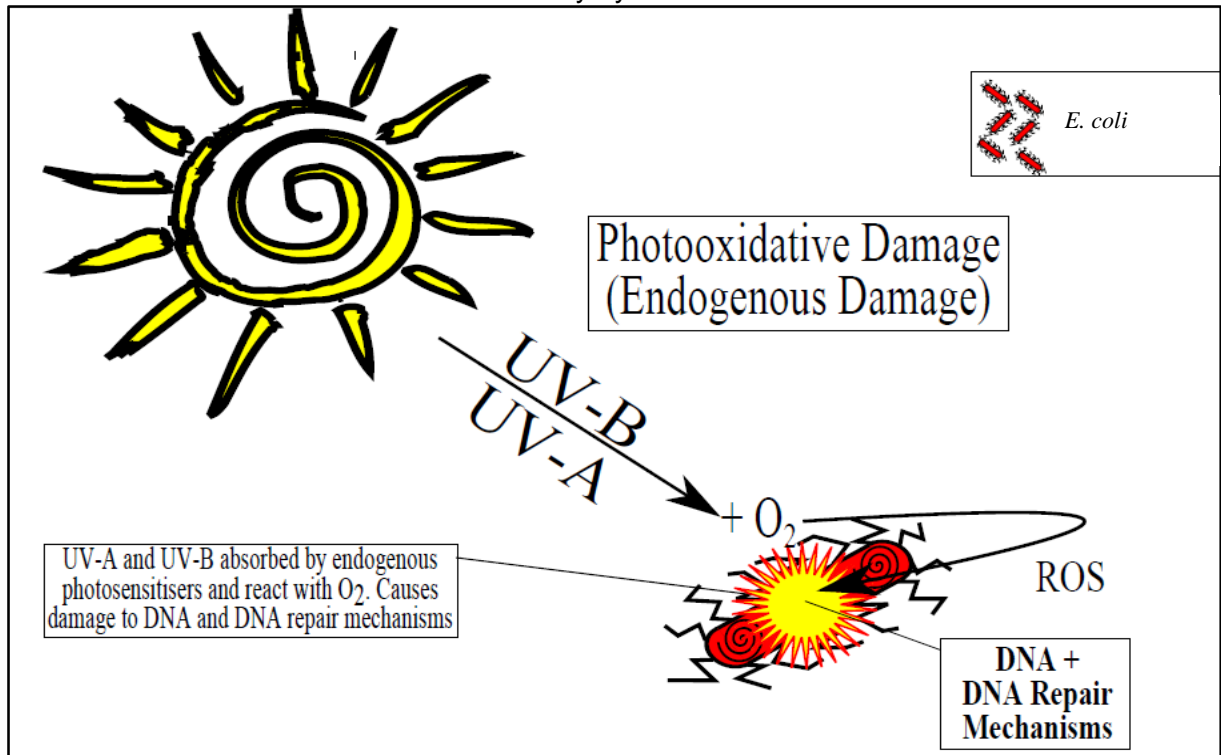
- **Mechanism 1** (*Direct photobiological damage*) – Solar UV-B (290–320 nm) is absorbed by DNA and causes direct damage to DNA (photobiological disinfection - Figure 4.9 (example: *E. coli*). This process does not depend on oxygen for potentially affecting the exposed mechanism. The problem is that the organisms are usually exposed to low dose, and this sometimes results in repair by the bacteria to correct much of the damage done to DNA, but only if the rate of damage is not overwhelming and if their repair capability has not been incapacitated.

Figure 4.9 - Direct photobiological damage caused to *E. coli* through UV-B.



- **Mechanism 2** (*Indirect endogenous photooxidation damage*) – Short wavelengths (UV-A and UV-B) from sunlight are absorbed by endogenous photosensitisers [e.g. porphyrin derivatives and flavins (Curtis, Mara and Silva, 1992a)] which react with oxygen under aerobic conditions to form highly reactive photooxidising species that cause damage to internal targets (photooxidation disinfection), such as DNA and, possibly, to DNA repair mechanisms (Figure 4.10). Just as with mechanism 1, damage is mainly caused, in this case indirectly, by UV-B and UV-A, but differs because it depends on DO in the medium.

Figure 4.10 - Indirect internal photooxidative damage to *E. coli* (Endogenous damage) caused indirectly by UV-A and UV-B.



UV radiation and PAR, the latter in a much lesser way, are able to also indirectly inactivate or damage bacteria/pathogens through photooxidation (Bolton *et al.*, 2010). This occurs when highly reactive oxygen species (ROS) are formed and react with bacteria/pathogens, therefore damaging or inactivating them. ROS can be generated from endogenous and exogenous sensitizers interacting with sunlight. Other reactions, such as Fenton's reaction are also important for causing oxidative stress to aerobic *E. coli* in dark conditions (Curtis *et al.*, 1992a; Acher *et al.*, 1997; Gracy *et al.*, 1999; Imlay, 2003; Kohn and Nelson, 2007; Nelson *et al.*, 2009). Sensitizers are light absorbing compounds which transfer their energy to other molecules and form ROS (Bolton *et al.*, 2010). In other words, a photosensitizer is a molecule that yields a chemical change in another molecule through photochemical processes. The internal sensitizers, or endogenous sensitizers, occur inside the bacteria cell (e.g. flavins) (Curtis *et al.*, 1992a; Kohn and Nelson, 2007). Bolton *et al.* (2010) stated that the presence of sensitizers would definitely affect sunlight-mediated disinfection of bacteria in a positive way, but hypothesized that it would not have any effect on viruses because they are not affected by endogenous photooxidation.

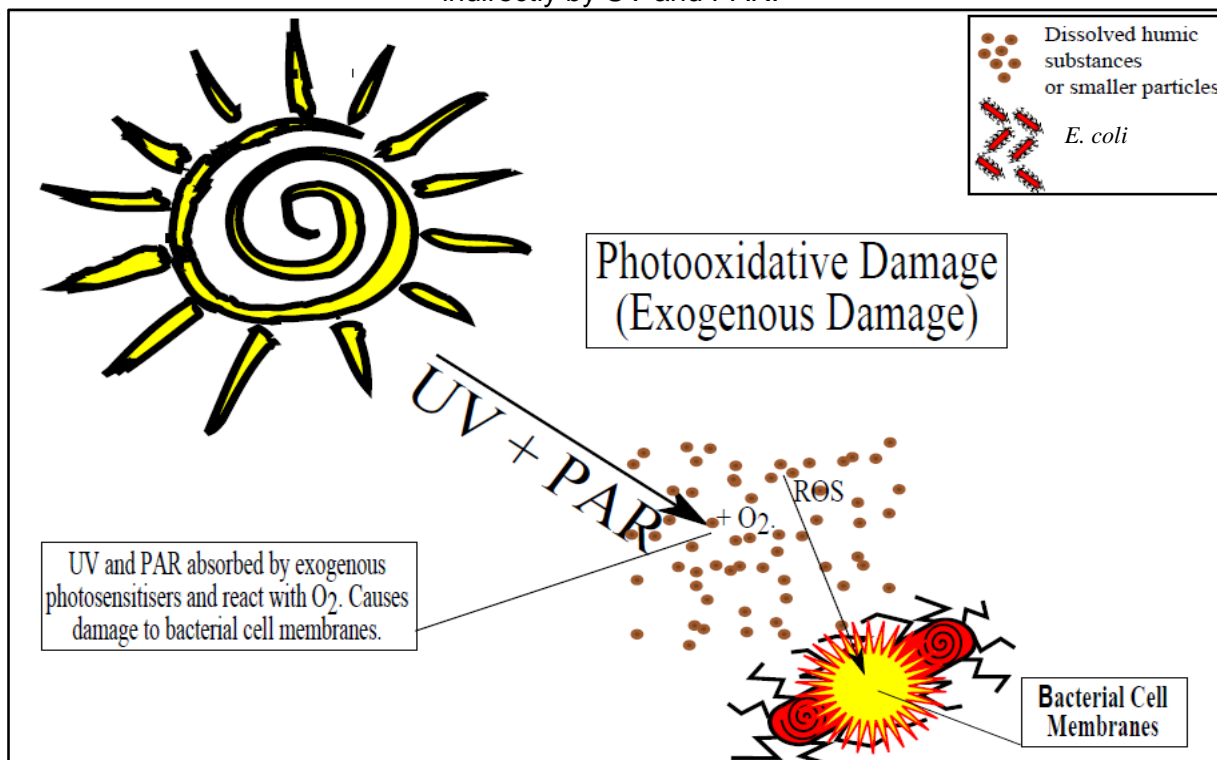
Reed (1997) considered endogenous sensitizers important for bacterial solar-mediated disinfection because it is dominant for *E. coli* disinfection and occurs when pH is close to neutral (Davies-Colley *et al.*, 1999; Kadir and Nelson, 2014). Santos *et al.* (2013) found that oxidative damage to lipids was determinant for bacterial disinfection during UV-B exposure. Nguyen *et al.* (2015) also considered indirect endogenous photooxidation damage to be the main contributor for *E. coli* disinfection based on modelling results from a pilot scale open-water wetland, but have found that it is constrained to wavelengths of 500 nm and less, therefore limiting penetration (Bolton *et al.*, 2011a) and consequently efficiency. Kadir and Nelson (2014) concluded that endogenous damage (contribution from UV-B and less contribution from UV-A) dominated *E. coli* disinfection and is strongly dependent on the presence of DO, but the disinfection rate did not increase with supersaturated mediums, as concluded by Davis-Colley *et al.*, (1999). Interestingly enough, Kadir and Nelson (2014) determined that this mechanism is not confined just to UV-B, noting that *E. coli* disinfection occurred in the absence of UV-B light and exogenous sensitizers. Their conclusions were that visible light also participates in *E. coli* disinfection, even though UV-B and UV-A dominate. Kadir and Nelson (2014) proposed to include UV-A and visible light in the second mechanism definition.

- **Mechanism 3** (*Indirect exogenous photooxidation damage*) – A wide range of wavelengths from sunlight, including the whole UV (290–400 nm) and PAR range (400–700 nm) is absorbed by external photosensitizers, or exogenous photosensitizers, found in WSP outside the microorganisms cells (e.g. humic substances (yellowish high-molecular-weight refractory forms of organic matter) and dissolved matter) (Curtis *et al.* 1992a; Curtis, Mara and Silva, 1992a; Muela *et al.* 2002; Kohn and Nelson 2007) (Figure 4.11). Smaller particles between 0.2 and 1 μm could also play a role (Kadir and Nelson, 2014). Humic substances can be a double-sided blade when ranging from sizes of 1 to 50 $\text{mg}\cdot\text{L}^{-1}$, by offering photoprotection against sunlight (Muela *et al.* 2002). Exogenous photosensitizers react with oxygen under aerobic conditions to form highly ROS such as singlet oxygen, hydroxyl radicals, superoxides and hydrogen peroxide (Zepp, 1988; Curtis *et al.*, 1992a) (exogenous photooxidation disinfection). Hydrogen peroxide combined with solar radiation causes bacterial disinfection and with proper dosages complete bacterial disinfection (Rodríguez-Chueca *et al.*, 2014). External ROS causes damage to the external structures of microorganisms such as the bacterial cell membranes. Dissolved matter may be the most important photosensitizer, but organic particulates could also be involved. UV-A is

responsible for most of the external photooxidation. Oxygen was identified to be a key variable, where without it, light would have less effect on *E. coli* (Curtis, Mara and Silva, 1992a).

Humic substances are ecologically important because they enhance the sun's bactericidal effects, allowing longer waves from the EM spectrum, PAR and UV-A, to cause damage to bacteria in the presence of DO. *E. faecalis* was found to be largely inactivated through mechanism 3 (UVA and PAR), with evidence that singlet oxygen is an important transient reactive species, while no significant effect for *E. coli* disinfection (Kadir and Nelson, 2014) or effect at all were observed (Nguyen *et al.*, 2015). However, Davies-Colley *et al.* (1999) considered that in the presence of high pH values, *E. coli* is vulnerable to the third mechanism. This requires further research to confirm these statements.

Figure 4.11 - Indirect internal photooxidative damage to *E. coli* (Exogenous damage) caused indirectly by UV and PAR.



The UV spectrum is nature's most powerful disinfection tool, especially UV-B by causing direct photobiological damage (mechanism 1) to DNA as well as indirect photooxidative damage (mechanism 2) to DNA (Sinton *et al.*, 2002). On the other hand, UV-B has a downfall for attenuating the most when penetrating water columns (Kirk, 1994) and may not contribute significantly enough for pathogen disinfection (Kadir and Nelson, 2014) as was once thought.

The other two waves cause indirect photooxidative damage to DNA (Table 4.5 and mechanisms 2 and 3), enhanced by oxygen and organic matter, therefore producing toxic agents such as singlet oxygen, oxygen free radicals, hydrogen peroxide and OH radicals (Kohn *et al.*, 2007; Maïga *et al.*, 2009a). DNA is the major target of UV radiation (Santos *et al.*, 2013), however, each bacteria has different sensitivities in relation to UV radiation (Joux *et al.* 1999; Matallana-Surget *et al.* 2008). Visser *et al.* (2002) believe that DNA damage alone does not account for bacterial disinfection, suggesting that other biomolecules and cellular structures are damaged by sunlight as well, consequently contributing for overall disinfection (Cheng *et al.*, 1981; Blanchetot *et al.*, 1984; Favre *et al.*, 1985; Jagger, 1985; Eisenstark *et al.*, 1989; Hoerter *et al.*, 2005; Santos *et al.*, 2013). Bosshard *et al.* (2010) understands that *E. coli* exposed to UV-A light in aerobic and sensitiser free conditions are first subjected to membrane damage and then loss of cultivability.

In shallow ponds, *E. coli* are inactivated faster than in deeper ponds, suggesting a relationship between solar radiation, bacterial disinfection rates and depth. Mayo (1989) performed a very interesting experiment, incubating wastewater in 600 mL fully transparent bottles. Some bottles were left above the water level and others placed at depths of 0.15 m and 1.0 m in the pond. The objective was to determine the disinfection rate of ThCB at different depths. The period for 90% disinfection ($t_{90\%}$) of the samples placed at the surface and depths of 0.15 m and 1.0 m took 21 hours, 90 hours and 150 hours respectively. The author concluded that bacterial disinfection increased with increasing direct solar radiation and HRT, and mortality rates were greater near the surface of the pond, decreasing as depth increased. The problem is that plastic bottles block most of the wavelengths incoming from sunlight, consequently underestimating disinfection times. James (1988) considered a general removal rate of 20 to 30 hours ($t_{90\%}$) for *E. coli* in ponds. Maïga *et al.* (2009a) results from an experiment in Burkina Faso with mesocosms operating at different depths showed that *E. coli* can be inactivated within hours and shallower depths (10 cm) had better removal rates than deeper depths. Maïga *et al.* (2009a, b) recommended shallow ponds (0.4 m) in areas with high temperatures, promoting high pH and DO levels. High pH levels results in a decrease in stability of microorganisms and therefore stimulating an increase in solar disinfection (Nelson *et al.*, 2009; Bolton *et al.*, 2010).

Kadir and Nelson (2014) suggested that damage from UV-B radiation alone is not a significant disinfection mechanism for *E. coli* and *enterococci*. The longer wavelengths like PAR and UV-

A are able to penetrate further and indirectly affect and inactivate microorganisms by reacting with organic matter to produce reactive oxygen species (ROS) (Muela *et al.*, 2002; Kohn and Nelson, 2007; Bolton *et al.*, 2011b; Kadir and Nelson, 2014). Santos *et al.* (2013) revealed that DNA damage to bacteria is possible upon UV-A exposure and that it indeed causes disinfection. Kadir and Nelson (2014) have questioned whether or not UV-A light may be more important for disinfection given that it reaches the Earth in greater strength, even though UV-B is better absorbed by DNA than UV-A (Sutherland and Griffin, 1981). This brings doubt on how important UV-B is for bacterial disinfection. Curtis (1990) considered that longer waves (e.g. visible light) are used mainly for photosynthesis and are not that good for removing ThCB. Curtis, Mara and Silva (1992a) studied the influence of pH, oxygen and humic substances in combination with sunlight for ThCB disinfection and concluded that wavelengths up to 700 nm were able to cause damage. This results in researchers concentrating on wavelengths from 290 nm to 700 nm to understand how penetration varies from wavelength to wavelength and pond to pond, possibly resulting in a better understanding on the impact of solar radiation on pathogenic organism disinfection (Curtis *et al.*, 1994).

It is possible to conclude that direct damage from sunlight radiation (direct photobiological disinfection) is limited, occurring only in the upper-most layers of ponds. Bacteria would need to remain for some time in the upper layers in order to be affected and for full photobiological disinfection to occur. The amount of algal mass changes the ponds optics by producing different light attenuation effects (Curtis *et al.*, 1994), meaning that disinfection largely depends on the medium in which bacteria are present. This influences *E. coli* disinfection and could as well protect algae from photoinhibition (Paerl *et al.*, 1985), resulting in a rise of algal productivity and leading to increasing DO and pH levels in WSPs (Curtis *et al.*, 1994).

Muela *et al.* (2002) showed the importance of oxygen participation and the role of exogenous and endogenous sensitizers for *E. coli* photoinactivation (UV-A, UV-B and PAR) suspended in freshwater. This was more pronounced when exposed to the UV spectrum. UV radiation also causes cellular damage to bacteria in the absence of oxygen, but may not be the dominant route for disinfection (Davies-Colley *et al.*, 1999; Kadir and Nelson, 2014). Bolton *et al.* (2010) found that *Enterococci* is primarily inactivated by UV-B, but not affected by the combination of DO and pH with UV-B, however UV-A in the presence of DO and pH further increases disinfection rates. Other studies indicated that *E. coli* disinfection increases with rising DO and pH levels

and solar radiation (Maïga *et al.*, 2009a; Davies-Colley *et al.*, 1999), but decreases enormously when UV-B is not present (Davies-Colley *et al.*, 1999). For that reason, the synergy of high pH and DO concentrations is very important for sunlight-mediated disinfection.

Noble *et al.* (2004) evaluated the effects that temperature, nutrients, total suspended solids and solar radiation had on total coliforms, *E. coli* and *enterococci*. Their results suggested that temperature and solar radiation had significant effects on disinfection rates. Through modelling, Mayo (1995) concluded that depth and solar radiation are the two most important factors influencing ThCB disinfection rate. On the other hand, he did argue that solar-mediated disinfection decreased in deeper ponds, leaving room for sedimentation to be considered a more dominant mechanism in deeper ponds.

E. coli are able to undertake photorepair in dark conditions, as revealed by Harm (1968), while Liltved and Landfold (1996) showed that this happens in a matter of minutes. Confirmed by Davies-Colley *et al.* (1999), dark photo repair occurs and some organisms can recover, although Sinton *et al.* (2002) and Kadir and Nelson (2014) considered that dark repair/disinfection is low for *E. coli* and has little impact for overall results. Mayo (1989) reached a surprising conclusion in dark repair tests, noticing that bacterial disinfection rates decreased with rising temperatures, although this contribution is also small in very shallow ponds. Simultaneous growth and disinfection rates explain this because growth rate is higher than the death rate in rising temperatures. Maïga *et al.* (2009a) research contradicts this theory, showing that dark *E. coli* disinfection increases in warmer seasons when compared to colder seasons, while Craggs *et al.* (2004) concluded that dark disinfection of *E. coli* accounts for 1/5 to 1/3 of the total disinfection.

4.3.5. Predation, starvation and competition (biological disinfection)

This mechanism is difficult to quantify, given that less work has been done in recent years when compared to the other mechanisms described above. On the other hand, scientists started investigating this mechanism in the 50's and 60's, proving to be an important mechanism for pond disinfection. The latest work on this mechanism was done by Vital, Hammes and Egli (2012).

Predation could be the second major disinfection mechanism in WSPs. In some cases could even be the most important, especially at times and places where sunlight exposure is low

(Shilton, 2005), therefore confirming Fernandez *et al.* (1992a,b) supposition that predation and competition are present and very important in WSPs for thermotolerant coliform bacteria disinfection. Mezrioui and Baleux (1992) observed an increase in disinfection when temperatures were higher and attributed it to an increase in predatory and lytic organism's activity in combination with an increase of toxic substances. Mayo and Noike (1996) confirmed that heterotrophic bacteria counts decreased because of an increase in competition at higher temperatures. Manage *et al.* (2002) showed that size-selective filtration or eukaryotic cell inhibitors, used to attenuate the role of microfauna, confirmed this mechanism to be important for disinfection. Davies and Bavor (2000) concluded that bacteria (ThCB, *enterococci* and heterotrophic bacteria) were protected from predators in pond systems by adhering to fine particles (clay). The authors also noted that predation is an important factor influencing bacterial survival.

Microorganisms compete over nutrients in wastewater, where some of them are considered pure predators and influence *E. coli* disinfection. Vital, Hammes and Egli (2012) considered that our knowledge on nutrient (organic matter included) competition is very limited. Gann *et al.* (1968) implied that coliforms are not capable of competing with other microorganisms for nutrients, even though *Chlorella vulgaris* algae can reduce heterotrophic bacteria growth due to competition for glucose (Mayo and Noike, 1996). Nutrients are important for the growth and survival of microorganisms that compete with coliforms, as shown by Atlas and Bartha (1981), Portier and Palmer (1989) and Mitchell, (1992). Interesting findings by Pearson *et al.*, (1987a), Almasi and Pescod, (1996) and Kaneko (1997) showed that high organic loads decreased pathogen removal in wastewater. This could be explained on the fact that high loads could decrease DO concentrations and therefore affect other disinfection mechanisms that depend on DO, or because of the nutrients, therefore decreasing competition for them amongst the microorganisms (Figure 4.12). Saqqar and Pescod (1992a, b) reached the same conclusion, showing that ThCB disinfection rates increased with decreasing BOD loads. Gameson and Gould (1985) revealed that starvation increased bacterial removal in the presence of low organic matter concentrations (20 mg/L), low light and predators.

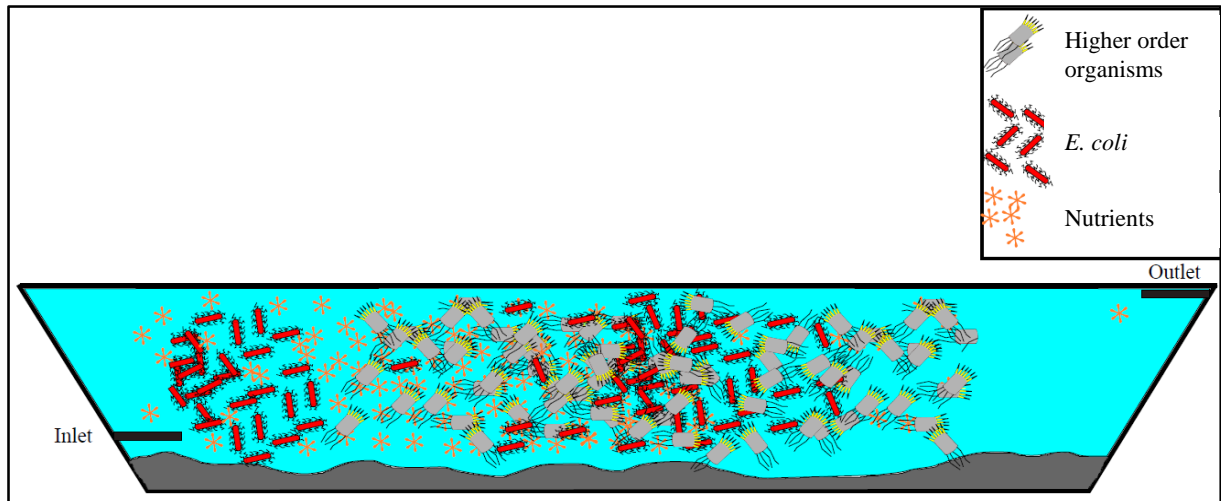
In an interesting study by Vital, Hammes and Egli (2012), the authors aimed at deepening the knowledge on the principles governing competition of enteric pathogens with natural bacterial flora (from drinking water) over nutrients from diluted wastewater. This was done by attributing

E. coli as the “opportunist”, specialised for growing at high nutrient concentrations, and the bacterial community as “gleaner”, more adapted to poor-nutrient environments. Results indicated that *E. coli* was able to flourish at low substrate concentrations in pure culture and also grow in competition with bacteria originating from poor-nutrient environments. On the other hand, *E. coli* was greatly restricted when in the presence of competing bacteria. The authors also considered temperature an important factor controlling heterotrophic growth and competition in the environment, making reference to the fact that *E. coli* growth is positively influenced by enhanced temperatures and for the first time elevated temperatures were shown to directly enhance enteric pathogen growth by increasing its competitive fitness.

When considering ThCB die-off rates, Klock (1971), Wu and Klein (1976) and Legendre *et al.* (1984) suggested that nutrient supply and competition for nutrients by the heterotrophic bacteria community should be taken in account. In fact, the addition of nutrients (e.g. glucose) and solutes (e.g. NaCl) increase bacterial survival under both dark and light conditions (Orlob, 1956; Van der Steen *et al.*, 2000).

Authors consider this mechanism as one of the most import of all the mechanisms (after sunlight-mediated disinfection), given that the effects for nutrient competition plays an important role in *E. coli* disinfection in pond systems. On the other hand, very little research about this mechanism has been done to fully quantify and understand its importance. Figure 4.12 shows that when there is an abundance of nutrients (inlet of the WSP), resulting in low penetration and competition because of the abundance of nutrients. As nutrient concentration decreases (towards the outlet of the WSP) predation of *E. coli* increases.

Figure 4.12 - Predation of *E. coli* by higher order organisms in the presence and absence of nutrients.



4.3.6. Algal toxins

Algae occur naturally in facultative and maturation ponds, with different species to occur during different seasons. Algae are important in any pond ecosystem because they produce oxygen at the expense of carbon dioxide, essential for aerobic organisms and species, and can cause biological disinfection. Pratt and Fong (1940) showed that *Chlorella vulgaris* produced toxins of long chain fatty acids when under stress and at high pH values which could affect the bacteria instead of the competition over glucose.

The effects of algae can vary from enhancing to protecting coliform growth from other mechanisms, like shielding from sunlight (Toms *et al.*, 1975) or having a bactericidal effect due to the toxins produced by them (Mezrioui *et al.*, 1994) (Figure 4.13), therefore varying the outcome on bacteria as shown by Mezrioui and Oudra (1998). Survival of *E. coli* in the presence of algal toxins is greater than that of *V. cholerae*, but in the presence of cyanobacteria the outcome is the opposite (Mezrioui *et al.*, 1994). The toxins which affected the different bacteria during the research were not identified unfortunately, but this should be recommendation taken in account when quantifying this disinfection mechanism. Interestingly, Mayo and Noike (1996) found that *Chlorella vulgaris* was responsible for heterotrophic bacteria reduction and attributed it to competition for glucose.

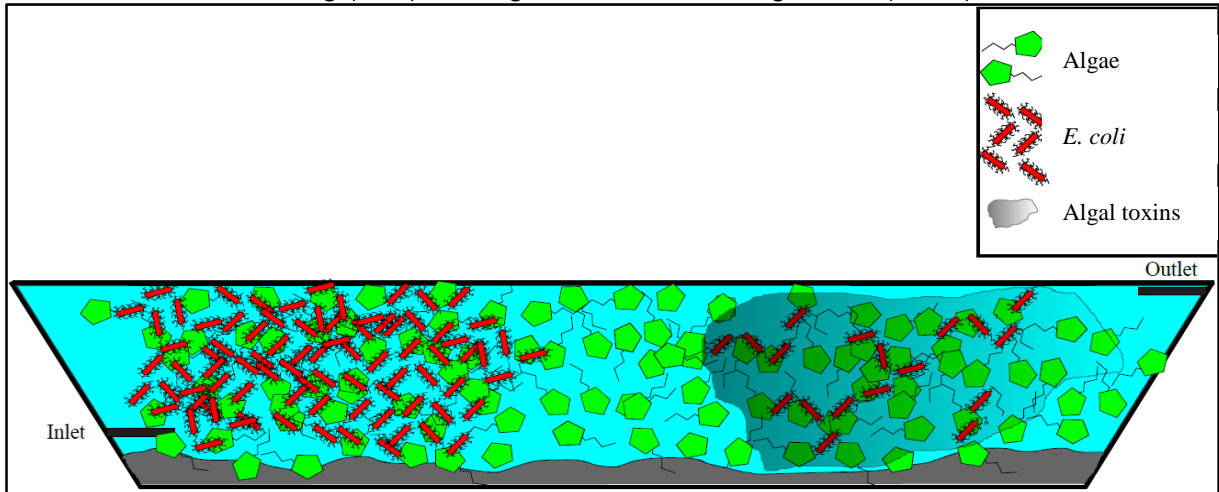
Toxin production could be initiated due to environmental changes or changes in the proportion of toxic strains (Kotut *et al.*, 2010). Araújo *et al.* (2016) found evidence that cyanobacteria were dominant in most of the seven WSP systems (facultative and maturation ponds in series)

analysed in Northeast Brazil, representing more than 60% of total algae composition. The authors noted that cyanobacteria concentrations decreased from facultative to maturation ponds and attributed it to less nutrients available in subsequent ponds in series, given that algae and cyanobacteria blooms are attributed to high temperatures and high nutrient availability (Paerl and Huisman, 2008). In fact, reducing nutrients (phosphorus (P) and nitrogen (N)) in ponds effectively reduces cyanobacteria biomass, especially N (Paerl and Otten, 2013). A previous research conducted in Brazil by Furtado *et al.* (2009) on a facultative pond showed that cyanobacteria and toxins were present in greater numbers, accounting for over 90% of the phytoplankton community during the summer and autumn months. In a more temperate climate, Esmoriz (North of Portugal), Vasconcelos and Pereira (2001) analysed the phytoplankton community in two ponds (facultative and maturation ponds) from January to July and found that cyanobacteria were regularly present in the ponds, ranging from 15.2% to 99.8% of the total phytoplankton community. All authors expressed concerns when cyanobacteria and their toxins were present, especially when discharging the final effluent into receiving waterbodies, but the toxins can prove to be detrimental towards *E. coli* and other bacteria as shown by Oufdou *et al.* (2001). Toms *et al.* (1975) and Mayo and Noike (1994) concluded that there was no indication that algae in ponds produced any bactericidal toxins.

One problem that arises is that algal populations in stabilisation ponds vary over time (Palmer, 1969) and toxins that some algae produce are pathogen selective. It is probably a good idea to identify algal groups in stabilisation ponds and determine their effect on microorganisms with other varying parameters (such as pH, DO, temperature, sunlight, etc.) as it is still unclear whether toxins are a major contributor for disinfection (Maynard *et al.*, 1999). The relationship N/P is an important factor for cyanobacteria growth (low N/P), but it is also important for chlorophytes (high N/P), so there is not necessarily a proliferation of cyanobacteria in ponds.

Figure 4.13 shows a WSP where at the inlet algae are protecting and enhancing *E. coli* growth from other mechanisms like sunlight or predation. Closer to the outlet, algae have produced toxins, in this case it could be cyanobacteria toxins which harmfully affects *E. coli*, therefore inactivating them.

Figure 4.13 - Algae protecting and inactivating *E. coli*: e.g.: sunlight-mediated protection with shading (inlet) and algal toxins inactivating *E. coli* (outlet).



4.3.7. Hydrodynamic factors influencing bacterial disinfection in ponds

Depth and hydraulic retention time (HRT) are key factors when designing pond systems as these physical attributes will influence overall disinfection mechanisms as shown below. Increasing length to breadth ratios will further enhance disinfection mechanisms as well as correct inlet and outlet structure.

4.3.7.1. Depth and hydraulic retention time

Pond depth is important because it influences overall performance regarding pathogen disinfection (Maynard *et al.*, 1999). Shallower ponds increase *E. coli* disinfection rates by remaining aerobic throughout the water column (higher DO and pH levels), consequently allowing for sunlight to better affect *E. coli*. On the other hand, for the same surface area, decreasing depth (H) will also reduce HRT, and could compromise the overall performance of the pond because the number of organisms removed during treatment is dependent on HRT (Oragui *et al.*, 1986). However, von Sperling (2005b), based on an evaluation of coliform removal in 186 ponds around the world, stated that the decrease in depth, even though it reduces the HRT, was compensated by higher coliform disinfection coefficient values. Maïga *et al.* (2009b) recommended a minimum depth of 0.4 m to increase disinfection efficiency while not affecting performance. This avoids also increased land costs, allows for easier construction of shallower embankments, and reduces the risk of macrophytes colonisation and sludge disturbance by the wind (Shilton, 2005). Mayo (1989) noticed that the mortality rate of ThCB was higher near the surface of a pond and decreased as depth increased. This conclusion was shared by Agunwamba (1991), Pearson *et al.* (1996) and Maïga *et al.* (2009a), who reported a

decrease in bacterial disinfection in deeper WSPs. However, as shown by Maïga *et al.* (2009a), *E. coli* disinfection rates in deeper microcosms were the same in cold and warm seasons in Burkina Faso, probably due to low pH and DO variation. Improving the uniformity of the effluent by increasing HRT does not necessary result in better disinfection efficiencies. Raising the water table increases HRT and negatively affects ThCB removal efficiencies (Pearson *et al.*, 1996). The only other way would be to use more land in order to maintain shallow depths and high HRT (Oragui *et al.*, 19870, therefore increasing disinfection (Rangeby *et al.*, 1996). Nevertheless, even when HRT in a pond is low, ThCB disinfection is still high, suggesting that other mechanisms could be playing a part in disinfection (Troussellier *et al.*, 1986).

WSPs should be designed to operate with optimal HRT and depth in order to treat more wastewater while using less land. In contrast, the HRT required for *E. coli* disinfection differs from place to place, as shown by Grimason *et al.*, (1996a, 1996b). Consequently, disinfection times could vary from place to place due to wastewater characteristics, overall temperature, rainfall, sunlight exposure, etc. Ideally, finding a relationship between HRT and depth (H) for optimal disinfection efficiency will improve pond systems while allowing to save on land requirements. Obviously, each place is different in each part of the world, needing special care when designing pond systems depending on meteorological data (temperature, weather, sunlight exposure, etc.).

4.3.7.2. Physical design and hydraulic behaviour

E. coli disinfection efficiencies are influenced by HRTs as discussed above. This dictates the time that microorganisms are in contact with various disinfection mechanisms. Considering pond configuration, namely length, width and depth, one should have in mind how they influence hydrodynamics and mixing (Shilton, 2005). As mentioned before, depth and HRT usually go hand in hand, where shallow depths imply shorter HRTs (considering the same surface area). On the other hand, shallow ponds in combination with sunlight exposure and long HRT are considered optimal (Davies-Colley *et al.*, 1999), but have a downfall of requiring large areas of land.

Maturation ponds in series are excellent for removing *E. coli* and perform better than a single pond with the same overall HRT. This is because ponds in series are more efficient for constituents that decay according to first-order kinetics, as is usually the case of coliforms. The length to breadth (L/B) ratio is another important factor to account for and if not considered

could affect the effluent quality (e.g. short-circuiting), even when considering other design factors (Fadel, Barakat and Fadel, 2011). Baffles can reduce short-circuiting and improve *E. coli* disinfection (Shilton, 2001; Shilton and Harrison, 2003) by increasing the L/B ratio and forcing wastewater to follow a predetermined path in the pond. The flow approaches ideal plug-flow conditions by decreasing dispersion in the pond and considered the ideal regime for *E. coli* disinfection (Bracho, Lloyd and Aldana, 2009). Pearson *et al.* (1995) concluded that the importance given to physical parameters of ponds (e.g. increasing L/B ratios) is exaggerated because it does not improve disinfection. However, they concluded that very shallow maturation ponds (0.4 m) with short HRT produced better results for ThCB disinfection than deeper ponds with the same area.

The improper inlet and outlet structure placement and construction can cause short-circuiting and blocking of the structures (embankment failures due to poor compression) (Fadel, Barakat and Fadel, 2011). Most inlet and outlet structures are placed at opposite ends and corners of ponds, but, even with this care, short-circuiting can occur (Shilton, 2005). It is recommended that the inlet structure should be placed at the bottom of the pond and the outlet structure close to the top of the water surface. This way, *E. coli* bacteria enter into the pond close to the bottom and can be incorporated faster into the sludge layer. By having the outlet structure at the surface of the pond, the effluent can be of a better quality since the surface layers receive more sunlight exposure, therefore promoting greater disinfection (Shilton, 2005).

Hawley and Fallowfield (2016) showed that increased solar exposure to wastewater is possible in any pond system by including the pond walls (inclined embankments) to increase the area available exposure and consequently disinfection. Wastewater trickles down the inclined embankments of the pond [high rate algal pond (HRAP) laboratory model and a pre-existing HRAP], therefore allowing for initial solar exposure opposed to the traditional inlet structure. Disinfection presented mixed results, but the authors concluded that this method should not be dismissed and further investigation is needed.

4.3.8. Summary of disinfection mechanisms affecting *E. coli*

Table 4.4 summarises the disinfection mechanisms for disinfection route and characteristics.

Table 4.4 - Summary of disinfection mechanisms, disinfection routes and characteristics.

Disinfection Mechanism	Disinfection Route	Characteristics
<u>Temperature</u>	<i>45 °C thermal shock for Coliforms.</i>	<ul style="list-style-type: none"> - Secondary factor generated from solar radiation; - Influences disinfection rates, higher temperatures, higher disinfection rates; - 1st design equation based on temperature; - <i>E. coli</i> counts are statistically well correlated to temperature.
<u>Attachment and Sedimentation</u>	<i>Attachment to larger objects (organic matter, algae, etc....) followed by sedimentation and eventually disinfection.</i>	<ul style="list-style-type: none"> - Second most important disinfection mechanism in primary pond units (facultative and maturation), first if solar radiation is not present; - <i>E. coli</i> cannot settle under their own weight, but if attached to larger objects they can; - Protection is granted from other mechanisms (solar radiation and predation) in ponds with low HRT and with low solar radiation exposure; - Could reduce the efficiency of biological disinfection by protecting bacteria from predators; - Disinfection is usually greater in the first ponds of any series.
<u>Dissolved Oxygen and pH</u>	<i>DO on its own does not cause disinfection; pH values need to be high (over 9.0) to cause disinfection on its own.</i>	<ul style="list-style-type: none"> - High concentrations of DO and pH in ponds promote an ideal environment for <i>E. coli</i> disinfection; - DO can reach concentrations over 30 mg/L; - DO is not statistically well correlated to <i>E. coli</i> disinfection; - pH values can be as high as 9.4. In some cases, 10 has been reported; - pH values as high as 10 can reduce <i>E. coli</i> by 8 logs in 15 seconds; - WSPs in tropical countries perform better than WSPs in temperate countries due to a combination of high pH values and high temperatures; - pH is statistically well correlated to <i>E. coli</i> concentration.
<u>Sunlight-mediated disinfection</u>	<i>Causes damage to DNA, DNA repair mechanisms and bacterial cell membranes</i>	<ul style="list-style-type: none"> - Most important disinfection mechanism for facultative and maturation ponds; - Percentage of radiation arriving at the surface at noon approximately: PAR: 50%; UV-A: 5%; and UV-B: 0.2%; - The UV spectrum attenuates the most when compared to PAR (UV is more bactericidal than PAR); - Downfall for wavelengths attenuating in ponds because of optical conditions; - Presence of high concentrations of DO and pH further enhances disinfection.

Disinfection Mechanism	Disinfection Route	Characteristics
<u>Sunlight-mediated disinfection</u>	<i>Mechanism 1 – direct photobiological damage (wavelength 290 – 315 nm)</i>	<ul style="list-style-type: none"> - Photobiological disinfection performed exclusively by UV-B; - Direct damage; - Limited to the first few centimetres in depth; - Targets DNA; - Repair can occur to DNA because of low UV dosages.
	<i>Mechanism 2 – indirect endogenous photooxidation damage (wavelength 290 – 400 nm) (400 – 700 nm?)</i>	<ul style="list-style-type: none"> - Endogenous photooxidation performed by UV-B (UV-A?) in combination with O₂; - Presence of internal photosensitisers; - The presence of O₂ is essential for this mechanism to occur; - Dominant disinfection mechanism for <i>E. coli</i>; - PAR participation is still unclear; - Indirect damage; - Occurs within the bacteria; - Targets DNA and DNA repair mechanisms.
	<i>Mechanism 3 – indirect photooxidation exogenous damage (wavelength 300 – 700 nm)</i>	<ul style="list-style-type: none"> - Exogenous photooxidation performed by UV-B, UV-A and PAR in combination with humic substances and smaller particles and O₂; - Presence of external photosensitisers; - Virtually the whole spectrum (UV-B; UV-A and PAR); - <i>E. coli</i> disinfection is limited through this mechanism; - Indirect damage occurs on the outside of the bacteria; - Targets cell membranes of bacteria's.
<u>Dark disinfection/repair</u>	<i>Dark conditions/absence of solar radiation</i>	<ul style="list-style-type: none"> - Disinfection or repair of <i>E. coli</i>; - Not in agreement in academia; - Low contribution for total disinfection (up to 1/3);
<u>Predation, starvation and competition</u>	<i>“Natural disinfection”</i>	<ul style="list-style-type: none"> - 2nd most important disinfection mechanism after passing the 1st pond in series, because nutrient concentration decreases in the following ponds (applicable if there are ponds in series); - Nutrients are vital for survival; - <i>E. coli</i> is not capable of competing for nutrients with other bacteria; - An abundance of nutrients reduces <i>E. coli</i> disinfection (low predation); - Low quantities of nutrients increases <i>E. coli</i> disinfection (high predation).
<u>Algal toxins/protection</u>	<i>Excreted toxins; Protection offered.</i>	<ul style="list-style-type: none"> - Cyanobacteria toxins are present in wastewater ponds and could be more of problem when discharging into waterbodies than for bacterial/pathogen disinfection; - Considered to have no effect on <i>E. coli</i> since it is unclear to what extent damage is caused as an isolated disinfection mechanism; - Protection could be offered to <i>E. coli</i> from other disinfection mechanisms – shading from solar radiation or hiding from higher forms of organisms (predation);

Disinfection Mechanism	Disinfection Route	Characteristics
<u>Algal toxins/protection</u>	<i>Excreted toxins; Protection offered.</i>	- Algal populations change throughout the year in ponds, complicating quantification of this disinfection mechanism seen that toxins could be selective on which bacteria they target.
<u>Physical design</u>	<i>Will dictate disinfection rates</i>	- Important for disinfection performance in ponds; - Ponds in series produce better disinfection efficiencies compared to a single pond with the same overall HRT as the ponds in series; - Ponds in series arrangement reduces short-circuiting - Each pond system should be designed according to the characteristics of the area in which it will be treating wastewater.
	<i>Depth, HRT and inlet/outlet structure placement; A favourable environment is formed within shallow ponds with optimal HRT and proper placement of inlet/outlet structures.</i>	- Shallow ponds produce better results for <i>E. coli</i> disinfection when compared to deeper ponds; - Shallow depths imply shorter HRTs; - Optimal depth should be around 0.40 m, promoting a long enough HRT for proper disinfection to occur; - Inlet/outlet structures should be placed opposite each other; - The inlet structure should be placed near the bottom of the pond to promote faster sedimentation, while the outlet structure should be at the top of the water level; - Inlet and outlet structures can be blocked by poor embankment compression.
	<i>Baffles, promoting longer actual mean HRT by forcing wastewater to travel a defined route.</i>	- Excellent intervention to increase true HRT without occupying more land with ponds; - Length to breadth (L/B) ratio is an important design factor to have in account since it affects the effluent quality; - Increases the uniformity of the effluent by approaching the plug flow regime; - Low cost intervention.
	<i>Pond walls to increase solar exposure</i>	- Improves solar radiation exposure to pathogens and increases disinfection; - Mixed initial results; - Virtually no intervention needed.

Table 4.5 presents the characteristics of the three main mechanisms of sunlight disinfection promoting disinfection in WSP's, as well as the inclusion of UV-A and PAR for mechanism 2 based on the literature review.

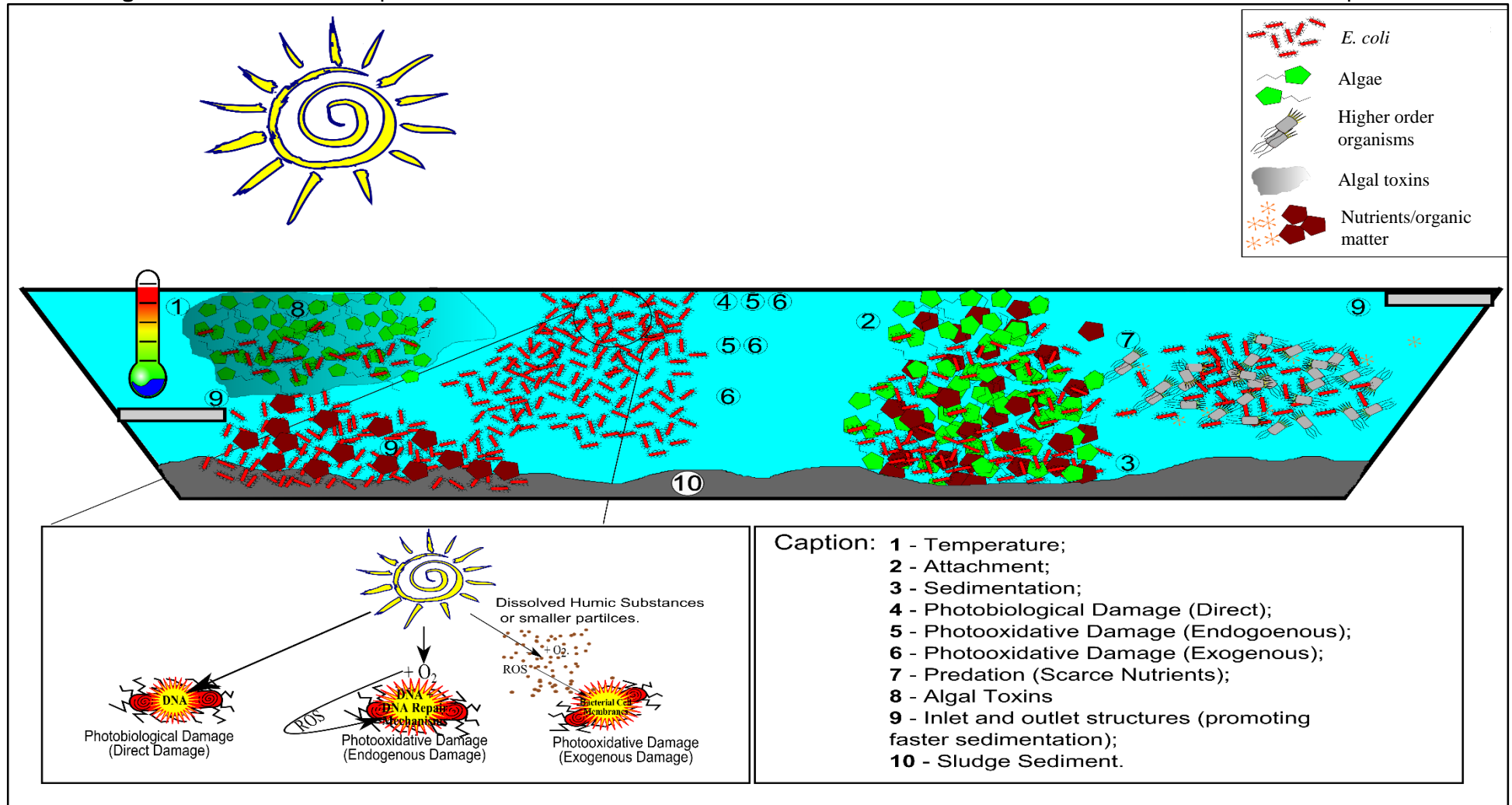
Sedimentation probably could be considered the second most important disinfection mechanism when considering the first pond of any series of WSP. This is because the amount of organic matter entering the first pond is greater than the amount entering subsequent ponds

of the series. As organic particulate matter and settleable suspended solids reduces, this mechanism loses its influence and therefore predation takes over as the second most important disinfection mechanism. Nutrient concentrations in the ponds after the first pond in series is much lower, consequently promoting predation. Both of these mechanisms could be considered the second most important for disinfection, especially for ponds in series. Figure 4.14 presents together all the removal mechanisms described above (except DO and pH influence on their own), as well as the inlet and outlet factor.

Table 4.5 - Characteristics of the three main mechanisms of sunlight disinfection promoting disinfection in WSP's (Adapted: SHILTON, 2005). *proposed inclusion due to recent research).

Mechanism	Contributing Wavelengths (nm)	Absorbed by	Primary target	Oxygen dependence	pH dependence	Repairable
1.Photo-biological damage	290-320 (UV- B)	DNA	DNA	-	-	X (bacteria)
2.Photooxidative damage (internal) – primary route for disinfecting <i>E. coli</i> *	290-320 (UV-B) + 320-400 (UV-A*) + 400-700 (PAR*)	DNA (+ other cell constituents?)	DNA	X	-	X (bacteria)
3.Photooxidative damage (external)	300-500 (UV-A + PAR)	Humic Organic Solids	Cell membrane, Capsid proteins?	X	Some bacteria (including <i>E. coli</i>)	-

Figure 4.14 – Schematic representation of the various disinfection mechanisms for *E. coli* disinfection in waste stabilisation ponds.



4.4. Pond arrangement, depth and HRT for *E. coli* disinfection

Choosing the number of ponds, type of ponds, depths and hydraulic retention times (HRT) depends on the desired final effluent quality. Land usage is also an issue because ponds require large areas of land to be implemented. Anaerobic and facultative ponds are good for removing biochemical oxygen demand (BOD), but not so good for pathogen disinfection. The best solution for natural wastewater disinfection are maturation ponds.

Pond systems can be arranged as a standalone treatment unit (single pond), in parallel or in series. Ponds in series are capable of achieving better removal efficiencies than a single pond with exactly the same overall HRT (Liu, Hall and Champagne, 2015).

A standalone system can consist of a single facultative pond for primary treatment, discharging the final effluent into a waterbody (Figure 4.15). This solution is good for BOD removal with efficiencies as high as 85%, but rather low coliform removal (99%) (von Sperling, 2007). Land requirement for this type of system is high, varying from 2.0 to 4.0 m²/inhab.. A setup comprised of an anaerobic pond followed by a facultative pond (Figure 4.16) is a good alternative to the standalone facultative pond system and requires less land (1.5 to 3.0 m²/inhab.). Most BOD is removed in the first pond, while remaining organic matter is further stabilised in the facultative pond. Yet again, coliform removal is just as low as the standalone system, reaching a removal efficiency of 99% (von Sperling, 2007).

Figure 4.15 - Standalone treatment system comprised of a facultative pond (von Sperling 2007).

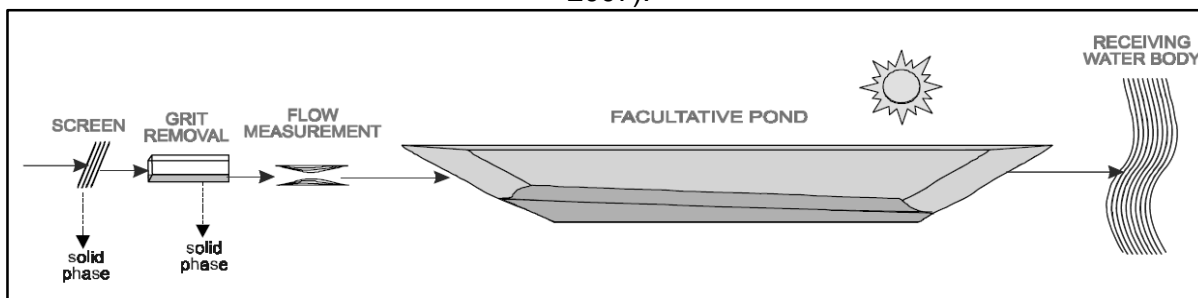
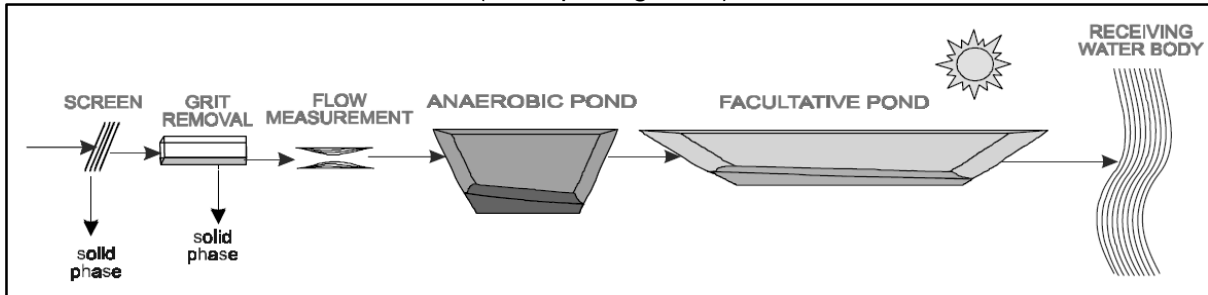
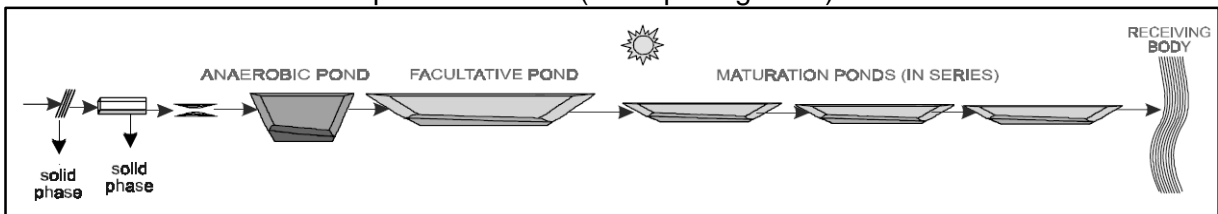


Figure 4.16 - Treatment system comprised of an anaerobic and facultative pond in series (von Sperling 2007).



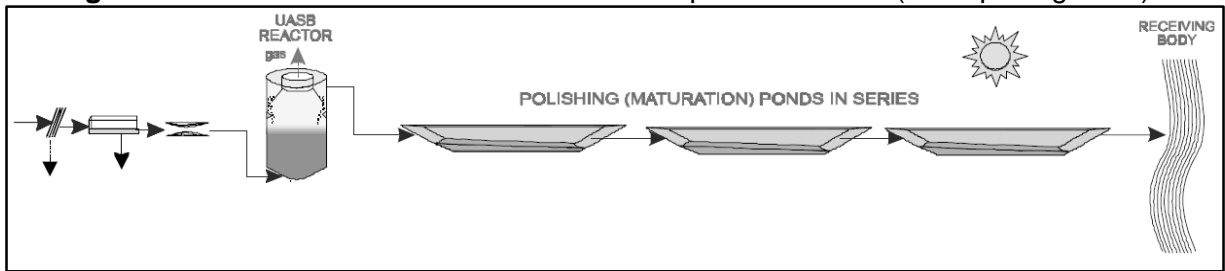
Maturation ponds are the ideal option for removing *E. coli* from the preceding ponds which have BOD removal as their main objective. Their shallow depths allow for high removal efficiencies of pathogens (up to 99.999%). Depth (subsection 4.3.7.), is an important factor for pathogen disinfection because it influences overall performance in maturation ponds. Shallower ponds increase *E. coli* removal by staying aerobic throughout the water column. On the other hand, for the same surface area, reducing depth will also reduce HRT and compromise the overall performance of the system. A system comprised of an anaerobic pond, a facultative pond and one or more maturation ponds, all in series (Figure 4.17), guarantees effective BOD and *E. coli* removal. The required land for implementing the system is probably the biggest obstacle.

Figure 4.17 - Treatment system comprised of an anaerobic, facultative and maturation ponds in series (von Sperling 2007).



To save on land requirement, maturation ponds can follow an anaerobic treatment unit such as a UASB reactor, removing most of the organic matter before entering the maturation ponds for disinfection (Figure 4.18). This setup is easier to implement than a setup composed of only ponds for treating wastewater.

Figure 4.18 - UASB reactor followed maturation ponds in series (von Sperling 2007).



Leite *et al.* (2009) evaluated a system in Brazil composed of one facultative pond and three maturation ponds in series. It had an overall HRT of 10 days even with shallow depths in the maturation ponds (0.44 m and 0.57 m). Overall removal efficiency was 3.8 logs for ThCB and considered low to other systems with shorter HRT.

Gonçalves *et al.* (2009) evaluated a treatment line in Brazil composed of a UASB reactor and one maturation pond in series. Overall removal efficiencies for ThCB were 92.2% during the summer months and 87.8% during the winter months, even with a high HRT (12.5 days) and shallow depth (1.0 m). Removal efficiencies were considered low when compared to other setups with more ponds in series and shorter overall HRT. An infinite number of ponds in series, in theory, could produce a plug flow regime (flow acts the same way as a piston, where no longitudinal mixing occurs), therefore increasing the removal efficiencies for constituents that follow first-order kinetics, such as *E. coli* (von Sperling, 2007). Having a single pond acting as a polishing unit after an anaerobic unit will not produce the desired bacteriological results. Four shallow maturation ponds in series reached a disinfection efficiency of 4.7 log units for *E. coli* until the third pond. The effluent from the third pond was already capable for unrestricted irrigation, whereas the fourth pond did not contribute for further disinfection (Bastos *et al.*, 2010, 2011). Von Sperling and Mascarenhas (2005) tried different HRT in a treatment line composed of a UASB reactor followed by four maturation ponds in series treating wastewater in Brazil. Results were excellent for BOD and *E. coli* removal. The ponds operated with very low HRT (1.4 to 2.5 days in each pond) and depths ranged between 0.65 m and 0.40 m. The effluent complied with the WHO guidelines for unrestricted irrigation (geometric mean less than 1000 MPN/100mL) even when the overall HRT was as low as 7.4 days. This was also reported by Dias *et al.* (2014) in a similar system composed of UASB reactor, three maturation ponds in series and a rock filter placed in the final third of the last pond. Removal efficiency of *E. coli* was excellent (5.7 log). Shallow depths (0.40 m to 0.80 m) and low HRTs (0.8 and 6.0 days) for individual units were also evaluated. The authors recommend shallow depths and low

HRT in each unit to produce a high quality final effluent, compatible with unrestricted irrigation. Ponds from both treatment setups operated sometimes below the minimum 3 day recommendation by Mara (2003), but still performed very well.

Bastos *et al.* (2010) reported that to achieve an effluent quality suitable for restricted irrigation, following the WHO guidelines, overall HRTs should be at least 10 days. For an effluent suitable for unrestricted irrigation, following the same guidelines, ponds should have an overall HRT of at least 17 days. The latter overall HRT is common in WSP setups, and by combining a favourable environment for disinfection, it is considered the main factor for producing a high quality effluent (low concentration of *E. coli*), suitable for reuse in agricultural irrigation (Mara, 1996).

Bastos *et al.* (2010) after compared four maturation ponds in series with four horizontal flow constructed wetlands (HFCW) treating UASB reactor effluent. Ponds HRT and depth varied between 4.1 and 9.4 days, and 0.4 and 0.9 m, respectively. *E. coli* disinfection was similar in both pond and wetland treatment lines, achieving efficiencies between 4 - 4.5 log units. The authors concluded that although disinfection efficiencies were similar, they were much less stable in the wetlands. This could be because of different disinfection mechanisms taking place in the wetlands and the absence of sunlight-mediated disinfection. Von Sperling *et al.* (2010) agreed and highlighted that disinfection occurs in all ponds in series and reinforces the role of solar radiation.

Moumouni *et al.* (2015) showed in a pilot scale baffled pond (1.05 m) in Burkina Faso that *E. coli* was not detected up to 0.60 m in depth, but it was deeper on. This shows the limitation that deeper depths can have on disinfection, allowing for bacteria to survive at deeper depths and not to be affected by solar radiation if other disinfection mechanisms do not intervene. Da Costa, Gomes and Filho (2011) showed the importance of not overloading shallow ponds (0.5 m) with too many solids in order to favour sunlight penetration. The research highlights the necessity of controlling influent loads in ponds, especially maturation ponds in order to promote photosynthesis and disinfection processes. Therefore, pre-treatment units that remove a major part of the solids is recommended before maturation ponds. A UASB reactor can perform this task and avoid organic waste overloading in ponds.

Summing up, *E. coli* disinfection depends on a number of factors such as HRT, depth, number of ponds in series, the primary treatment applied and pond conditions (aerobic). These systems can perform very well and are very robust. They are cheap to construct and run, but poor planning and ill upkeep can cause them to be a nuisance. Consequently, they can cause serious problems to communities if the final effluent is treated poorly and discharged into waterbodies or used for other practices, such as irrigation and fish farming. *E. coli* removal efficiencies are also affected by seasonal patterns, implying that location and climate affect disinfection, therefore increasing the difficulties when treating wastewater with natural systems like ponds (Liu, Hall and Champagne, 2015). This should also be taken into consideration when planning pond systems.

4.5. Baffles to increase *E. coli* disinfection

As shown in subsection 4.4, maturation ponds in series are an excellent option for inactivating *E. coli*. Baffles (divisions) in ponds are an excellent option to increase actual mean HRT while not increasing land requirement. The most common setup is applying baffles perpendicular to the pond's length, therefore reducing short-circuiting and increasing actual HRT (the theoretical HRT remains the same) by creating a zigzag pattern for wastewater to flow. Baffles running parallel to the pond's length are an alternative way and create channels in the pond. The length/breadth (L/B) ratio increases dramatically (the L/B ratio also increases with perpendicular baffles), therefore approaching plug flow and reducing short-circuiting. Baffles are commonly employed to reduce occurring short-circuiting in ponds, and according to first order kinetics, the removal efficiency increases because it approaches plug flow. Depth is important to have in account, since increases in depth for a given breadth tend to increase dead volume fractions in dead zones (Thackston, Shields and Schroeder, 1987). James (1988) considered that short-circuiting in ponds produced a negative effect for *E. coli*/pathogen disinfection, verifying that the final effluent was leaving the pond only one day after entering. If this proportion leaving the pond could remain in the pond for at least two days, the bacterial concentration in the final effluent could be reduced by 40%. Baffles seek to improve disinfection by promoting three purposes:

- approach the plug-flow regime (important for using first-order kinetics);
- reduce dead zones (approach actual HRT to theoretical HRT);

- and reduce short-circuiting.

Baffles are much easier to install in existing pond units than modifying the inlet/outlet position of a pond or building another pond in series, although uncertainty arises on the number and position of the baffles to include in the system.

Shilton (2001) investigated the ideal length for baffles in ponds, concluding that baffles running 70% the width of the pond produced the best results for bacterial disinfection, while other lengths were either too short (50%) or too long (90%). This was verified with computational fluid dynamics (CFD) and is also valid for baffles running the pond's length. Equally, Olukanni and Ducoste (2011) also used CFD modelling to determine the ideal length and configuration of baffles, contradicting Shilton's (2001) findings. The best configuration for Olukanni and Ducoste (2011) are two baffles running 90% the length of the pond, and not the width. The CFD programme was able to predict over 5 log unit reduction for ThCB. Although these results are promising, they still need to be tested against real WSP treating real sewage. Thackston, Shields and Schroeder (1987) recommended that baffles should be 75% the length of the parallel basin side, which is in accordance with Shilton's (2001) findings.

Bracho, Lloyd and Aldana (2006) modified a maturation pond's L/B ratio from 9:1 to 79:1 with two baffles running the length of the pond. Through tracer tests (rhodamine) the authors verified a decrease in the dispersion number (d) from 0.37 (dispersed flow), to 0.074 (plug flow), corresponding to an 89% reduction, approaching the plug flow regime (Bracho, Lloyd and Aldana, 2009). Actual HRT (39.35 hours) increased 5 hours when compared to the previous setup without baffles (HRT= 34.66 hours), therefore exposing bacteria to the environment in the pond for longer periods.

Kilani and Ogunrombi (1984) also verified a decrease in the dispersion number by progressively applying baffles perpendicular to the length of laboratory-scale facultative ponds. 9 baffles produced a $d = 0.096$, very close to that verified by Bracho, Lloyd and Aldana (2006, 2009). Kilani and Ogunrombi (1984) considered – *“In order to compare these favourable laboratory results with actual field tests, it is recommended that when ponds are constructed in the future, provision should be made for large scale operating data to be obtained by providing at least one cell with facilities for studying the effect of inserting baffles”*. This recommendation is important in order to understand better the influence and enhancement baffles can provide

when treating real wastewater, because it is very easy to reach desired results in a controlled environments opposed to an environment not controlled.

According to Thackston, Shields and Schroeder (1987), hydraulic efficiency (t/T , or actual mean HRT divided by theoretical HRT) can be improved by increasing the L/B ratio, and reducing the effect of wind and depth. L/B ratios of 5-10 are sufficient and above these values little improvement for hydraulic efficiency is achieved. This led to the conclusion that plug flow is impossible to achieve in practice. On the contrary, Bracho, Lloyd and Aldana (2006, 2009) with a L/B ratio greater than 10 induced plug flow and better hydraulic efficiency. Thackston, Shields and Schroeder (1987) recommended floating baffles should be considered because they are easy to transport and remove, use little volume in the pond and can be easily applied. James (1988) concluded that if plug flow were able to be induced without changing the HRT, then bacterial disinfection would improve from less than 90% to theoretically 99.99%. James (1988) commented that configurations inducing plug flow are more efficient than completely mixed configurations for bacterial disinfection.

Lloyd, Vorkas and Guganesharajah (2003) applied four different sequential interventions on a treatment line consisting of an anaerobic and facultative pond system. The first intervention consisted in annexing a maturation pond (depth = 1.1 m and L/B = 4:1). This intervention only achieved a disinfection efficiency of 90.26% for thermotolerant coliforms, concluding that short-circuiting was the culprit for poor performance. The standalone maturation pond of the treatment line was only able to reduce ThCB by 90%. Tracer studies showed that mean HRT was only 1.07 days, again supporting the short-circuiting theory. The dispersion number (d) was 0.79. The second intervention consisted in inserting two baffles running 94% the length of the maturation pond, increasing the L/B from 4:1 to 35:1. Thermotolerant coliforms disinfection efficiency increased from 90.36% to 96.03%. Tracer studies showed the overall HRT increased from 1.07 days to 1.25 days. The dispersion number was not mentioned or calculated. The third intervention consisted in using top baffles in the gap between the pond and the baffle, with a 10 cm freeboard in an attempt to reduce the effect of high surface and subsurface velocities on short-circuiting. This intervention did not improve ThCB disinfection and performance efficiency was reduced from 96.03% to 92.64%. The fourth intervention consisted in using wind breakers around the pond to reduce wind effect. Thermotolerant coliform disinfection

efficiency increased from 96.03% (baffled) to 98.13%, a 2.10% increase. Tracer tests showed actual HRT increased from 1.25 days to 1.86 days with this intervention.

The authors concluded that increasing L/B ratios with baffles increased mean HRT and would definitely enhance thermotolerant coliform disinfection efficiency. Combining baffles with wind breakers would further improve disinfection performance and increase HRT, possibly leading to plug flow in a shallow channel. Then again wind could be very important seen that it could induce gentle mixing. Lloyd, Vorkas and Guganesharajah (2003) also advert to the fact that baffles do not necessarily improve thermotolerant coliform disinfection performance, as their design requires further care and evaluation.

Moumouni *et al.* (2015) produced excellent results for *E. coli* disinfection in a pilot sized scale wastewater treatment system comprised of a two stage anaerobic reactors feeding a pond with three vertical baffles made from recycled plastic media for attached growth and a control pond in parallel in Burkina Faso. Both the ponds were 1.05 m deep. At the outlet of the baffled pond, *E. coli* was not detected (<1.0 per 100 mL), while at the outlet of the control pond *E. coli* concentrations were on average 4000 per 100 mL. The authors attributed the excellent results to the baffles because they increased HRT and allowed for attached growth, therefore enhancing disinfection when compared to the control pond

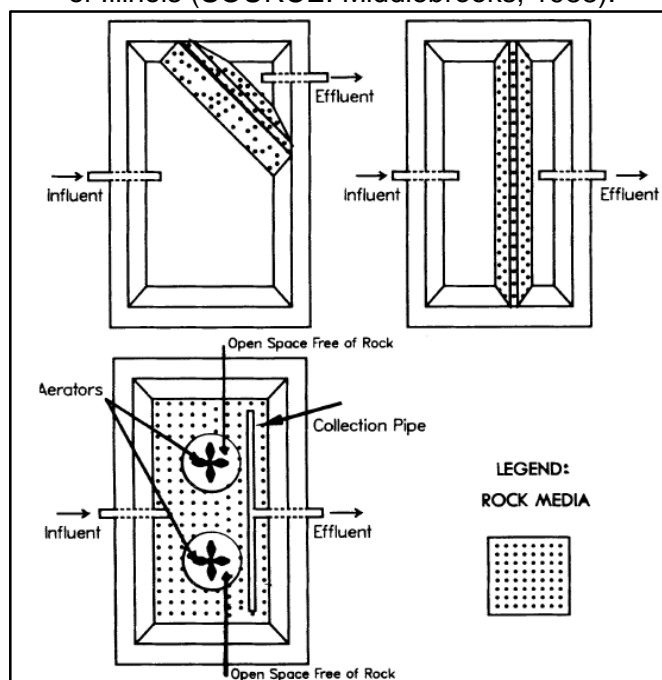
This type of intervention increases actual HRT and affects ThCB disinfection efficiency positively while saving on land requirement. It is a low-cost upgrade where virtually no maintenance is needed. However, special care is needed because baffles do not essentially prevent the formation of dead zones, and planning the gap between the pond and the baffle is considered key to improve hydrodynamics. Using the correct distance will prove to be important in order to maintain disinfection efficiency up to standard. Other hydraulic interventions, such as freeboards placed on the surface of the pond, supposedly reduce the effect of different flow velocities in the pond due to different temperatures. This could increase disinfection, but needs further research to determine the depth they should be placed to have a positive effect. Wind breakers are also another intervention which could reduce mixing caused by wind and therefore increase disinfection.

4.6. Discharging the final effluent into waterbodies: concerns

One of the problems that arises with maturation ponds is the need to control algae in the final effluent. Although excellent performance is achieved for bacterial disinfection through various mechanisms (subsections 4.1, 4.3 and 4.4), organic matter in the form of algae, quantified as total suspended solids (TSS), is discharged into the environment at high concentrations. When discharged into the receiving waterbody, algae usually die, settle, decay and consequently increase oxygen demand. Investigations and research has arisen due to the concern about the relationship between decay and oxygen consumption in waterbodies and how to reduce the amount of algal bio mass discharged (Crites *et al.*, 2014). Tom *et al.* (1975) studied algae growth rates over a period of 18 months in a full-scale polishing pond treating activated sludge effluent, concluding that with a HRT lower than 2.0 d algal growth would not become a problem in the receiving basin. With HRTs greater than 2.5 d in the pond, TSS increased and consequently caused problems to the receiving waterbody.

Rock filters as a final step after maturation ponds are a very good method to reduce algae concentration and also known as a polishing stage (maturation ponds proceeding other units are also known as polishing ponds). The pond effluent passes through the void spaces in a submerged porous rock bed, causing algae to adhere and settle to the media and consequently degrade biologically (Crites *et al.*, 2014) and form sludge which could clog the unit. Rock filters are not a new type of technology and have been installed and studied extensively throughout the world, especially in the United States (USEPA 1983; Adam 1986; Middlebrooks 1988; and Saidam *et al.* 1995). Examples of rock filters applied in Illinois are shown in Figure 4.19 (Middlebrooks 1988). The main advantages of rock filters are low construction costs opposed to other filtration systems such as biodiscs or trickling filters, and simple operation. The disadvantages are odour problems that occur due to the nature of the unit (anaerobic decay) and the lifespan and cleaning of the filters. Nonetheless, several units have been in operation for over 20 years and no problems have arisen (Crites *et al.* 2014).

Figure 4.19 - Rock filter designs from the State of Illinois (SOURCE: Middlebrooks, 1988).



A rock filter inserted in the final third of the last pond of a system comprised of a UASB reactor and three ponds in series (same treatment system investigated in the current research, but before the adaptations) was able to reduce BOD, COD and TSS by 7%, 22% and 58%, respectively during the warmer months, providing complementary polishing of the effluent before discharging into a waterbody (Dias *et al.*, 2014). Surprisingly, complementary *E. coli* removal was also accounted for in the rock filter, with 0.9 log reduction during the warmer months, suggesting that mechanisms like attachment and predation are present within these filters. HRT in the rock filter was often very low (0.8 to 2.5 d).

4.7. Quantifying bacterial disinfection in waste stabilisation ponds

This section will concentrate first on hydraulic models used in the pond designs, a crucial step for the project engineer. The dimensions of the pond (length, breadth and depth) depend on the expected final concentration of *E. coli*. A disinfection/die-off coefficient (K_d) for *E. coli* is used to quantify disinfection rates. Disinfection coefficients incorporating different parameters by numerous researchers are presented from different time periods. Some of these equations are simple, while others prove to be difficult to use when considering pre-planning.

Mathematical modelling of bacteria in ponds is an important stage of any project. Final *E. coli* estimations are determined and usually modelled by first-order kinetics based on Chick's Law.

Maturation pond goals are to remove *E. coli*, therefore they are designed regarding the final estimated concentration of *E. coli* and represented by one of the following hydraulic models (von Sperling, 2007):


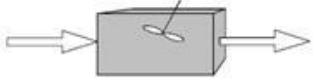
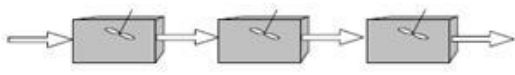

- **Plug-flow** – this flow model is used when fluid particles enter the reactor continuously at one end, travelling right through and discharged at the other end of the reactor in the same order as they entered. Therefore, no longitudinal particle mixing takes place and fluid flows just like a plug, maintaining its identity and remaining in the reactor for a period equal to the HRT. This type of flow is achievable when length/breadth (L/B) ratios are high. This is considered an idealised flow, since complete absence of longitudinal mixing is difficult to reproduce in practice.
- **Ponds in series** – this hydraulic model is applied when ponds are in series or when the hydraulic regime is considered between an idealised plug flow and a completely mixed reactor. An infinite number of ponds in series theoretically reproduces plug flow.
- **Dispersed flow** – this type of hydraulic model is used when a reactor has an intermediate degree of mixing between the idealised regimens of plug flow and completely mixed. Most reactors present this type of flow. Their modelling is considered more difficult compared to the other flow models and as a result the pattern is usually portrayed by either plug flow or completely mixed flow. Flow is considered continuous.
- **Complete mix or continuously stirred tank reactor (CSTR)** – this hydraulic model considers that particles enter the reactor and are immediately dispersed all over, meaning that the particles leave the reactor in proportion to their statistical population. This type of hydraulic model is also considered idealised because total and identical dispersion is difficult to reproduce in reality.

Choosing a hydraulic model depends on the hydraulic regime assumed by the project designer, where different regimes estimate different concentrations of *E. coli* in the final effluent (von Sperling, 2007). In other words, choosing the proper model for the project will translate into efficient performance of the treatment line.

Figure 4.20 depicts different equations for all four of the hydraulic patterns for estimating coliform concentrations. Best quality estimations are obtained when ponds approach plug flow or equal completely mixed cells in series. For design purposes, the dispersion number (d) for

dispersed flow can be estimated by the equations proposed by Polprasert and Bhattarai (1985) (Equation 4.1), Agunwamba *et al.* (1992) (Equation 4.2), Yanez (1993) (Equation 4.3) or von Sperling (1999) (Equation 4.4). Some of the equations are quite complex while others are simple to use. A more accurate way of determining the dispersion number can be through dye tracer tests (Thackston, Shields and Schroeder, 1987).

Figure 4.20 - Formulas for calculation of the effluent coliform concentration (N) for ponds (Source: von Sperling (2007)).

Hydraulic regime	Scheme	Formula for the effluent coliform concentration (N)
Plug flow		$N = N_o e^{-K_b \cdot t}$
Complete mix (1 cell)		$N = \frac{N_o}{1 + K_b \cdot t}$
Complete mix (equal cells in series)		$N = \frac{N_o}{(1 + K_b \cdot t/n)^n}$
Dispersed flow		$N = N_o \cdot \frac{4ae^{1/2d}}{(1+a)^2 e^{a/2d} - (1-a)^2 e^{-a/2d}}$ $a = \sqrt{1 + 4K_b \cdot t \cdot d}$

N_o = coliform concentration in the influent (org/100mL) t = detention time (d)
 N = coliform concentration in the effluent (org/100mL) n = number of ponds in series (-)
 K_b = bacterial die-off coefficient (d^{-1}) d = dispersion number (dimensionless)

For design purposes, the dispersion number (d) can be obtained by the following Equations (4.1), (4.2), (4.3) or (4.4):

➤ Polprasert and Bhattarai (1985)

$$d = \frac{0.184 \cdot t \cdot v \cdot (B+2H)^{0.489} \cdot B^{1.511}}{(L \cdot H)^{1.489}} \quad (4.1)$$

➤ Agunwanba *et al.* (1992), original formula simplified by von Sperling (2007)

$$d = 0.102 \cdot \left(\frac{B \cdot (B+2H) \cdot t \cdot v}{4 \cdot L \cdot B \cdot H} \right)^{-0.410} \cdot \left(\frac{H}{L} \right) \cdot \left(\frac{H}{B} \right)^{-(0.981+1.385 \cdot \left(\frac{H}{B} \right))} \quad (4.2)$$

➤ Yanez (1993)

$$d = \frac{\left(\frac{L}{B} \right)}{-0.261 + 0.254 \cdot \left(\frac{L}{B} \right) + 1.014 \cdot \left(\frac{L}{B} \right)^2} \quad (4.3)$$

➤ von Sperling (1999)

$$d = \frac{1}{(L/B)} \quad (4.4)$$

where,

- L – length of pond (m);
- B – breadth of pond (m);
- H – depth of pond (m);
- t – hydraulic retention time (d);
- ν – kinematic viscosity of the water ($\text{m}^2 \cdot \text{d}^{-1}$).

The kinematic viscosity of the water is calculated according to the temperature (T), where von Sperling (2007) proposed a correlation Equation 4.5 (for $T = 10$ to 30 °C; $R = 0.986$).

$$\nu = 0.325 \cdot T^{-0.450} \quad (4.5)$$

where,

- ν – kinematic viscosity of the water ($\text{m}^2 \cdot \text{d}^{-1}$);
- T – water temperature (°C).

The disinfection rate/coefficient (K_b) quantifies decay rates and influences *E. coli* concentration estimations. This is expected because all equations used for estimating the final concentration present a dimensionless product $K_b \cdot \text{HRT}$, which is an integral part of the concept. Literature has shown that coefficients vary a great deal (0.2 to 43.6 d^{-1} at 20 °C), because different coefficient values have been obtained supposing different hydraulic regimes, which are not always reported (von Sperling, 1999). Other factors also influence K_b , such as solar radiation, DO concentration, pH levels, BOD loading and of course the actual configuration of the pond and does not depend on the hydraulic regime. Depth is important for determining K_b , since shallower ponds produce higher K_b values. Von Sperling (2007) recommends that the combined effect of shallow ponds and low HRT (t) should be investigated.

E. coli concentration estimations (N) generally involve simple equations that only depend on the influent concentration (N_0), HRT (t), number of ponds in series (n), the dispersion number

(*d*) and the disinfection coefficient (K_b) (Figure 4.20). The disinfection coefficient can be expressed as a function of a few parameters or an array of parameters, such as depth (H), hydraulic retention time (t ; HRT), temperature (T), solar irradiance (S_0 ; I_r), light attenuation (K), organic matter (BOD_5), dissolved oxygen (DO) and pH (Marais, 1974; Sarikaya and Saatçi, 1987; Sarikaya, Saatçi and Abdulfattah, 1987; Qin *et al.*, 1991; Curtis, Mara and Silva 1992a; Saqqar and Pescod, 1992a; Mayo, 1995; von Sperling, 1999; von Sperling 2005; von Sperling, Bastos and Kato, 2005; von Sperling, 2007; Ouali *et al.*, 2014).

Many maturation ponds were designed based on Marais (1974) Equation 4.6 for completely-mixed conditions (Figure 4.20). It only considers N_0 , t , n and K_b for estimating the final concentration (N) and is water temperature dependent.

$$N = \frac{N_0}{(1+K_b t_f)(1+K_b t_m)^n} \quad (4.6)$$

where,

- N – *E. coli*/100 mL in effluent;
- N_0 – *E. coli*/100 mL in influent;
- K_b – first order *E. coli* disinfection rate/coefficient for the pond temperature (d^{-1});
- t_f and t_m – theoretical hydraulic retention time in facultative and maturation ponds respectively (d);
- n – number of maturation ponds.

Equation 4.6 assumes that the K_b value is the same for facultative and maturation ponds, which is not the case. There is big disparity between the predicted values using Marais (1974) Equation 4.6 and observed values, where measured counts can be 1.0 log unit or higher than the predicted counts (Buchanan *et al.*, 2011). Many WSPs designed with this equation underestimate the disinfection rate of ThCB, consequently leading to poor pond performance.

Simple equations to estimate the disinfection rate/coefficient (K_b) of *E. coli* with temperatures *in loco* in WSPs can be used by measuring the concentration of *E. coli* in the influent and effluent of a pond, or samples before and after an experiment, as well as exposure time (days/hours). This is similar to the equation presented by Marais (1974). Equation 4.7 estimates

the final concentration of *E. coli* for plug flow regime (Figure 4.20). Plug flow regime considers no horizontal mixing, only vertical mixing, and can also be used for estimating disinfection rates/coefficients in batch flow regimes (plug flow = batch flow). Equation 4.7 was rearranged from predicting the final concentration of *E. coli* for estimating K_b , as shown in the following steps and ending at Equation 4.10.

❖ First order *E. coli* disinfection rate/coefficient at temperature T for plug-flow regime.

$$N = N_0 \cdot e^{-K_b \cdot t} \quad (4.7)$$

$$\frac{N}{N_0} = e^{-K_b \cdot t} \quad (4.8)$$

$$\ln\left(\frac{N}{N_0}\right) = -K_b \cdot t \quad (4.9)$$

$$K_b = \frac{-\ln(N/N_0)}{t} \quad (4.10)$$

where,

- N – *E. coli* concentration in the effluent (MPN/100 mL);
- N_0 – *E. coli* concentration in the influent (MPN/100 mL);
- K_b – first order *E. coli* disinfection rate/coefficient (d^{-1}/h^{-1});
- t – Retention time (d/h).

K_b can be obtained through linear regression (Equation 4.9) with several pairs of N and t values or by Equation 4.10 based on exposure time and temperature that *E. coli* endured in the pond. Standardising the disinfection coefficient is essential for comparing with values from ponds in different areas of the world. This can be estimated by the first order kinetics Equation 4.11, based on the Arrhenius/van't Hoff function. Equation 4.11 is rearranged to estimate the disinfection coefficient for a standardised temperature of 20 °C (Equation 4.12).

❖ First order K_b equation for the *E. coli* disinfection rate/coefficient at 20 °C.

$$K_T = K_{20}[\theta]^{(T-20)} \quad (4.11)$$

$$K_{20} = \frac{K_T}{[\theta]^{(T-20)}} \quad (4.12)$$

where,

- T – average air/water temperature (°C);
- K_T – first order *E. coli* disinfection rate/coefficient at temperature T (d^{-1}/h^{-1});
- K_{20} or K_b – first order *E. coli* disinfection rate/coefficient at 20°C (d^{-1}/h^{-1});
- θ – temperature coefficient [considered 1.07 (Yanez, 1993) or 1.19 (Marais, 1974)].

Von Sperling, Bastos and Kato (2005), von Sperling (2005b) and von Sperling (2007) estimated K_b considering only depth (H) and mentioned that the combination of UV radiation, pH and DO are responsible for high coliform disinfection efficiencies in shallow ponds, accomplished with short HRT when compared to deeper ponds with longer HRT. For any surface area, short HRT is synonymous with shallow depths, therefore strongly associated with high pH and DO values. Von Sperling (1999) presented two models for estimating K_b based on 33 facultative and maturation ponds operating in Brazil. The first model is for dispersed-flow (Equation 4.13) considering depth (H) and HRT (t). The second model is for CSTR flow regime (Equation 4.14). This equation transforms the dispersed flow K_b value estimated in Equation 4.13 (better representation of the kinetics in a pond) into an idealised K_b flow value, in this case, completely mixed.

❖ First order K_b for *E. coli* disinfection rate/coefficient for dispersed-flow considering H and t (von Sperling, 1999)

$$K_b = 0.917 \cdot H^{-0.877} \cdot t^{-0.329} \quad (4.13)$$

❖ First order K_b for *E. coli* disinfection rate/coefficient for CSTR considering $K_{b(\text{dispersed})}$, t , L and B (von Sperling, 1999)

$$K_b = 1.753 \cdot K_{b(\text{dispersed})} + [0.0011 \cdot K_{b(\text{dispersed})}^{4.189} \cdot t^{3.189} \cdot (L/B)^{1.501}] \quad (4.14)$$

where,

- K_b – first order *E. coli* disinfection rate/coefficient (d^{-1}/h^{-1});
- H – depth (m);
- t – hydraulic retention time (d/h);

- $K_{b(\text{dispersed})}$ – dispersed flow *E. coli* disinfection rate/coefficient ($\text{d}^{-1}/\text{h}^{-1}$);
- L – length of the pond (m);
- B – width of the pond (m).

K_b values obtained experimentally and from pond inlet and outlet samples, are always associated with hydraulic models (plug flow, completely mixed, dispersed flow), bringing about imperfections of idealised regimes.

A very thorough evaluation on coliform disinfection in facultative and maturation ponds was undertaken by Von Sperling (2005b) in an attempt to produce a K_b estimation equation which could predict disinfection rates/coefficients for any pond in any part of the world. Acquired data from 186 ponds from all over the world, majority Brazilian, was used. Two K_b equations (4.15 and 4.16) for facultative and maturation ponds were presented considering dispersed-flow (Figure 4.20). Equation 4.15 is similar to Equation 4.13, considering also depth (H) and HRT (t). Equation 4.16 considers only H , simpler to use than the previous equations.

- ❖ First order K_b for *E. coli* disinfection rate/coefficient for dispersed-flow model considering H and t (von Sperling, 2005b) for *in situ* temperature.

$$K_b = 0.682 \cdot H^{-1.286} \cdot t^{-0.103} \quad (4.15)$$

- ❖ First order K_b for *E. coli* disinfection rate/coefficient for dispersed-flow model considering H (von Sperling, 2005b).

$$K_b = 0.549 \cdot H^{-1.456} \quad (4.16)$$

where,

- K_b – first order *E. coli* disinfection rate/coefficient ($\text{d}^{-1}/\text{h}^{-1}$);
- H – depth (m);
- t – hydraulic retention time (d/h).

Von Sperling, Bastos and Kato (2005) analysed *E. coli* and helminth eggs disinfection in Brazil from five different wastewater treatment plants, all comprised of UASB reactors followed by a maturation pond system. Most of the systems had ponds in series, except for two with only one pond following the UASB reactor. Depths were shallower than 1.0 m, a typical parameter for

maturation ponds. The authors proposed an *E. coli* disinfection rate/coefficient (Equation 4.17) for dispersed-flow models for maturation ponds, very similar to Equation 4.16, but standardised for a temperature of 20 °C.

❖ Standardised first order K_b for *E. coli* disinfection rate/coefficient for dispersed-flow model at 20 °C considering H (von Sperling, Bastos and Kato 2005).

$$K_b = 0.710 \cdot H^{-0.995} (20^\circ C) \quad (4.17)$$

- K_b – first order *E. coli* disinfection rate/coefficient (d⁻¹/h⁻¹);
- H – depth (m).

Von Sperling (2005b) considered that the proposed models have better representativeness compared to other K_b equations in literature. The K_b equations presented by von Sperling (1999; 2005) and von Sperling, Bastos and Kato (2005) for bacterial/coliform disinfection rates/coefficients only consider H and t or just H for design purposes. These equations are simpler to use because the variables are known before hand when designing a pond system.

Complex K_b models in function of pH, solar irradiance (S_0), temperature (T) and depth (H) (includes light extinction and settling) (Mayo, 1995) consider an array of variables. Mayo (1995) proposed Equation 4.18 to include these variables for plug-flow regime.

❖ First order K_b for *E. coli* disinfection rate/coefficient for plug-flow regime considering pH, S_0 , T and H (Mayo 1995).

$$K_b = K_{20} \cdot \theta^{(T-20)} + \frac{k_s \cdot S_0}{K \cdot H} + k_{pH} \cdot pH \quad (4.18)$$

where,

- K_b – first order *E. coli* disinfection rate/coefficient (d⁻¹/h⁻¹);
- K_{20} – first order *E. coli* disinfection rate/coefficient at 20°C (d⁻¹/h⁻¹);
- θ – temperature coefficient;
- k_s – rate constant for light disinfection term (cm².cal⁻¹)/(m².W⁻¹);
- S_0 – solar irradiance received at pond surface per day (cal.cm⁻².d⁻¹)/(W.m⁻².d⁻¹);
- K – light attenuation coefficient (m⁻¹);

- H – pond depth (m);
- k_{pH} – rate constant for pH;
- pH – pH value.

Authors debate whether to include the disinfection/repair rate/coefficient for dark conditions (K_d) or not, because some believe that dark conditions allows for repair (Harm, 1968 and Davies-Colley *et al.*, 1999), while others consider that it contributes for disinfection (Maïga *et al.*, 2009a and Craggs *et al.*, 2004). Mayo (1995) believes that the disinfection/repair rate/coefficient in dark conditions has little contribution for overall K_b , and was not included in his equations. Sarikaya and Saatçi (1987) and Sarikaya, Saatçi and Abdulfattah (1987) on the other hand considered that the disinfection/repair rate/coefficient for dark conditions (K_d) was important and included it in their equation. Davies-Colley *et al.* (1999) and Davies-Colley, Donnison and Speed (2000) recommended a better understanding of the slower dark disinfection.

Sarikaya and Saatçi (1987) proposed Equation 4.19 for *E.coli* disinfection rate/coefficient (K_b) in vertically mixed ponds. The equation is very similar to Mayo's (1995), with the exception of pH and K_d . The flow regime considered was plug-flow.

❖ First order K_b for *E. coli* disinfection rate/coefficient for plug-flow regime considering K_d , S_0 and H (Sarikaya and Saatçi 1987).

$$K_b = K_d + \frac{k_s S_0 (1 - e^{-K.H})}{K.H} \quad (4.19)$$

where,

- K_b – first order *E. coli* disinfection rate/coefficient (d^{-1}/h^{-1});
- K_d – first order *E. coli* disinfection/repair rate/coefficient in the dark (d^{-1}/h^{-1});
- k_s – rate constant for light disinfection term ($cm^2 \cdot cal^{-1} / (m^2 \cdot W^{-1})$);
- S_0 – solar irradiance received at pond surface ($cal \cdot cm^{-2} \cdot d^{-1} / (W \cdot m^{-2} \cdot d^{-1})$);
- K – light attenuation coefficient (m^{-1});
- H – pond depth (m).

Sarikaya, Saatçi and Abdulfattah (1987) rearranged Equation 4.19 to produce Equation 4.20 for K_b prediction. This equation can be used when depths are greater than 0.9 m, neglecting the term $e^{-K.H}$ and considering an error of less than 1%. The authors considered that disinfection in WSP depends on sunlight exposure, therefore existing a very strong relationship with depth and consequently sunlight penetration. Again, the authors considered plug-flow.

❖ First order K_b for *E. coli* disinfection rate/coefficient for plug-flow regime considering K_d , S_0 and H (Sarikaya and Saatçi 1987).

$$K_b = K_d + \frac{k_s S_0}{KH} \quad (4.20)$$

where,

- K_b – first order *E. coli* disinfection rate/coefficient (d^{-1}/h^{-1});
- K_d – first order *E. coli* disinfection/repair rate/coefficient in the dark (d^{-1}/h^{-1});
- k_s – rate constant for light mortality term ($cm^2.cal^{-1}/(m^2.W^{-1})$);
- S_0 – solar irradiance received at pond surface ($cal.cm^{-2}.d^{-1}/(W.m^{-2}.d^{-1})$);
- K – light attenuation coefficient (m^{-1});
- H – pond depth (m).

Qin *et al.* (1991) developed a model for predicting bacterial disinfection considering the combination of environmental factors (temperature, pH and organic loading), illumination-related factors (sunlight irradiance, depth, algal concentration and turbidity) and physical configuration factors [pond dimensions (depth, length and width), HRT and dispersion number]. The experiment was conducted on a maturation pond and results showed that the models predictions were in agreement with the measured values. A simple model for overall *E. coli* rate/coefficient (K_b) was produced (Equation 4.21). Note that the model depends on the sum of two different coefficients, the disinfection/repair coefficient due to dark conditions (K_d) and the disinfection coefficient due to sunlight conditions (K_l). This equation is very complete because it considers a magnitude of parameters, although it is difficult to calculate the overall disinfection coefficient (K_b) when compared to other equations that consider one or two parameters.

❖ First order K_b for *E. coli* disinfection rate/coefficient for any regime considering environmental factors, illumination-related factors and physical configuration factors (Qin *et al.*, 1991).

$$K_b = K_d + K_s \cdot I = K_d + K_I \quad (4.21)$$

where,

- I – solar irradiance at depth H per day/hour ($\text{cal.cm}^{-2}.\text{d}^{-1}$)/($\text{W.m}^{-2}.\text{d}^{-1}$)/($\text{W.m}^{-2}.\text{h}^{-1}$);
- K_I – disinfection coefficient due to sunlight irradiance at depth H (m^{-1});
- K_s – rate constant for light mortality term ($\text{cm}^2.\text{cal}^{-1}$)/($\text{m}^2.\text{W}^{-1}$);
- K_b – first order *E. coli* disinfection rate/coefficient ($\text{d}^{-1}/\text{h}^{-1}$);
- K_d – first order *E. coli* disinfection/repair rate/coefficient in the dark ($\text{d}^{-1}/\text{h}^{-1}$).

Equations 4.22 and 4.23 were proposed for estimating disinfection/repair in dark conditions and disinfection for sunlight conditions at a given depth, correspondingly. The results from the estimations for dark and light conditions are then used to determine the overall K_b value in Equation 4.21.

$$K_d = K_T + K_{pH} + K_{BOD_5} \quad (4.22)$$

$$I = \frac{I_0 \cdot (1-B) \cdot (1-e^{-K_\ell H})}{K_\ell \cdot H} \quad (4.23)$$

where,

- K_d – first order *E. coli* disinfection/repair rate/coefficient in the dark ($\text{d}^{-1}/\text{h}^{-1}$);
- K_T – first order *E. coli* disinfection rate/coefficient due to temperature ($\text{d}^{-1}/\text{h}^{-1}$);
- K_{pH} – first order *E. coli* disinfection rate/coefficient due to pH ($\text{d}^{-1}/\text{h}^{-1}$);
- K_{BOD_5} – first order *E. coli* disinfection rate/coefficient due to BOD₅ ($\text{d}^{-1}/\text{h}^{-1}$);
- I – solar irradiance at depth H per day/hour ($\text{cal.cm}^{-2}.\text{d}^{-1}$)/($\text{W.m}^{-2}.\text{d}^{-1}$)/($\text{W.m}^{-2}.\text{h}^{-1}$);
- I_0 – solar irradiance at surface per day/hour (lux)/($\text{W.m}^{-2}.\text{d}^{-1}$)/($\text{W.m}^{-2}.\text{h}^{-1}$);
- K_ℓ – light extinction coefficient;

- BOD₅ – concentration of organic loading (mg/L).

The dark disinfection/repair coefficient (Equation 4.22) is estimated by the sum of temperature (Equation 4.24), pH (Equation 4.25) and biochemical oxygen demand (BOD₅) (Equation 4.26) disinfection rate/coefficients. Light irradiance at depth H (Equation 4.23) considers solar irradiance at the surface of the pond, breadth and depth of the pond and the light extinction coefficient (Equation 4.27). The light extinction coefficient depends on disinfection rates/coefficients influenced by depth (K_H), algae (K_A) and turbidity (K_{TUR}), as well as algal (A) concentration and turbidity units (TUR).

$$K_T = 0.0279 + 0.00898 \cdot T \quad (4.24)$$

$$K_{pH} = 0.2207 \cdot (pH)^2 - 3.5797 \cdot (pH) + 14.489 \quad (4.25)$$

$$K_{BOD_5} = 0.406 - 0.184 \cdot \log(BOD_5) \quad (4.26)$$

$$K_\ell = K_H + K_A \cdot A + K_{TUR} \cdot TUR \quad (4.27)$$

where,

- K_T – first order *E. coli* disinfection rate/coefficient due to temperature (d⁻¹/h⁻¹);
- K_{pH} – first order *E. coli* disinfection rate/coefficient due to pH (d⁻¹/h⁻¹);
- K_{BOD_5} – first order *E. coli* disinfection rate/coefficient due to BOD₅ (d⁻¹/h⁻¹);
- K_ℓ – light extinction coefficient;
- T – temperature (15°C < T < 35°C);
- pH – pH value (-);
- BOD₅ – surface organic loading concentration (mg/L);
- K_H – first order *E. coli* disinfection rate/coefficient due to depth (d⁻¹/h⁻¹);
- K_A – first order *E. coli* disinfection rate/coefficient due to algae (d⁻¹/h⁻¹);
- A – algal concentration (mg/L);
- K_{TUR} – first order *E. coli* disinfection rate/coefficient due to turbidity (d⁻¹/h⁻¹);
- TUR – Turbidity (NTU);
- B – surface layer effect coefficient (0.0 – 0.03);
- t – hydraulic retention time (d).

After estimating the *E. coli* disinfection rate/coefficient (Equation 4.21), it is used in equation 4.29 and subsequently equation 4.28 for predicting the total concentration of bacterial organisms. The dispersion number (d) was obtained using the equation proposed by Polprasert and Bhattarai (1983), although other equations can be used from different authors. Equation 4.28 is for the plug-flow regime or for ponds with a dispersion number (d) < 0.2.

$$N = N_0 \cdot \frac{4.F}{(1+F)} \cdot e^{[(F-1)/2.d]}, \text{ for } d < 2.0 \quad (4.28)$$

$$F = (1 + 4.K_b.d.t)^{1/2} \quad (4.29)$$

where,

- N – *E. coli*/100 ml in effluent;
- N_0 – *E. coli*/100 ml in influent;
- d – dispersion number (-).

Curtis, Mara and Silva (1992b) proposed equation 4.30 for ThCB disinfection based on a multiple regression analysis considering only solar irradiance (Ir), pH and DO. The model produced a good fit, accounting for 88.5% of the observed and measured concentrations ($p < 0.001$). The authors had a different position from that derived from the research done by Sarikaya and Saatçi (1987) and Mayo (1989), and stated that “*Consequently recent attempts to predict the performance of WSP using light alone are not likely to work*”. Curtis, Mara and Silva (1992b) considered that the combination of high pH and high oxygen concentration is essential for solar irradiance to have adverse effects ThCB removal. The log removal rate presented in hours⁻¹ (h^{-1}), while most of the other equations are usually in days⁻¹ (d^{-1}).

❖ Thermotolerant coliform removed logs considering solar irradiance, pH and dissolved oxygen (Curtis, Mara and Silva 1992b).

$$\log FC \text{ removed } (h^{-1}) = -2.76 + 0.000446.(Ir) + 0.323.(pH) + 0.0708.(DO) \quad (4.30)$$

where,

- Ir – solar irradiance at surface of pond ($W.m^{-2}$);
- pH – pH value (-);

- DO – dissolved oxygen (mg/L);

The variable from equation 4.30 cover a wide range of values (Table 4.6), therefore allowing for it to be used in different parts of the world, as long as their parameters are in the range of the parameters used to produce the multiple regression curve.

Table 4.6 - Ranges of variable values used for calculating equation 4.33. Source: Curtis, Mara and Silva (1992b).

Variable	Range
Solar intensity/irradiance (W/m ²)	429 – 1096
pH	7.2 – 9.5
Dissolved Oxygen (mg/L)	0.8 – 7.5
Temperature (°C)	30 – 40

The authors also presented Table 4.7 showing the minimum and maximum monthly solar irradiance of five different locations in order to put the equation into context.

Table 4.7 - Annual range of mean monthly irradiances from various locations. Source: Curtis, Mara and Silva (1992b).

Location	Monthly Irradiance (W/m ²)	
	Min	Max
London, UK	74	477
Lisbon, Portugal	261	800
Marseille, France	189	704
Cairo, Egypt	417	824
Recife, Brazil	744	915

Saqqar and Pescod (1992a) considered water temperature, received solar irradiance, pH, soluble BOD₅, total BOD₅ and surface organic loading for their disinfection model. Considering these parameters increased coliform disinfection rates, but only water temperature, pH and soluble BOD₅ took part in the proposed Equation 4.34 for coliform disinfection rate/coefficient (K_b). Algal concentration was not considered in the model, unlike Qin *et al.* (1991) because generally the greater algal concentration is, the higher pH values will be.

❖ First order K_b for *E. coli* disinfection rate/coefficient considering temperature, pH and soluble BOD₅ (Saqqar and Pescod (1992a)).

$$K_b = 0.50 \cdot (1.02)^{(T-20)} \cdot (1.15)^{(pH-6)^2} \cdot (0.99784)^{(SBOD-100)} \quad (4.31)$$

where,

- K_b – first order *E. coli* disinfection rate/coefficient (d⁻¹/h⁻¹);

- T – water temperature (°C);
- pH – pH value (-).
- SBOD – soluble BOD₅ (mg.L⁻¹).

Equation 4.31 is much simpler than those presented by previous authors seen that it only has three of the same variables. It uses indirect values (temperature) instead of solar irradiance.

Ouali *et al.* 2014 considers there are big differences between empirical models developed over the years estimating coliform/*E. coli* disinfection, and that disinfection is increased with optimised pond design. Modelling was based on a laboratory pilot scale maturation pond. The authors sought out to find which parameters influenced *E. coli* disinfection the most, concluding that K_b values increased with increasing pH, solar irradiance (I), water temperature and DO, with a strong dependence on pH and DO. Dark disinfection/repair (K_d) was also quantified, consequently falling into agreement with literature for its low disinfection participation. After considering all these coefficients and parameters, Equation 4.32 was proposed.

❖ First order K_b for *E. coli* disinfection rate/coefficient considering dark disinfection/repair coefficient, pH value and pH coefficient, dissolved oxygen concentration and DO coefficient, solar irradiance received and solar irradiance coefficient and temperature (Ouali *et al.* 2014).

$$K_b = (K_d + K_{pH} \cdot pH + K_{DO} \cdot DO + K_I \cdot I) \cdot \theta^{(T-20)} \quad (4.32)$$

- K_b – first order *E. coli* disinfection rate/coefficient (d⁻¹/h⁻¹);
- K_d - first order *E. coli* repair/disinfection rate/coefficient in dark conditions (d⁻¹/h⁻¹);
- K_{pH} – first order *E. coli* disinfection rate/coefficient due to pH (d⁻¹/h⁻¹);
- pH – pH value;
- K_{DO} – first order *E. coli* disinfection rate/coefficient due to dissolved oxygen (d⁻¹/h⁻¹);
- DO – dissolved oxygen in the medium (mg/L);
- K_I – first order *E. coli* disinfection rate/coefficient due to solar irradiance (d⁻¹/h⁻¹);
- I – solar irradiance (W/m²);
- θ – temperature coefficient;

- T – temperature ($15^{\circ}\text{C} < T < 35^{\circ}\text{C}$).

The model does not depend on the hydrodynamic flow since the results were obtained from a batch flow reactor with a shallow depth. K_b can be used in other hydrodynamic models, such as plug flow, dispersed flow and even with computational fluid dynamics (CFD) to simulate bacterial disinfection in maturation ponds.

Modelling tools and equations are important for designing WSP, allowing to predict the final concentration of coliforms/*E. coli* and accordingly the dimensions of a pond. The correct choice of flow type, as well as the right dispersion number can sometimes be limited, as perfect regimes such as plug flow or completely mixed flow cannot be achieved. As a consequence, pond designers must have this in mind when using these equations, and ensure that the main objective of maturation ponds because reports have shown that systems are underperforming due to improper designing (Buchanan *et al.*, 2011). Understanding better disinfection mechanisms in maturation ponds for bacteria and how they interact with each other and the environment would optimise disinfection and reduce required areas. Some disinfection coefficient models (K_b) are simple because they only consider depth, not including direct and indirect solar irradiance influence. Other models consider an array of parameters such as turbidity, pH, DO, temperature, solar irradiance, BOD, etc., therefore difficult and impractical to use for design purposes. K_b models need to be revised for better predictions of *E. coli* to be made.

It is important that K_b models are simple and easy to use, making them practical for planning and designing maturation ponds, and not evaluating them. It is widely recognised that disinfection models for WSPs that incorporate sunlight exposure produce more satisfactory results than others that do not (Mayo, 1995), but there is still a gap to be filled about sunlight-mediated disinfection mechanisms and how they interact with other environmental factors (Davies-Colley *et al.*, 1999). Rudolph, Weil and Fuchs (2016) recommended that solar radiation should be applied in practice as a driver for innovations in pond design, seen that it influences a multitude of reactions occurring within the pond.

Seen that physical-chemical conditions in WSPs vary from place to place, as well as the diversity of environmental factors on sunlight-mediated disinfection, Davies-Colley *et al.* (1999) and Davies-Colley, Donnison and Speed (2000) recommend that this should translate in implications for modelling *E. coli* disinfection in WSPs. To produce reliable predictions of

disinfection efficiency, the model should be robust and physically meaningful, bearing in mind pH, DO, temperature, pond geometry, pond effluent optics, solar irradiance and mixing depth, as well as the better understanding of the slower dark disinfection/repair.

Table 4.8 shows a summary of the models reviewed in this section and included the variables and coefficients used in each K_b model. Note that the most used variables for the equations were depth and temperature, while Qin *et al.* (1991) accounted for virtually every variable (except DO). K_d and K_s were the most used coefficients.

Table 4.8 - Summary of K_b models, parameter and constants reviewed.

AUTHORS	VARIABLES									COEFFICIENTS													
	H	t	T	$S_0/I/r$	pH	DO	TUR	A	$BOD_5/SBOD$	K_d	K	K_ϕ	K_{BOD5}	K_I	K_T	K_{20}	θ	K_s	K_H	K_{pH}	K_{DO}	K_A	K_{TUR}
Marais (1974)	-	X	X	-	-	-	-	-	-	-	-	-	-	-	-	-	-	-	-	-	-	-	-
Curtis, Mara and Silva (1992b)	-	-	-	X	X	X	-	-	-	-	-	-	-	-	-	-	-	-	-	-	-	-	-
von Sperling (1999)	X	X	-	-	-	-	-	-	-	-	-	-	-	-	-	-	-	-	-	-	-	-	-
von Sperling (2005)	X	X	-	-	-	-	-	-	-	-	-	-	-	-	-	-	-	-	-	-	-	-	-
von Sperling (2005)	X	-	-	-	-	-	-	-	-	-	-	-	-	-	-	-	-	-	-	-	-	-	-
von Sperling, Bastos and Kato (2005)	X	-	X	-	-	-	-	-	-	-	-	-	-	-	-	-	-	-	-	-	-	-	-
Mayo (1995)	X	-	X	X	X	-	-	-	-	-	X	-	-	-	-	X	X	X	-	X	-	-	-
Sarikaya and Saatçi (1987)	X	-	-	X	-	-	-	-	-	X	X	-	-	-	-	-	X	-	-	-	-	-	-
Sarikaya, Saatçi and Abdulfattah (1987)	X	-	X	X	-	-	-	-	-	-	-	-	-	X	-	-	X	-	-	-	-	-	-
Qin et al. (1991)	X	-	X	X	X	-	X	X	X	X	-	X	X	-	X	-	-	X	X	X	-	X	X
Saqqard and Pescod (1992)	-	-	X	-	X	-	-	-	X	-	-	-	-	-	-	-	-	-	-	-	-	-	-
Ouali (2014)	-	-	X	X	X	X	-	-	-	X	-	-	-	X	-	-	X	-	-	X	X	-	-

4.8. Solar irradiance attenuation rate with depth in ponds

Solar irradiance in facultative and maturation ponds is very much attenuated, especially the UV waves (UV-A and UV-B), because of the high algal concentrations, consequently producing different attenuation properties in different ponds (Curtis, *et al.*, 1994). The longer wave, PAR, penetrates deeper compared to the other two waves and produces better attenuation models.

Solar irradiance can be measured as irradiance (I) and represents the number of photons per unit area per time ($\text{m}^{-2} \cdot \text{s}^{-1}$) or the amount of energy per unit area ($\text{W} \cdot \text{m}^{-2}$), the latter according to the International System of Units (SI). There are two types of irradiance, downward irradiance (I_a) on horizontal surfaces facing up, and upward irradiance (I_u) on horizontal surfaces facing downward. Downward irradiance is of particular interest in this research, therefore upward irradiance will not be included. $I_{a(z)}$ attenuates with depth z and is shown by Equation 4.33, following Beer-Lambert's law (Curtis *et al.*, 1994).

$$I_{a(z)} = I_{a(0)} \cdot e^{-K_a \cdot Z} \quad (4.33)$$

where,

- $I_{a(z)}$ – downward irradiance at a depth z ($\text{m}^{-2} \cdot \text{s}^{-1}$) or ($\text{W} \cdot \text{m}^{-2}$);
- $I_{a(0)}$ – downward irradiance at surface ($\text{m}^{-2} \cdot \text{s}^{-1}$) or ($\text{W} \cdot \text{m}^{-2}$);
- $K_{a(z)}$ – attenuation coefficient for downward irradiance (m^{-1});
- Z – depth from surface or reference point (m).

$K_{a(z)}$ is estimated by equations 4.34 and 4.35 for the different wavelengths as the slope of an exponential regression between irradiance and depth.

$$K_{a(z)} = \frac{\ln I_{a(0)} - \ln I_{a(z)}}{Z} \quad (4.34)$$

or,

$$K_{a(z)} = \frac{-\ln(I_{a(z)}/I_{a(0)})}{Z} \quad (4.35)$$

where,

- $K_{a(z)}$ – attenuation coefficient for downward irradiance (m^{-1});

- $I_{a(0)}$ – downward irradiance at surface ($\text{m}^{-2} \cdot \text{s}^{-1}$) or ($\text{W} \cdot \text{m}^{-2}$);
- $I_{a(z)}$ – downward irradiance at a depth z ($\text{m}^{-2} \cdot \text{s}^{-1}$) or ($\text{W} \cdot \text{m}^{-2}$);
- Z – Depth from surface or reference point (m).

Bolton *et al.* (2011a) used surrogate parameters such as suspended solids (SS), chlorophyll-a (CHLa) and turbidity (NTU) to predict UV and PAR attenuation. These showed a good fit when correlated with UV radiation attenuation measurements, where UV-A ($R^2=0.72$) and UV-B ($R^2=0.732$) were well correlated with turbidity and consequently can be considered a good predictor of attenuation in ponds.

The coefficient of determination was used to explain the variability of observed irradiance values and estimated irradiance values when calibrating the different models. The coefficient of determination = $1 - (\sum \text{squared errors of the data} / \sum \text{variance of the data})$.

4.9. Solar irradiance dose

Sunlight is very important for *E. coli* disinfection in natural wastewater treatment systems such as WSP. Doses from the UV and PAR spectrum present the amount of radiation that each organism receives. Applied surface dose is the amount of energy reaching the surface of the pond and received doses are the amount of energy that was received by the liquid and bacteria at different depths. Therefore, the effectiveness of sunlight disinfection is dependent on the dose that microorganisms are exposed to. The dose, D , is characterised as follows (Metcalf and Eddy, 2013) in Equation 4.36:

$$D = I \times t \quad (4.36)$$

where,

- D – dose, $\text{mJ} \cdot \text{cm}^2$ ($\text{mJ} \cdot \text{cm}^2 = \text{mW} \cdot \text{s} \cdot \text{cm}^{-2}$);
- I – Intensity or irradiance ($\text{mW} \cdot \text{cm}^{-2}$);
- t – exposure time (s).

4.10. Research gaps that were drivers for the current research

1. Most natural treatment systems use substantial surface areas. Natural treatment systems that are less land intensive need to be evaluated within a long term.
2. Literature does not present long term solar radiation penetration monitoring of the three consolidated wavelengths for bacterial disinfection in WSP, especially extinction rates in a shallow maturation pond treating sewage in tropical climates.
3. There is a difference between *E. coli* disinfection during morning and afternoon for different depths. Nothing in literature was found reporting on this matter.
4. In existing ponds, K_b coefficients are usually calculated based on measured values of the inlet and outlet concentration of bacteria and as a function of parameters (depth, pH, DO, sunlight radiation) and consider the hydraulic regime as well. But the K_b coefficient changes along pond depth, being greater near the surface. This research aims at better understanding how depth, in relation with solar radiation, pH, DO and temperature affects the K_b coefficient.
5. Literature is clearly not in agreement about the K_d coefficient on whether it represents disinfection or repair. There are probably two dark disinfection and repair coefficients, different from each other. Mostly every experiment is done in controlled environments, but results for K_d here are presented in function of depth and temperature in the real environment. Again, depth affects this parameter, and no research has been done about the K_d coefficient from different depths in WSP.
6. No study was found showing the amount of solar radiation that *E. coli* receive during the morning and afternoon periods in a waste stabilisation pond. Even more so from different depths in a pond, where disinfection proceeds to decrease as depth increases, due solar attenuation.
7. Usually, literature only reports either applied doses or received doses for *E. coli* disinfection, and here both results are presented.
8. Determining received solar doses required for *E. coli* disinfection instead of light extinction depths.

5. MATERIAL AND METHODS

5.1. *Location of the experimental apparatus and climate characteristics*

The experiment was conducted at the Centre for Research and Training on Sanitation (CePTS UFMG/COPASA), located between Belo Horizonte and Sabará/MG, Brazil, at the Arrudas wastewater treatment plant (WWTP), managed by the water and sanitation company of Minas Gerais (COPASA) (Figure 5.1 (A)). The UTM coordinates of CePTS are: 19°53'44.1"S and 43°52'42.9"W.

The climate in the region according to the Köppen classification system is Cwa – tropical altitude, average annual temperature of 22.1 °C and a precipitation of 1540 mm/year. The dry and cool season occurs between April and September, and the rainy and warm season is from October to March. During the dry season, the average temperature and monthly rainfall is 20.9 °C and 33 mm/month, respectively. The rainy season presents higher average temperature and rainfall of 23.4 °C and 254 mm/month, respectively.

The WWTP was constructed to treat urban wastewater from a portion of the metropolitan area of Belo Horizonte. Before raw domestic sewage enters the treatment line it passes through preliminary treatment, i.e., mechanised solids removal for dimensions above 15 mm and sand sedimentation in a grit chamber. A small amount of domestic raw sewage is diverted to the various treatment units at CePTS after passing through the preliminary treatment. CePTS has been in operation since 2002 and many of the treatment units have undergone changes over the years. The treatment line studied here is no exception and has experimented different setups as well. Figure 5.1 (B) shows the previous treatment line, before the current research, composed of an upflow anaerobic sludge blanket (UASB) reactor followed by three maturation ponds in series and a rock filter inserted in the final third of the last pond. Some of the units underwent renovation and upgrades for this research and Figure 5.1 does not accurately depict the current setup. This is covered in subsection 5.2.

Figure 5.1 - Overview of Waste Water Treatment Plant (A) and Experimental Plant (CePTS) (B).



5.2. Experimental apparatus

The UASB reactor and the first pond of the series did not undergo any renovation because the first pond was under research to evaluate the sludge layers' role in the removal of specific constituents (Rodrigues *et al.*, 2015, 2016). The first pond has accumulated sludge from the last 13 years of continuous operation. The physical characteristics of the three ponds are shown in Table 5.1.

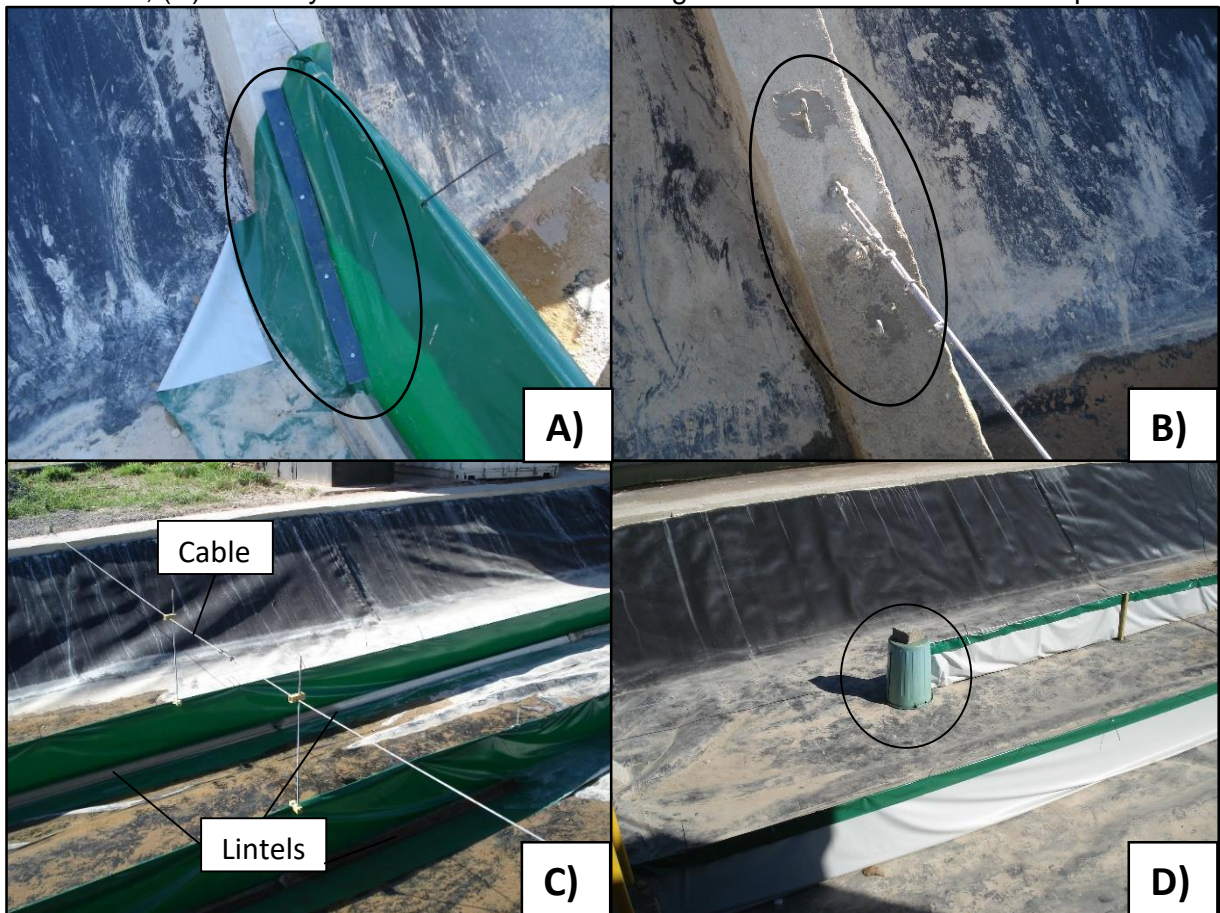
At the beginning of 2014 the second and third ponds underwent complete desludging and removal of the existing geomembrane covering the embankments and pond bottom (Figure 5.2 (A)). The embankment slopes were corrected and compacted, and the bottom of the ponds were also compacted with clay. A new geomembrane was placed (Figure 5.2 (B)), except on the bottom of the third pond because it was compacted with two 0.20 m layers of clay, totalling 0.40 m (Figure 5.4 (A)). The second pond received four small concrete pillars (in pairs, opposite to one another) on the embankments (Figure 5.2 (C)) to fix the cables that hold the two baffles. The baffles run parallel to the ponds length and are flexible enough to change from 70 % to 100 % the total length of the pond (Figure 5.2 (D)). The baffles were made out of waterproof awning material and are attached to the metal cables with plastic ties. The cables are linked to the pillars opposite each other on the embankment (Figure 5.2 (C)). The baffles can also change height in order to evaluate different depths in the pond. During the experiment the baffles were positioned at 90% of the length of the pond and at 0.55 m height.

Figure 5.2 - Pond 2 renovation. **(A)** Desludging and removal of the existing geomembrane canvas (Pond 2); **(B)** Placement of new geomembrane canvas (Pond 2); **(C)** Pillars constructed at each end; **(D)** baffles 90% the length of the pond are anchored to the pillars.



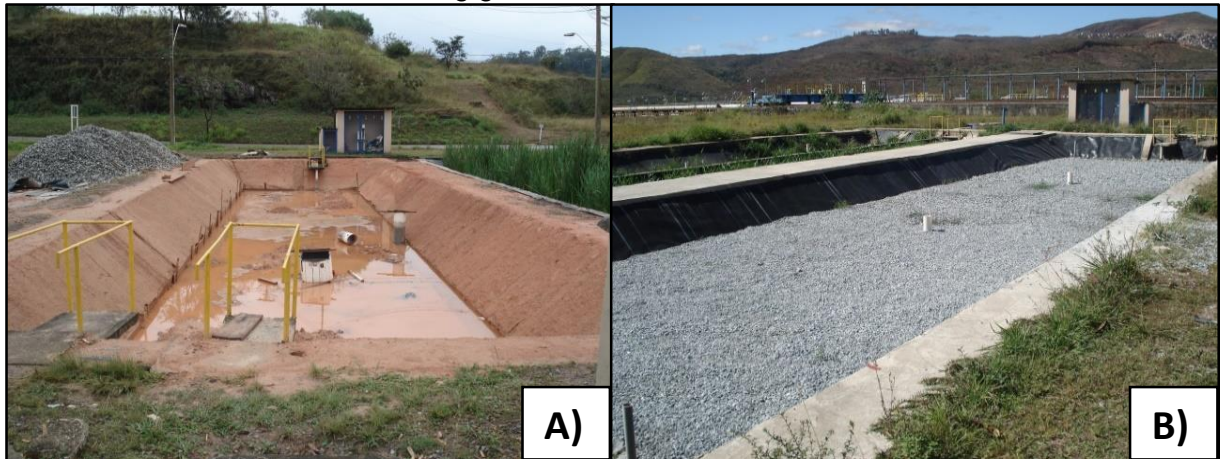
The baffles were permanently fixed on one side of the pond with a metal plate and rubber to minimise liquid passing behind (Figure 5.3 (A)). The other side was bolted to the pillar to allow length changes (Figure 5.3 (B)). Three different baffled heights can be researched (0.55 m, 0.65 m and 0.75 m), with a minimum difference of 0.10 m between the liquid layer and the top of the baffle, and a maximum difference of 0.30 m (Figure 5.3 (B)). The bottom of the baffles were weighted down with concrete lintels in series to also minimise liquid passing underneath (Figure 5.3 (C)). Over time sludge, will accumulate and possibly seal the interface of the baffles with the bottom of the pond. A pair of cables was used to cross the breadth of the pond to counter the sagging caused by the weight of the cables and awning material (Figure 5.3 (C)). Ordinary dustbins were used to round off the edges of the baffles to create a smooth pass for wastewater to flow around and facilitate computer fluid dynamics (CFD) drawings and flow estimations (Figure 5.3 (D)). This upgrade allows for future evaluations of different baffle lengths and depths, as well as removing the baffles completely without stopping treatment, as opposed to solid-state baffles.

Figure 5.3 - (A) Metal plate and rubber fixing baffle to the pillar; (B) Three different heights for bolting the cable of the baffle; (C) Cable crossing breadth of the pond to avoid sagging caused by the weight of the baffles and lintels to minimise water passing underneath the baffles; (D) Ordinary dustbin to round off the edge of the baffle not fixed to the pillars.



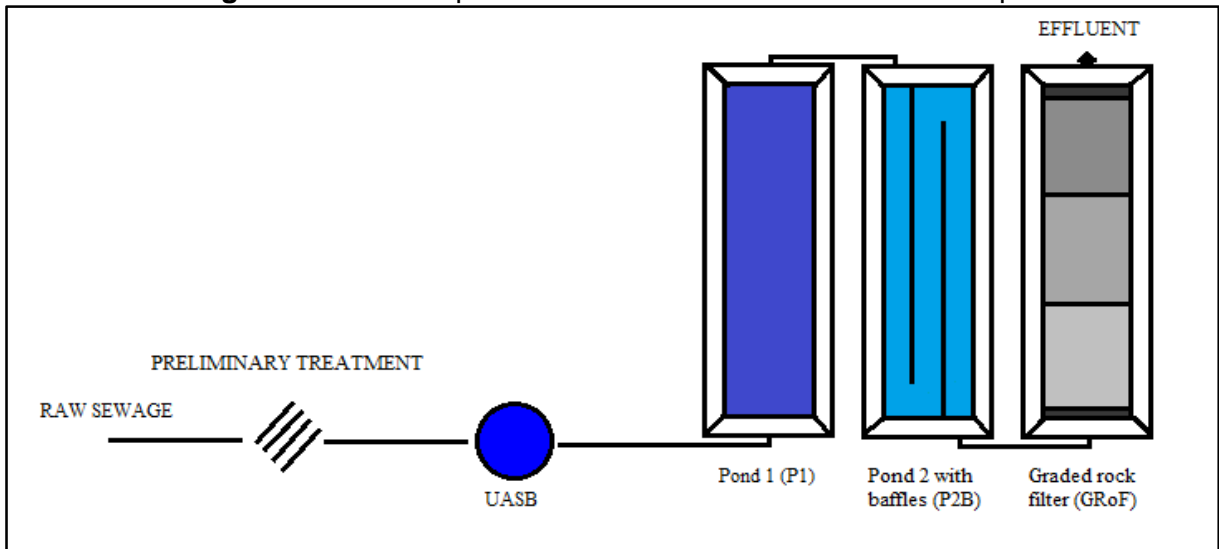
The third pond was transformed into a graded rock filter (GRoF) as shown in Figure 5.4 (A; B). To avoid tearing or ripping because of the gravel stones, a geomembrane canvas was not placed on the bottom (Figure 5.4 (A)). The GRoF consisted of three different grain sizes, decreasing in size from the inlet to the outlet (Figure 5.4 (B), Figure 5.5 and Figure 5.6 (D)).

Figure 5.4 - Renovation of Pond 3. **(A)** Compacting the bottom and embankments; **(B)** GRoF with decreasing grain size from the inlet to the outlet.



The treatment line was designed to serve a population of 250 inhabitants ($40 \text{ m}^3 \cdot \text{d}^{-1}$) and the setup can be seen in Figure 5.5: a UASB reactor followed by two maturation ponds, the first pond without baffles and the second pond with baffles, and a graded rock filter (GRoF) in series. The area required to treat the wastewater decreased to $1.50 \text{ m}^2/\text{inhabitant}$, a 0.50 to $1.00 \text{ m}^2/\text{inhabitant}$ improvement compared to the previous setups (Dias *et al.*, 2014). The UASB reactor (Figure 5.6 (A)) removes up to 70% of organic matter from raw sewage. The UASB reactor is made from ferrocement and is 2.0 m in diameter and 4.5 m in height, resulting in a volume of 14.2 m^3 . The reactor has been in continuous operation for the last 13 years and no problems have occurred, nor have strong odours been detected. The first pond (Figure 5.6 (B)) of the series has also been in continuous operation over the same period, resulting in sludge accumulation at the bottom (up to 40% of the useful volume) (Possmoser-Nascimento *et al.*, 2013, 2014).

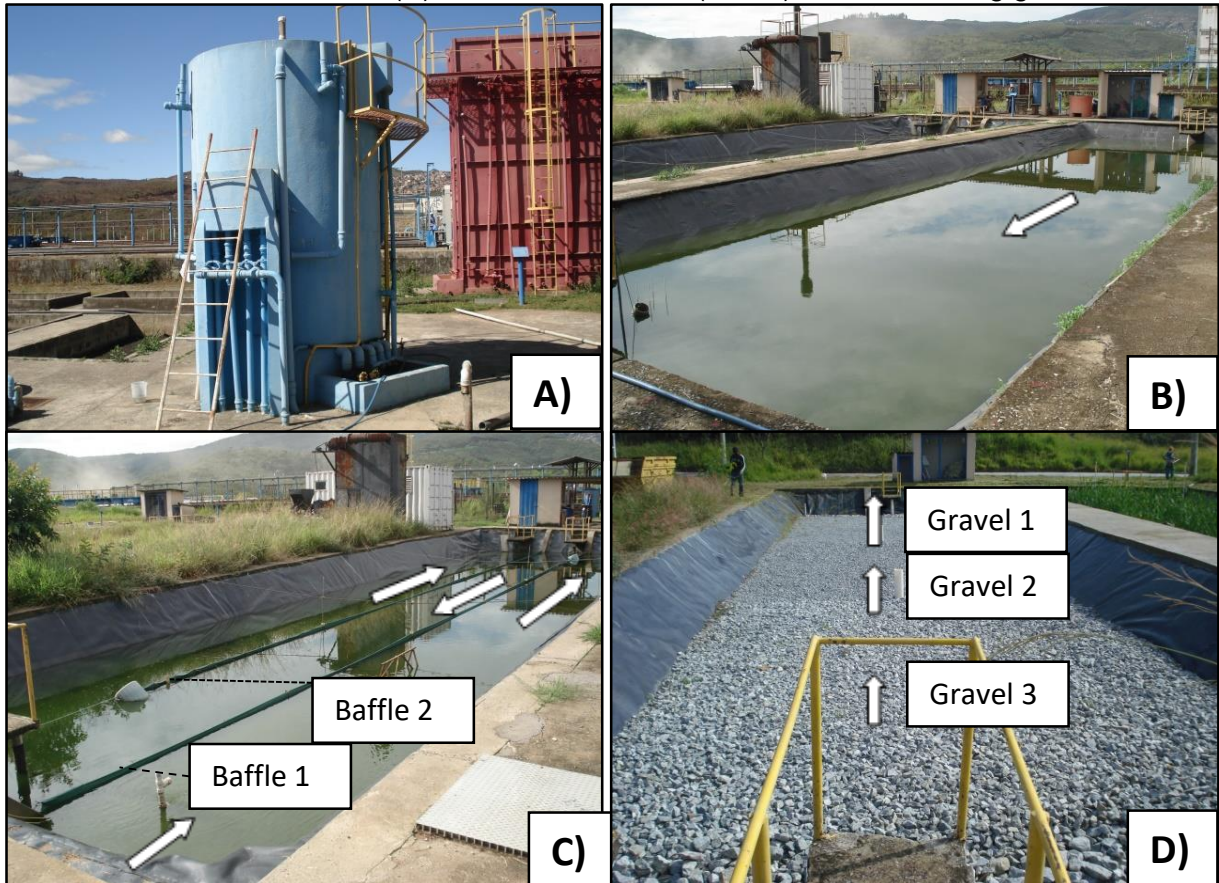
Figure 5.5 – The experimental wastewater treatment line setup.



Depth did not vary much in the first pond compared to previous studies and was maintained at an average of 0.77 m (Figure 5.6 (B) and Table 5.1) to promote complementary organic matter removal. The second pond (Figure 5.6 (C)) average depth was 0.44 m (Table 5.1), seeking to further increase disinfection but resulting in a decrease in actual HRT. The baffles are to increase actual HRT and consequently promote longer contact times of the medium with solar radiation. The L/B ratio of the second pond before inserting the baffles was 5:1, and increased to 43:1 after upgrading.

The third pond, GRoF, was divided into three equal compartments in series (8.0 m), and each compartment received different grain sizes (Figure 5.6 (D)). From the inlet to the outlet, grain size decreased to avoid clogging caused by organic matter in the form of algae produced in the ponds. Larger stones were placed over 0.5 m from the inlet and the outlet of the GRoF (Figure 5.5 – darker grey areas), to uniformly distribute the liquid at the inlet and the outlet. The GRoF used common gravel 3 (25.0 – 50.0 mm), gravel 2 (19.0 – 25.0 mm) and gravel 1 (9.5 – 19.0 mm), as shown in Figure 5.5 and Figure 5.6 (D).

Figure 5.6 – (A) Units from the treatment line. UASB reactor; (B) Pond 1 without baffles; (C) and Pond 2 with baffles; (D) Graded Rock Filter (GRoF) with decreasing grain size.



A granulometric analysis was performed to characterise the gravel and results for the main indexes (largest to smallest) are:

- Gravel 3: $d_{10} = 27 \text{ mm}$; $d_{90} = 48 \text{ mm}$; unifor. coef. $d_{60}/d_{10} = 1.37$; void ratio (porosity) = 0.48
- Gravel 2: $d_{10} = 14 \text{ mm}$; $d_{90} = 26 \text{ mm}$; unifor. coef. $d_{60}/d_{10} = 1.55$; void ratio (porosity) = 0.45
- Gravel 1: $d_{10} = 9 \text{ mm}$; $d_{90} = 18 \text{ mm}$; unifor. coef. $d_{60}/d_{10} = 1.50$; void ratio (porosity) = 0.43

The void ratio is greater for gravel 3 and decreases with gravel 2 and gravel 1. The analysis shows that the effluent from pond 2 should flow easier through gravel 3 and remove most of the organic matter before passing through gravel 2 and 1 for further polishing. This should avoid premature clogging.

Table 5.1 - Physical and operational characteristics of pond and filter units.

Characteristics	Unit	Pond 1 (P_1)	Pond 2 (P_2B)	Graded Rock Filter (GRoF)
Bottom length	m	25	25	8.0 [#]
Bottom width	m	5.25	1.75*	5.25
Water depth	m	0.77	0.44	0.50**
Slope	degrees	45	45	45
Surface area	m ²	155	145	147
Average Flow	m ³ .d ⁻¹	36	36	36
HRT (theoretical)	d	3.5 ⁺ /3.4	1.8/1.8	1.0/1.0

*Width between baffles; ⁺The theoretical calculation of the mean HRT took in account the full depth of the first pond, not considering the volume occupied by the sludge layer; [#]Length of each of the 3 compartments, not accounting the length of the larger stones at the inlet and outlet (1.0 m); **Gravel height = 0.60 m; HRT – mean/median.

The overall theoretical mean and median HRT of the overall treatment system were 6.7 d and 6.6 d, considered a short time for treating wastewater by natural processes.

5.3. Sampling points and methods for routine monitoring of the treatment system

This section outlines the sampling points and methods used to evaluate the treatment system. Monitoring started on the 24/01/2014 and ended on 19/04/2016, totalling two years and three months of continuous sampling and analysis, with the exception of public and school holidays. Sampling and analyses were done on a weekly basis, with sample numbers (n) varying for each constituent from 18 to 75. This resulted in some total concentrations not equalling the sum of their parts because they are associated with different sample numbers. Awuah (2006) advises that sampling in ponds should be done in the early hours of the morning (before strong sunlight) in order to evaluate bacterial removal performance after photo-repair overnight.

5.3.1. Sampling methods and analysis

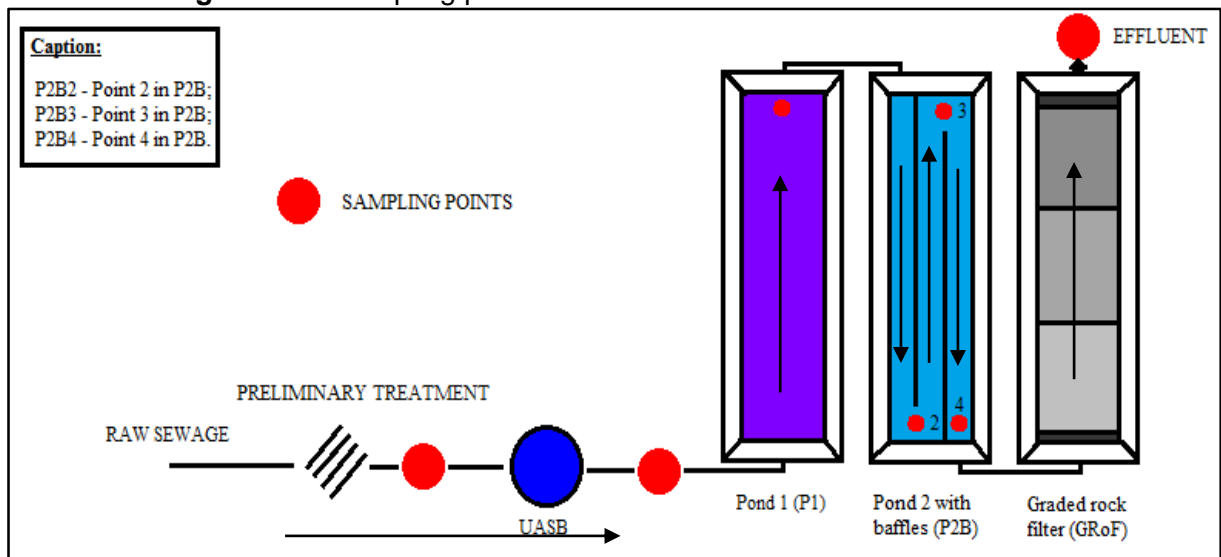
Sampling took place in the morning, usually between 08:00 and 09:30 on a weekly basis. Grab samples were collected every week. The samples were preserved and sent to the physicochemical and microbiology laboratories at the Department of Sanitary and Environmental Engineering (DESA), Federal University of Minas Gerais (UFMG), Brazil. Samples were collected and analysed according to Standard Methods for Examination of Water and Wastewater APHA-AWWA-WEF (2005). Analysis were carried out for biochemical oxygen demand (BOD) (total, particulate and filtered), chemical oxygen demand (COD) (total, particulate and filtered), total suspended solids (TSS), volatile suspended solids (VSS), fixed suspended solids (FSS), total Kjeldahl nitrogen (TKN) and ammonical nitrogen (Ammonia-N). Microbiological analysis for total coliforms and *E. coli* was done using the chromogenic

substrate (Colilert®) technique. The results are expressed as the most probable number of the organism in per 100 mL (MPN/100 mL). Onsite monitoring during sampling was carried out for temperature, dissolved oxygen (DO), pH, redox potential (ORP), electrical conductivity, turbidity and settleable solids.

5.3.2. Sampling points

Sampling points are shown in Figure 5.7.

Figure 5.7 - Sampling points in the treatment line and flow direction.

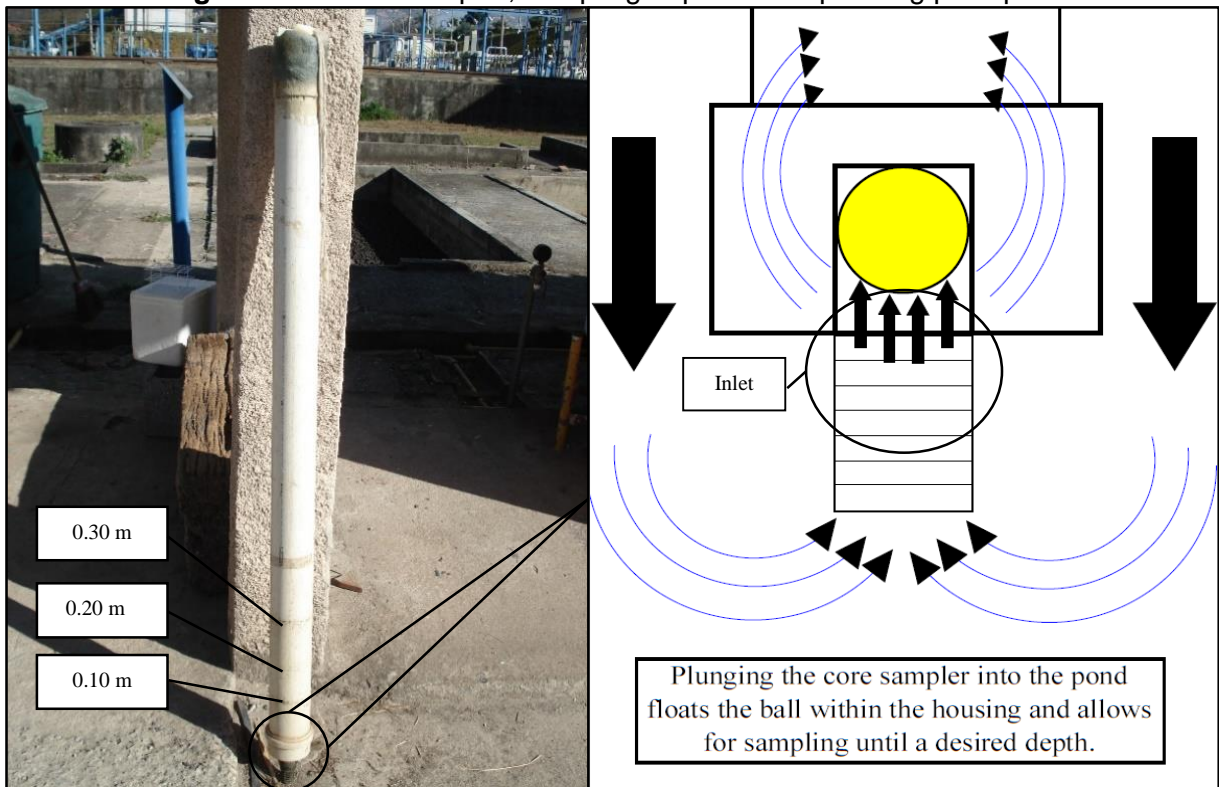


Raw sewage was sampled after preliminary treatment and was then directed to the UASB reactor and the effluent sampled before entering the first pond of the series. The UASB effluent enters the first pond (P_1) and exits at the end. Sampling was done at the outlet of P_1 . The second pond (P_2B) had three sampling points, one at the end of each baffle (P_2B_2 and P_2B_3) and the third at the outlet of the second pond (P_2B_4) (Figure 5.7). Mid-section sampling in the second pond was carried out to evaluate the effect of baffles and shallow. All pond samples were collected with a core sampler (see subsection 5.3.3) up to a depth of 0.30 m. The seventh and final sampling point was at the outlet of the graded rock filter (GRoF), i.e., the final effluent (Figure 5.7).

5.3.3. Core sampler

Pond sampling along the liquid column was done using a core sampler (Figure 5.8). It was made with polyvinyl chloride (PVC) pipe with 0.20 m diameter and 1.50 m height. The sampler allowed for sampling at various depths, but for this research the maximum sampling depth was 0.30 m because of sludge disturbance occurring when the sampler reached depths greater than 0.30 m (the core sampler sometimes came in contact with the sludge layer at the bottom of the pond, especially in P_1). Other sampling depths of 0.10 m, 0.20 m and 0.30 m were performed (Figure 5.8) (subsections 5.4 and 5.5).

Figure 5.8 - Core sampler, sampling depths and operating principle.



The operating principle of the core sampler is simple, as shown in Figure 5.8. As the sampler is plunged into the pond, a small sphere floats to the top of the housing and allows wastewater to be sampled until a desired depth (0.10, 0.20 or 0.30 m). After reaching the desired depth, the core sampler is pulled up and the sphere now covers the inlet of the sampler because of the weight of the wastewater now above it. This creates a water tight seal, trapping the sample within the PVC pipe. The top of the sampler is open, allowing for the sample to be poured into a beaker or recipient for analysis or experiments (Figure 5.9).

Figure 5.9 - Pouring the effluent from the core sampler into beaker and recipient after sampling.



5.4. Solar radiation measurement

5.4.1. Measuring principal

Solar radiation (solar irradiance) was recorded with two different sets of sensors. One set was permanently placed on the ground surface, continuously recording total solar irradiance (TSI) over 24 hour periods. The other set of sensors were placed at different depths in the second pond, also continuously recording the energy from different wavelengths over 24 hour periods. This resulted in modelling attenuation rates and evaluating the extinction of the different wavelengths. Recording solar radiation was done in second pond of the series, with the exception of it being used in the first pond of the series on some days to aid another PhD student's research.

5.4.2. Total solar irradiance (TSI) at ground level

A meteorological station from DAVIS INSTRUMENTS[®] was purchased and placed onsite for continuous weather monitoring. The Wireless Vantage pro 2 Plus[®] (Figure 5.10) recorded the following environmental data over the research period, wind speed and direction, temperature,

humidity, rainfall, atmospheric pressure, UV index and total solar irradiance (TSI). It was set up at the beginning of July 2014 and data was recorded until November 2015. Of the many parameters recorded only TSI and atmospheric pressure were used for this research. The station was installed according to recommendations made by the manufacturer and Brazilian legislation for weather monitoring.

Figure 5.10 - Meteorological Station installed at CePTS for onsite monitoring of various environmental parameters.



TSI, expressed in $\text{W}\cdot\text{m}^{-2}$, is the amount of total sunlight or visible light (watts) per unit area (m^2) recorded at the meteorological station. Recorded intervals were set for every 10 minutes. The solar irradiance sensor captured radiation between 300 nm and 1100 nm, accounting for the whole PAR and UV-A range, while only partially accounting for the UV-B wavelength (280 nm – 315 nm). The amount of solar radiation reaching the top of the atmosphere is made up 50% of infrared radiation, 40% of visible radiation and 10% of ultraviolet radiation. Radiation decreases in strength as it penetrates the atmosphere and reaches the surface with about 43% infrared radiation, 44% visible radiation and 3% of ultraviolet radiation (Qiang, 2003). These percentages are similar to those reported by Shilton (2005) for UV-B (0.2%), UV-A (5%) and visible radiation (50%) at noon. All data was stored on a datalogger and downloaded to a computer for further analyses on a monthly basis.

Another form of predicting UV-A, UV-B and PAR is to use the same program that Silverman *et al.* (2015) used, known as a Simple Model of the Atmospheric Radiative Transfer of Sunshine (SMARTS – global horizontal irradiance). The program was developed and tested by Gueymard (1995, 2001). Surface UV-A, UV-B and PAR was predicted for each hour (9:00 – 16:00) based on atmospheric pressure data for each hour and day from the meteorological station and input to SMARTS. The parameters are presented in APPENDIX I. SMARTS considers 24-hour and seasonal changes in light intensity, but assumes clear-sky conditions and does not account for differences in atmospheric conditions or cloud cover. Percentages of UV-A, UV-B and PAR were calculated based on SMARTS predictions and TSI data acquired from the meteorological station.

5.4.3. Depth profiling of solar irradiance in a shallow maturation pond

The environment in maturation ponds can be considered harsh for any type of electronic equipment because of high algal population and pH values. Solar irradiance sensors placed in this environment needed to be robust, watertight, rustproof and easy to clean and operate. Measuring solar radiation in maturation ponds helped determining attenuation rates, extinction rates, penetration depths and received irradiance doses for *E. coli* disinfection in the natural environment.

Three different sensors, UV-A (SKU 421/I 43814), UV-B (SKU 430/I 43815) and PAR (SKL 2623/I 43817), a data logger (Datahog 2[®]) and a levelling plate were acquired from SKYE INSTRUMENTS[®] (Figure 5.11 (A)) and used to measure radiation in *P₂B*. The PAR sensor captured radiation from 400 to 700 nm, and UV-A and UV-B sensors detected radiation between 315 to 400 nm and 280 to 315 nm, respectively. A concrete base was built and four helical ridge rods with bolts were embedded into it.

Each of the three sensors recorded irradiance in the datalogger (DATAHOG 2[®]). The data was downloaded with the SKYELYNX COMMS[®] program onto a computer via cable, for analysis (Figure 5.12 (A and B)). This software allowed logging intervals to be set in unison with the data recorded from the meteorological station (Table 5.2). Therefore, solar irradiance was also recorded every 10 minutes.

Figure 5.11 - (A) UV-A, UV-B and PAR sensors, data logger and levelling plate from SKYE INSTRUMENTS®; **(B)** Concrete base with helical ridge rods and bolts for height adjustment.

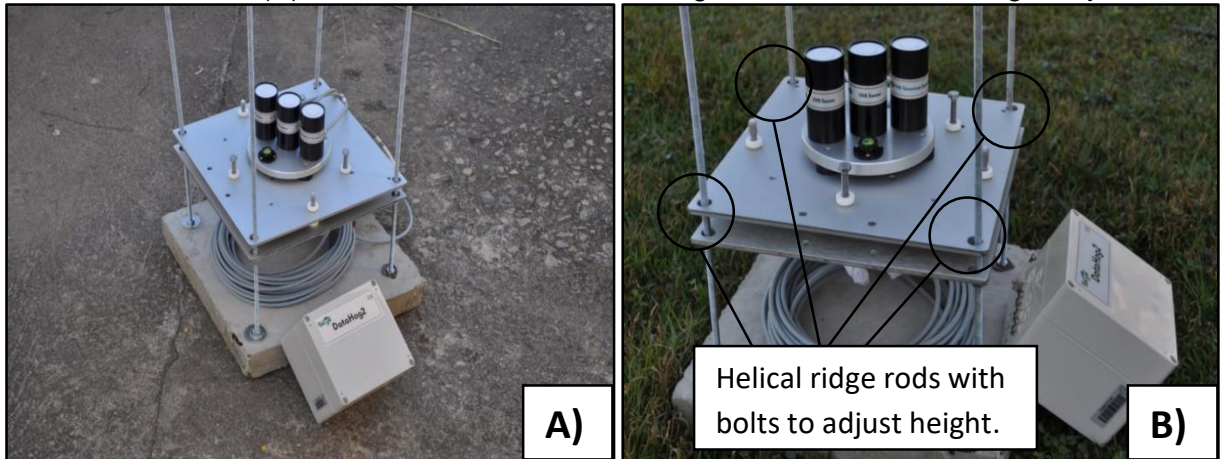
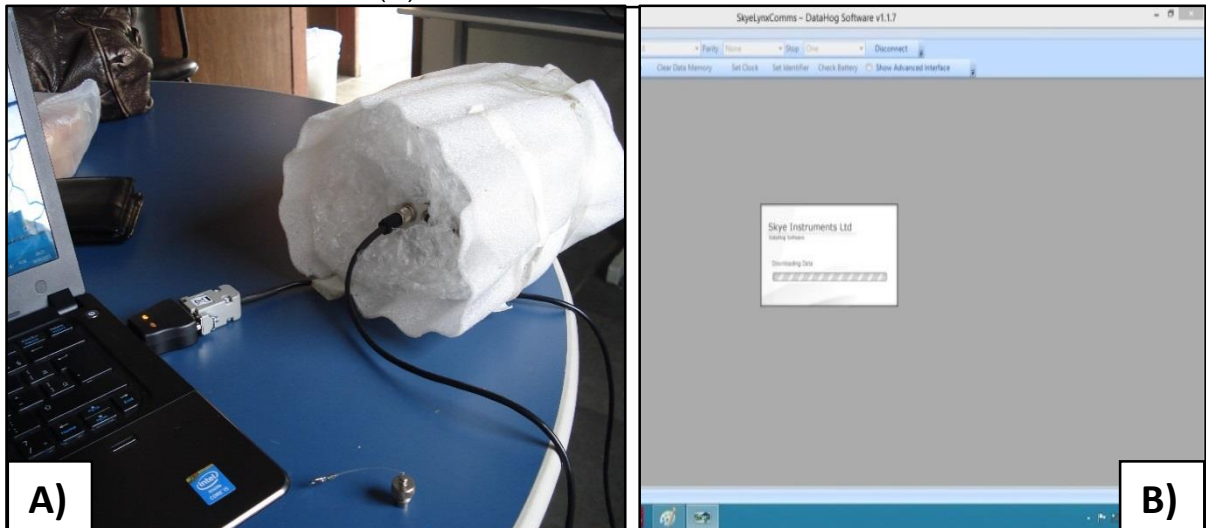


Figure 5.12 - (A) Downloading solar irradiance data from the datalogger on to a computer; **(B)** SKYELYNX COMMS® software.



The PAR sensor captured and measured solar irradiance in $\mu\text{moles.m}^{-2}.\text{s}$, while UV-A and UV-B captured and measured irradiance in W.m^{-2} . The desired unit for solar irradiance and used in the S.I. is W.m^{-2} , therefore PAR units were converted from $\mu\text{moles.m}^{-2}.\text{s}$ to W.m^{-2} . By dividing each PAR irradiance value measured and stored on the datalogger by 4.6 (information and conversion rate provided by SKYE INSTRUMENTS®), the results were converted to W.m^{-2} . The sensors were fixed to a levelling plate to ensure that they were level with the bottom of the pond (Figure 5.11 (A and B)). The sensors were fitted tightly on the levelling plate, ensuring that no movement was possible. The levelling plate slid along the stand made out of a concrete base and iron rods as sliding poles, allowing height adjustments to be made by screwing and unscrewing bolts (Figure 5.11 (B)). This was important to control the height the sensors were placed for continuous monitoring (Figure 5.14).

Sensor placement depth varied on a weekly basis as shown in Table 5.2 (example of two months of continuous monitoring), Figure 5.13 and Figure 5.14. Sensors were placed at points P_2B_2 and P_2B_3 during the research, prevailing during longer periods at P_2B_3 (Figure 5.14).

Table 5.2 - Monitoring Programme for UV-A, UV-B and PAR at different depths over a time frame.

Month	Sampling Days	Time monitoring per day (hours)	Sampling interval (minutes)	Depth profiling – from water surface of pond (m)	Parameters measured in the field
1 st month	1 st week	24	10	0.05-0.10*	UV-A, UV-B and PAR
	2 nd week			0.15-0.20*	
	3 rd week			0.30	
	4 th week			0.05-0.10*	
2 nd month	1 st week			0.15-0.20*	
	2 nd week			0.30	
	3 rd week			0.05-0.10*	
	4 th week			0.15-0.20*	

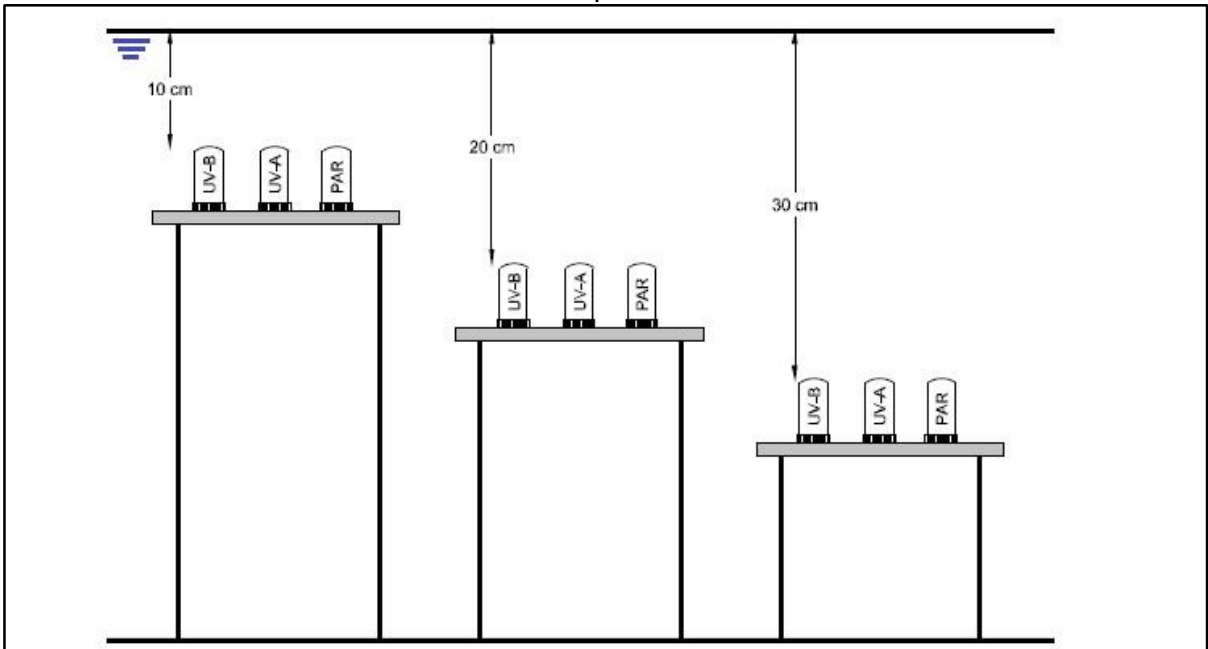
*depth placement changed every time for different weeks in order to obtain more points throughout the depth and produce a better profile

After reaching the end of the 3rd week of the 1st month and starting on the 4th week of the same month, the sensors were placed at the same depth as that of the 1st week of the first month, as shown in Table 5.2. Consequently, when the 4th week ended, this corresponded to the end of the 1st month, and the sensors were placed at the same level as the 2nd week of the first month, but now corresponding to the first week of the second month, as shown in Table 5.2. This did not interrupt the monitoring cycle and allowed to have data from different depths, during different weeks, in different months, and consequently not only results for 0.05/0.10 m depth monitoring during the first week of every month. The sensors only recorded data at a given depth and time, meaning that data recorded from the three different waves from a particular week are in relation to one depth only.

Figure 5.13 - UV-A, UV-B and PAR sensors placed at P_2B_3 at 0.05 m in depth for continuous monitoring over one week.



Figure 5.14 - Level changing and heights of UV-A, UV-B and PAR sensors for monitoring in the pond.



Recording long-term solar irradiance at various depths allowed to produced predictive curves for attenuation rates and minimum irradiance until 0.30 m depth.

Turbidity was measured at least twice a week, up to a maximum of five times a week (an average of four times a week). Sampling was done every hour, either in the morning from 08:00 to 12:00 h or in the afternoon from 12:00 to 16:00 h with the core sampler. Sampling was done up to the depth of the solar irradiance sensors.

5.4.4. Cleaning and upkeep of the sensors

Algae and biofilm accumulated rapidly on the levelling plate and sensors. Sensors had to be cleaned at least once a week (twice a week is recommended) with a soft damp cloth and distilled water to remove algae and biofilm, and the levelling plate was cleaned once a week. Ideally, sensors should be cleaned every day to allow maximum passage of light through the lenses and remain as shown in Figure 5.15 (A). The closer the sensors were to the surface of the pond, the greater algal and biofilm accumulation was; e.g., sensors placed at 0.30 m in depth accumulated less algae and biofilm probably due to the amount of light reaching that depth opposed to 0.05 m where greater accumulation was noticed, as shown in Figure 5.15 (B) after just three days in the pond. Cleaning the sensors at least once or twice a week guaranteed that they on average received the maximum amount of solar irradiance possible over the research period.

Figure 5.15 - (A) Clean sensors before placed in the pond; (B) Algal and biofilm accumulation after three days in the pond at 0.05 m.



5.4.5. Attenuation coefficients (K_a) estimated and modelled with turbidity and \log_{10} of turbidity for predicting irradiance attenuation.

Light attenuation coefficients (K_a) for PAR, UV-A and UV-B were calculated based on the pairs of irradiance and depth, in which $I_{a(z)}$ were the mean values of irradiance and Z the depths in which irradiance was measured. Equation 4.36 was used. For the surface of the pond ($Z=0$ m), irradiance for the three wavelengths was estimated based on the percentages (UV-A = 5%; UV-B = 0.2%; PAR = 50%) recommended by Shilton *et al.* (2005) and multiplied by the TSI reaching the surface ($I_{a(0)\%}$). Surface irradiance was also estimated by the SMARTS program ($I_{a(0)SMARTS}$). Several pairs of I-Z (0.0 m, 0.10 m, 0.20 m and 0.30 m) were used to estimate

K_a through the non-linear least squares method, and applying the solver tool in Excel[®] for finding the K_a value that minimized the sum of the squared errors. Mean values were used.

As suggested by Bolton *et al.* (2011a), turbidity was also measured during the whole experiment. It was measured every hour for four hours on selected days, either in the morning or afternoon by using the column sampler to sample up to the depth of the solar sensors. Turbidity values were condensed into one day (09:00 – 16:00) and used in both attenuation equations containing turbidity (TUR) and the transformed values of turbidity ($\log_{10}\text{TUR}$).

5.5. *Escherichia coli* disinfection in a shallow maturation pond

The main interest of this research was to evaluate the effect of solar radiation on *Escherichia coli* (*E. coli*) at different depths in the pond and over a long period of time. All samples came from the outlet of the first pond (P_1), meaning that some degree of disinfection and photo-repair had already occurred. *E. coli* disinfection during the experiments was associated to the solar-mediated mechanism by reducing the effect of other mechanisms affecting *E. coli* disinfection, such as attachment/sedimentation, predation and starvation and algal toxins. This was done by isolating samples and solely exposing them to solar radiation. On the other hand, control over other parameters such as pH, dissolved oxygen (DO) and temperature (T) could not occur since every day presented different values. These values were probably sustained during each experiment and their participation was considered for either enhancing or decreasing disinfection, although it is not clear whether DO and pH levels increased in the isolated environments (subsection 5.5.2). DO and pH levels varied considerably when morning experiments were compared to afternoon experiments. This part of the research used the effluent from P_1 and was conducted in the second pond of the series (positions P_2B_2 and P_2B_3).

5.5.1. *E. coli* disinfection rate at different depths in a shallow maturation pond

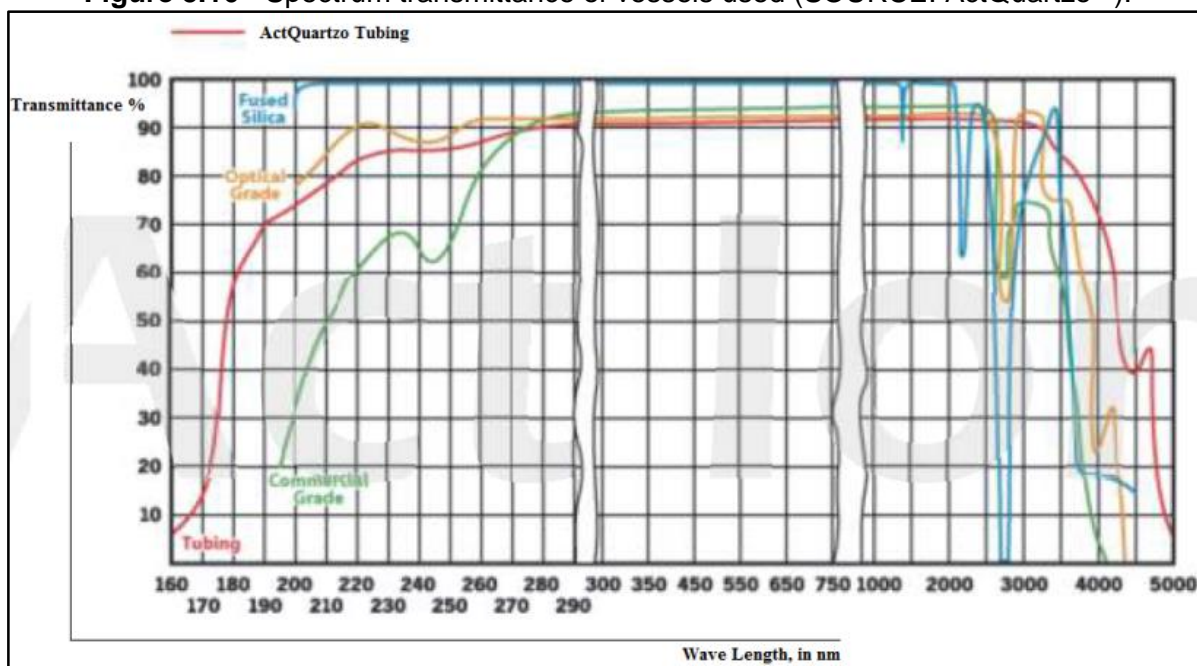
E. coli disinfection in a maturation pond is expected to decrease as depth increases since solar radiation is limited or absent from a certain depth downwards. Solar-mediated disinfection is more intense in the top layers of maturation ponds, especially from 10:00 to 16:00 at the site. *E. coli* disinfection efficiencies associated with solar radiation at different depths and over different time intervals in a controlled and isolated environment produced actual results, attenuating or completely eliminating other mechanisms while promoting a certain amount of control of the sample used. Vessels were used to create the isolated environments inside the

pond. The vessels were placed at different depths within P_2B , therefore quantifying different disinfection depths for *E. coli* regarding the solar radiation received.

5.5.2. Vessels (isolated environments) used to conduct the experiments

The vessels used for the experiment needed to be airtight and watertight (no exchanges with the external environment could take place), as well as allowing solar radiation to pass through without being distorted, reflected or attenuated. Normal glass or plastic does not allow a great amount of radiation to pass (PAR and Infrared passes), blocking all of the UV range. Borosilicate is also transparent but only allows PAR and a small part of UV-A to pass (380 to 720 nm)). This was a setback because these materials were relatively cheap. To work around this problem, specially manufactured vessels by ACTQUARTZO® (<http://www.actquartzo.com/>) were acquired for the experiments. The vessels were made of 99.995% silicon dioxide, commonly known as quartz (Figure 5.17 (A)), and therefore allowed more than 90% of solar radiation within the 270 to 3000 nm range to pass through (Figure 5.16).

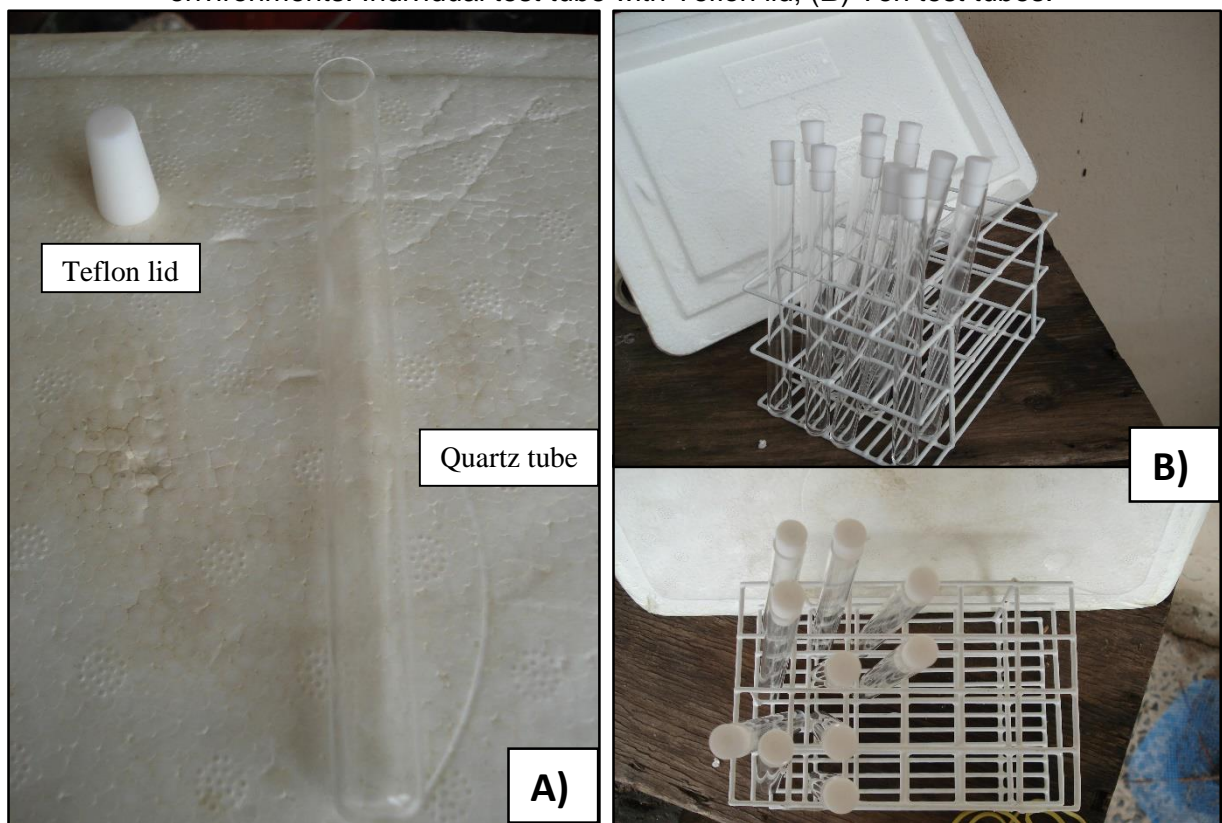
Figure 5.16 - Spectrum transmittance of vessels used (SOURCE: ActQuartzo®).



The vessels also needed to be sterilised in an autoclave that reaches high temperatures and pressures to destroy any residual bacteria from previous experiments. This ruled out the use of any transparent plastic bottles because it could damage and tarnish the plastic.

Initially one vessel with a capacity of 100 mL was considered, but this did not guarantee that the sample inside the vessel was evenly exposed to solar radiation during the experiments as opposed to numerous smaller vessels. Using various vessels was the best solution (Figure 5.17 (B)), i.e., vessels were distributed over a horizontal plane in P_2B and not concentrated in one place (which would occur with one 100 mL vessel), therefore maximising solar radiation exposure to each individual sample. Thirteen 10 mL test tubes were acquired totalling 130 mL. Teflon lids completed the tubes and created an airtight and watertight environment, as well as being anticorrosive (Figure 5.17 (A)). Because the lids occupy a portion of the tubes (around 2 cm in length), each tubes capacity was reduced to around 90 mL. Therefore, twelve tubes were used for each experiment, totalling 108 mL.

Figure 5.17 - (A) Vessels for conducting experiments for *E. coli* disinfection in isolated environments. Individual test tube with Teflon lid; (B) Ten test tubes.



Each tube was 130 mm tall and 10 mm wide (Figure 5.17), characterising layers of 10 in the pond.

5.5.3. Submerging and sampling of the vessels in the pond

The watertight and airtight test tubes were filled with P_1 effluent and submerged at different depths inside Pond 2 for a given time interval of the day. Each tube was always at the same depth as the other for each individual experiment. The experiments were conducted two to four days a week, at least one day in the morning and the other day in the afternoon, or two days in the morning and two days in the afternoon. Morning experiments started at 08:00 a.m. and finished at 12:00 noon, totalling four hours of exposure to solar radiation. In the afternoon, sample exposure time was from 12:00 to 16:00 (also four hours).

For each experiment three samples were collected (Figure 5.18):

- **BEFORE** sample – not subjected to solar radiation exposure in the test tubes and served as the initial concentration of *E. coli* before exposure;
- **AFTER** sample – subjected to solar radiation exposure in the test tubes for four hours;
- **DARK CONTROL** sample – not subjected to solar radiation only to temperature at the same depth and time period as the **AFTER** sample.

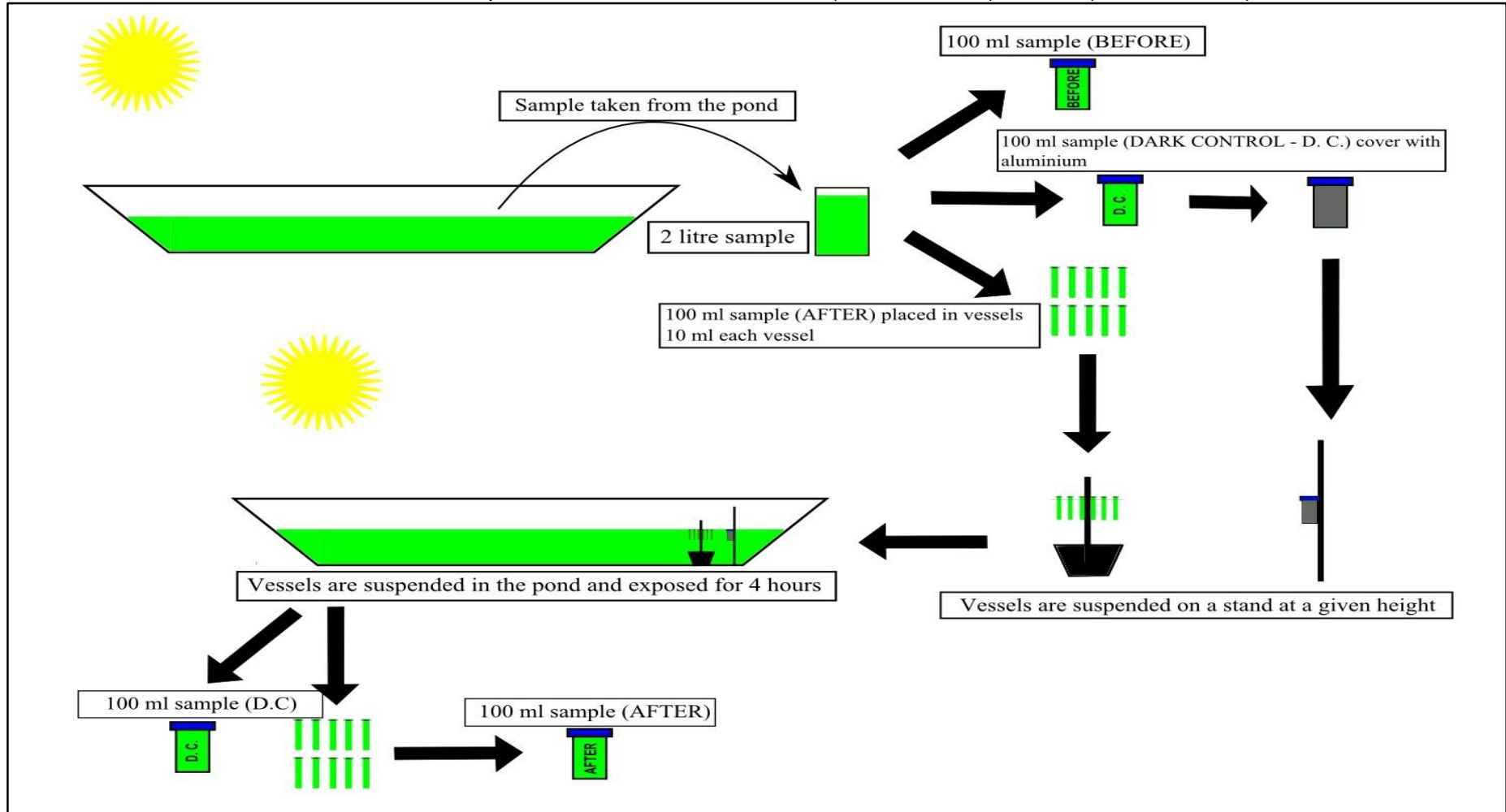
A two litre grab sample was collected from the outlet of P_1 (Figure 5.7) with the core sampler until 0.30 m in depth. The two litre sample was mixed and 100 mL were poured into a sterilised container and placed into a cooler box containing icepacks for refrigeration and preservation. This sample was the **BEFORE** sample because it was not subjected to any solar radiation exposure in the test tubes in P_2 . Another 100 mL was poured from the two litre grab sample into the test tube vessels (Figure 5.18) and closed with the Teflon lids. The test tubes hung on a stand with a net plane (Figure 5.19 (A)), all remaining at the same level and depth within the pond during the experiment. After four hours of solar radiation exposure at a given depth, the stand with the test tubes was removed from the pond and the sample in the test tubes was poured into a sterilised vessel and placed into the cooler box containing icepacks for refrigeration and preservation. This was the **AFTER** sample. The **DARK CONTROL** sample consisted in pouring 100 mL into a sterilised vessel (0.10 cm in height) covered up with aluminium foil (Figure 5.21). The **DARK CONTROL** sample was attached to a PVC pipe with elastic bands and also hung in the shallow maturation pond at the same depth and level as the test tubes, staying submerged during the same four hour period (Figure 5.18). The aluminium foil was to block all solar radiation from entering the sterilised vessel. During the experiment, the test tubes

with the stand and the dark control sample attached to the PVC pipe were placed either at sampling point P_2B_2 or P_2B_3 , the latter being the most used (Figure 5.7). When sampling and pouring the effluent from the two litre sample into the other vessels for the experiment, care was taken to do it in the shade and avoid any direct sunlight which could influence overall results.

The **BEFORE**, **AFTER** and **DARK CONTROL** were analysed within six hours after sampling (APHA. AWWA. WEF. – Standard Methods (2005)).

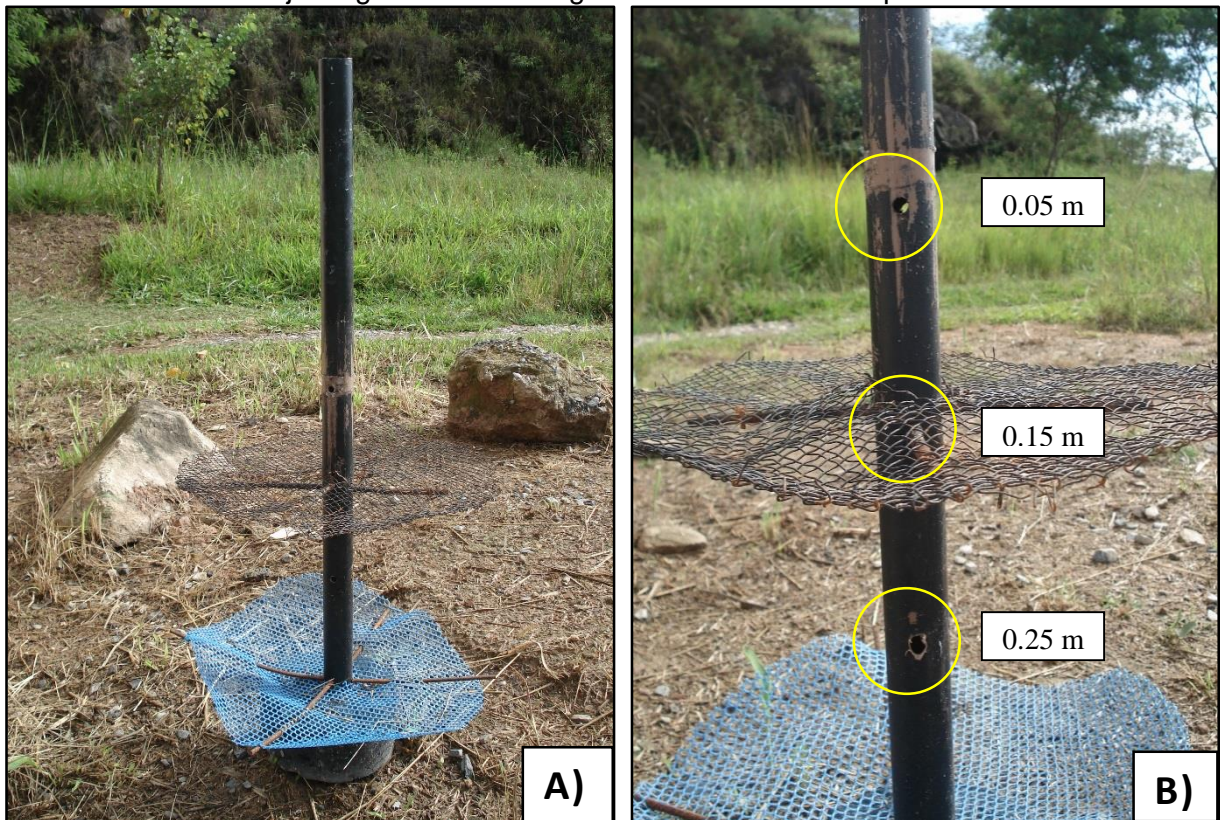
The remaining effluent from the two litre sample (1700 mL left), was analysed onsite for a few variables that could enhance or affect bacterial disinfection: dissolved oxygen (DO), pH, turbidity and temperature.

Figure 5.18 - Flowsheet of the steps for the experiment in the shallow maturation pond with vessels exposed to solar radiation for four hours. The vessels were suspended in Pond 2 either at P_2B_2 (end of baffle 1) or P_2B_3 (end of baffle 2).



The stand for hanging the test tubes was made of 1.20 m long PVC pipe anchored onto a concrete base (Figure 5.19 (A)). A net made of iron and painted black (which was later substituted with a stainless steel net, therefore avoiding rust) was used to hang the test tube vessels and distribute them across the horizontal plane in different places (Figure 5.20). The metal net had fifteen holes drilled in it to hang the test tubes in different places. Levels of the net changed every 0.10 m on the stand because of holes drilled in the PVC pipe (Figure 5.19 (B)), where the first hole at the top was located roughly 0.05 m from the surface of the pond (Figure 5.19 (B)). The following holes were drilled roughly at 0.15 m and 0.25 m from the ponds surface. The net level was not always precise because the ponds water level always varied week to week. Therefore, individual level adjustments of the test tubes were made depending on the experimental depth.

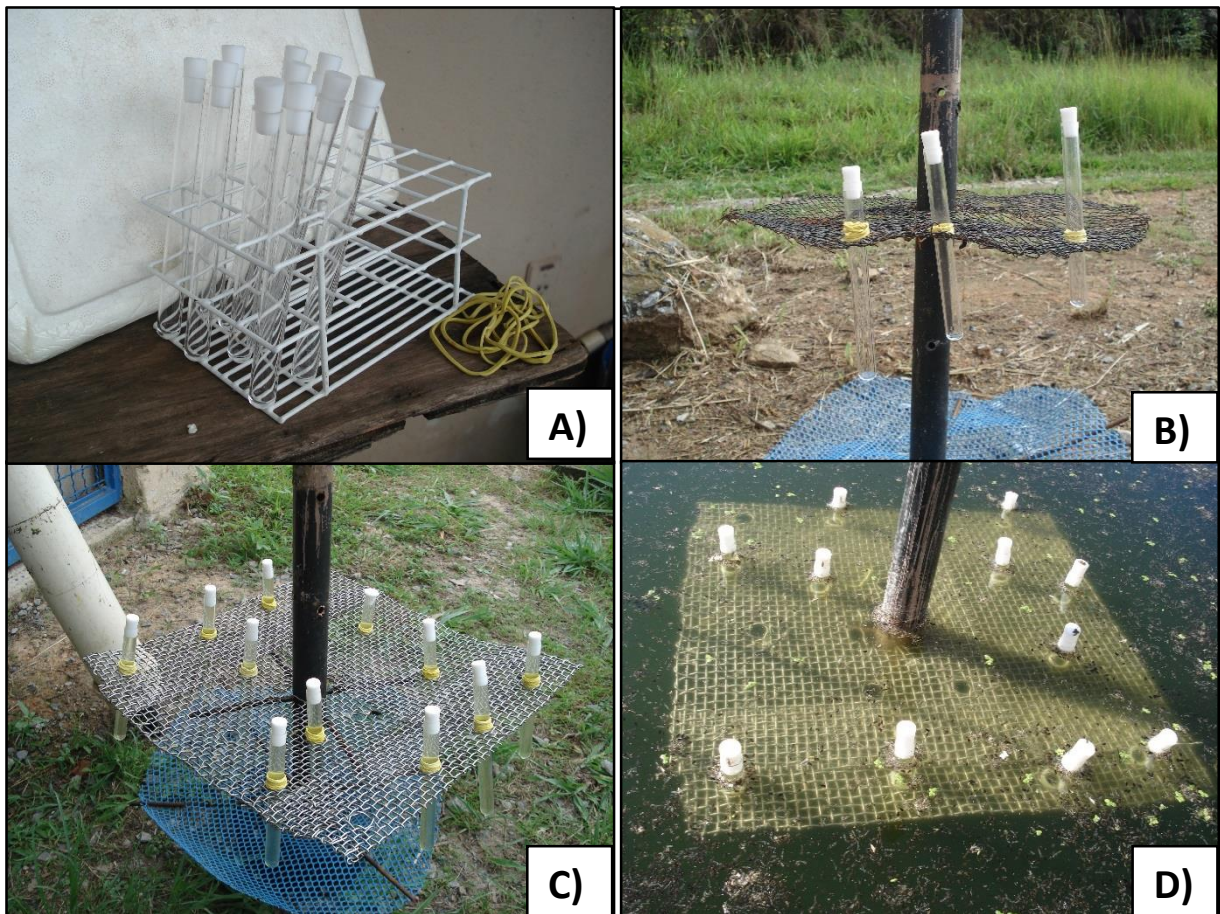
Figure 5.19 - (A) Stand and net plane used for hanging the vessels and; (B) Holes for adjusting the vertical height of the horizontal net plane.



Every day the water level in P_2B changed due to flow fluctuations, rainfall and other events but maintained an average depth of 0.44 m. The test tubes were placed to accompany the water level changes because the metal net was always fixed. The test tubes were suspended and kept vertically in place on the net by wrapping elastic bands around them (later, orthodontic elastic

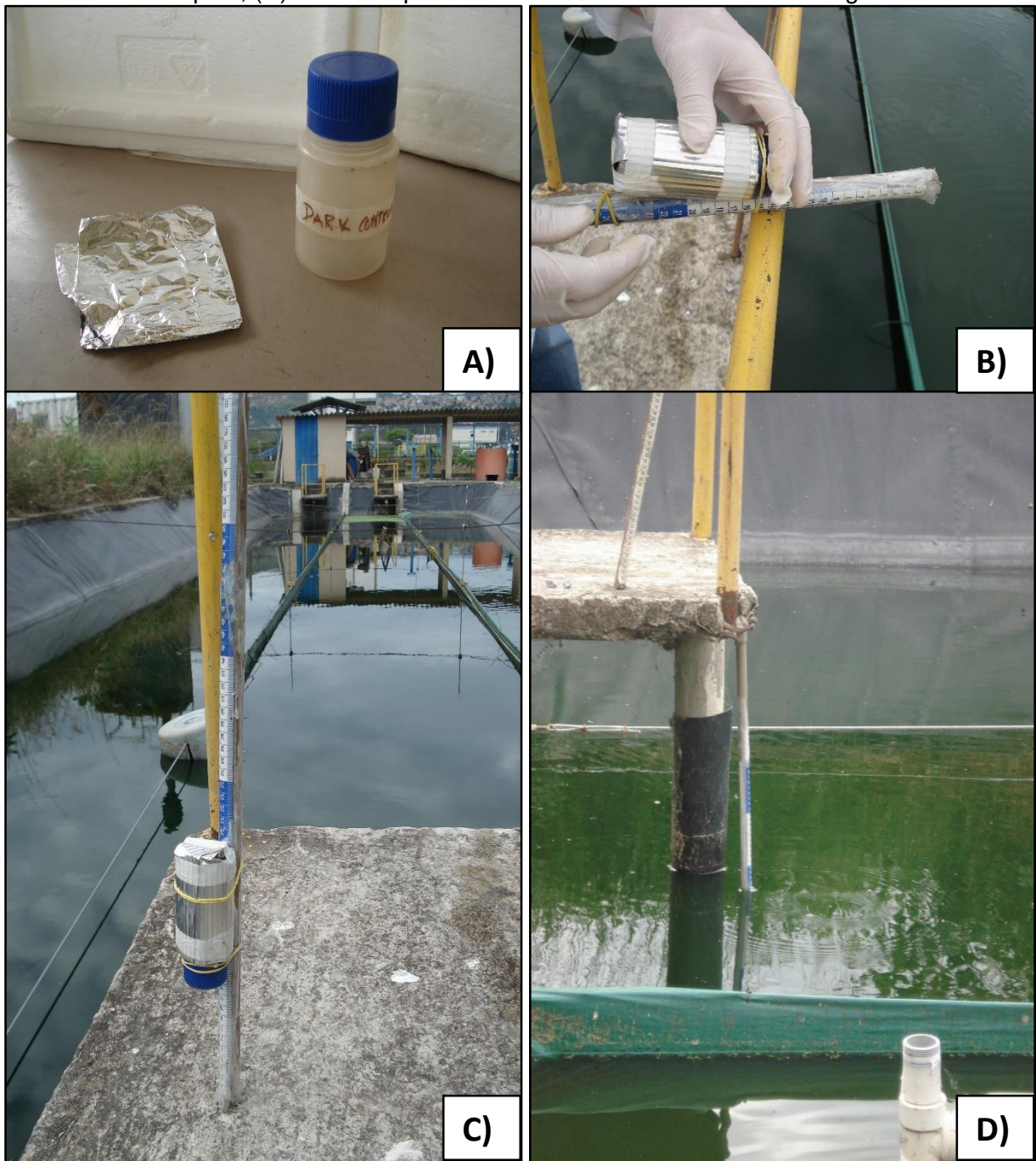
bands were used and proved to be easier to wrap around the test tubes and lasted longer), widening the area of the test tube and allowing for changeable heights of the test tubes as well (Figure 5.20 (A)). This simple solution minimised the amount of sunlight that could eventually be blocked by any other structure used to suspend the test tubes, as well as enabling changeable heights of the test tubes (Figure 5.20 (B)). During each experiment the test tubes were suspended at the same height (Figure 5.20 (C)) with the net plane set at one height. The apparatus was then submerged in P_2B_2 or P_2B_3 (Figure 5.7 and Figure 5.20 (D)) and remained there for four hours.

Figure 5.20 – (A) Test tubes and elastic bands; (B) Elastic bands wrapped around the test tubes and suspended at different levels and the net plane at a constant level; (C) All test tubes suspended on the same net plane with the same height adjustments before submerging in P_2B ; (D) The apparatus (test tubes and stand) submerged in P_2B , profiling 0.10 m disinfection.



The **DARK CONTROL** vessel was an ordinary 100 mL flask (height: 0.10 m) wrapped up with aluminium foil (Figure 5.21 (A)). It was attached to a PVC pipe with elastics (Figure 5.21 (B, C)) to mimic the same depth as the test tubes and submerged also at P_2B_2 or P_2B_3 (Figure 5.21 (D)).

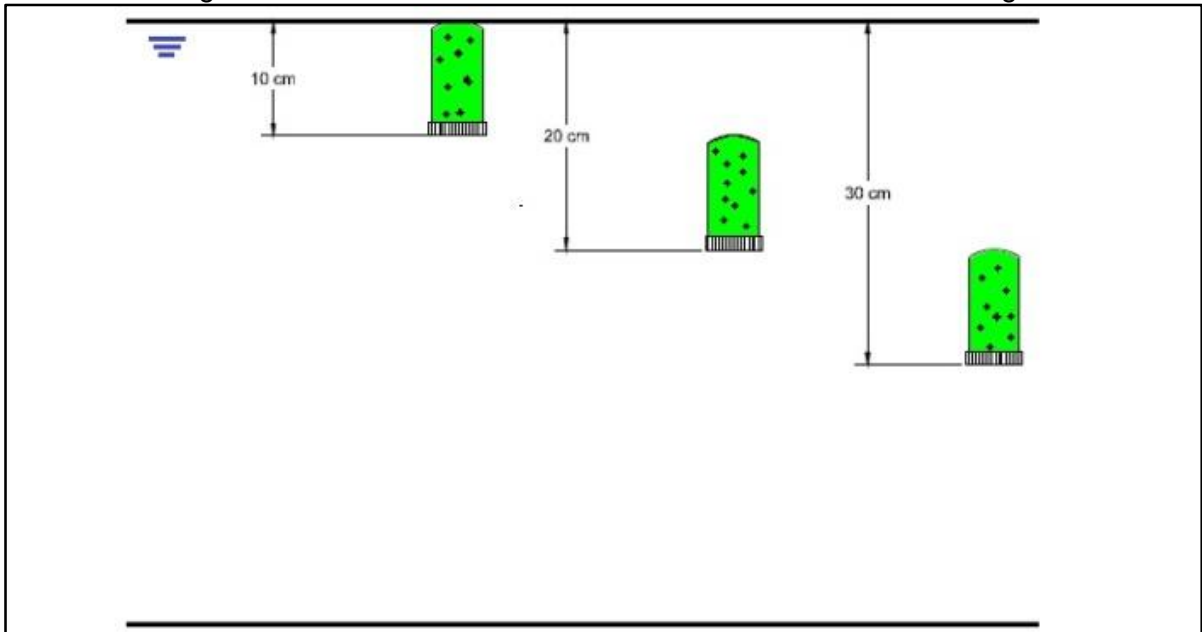
Figure 5.21 - (A) Vessel and aluminium foil used for dark control tests; (B) Attaching the container to the PVC pole; (C) The container covered with the aluminium sheet and attached to the PVC pole; (D) The PVC pole and the dark control vessel submerged in P_2B .



E. coli disinfection and dark control depth profiling were monitored up until 0.30 m and divided into three different layers of 0.10 m (Figure 5.22), i.e., 0.10 m = 0 to 0.10 m; 0.20 m = 0.10 to 0.20 m; and 0.30 m = 0.20 to 0.30 m. The test tubes were 0.13 m tall, however the teflon lid occupied 0.02 m of the tube, leaving 0.11 m to be filled with effluent from P_1 . Each depth

profile received different strengths and wavelengths of solar radiation at different times and different atmospheric conditions, consequently affecting disinfection rates.

Figure 5.22 – Depth profiling up to 0.30 m with three different 0.10 m profiles evaluated for determining *E. coli* disinfection because of the effect of different wavelengths in P_2B .



Sampling of the medium around the test tubes was done over the course of the four-hour exposure with the core sampler up until the depth of the bottom of the tubes (and top of solar sensors). This was to characterise turbidity at the time of the experiments to aid modelling irradiance attenuation. Sampling of the medium was done every hour, totalling four different readings for turbidity for each experiment.

5.6. Research phases and monitoring routine

The research was divided into two phases. Each phase consisted of different hydrodynamic interventions in the second pond. Monitoring of the whole system during the 1st phase was vital to validate the 2nd phase and compare results from both phases. The main hydraulic interventions are listed below and detailed subsequently:

- 1st phase: Pond 2 with only the longitudinal baffles (as described so far);
- 2nd phase: Pond 2 with longitudinal and “vertical baffles”.

Phase 1. After upgrading the treatment line, the 1st phase consisted in; (i) monitoring the whole system for the variables mentioned in section 5.3.1; (ii) characterising penetration depths of both UV and PAR waves; (iii) determining *E. coli* disinfection coefficients at different depths; (iv) and a better understanding of the second pond’s hydrodynamics for vertical mixing and stratification. Preliminary results (over two months) served to set up the monitoring phase, deciding on the different depths for placing the sensors and time intervals for conducting the test tube/vessel experiments. This was done by placing the sensors at different depths receiving radiation and determining extinction depths of UV-A, UV-B and PAR. It was subsequently implemented as standard and monitoring solar radiation continued and was joined by the test tubes experiment. This characterised the three different waves (UV-A, UV-B and PAR) and attenuation coefficients (K_a) were calculated, as well as, wavelength extinction, minimum and maximum energy received at different depths, overall behaviour of each wave at different depths and modelling irradiance in accordance with depth, and depth and turbidity. *E. coli* disinfection was monitored during one year and two months for three different depths, therefore characterising different disinfection rates at, the amount of received solar irradiance doses at each depth regarding *E. coli* disinfection, modelling *E. coli* disinfection with measured environmental variables and relating *E. coli* disinfection with various environmental variables. During this period, another experiment was conducted in cooperation with a PhD student (Ricardo Gomes Passos) to understand the hydrodynamics of the two ponds, but emphasising the second pond, with the aid of computational fluid dynamics (CFD). Tracer tests and temperature depth readings were used to determine if stratification and thermal turn-over occurred in the second pond. This part of the research helped understanding the occurrence of stratification in the second pond, therefore short-circuiting and possible reduction of disinfection efficiencies.

Phase 2. The 2nd phase of the experiment consisted in altering the second pond's hydrodynamics by placing vertical baffles in-between the existing baffles and slopes at predetermined distances, based on the data gathered in the 1st phase. This aimed at altering the hydrodynamics in the pond by destratifying the wastewater, reducing short-circuiting and improving disinfection in the second pond, as well as the overall disinfection of the treatment system.

The parameters monitored and analysed during both phases are shown in Table 5.3 and the sampling points are shown in Figure 5.7. The measured and analysed parameters showed the efficiency of the treatment system and the effect of the upgrades made to the treatment system (*P₂B* and GRoF) during both phases. Only bacteriological analyses were done during the 2nd phase.

Table 5.3 - 1st phase and 2nd phase: measurement and analysis of parameters and sample frequency in the treatment system.

Sampling Days	Samples	Parameters measured in the field	Parameters analysed in the laboratory
Once-a-week	<u>Raw Sewage</u>		
	<u>UASB</u> (effluent)	Flow, Depth, DO, pH, EC,	TSS, VSS, FSS, COD and
	<u>P₁</u> (effluent)	Redox Potential, Settleable	BOD (Total + Filtered +
	<u>P₂B₂, P₂B₃ and P₂B₄</u> (<i>P₂B</i> effluent)	Solids, Temperature and Turbidity	Particulate), TKN, Ammonia N, <u>Total Coliforms</u> and <u><i>E. coli</i></u>
	<u>GRoF</u> (effluent)		

Only the underlined units and parameters were measured during the 2nd phase.

5.6.1. 1st Phase

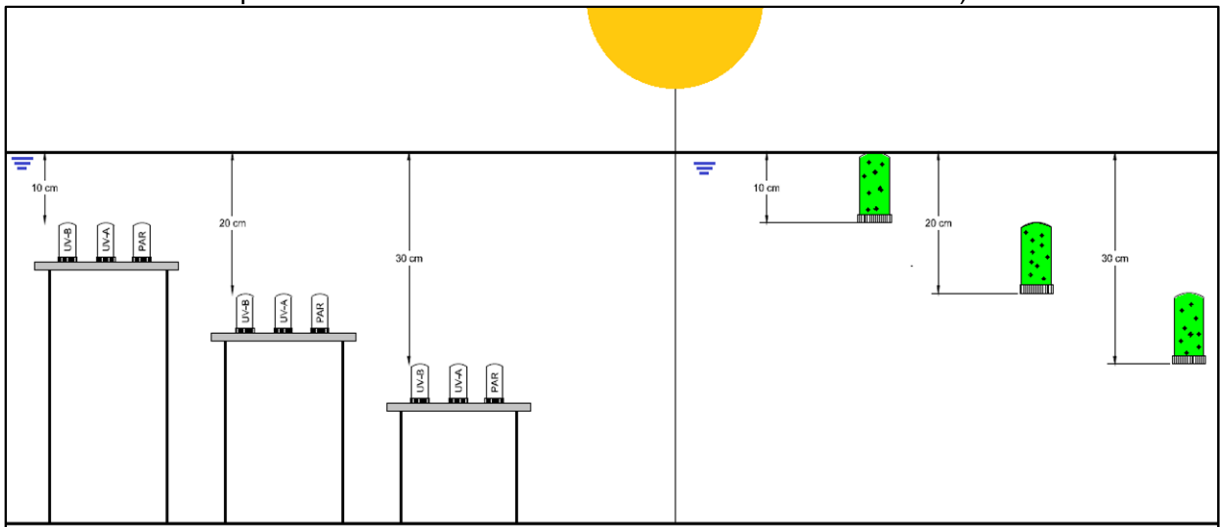
During the 1st phase, the second pond received an upgrade compared to its previous configuration (before this research) and hydraulics were improved with the application of baffles running 90% the length of the pond. The previous third pond was transformed into a graded rock filter (GRoF) to remove reminiscent organic matter (mostly in the form of algae) inflowing from the second pond. The flowsheet of the treatment line was as follows: raw sewage was directed to the UASB reactor, pond 1 (*P₁*), pond two with baffles (*P₂B*) and the graded rock filter (GRoF), all operating in series (Figure 5.5). Operating the second pond with shallow depths aimed to improve some mechanisms associated with *E. coli* disinfection, and consequently pathogenic bacteria disinfection, but HRT was reduced as a consequence.

Solar radiation penetration in the second pond was measured to determine the depth at which the liquid column should be characterised. The sensors were placed at different depths every week to evaluate irradiance received at these depths. After analysing the amount of solar irradiance received at different depths, a protocol for solar radiation monitoring at different depths was implemented (Table 5.2) where a significant amount of PAR was still captured by the sensor at 0.30 m from the surface of the pond. Further depths could not be monitored in the second pond because the sensors and levelling plate as a set are 0.15 m and therefore the set was placed on the bottom of the 2nd pond to measure irradiance received at 0.30 m. Solar radiation measurement was a non-stop activity and produced over one year of continuous solar irradiance data from different depths, only stopping for 30 minutes a week (15 minutes each day) for cleaning the sensors and downloading data from the datalogger (Figure 5.12 and Figure 5.15). A detailed description of the solar sensors and procedures is shown in subsection 5.4. The test tube experiment was initiated for *E. coli* disinfection up to 0.30 m in the second pond based on the results from preliminary solar penetration data.

During solar irradiance monitoring at different depths, the test tubes or vessels were filled with effluent from the first pond and closed with the Teflon lids and suspended in the second pond, creating an isolated environment from the external environment. A detailed description of this procedure is shown in subsection 5.5.

The vessels were hung in the medium at three different depths together with the solar sensors, which were placed at the same level as the bottom of the test tubes in the medium, therefore recording solar irradiance received for each wave at that given depth and the minimum solar irradiance that the medium in the tubes were exposed to (Figure 5.23). Sometimes the solar sensors were placed at intermediate depths (0.05 m and 0.15 m) to collect solar irradiance data, especially for UV-A and UV-B, to draw a better depth profile of these two waves (Table 5.2). For each *E. coli* disinfection test tube experiment there was a **BEFORE**, **AFTER** and **DARK CONTROL** sample. The experiment (test tubes and solar sensors) was performed two to four times a week to collect as much data on morning and afternoon *E. coli* disinfection (Table 5.4).

Figure 5.23 - Solar sensors placed in the pond at the three different depths, accompanied by the suspended test tubes in the pond at the same heights as sensors (sensors lenses were placed at the same level as the bottom of the test tubes).



The grab sample used in the **BEFORE**, **AFTER** and **DARK CONTROL** recipients was analysed in the field for pH, turbidity, DO, EC, REDOX and temperature (Table 5.4) – subsection 5.5, and at every hour after the experiment had commenced a one litre sample surrounding the test tubes and sensors was analysed for turbidity. The sample was limited to the depth that the sensors and test tubes were placed during the experiment, therefore only characterising the medium surrounding and above the sensors and tubes, and not beneath them. The monitoring programme used for quantifying *E. coli* disinfection in a closed environment and the variables used in the experiment and the medium around the vessels and sensors are shown in Table 5.4. Figure 5.23 shows the sensors and vessels placed at three different depths.

Table 5.4 – Monitoring programme used for *E. coli* disinfection during the 1st phase.

Sample	Sampling Days	Time interval (hours)	Sampling interval	Depth profiling (cm)	Variables in the inside environment (test tubes)	Variables every hour in the outside environment	Variables analysed in laboratory
First pond effluent	Once to five times a week	08:00 – 12:00 and 12:00 – 16:00	1 st week	0 – 10	pH, turbidity, DO, and temperature	Turbidity	<i>E. coli</i> (BEFORE , AFTER and DARK CONTROL samples)
			2 nd week	10 – 20			
			3 rd week	20 – 30			
			4 th week	0 – 10			
			1 st week	10 – 20			

5.6.1.1. Hydrodynamic studies during the 1st phase

Hydrodynamic studies were performed in the second pond with computational fluid dynamics (CFD) simulations to detail vertical profiling of stratified layers. Field experiments with tracers and temperature probes were carried out as well. Saline tracers (NaCl) are a low cost form to characterise the HRT and stratified layers quantified with electrical conductivity sensors positioned at the top and bottom of the pond. Temperature probes were also placed near the surface and the bottom of the second pond with the aim to understanding thermal stratification.

This study validated the 2nd phase of the experiment and allowed a better understanding of the hydrodynamics in the shallow baffled maturation pond (0.44 m). This part of the research was conducted together with another PhD student (Ricardo Gomes Passos), who investigated in more detail aspects related to hydrodynamics in the ponds, including CFD modelling.

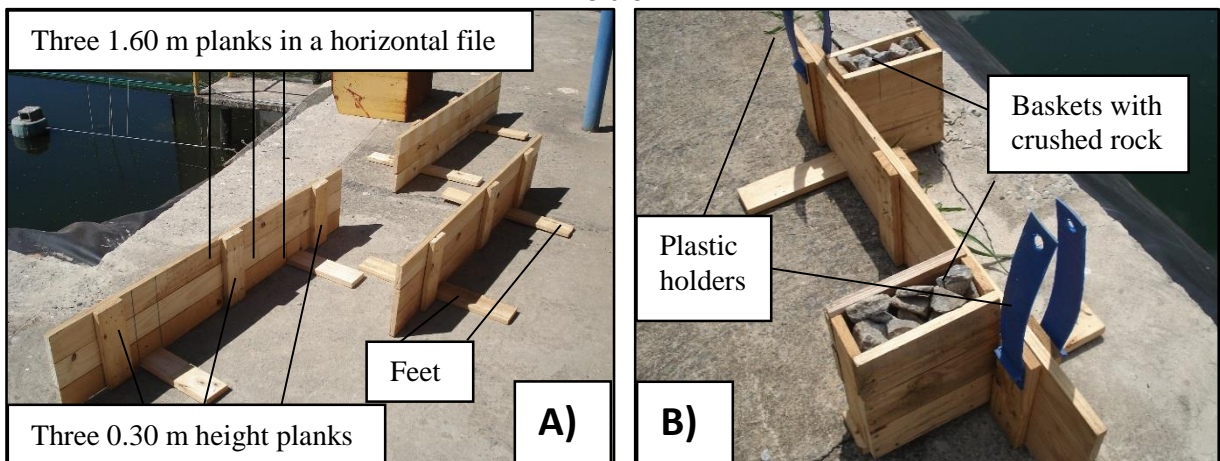
5.6.2. **2nd Phase**

The 2nd phase of the experiment started at the beginning of November 2015 and extended until April 2016. The flowsheet of the treatment was the same as the 1st phase with the difference that the second pond received an upgrade by placing three “vertical baffles” at the bottom of in the first channel (between the inlet and P_2B_2).

5.6.3.1. Vertical baffles: fabrication and placement in P_2B

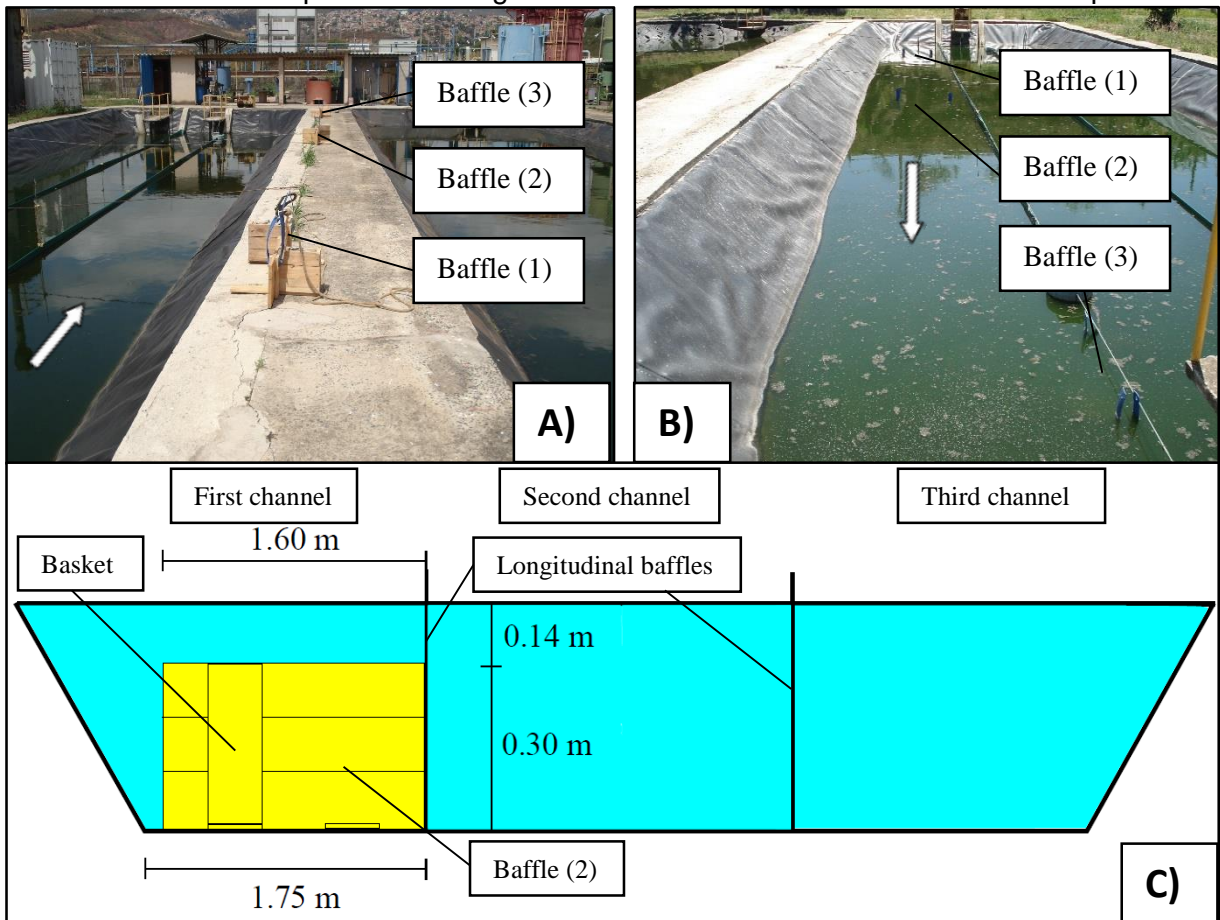
The “vertical baffles” were built from ordinary pallet wood planks as shown in Figure 5.24. Three 1.60 m planks were placed in a single horizontal file (totalling 0.30 m in height) (Figure 5.24 (A)). Two other planks were used as feet for standing the “vertical baffles” up. The “vertical baffles” were weighed down by building two baskets on opposite sides of the feet and filled up with crushed rock (Figure 5.24 (B)). Plastic holders were also incorporated into the baffles in order to lower them into the pond and to make them visible whilst in the pond (Figure 5.24 (B) and Figure 5.25 (B)).

Figure 5.24 - (A) Anatomy of the "vertical baffles" and; (B) baskets with crushed stone to weight down the baffles. Plastic holders to lower the baffles into the pond and make them visible.



The “vertical baffles” were set between and perpendicular to the existing longitudinal baffles (Figure 5.25 (A, B)). The “vertical baffles” were 0.30 m in height and reduced the water level above it to 0.14 m, while promoting vertical mixing/destratification of the medium (Figure 5.25 (C)). The first baffle (1) was positioned 2.0 m from the inlet, the following baffle was placed 12.5 m (2) from the inlet and the third baffle (3) was located on the curve (P_2B_2) (Figure 5.25 (B)). The parameters monitored during the 2nd phase are shown in Table 5.3 and were compared with the 1st phase.

Figure 5.25 - (A) Positioning of the “vertical baffles”; **(B)** and placement of the “vertical baffles” in the first channel of the second pond (between the inlet and P_2B_2); **(C)** and a cross-section of the second pond illustrating a front view of the second “vertical baffle” in position.



5.7. Data analysis

Descriptive statistics were used to prevent the variability of the several variables monitored at different points of the treatment line, as well as during the experiments for solar radiation and *E. coli* depth disinfection. Scatter charts, calculations of central tendencies, dispersion calculation (variance), box-plot graphs and non-parametric tests were performed for comparing independent samples. Wilcoxon-Mann-Whitney U test was used to compare two independent samples and Kruskal-Wallis was for comparing multiple independent samples. Where a significant difference existed, a multiple comparison of mean ranks for all groups was then used. The programs used were Statistica 10[®] and Action Stat[®].

6. RESULTS AND DISCUSSION

Section 6.1 focuses on the overall treatment system for concentrations and removal efficiencies. In Section 6.2, total solar radiation reaching the Earth's surface as well as depth penetration profiling of UV-A, UV-B and PAR, and extinction coefficients regarding depth and turbidity in the second pond are discussed. *E. coli* disinfection concerning depth and environmental variables (DO, pH, turbidity, solar irradiance, temperature, etc.), as well as modelling disinfection coefficients (K_b) considering depth, environmental variables and dark disinfection/repair coefficients (K_d) are covered in Section 6.3. Applied and received doses at different depths for *E. coli* disinfection, vertical profiling (hydrodynamics) and finally, a comparison between both phases (before and after the installation of the “vertical baffles”) for *E. coli* disinfection are also shown in Section 6.3.

6.1. Overall evaluation of the treatment system

Table 6.1 exhibits the mean and median concentrations and standard deviations of the constituents analysed in raw sewage (RS) and in the effluents of each treatment unit. Overall, the systems performance was excellent, with low concentrations for all of the constituents, especially when considering the low hydraulic retention time (HRT) for a natural treatment system. Each constituent is discussed individually in detail in the following subsections. Table 6.2 shows the mean and median environmental variables in each treatment unit, as well as in the RS. Intermediate points in the 2nd pond (P_2B_2 and P_2B_3) are shown to quantify the effect of the baffles. The ponds remained aerobic during the whole period and the UASB reactor and GRoF presented an anaerobic environment. Table 6.3 presents median removal efficiencies for each individual treatment unit, including intermediate points in the 2nd pond (P_2B_2 and P_2B_3) for coliforms and *E. coli*, with the same objective as mentioned above. Overall cumulative removal efficiencies from raw domestic sewage (RS) by pond 1 (P_1), pond 2 (P_2B_4) and the graded rock filter (GRoF) are also shown. Regarding organic matter, low concentrations were observed in the final effluent and are attributed to the GRoF as the final polishing step of the treatment line, therefore proving to be an excellent addition to the pond system. Overall, removal efficiencies were excellent for biochemical oxygen demand removal (BOD) and *E. coli*. *E. coli* removal efficiency in the 2nd pond was not as good as expected, seeing that shallow depths combined with baffles should have increased disinfection even further. This could be attributed to short circuiting occurring in the second pond due to different velocities at the

bottom and top of the pond and wastewater could be passing behind and underneath the baffles (Figure 5.3 (A)).

Table 6.1 - Mean/median (standard deviation) concentrations for raw sewage and effluents along the treatment line.

Parameter	Raw Sewage (RS)	UASB reactor	Pond 1 (P ₁)	Pond 2 (P ₂ B ₄)	Graded Rock Filter (GRoF)
BOD Total	261/234 (95)	81/72 (30)	65/59 (25)	65/62 (24)	16/17 (3)
BOD Particul.	158/148 (52)	40/33 (23)	37/39 (18)	39/36 (19)	3/2 (3)
BOD Filtered	76/64 (39)	44/42 (17)	29/26 (17)	26/25 (15)	14/14 (3)
COD Total	432/424 (134)	186/181 (72)	176/143 (72)	192/181 (80)	74/79 (19)
COD Particul.	266/74 (100)	109/103 (50)	106/102 (63)	129/102 (77)	50/52 (13)
COD Filtered	136/120 (55)	78/69 (54)	75/50 (62)	70/44 (54)	31/28 (15)
TSS	183/160 (89)	28/27 (11)	60/57 (29)	90/83 (45)	27/25 (15)
FSS	44/24 (76)	6/4 (6)	6/5 (7)	7/4 (9)	4/2 (5)
VSS	152/149 (76)	24/24 (10)	62/63 (27)	85/82 (43)	23/22 (15)
TKN	28/27 (8)	30/31 (6)	25/24 (7)	19/18 (8)	17/14 (8)
Ammonia N	26/25 (8)	30/31 (7)	23/22 (8)	17/18 (7)	17/19 (7)
Total Coliforms*	4.53×10 ⁺¹⁰ / 5.48×10 ⁺¹⁰	3.00×10 ⁺⁰⁹ / 3.47×10 ⁺⁰⁹	1.53×10 ⁺⁰⁷ / 1.97×10 ⁺⁰⁷	3.90×10 ⁺⁰⁵ / 4.88×10 ⁺⁰⁵	9.08×10 ⁺⁰⁴ / 1.05×10 ⁺⁰⁵
<i>E. coli</i>*	7.79×10 ⁺⁰⁹ / 7.29×10 ⁺⁰⁹	5.95×10 ⁺⁰⁸ / 4.53×10 ⁺⁰⁸	2.89×10 ⁺⁰⁶ / 2.78×10 ⁺⁰⁶	3.55×10 ⁺⁰⁴ / 4.26×10 ⁺⁰⁴	4.81×10 ⁺⁰³ / 6.09×10 ⁺⁰³

Units: mg/L, except total coliforms and *E. coli* (MPN/100 mL).

* Total coliforms and *E. coli*— geometric mean/median;

Table 6.2 – Mean/median (standard deviation) values for environmental variables for raw sewage and the effluents from each unit along the treatment line, including intermediate sample points from the 2nd pond.

Parameter	Raw. sew. (RS)	UASB reactor	Pond 1 (P ₁)	Pond 2 (P ₂ B ₂)	Pond 2 (P ₂ B ₃)	Pond 2 (P ₂ B ₄)	Graded Rock Filter (GRoF)
Turbidity (NTU)	225/195 (134)	56/51 (21)	77/67 (43)	84/66 (60)	83/67 (56)	83/64 (61)	30/25 (23)
Temp. (°C)	24.3/24.2 (1.7)	24.3/23.8 (2.0)	22.5/22.3 (2.5)	22.1/21.4 (2.6)	22.0/21.5 (2.6)	21.8/20.9 (2.5)	22.5/22.1 (2.8)
DO (mg/L)	-	-	7.0/6.3 (4.1)	8.5/6.9 (5.0)	9.2/8.8 (5.1)	9.7/8.5 (4.8)	-
pH (-)	7.6/7.6 (0.2)	7.3/7.3 (0.1)	7.9/7.8 (0.3)	8.5/8.4 (0.4)	8.6/8.6 (0.4)	8.8/8.7 (0.5)	8.1/8.0 (0.3)
ORP (mV)	-194/-216 (80)	-183/-176 (37)	24/28 (49)	37/33 (36)	35/29 (38)	42/39 (35)	-179/-224 (223)
Alkalinity (mgCaCO₃/L)	193/195 (35)	234/246 (52)	205/200 (44)	-	-	182/180 (30)	204/206 (41)
Settleable solids	3.8/3.2 (3)	0.6/0.4 (1)	-	-	-	-	-

Table 6.3 – Median removal efficiencies in each treatment unit and in the overall treatment system, as well as in the intermediate (P_2B_2 and P_2B_3) points in the 2nd pond.

Parameter	UASB reactor	Pond 1 (P ₁)	Pond 2 (P _{2B₂})	Pond 2 (P _{2B₃})	Pond 2 (P _{2B₄})	Graded Rock Filter (GRoF)	RS – P ₁	RS – P _{2B₄}	Overall (RS – GRoF)
BOD Total	69.1	23.0	-	-	-4.9	72.0	74.9	73.6	92.6
BOD Parti.	77.1	-4.2	-	-	-5.4	91.8	77.7	76.1	97.8
BOD Filter.	36.4	42.0	-	-	0.2	7.1	68.2	66.7	77.4
COD Total	62.8	6.9	-	-	-6.8	60.1	62.8	56.6	79.4
COD Parti.	59.1	0.8	-	-	-2.8	71.8	65.6	50.3	78.5
COD Filter.	64.5	21.6	-	-	-21.6	22.3	71.7	67.6	80.3
TSS	85.1	-106.9	-	-	-18.5	70.8	65.8	51.3	86.9
FSS	77.5	21.4	-	-	-7.1	44.9	84.6	73.3	89.4
VSS	82.2	-137.2	-	-	-42.1	73.1	55.8	44.1	85.5
TKN	-14.3	15.0	-	-	28.9	10.6	11.4	31.9	54.9
Ammonia N	-24.2	19.6	-	-	28.3	0.0	9.6	37.2	42.6
Turbidity	73.3	-20.3	-13.7	0.1	2.9	66.7	65.3	66.3	88.9
Total Colif.	1.1	2.2	0.6	0.9	0.3	0.8	3.5	5.2	5.9
<i>E. coli</i>	1.0	2.2	0.6	0.8	0.4	1.0	3.5	5.3	6.1

Removal efficiency (%), except total coliforms and *E. coli* (log units). (RS = raw domestic sewage; P₁ = Pond 1; P_{2B₂}, P_{2B₃} and P_{2B₄} = Pond 2, end of each baffle and outlet; GRoF = graded rock filter)

6.1.1. Flow, hydraulic retention time (HRT) and depth

During the operational period the flow varied for each measurement, presenting a mean and median flow rate of 36 m³.d⁻¹ (equivalent to treating RS of approximately 225 inhabitants) and 35 m³.d⁻¹ (equivalent to treating RS of approximately 219 inhabitants), respectively. These values are slightly lower than the designed flow rate of 40 m³.d⁻¹, equivalent to treating RS of a population of approximately 250 inhabitants. This illustrates the difficulty in controlling the flow rate due to variations occurring in the influent for various reasons. As shown in Table 5.1, the 1st pond, 2nd pond and GRoF had a mean HRT of 3.5 d, 1.8 d and 1.0 d, respectively, while the UASB reactor had a HRT of 0.4 d, therefore totalling an overall mean theoretical HRT of 6.7 d. The HRT achieved in this system is lower by 0.7 d than the 7.4 d presented by von Sperling and Mascarenhas (2005) in a similar system composed of a UASB reactor and four maturation ponds in series. HRT in the 2nd pond (Table 5.1) was lower than the minimum recommendation of 3.0 d suggested by Mara (2003), while the first pond HRT was slightly higher than this value. The minimum value is supposed to insure no algal wash-out occurs in ponds, but up to the end of the monitoring period no difficulty in algal growth and establishment was observed in both ponds. Depth in the 1st and 2nd ponds was maintained at a mean value of 0.77 m and 0.44 m, respectively (Table 5.1). The GRoF presented a mean depth of 0.50 m during the monitoring period (Table 5.1). The mean surface hydraulic loading rate of the 1st and

2nd pond was $0.232 \text{ m}^3 \cdot \text{m}^{-2} \cdot \text{d}^{-1}$ and $0.247 \text{ m}^3 \cdot \text{m}^{-2} \cdot \text{d}^{-1}$. The mean surface hydraulic loading rate of the GRoF was $0.237 \text{ m}^3 \cdot \text{m}^{-2} \cdot \text{d}^{-1}$.

6.1.2. Biochemical oxygen demand (BOD)

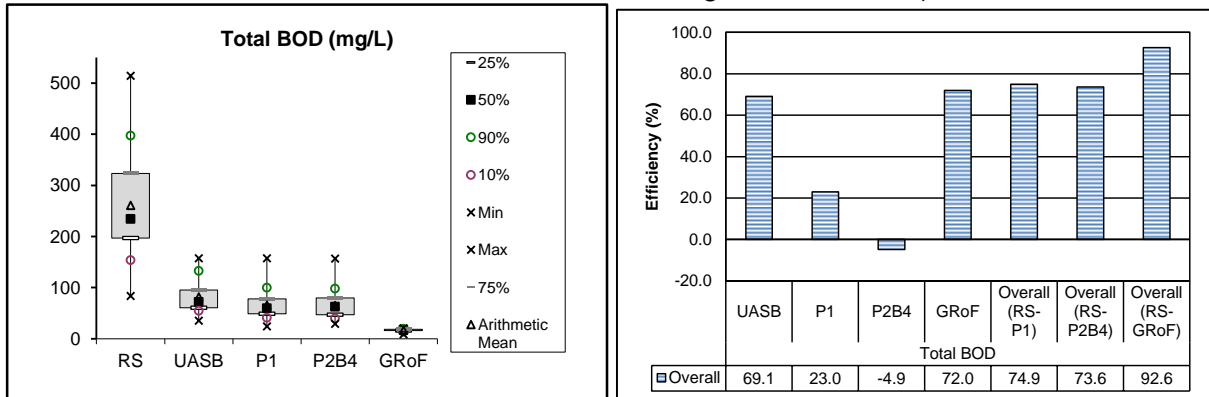
Figure 6.1 presents total biochemical oxygen demand (BOD) concentration and median removal efficiencies in each treatment unit and overall cumulative removal efficiency from RS to P_1 , P_2B_4 and GRoF. Particulate and filtered BOD median removal efficiencies in each individual treatment unit and overall cumulative removal efficiency from RS to P_1 , P_2B_4 and GRoF are shown in Figure 6.2. All results and figures discussed below are in accordance with median concentrations and removal efficiencies.

The UASB reactor removed 69.1% of the incoming BOD (Table 6.3 and Figure 6.1), presenting a median effluent concentration of 72 mg/L (Table 6.1). The 1st maturation pond of the series did some complementary BOD removal by decreasing concentration to 59 mg/L, corresponding to a 23.0% reduction from the UASB reactor (Table 6.1, Table 6.3 and Figure 6.1). This is endorsed by the mean and median surface loading rate of $191.0 \text{ kgBOD} \cdot \text{ha}^{-1} \cdot \text{d}^{-1}$ and $173.0 \text{ kgBOD} \cdot \text{ha}^{-1} \cdot \text{d}^{-1}$, respectively and indicated that from an organic loading point-of-view, the 1st pond approached a facultative pond which usually has design values between 100 and 350 $\text{kgBOD} \cdot \text{ha}^{-1} \cdot \text{d}^{-1}$ (von Sperling, 2007). The 2nd pond increased BOD concentration to 65 mg/L, corresponding to a 4.5% increase (Table 6.1, Table 6.3 and Figure 6.1) due to algal mass production. Von Sperling *et al.* (2008b) and Dias *et al.* (2014) observed the same tendency for a system with a similar configuration. The graded rock filter (GRoF) reduced most of the BOD to a very low 17 mg/L, resulting in a 72.0% decrease (Table 6.1, Table 6.3 and Figure 6.1). This is considered a low concentration, especially because it was achieved by a natural treatment system.

Cumulative removal efficiency of total BOD from RS to P_1 (RS – P_1) was 74.9% (Table 6.3 and Figure 6.1). P_2B_4 increased BOD concentration and slightly decreased cumulative efficiency to 73.6% (Table 6.3 and Figure 6.1). The overall BOD removal efficiency, RS – GroF, can be considered excellent. A 92.6% decrease emphasises the role of the UASB reactor and especially the GRoF. This resulted in an improvement of 12.6% when compared to a similar system studied by Dias *et al.* (2014) (UASB reactor + 3 ponds in series + rock filter in final

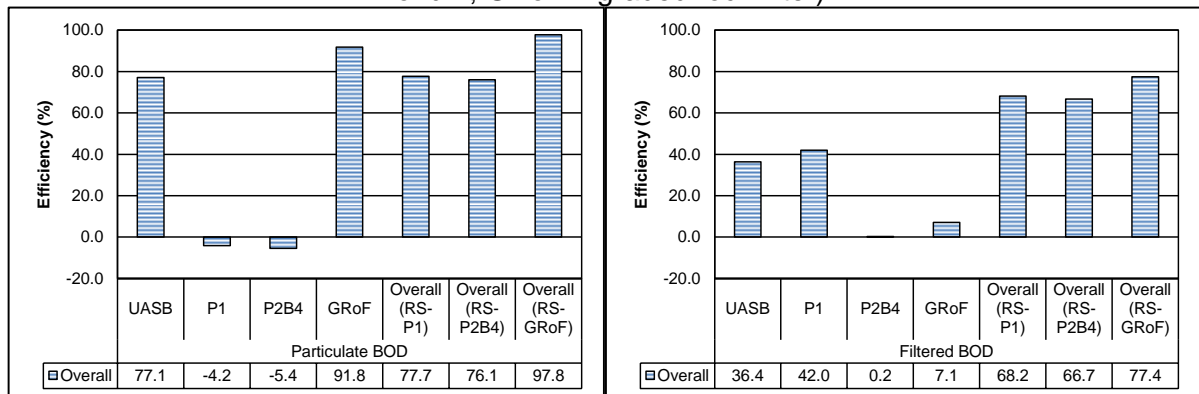
third of the last pond in the series). Noticeably the GRoF BOD effluent concentration ($n = 45$) in Figure 6.1 varied very little, therefore indicating the stability of the GRoF in removing BOD.

Figure 6.1 - Box-plot and column graph of Total BOD concentrations and median removal efficiencies in the treatment line for each unit and overall (RS = raw domestic sewage; P_1 = Pond 1; P_2B_4 = Pond 2; GRoF = graded rock filter).



Particulate BOD decreased in concentration only in the UASB reactor and GRoF. The 1st and 2nd pond of the series both increased particulate BOD concentrations by 4.2% and 5.4% (Table 6.3 and Figure 6.2) because of algal activity. The GRoF was integrated in the treatment system as the final step to reduce the amount of particulate BOD incoming from the ponds. The unit proved to be very effective and reduced particulate BOD by 91.8%, resulting in a final concentration of 2 mg/L (Table 6.1 and Table 6.3). Overall efficiency from RS – GroF was 97.8% (Table 6.3 and Figure 6.2), an excellent reduction in overall particulate BOD and therefore justifying the incorporation of the GRoF in the treatment system. Filtered BOD decreased throughout the treatment line, including in both ponds (Table 6.1, Table 6.3 and Figure 6.2), with P_2B_4 maintaining the concentration (UASB reactor – 42 mg/L, P_1 – 26 mg/L and P_2B_4 – 25 mg/L). In fact, P_1 reduced filtered BOD by 42.0%; and surprisingly, the GRoF only reduced filtered BOD by 7.1%. The UASB reactor was able to remove up to 36.4%, proving to be the second most efficient unit for filtered BOD. Cumulative overall efficiency was good, presenting a final concentration of 14 mg/L - 77.4% (Table 6.1, Table 6.3 and Figure 6.2). Filtered BOD removal was not significant in the GRoF, that its main objective is indeed to remove particulate BOD.

Figure 6.2 - Column graphs of particulate and filtered BOD median removal efficiencies in the treatment line for each unit and overall (RS = raw domestic sewage; P_1 = Pond 1; P_2B_4 = Pond 2; GRoF = graded rock filter).

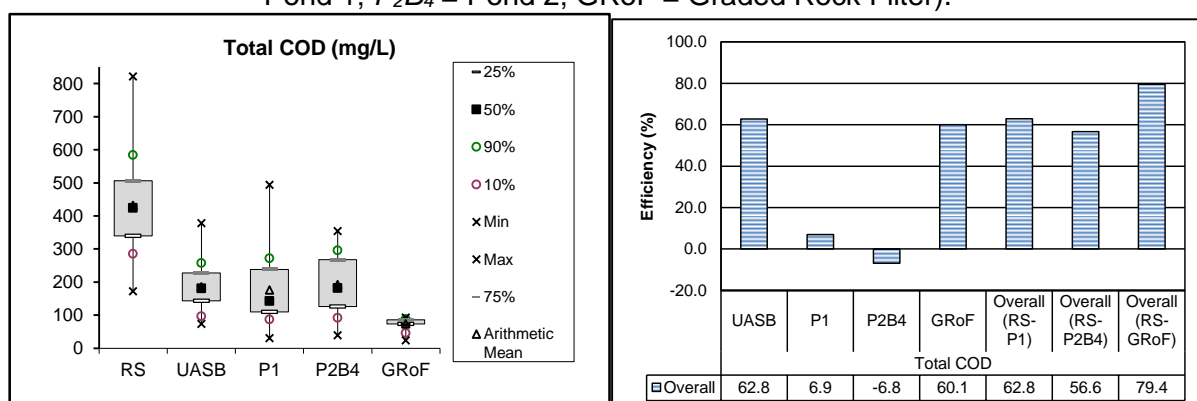


6.1.3. Chemical Oxygen Demand (COD)

Concentrations and removal efficiencies for total chemical oxygen demand (COD) in each treatment unit and overall cumulative removal efficiency from RS to P_1 , P_2B_4 and GRoF are shown in Figure 6.3. Removal efficiencies for particulate and filtered COD are shown in Figure 6.4 for each treatment unit and overall cumulative removal efficiency from RS to P_1 , P_2B_4 and GRoF.

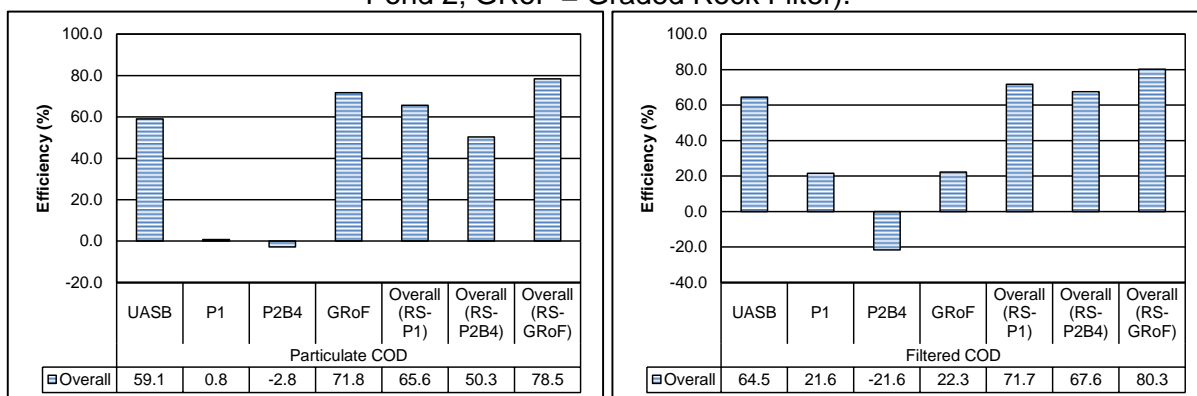
The overall cumulative removal efficiency for the full treatment line (RS – GRoF) was good, 79.4%, with the UASB reactor (62.8%) and GRoF (60.1%) contributing the most to removing total COD (Table 6.3 and Figure 6.3). Overall removal efficiency for COD 13 % lower than that of BOD, which was expected. Overall removal efficiency from RS – P_1 remained the same as the removal efficiency in the UASB reactor (62.8%) and then decreased from RS – P_2B_4 (56.6%), due to algae growth in the 2nd pond (Table 6.3 and Figure 6.3). It is worth noticing that, just as with the total BOD, the concentration of COD in the GRoF effluent ($n = 20$) in Figure 6.3 varied very little.

Figure 6.3 - Box-plot and column graph of total COD concentrations and median removal efficiencies in the treatment line for each unit and overall (RS = raw domestic sewage; P_1 = Pond 1; P_2B_4 = Pond 2; GRoF = Graded Rock Filter).



The UASB effluent presented a total COD concentration of 181 mg/L, which decreased in P_1 (143 mg/L) with complementary removal occurring (6.9%), just as observed with total BOD (Table 6.1, Table 6.3 and Figure 6.3). Total COD increased in P_2B_4 (181 mg/L), therefore producing negative removal efficiencies (-6.8%) (Table 6.1, Table 6.3 and Figure 6.3) in the 2nd pond due to the presence of algae. The GRoF presented a low concentration of total COD in the final effluent of 79 mg/L (Table 6.1 and Figure 6.3). The final effluent concentration of COD in a similar treatment line studied by Dias *et al.* (2014) was 97 mg/L, 18 mg/L more than in this setup and with a longer HRT. This once again highlights the importance of the GRoF, although removal efficiencies for BOD were higher.

Figure 6.4 - Column graphs of particulate and filtered COD median removal efficiencies in the treatment line for each unit and overall (RS = raw domestic sewage; P_1 = Pond 1; P_2B_4 = Pond 2; GRoF = Graded Rock Filter).



Particulate COD concentration decreased 59.1% in the UASB reactor (103 mg/L), only slightly in the 1st pond (102 mg/L – 0.8%) and then substantially in the GRoF (52 mg/L – 71.8%), following the same trend as particulate BOD (Table 6.1, Table 6.3 and Figure 6.4). The 2nd

pond maintained particulate COD concentration, therefore no complementary removal occurred in the 2nd pond. Overall removal efficiency for RS – GRoF was 78.5% for particulate COD (Table 6.3 and Figure 6.4), considered good, but not as good as for particulate BOD. Regardless, the GRoF performed well and removed a good amount of the incoming particulate COD from *P_{2B4}*, therefore achieving what it was designed to. Filtered COD was removed in the UASB reactor (64.5%), *P₁* (21.6%) and GRoF (22.3%), with most of it done in the UASB. The 2nd pond increased COD concentration by 21.6%, but then compensated by the GRoF (Table 6.3 and Figure 6.4). Overall, the treatment line presented a final effluent concentration for filtered COD of 28 mg/L, corresponding to an overall removal efficiency (RS – GRoF) of 80.3% (Table 6.1, Table 6.3 and Figure 6.4), also considered a good reduction and slightly higher than filtered BOD removal efficiency.

6.1.4. COD/BOD ratio in the raw sewage

The ratio between COD and BOD indicates the biodegradability of the raw sewage. The median values were: COD = 424 mg/L; and BOD = 234 mg/L, $COD/BOD = 424/234 = 1.81$.

This value indicates a low COD/BOD ratio, therefore showing that the wastewater had a high biodegradable fraction, (von Sperling, 2008a). This means that the natural treatment system used is recommended for this type of wastewater, therefore justifying the positive removal efficiencies obtained for organic matter.

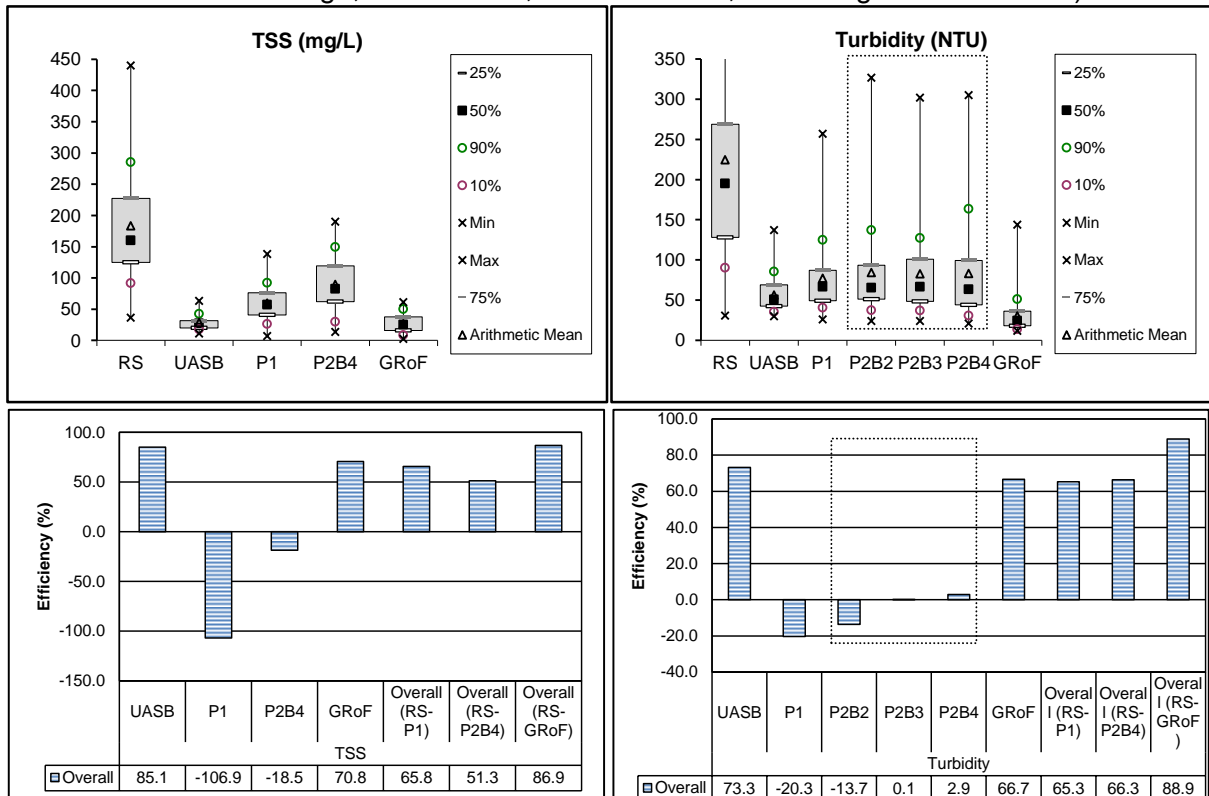
6.1.5. Suspended Solids and Turbidity

Figure 6.5 exhibits the concentrations and removal efficiencies of total suspended solids (TSS) and turbidity for each treatment unit and the overall cumulative removal efficiencies from RS to each pond (*P₁* and *P_{2B4}*) and the GRoF. Removal efficiencies for fixed suspended solids (FSS) and volatile suspended solids (VSS) in each treatment unit and overall cumulative removal efficiency (RS to *P₁*, *P_{2B4}* and GRoF) are shown in Figure 6.6.

The UASB reactor removed 85.1% of TSS from the RS (Table 6.3 and Figure 6.5), resulting in 27 mg/L. This decrease further endorses the objective of the UASB. In *P₁* and *P_{2B4}*, on the other hand, TSS concentration increased by 106.9% and 18.5%, respectively, due to the presence of algae (Table 6.3 and Figure 6.5). The GRoF decreased TSS concentration from *P_{2B4}* by 70.8% to 25 mg/L, therefore removing residual algae and remaining suspended solids from the effluent

(Table 6.1, Table 6.3 and Figure 6.5). Overall, the ponds undid the work carried out by the UASB reactor, therefore decreasing cumulative removal efficiencies from RS – P_1 and RS – P_2B_4 to 65.8% and 51.3%, respectively. From RS – GRoF the removal efficiency increased to 86.9% because of the GRoF, once again highlighting its role in removing organic matter (Table 6.3 and Figure 6.5).

Figure 6.5 - Box-plot and column graphs of TSS and turbidity concentrations (top graphs) and median removal efficiencies (bottom graphs) for each unit and overall (RS = raw domestic sewage; P_1 = Pond 1; P_2B_4 = Pond 2; GRoF = graded rock filter).

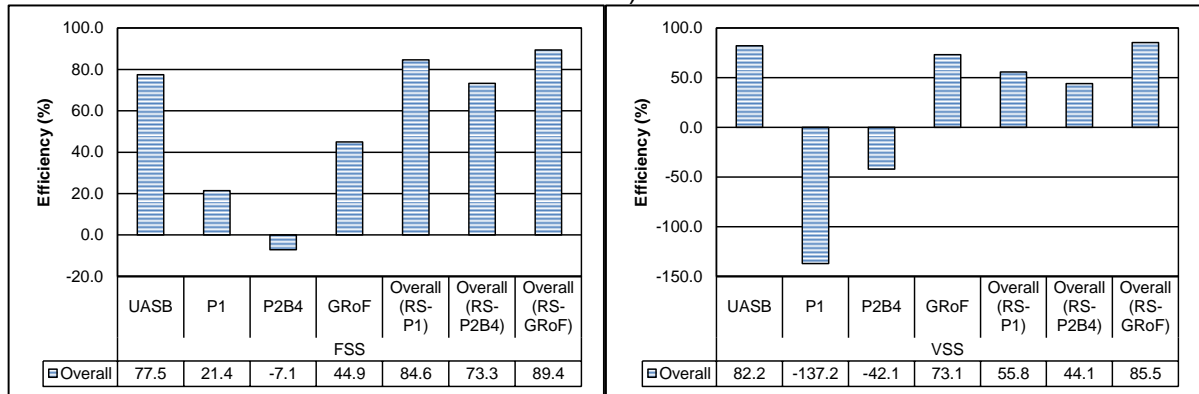


Turbidity was reduced by 73.3% in the UASB reactor, increasing again in P_1 by 20.3% and maintaining roughly the same value of 67 NTU at P_2B_2 , P_2B_3 and P_2B_4 points (Figure 5.7, Table 6.2, Table 6.3 and Figure 6.5) due to the presence of algal mass. In the final effluent, turbidity was reduced by 66.7% in relation to P_2B_4 , presenting a final value of 25 NTU. Overall (RS – GRoF), the system was able to reduce turbidity by 88.9%. Even though the GRoF performed very well, it was the UASB reactor that reduced turbidity the most.

Removal efficiencies of FSS (77.5%) and VSS (82.2%) were greater in the UASB reactor than in the GRoF (FSS – 44.9% and VSS – 73.1%), with VSS reduced the most in both reactors (Table 6.3 and Figure 6.6). Overall (RS – GRoF), the treatment system performed very well for

FSS and VSS removal, presenting cumulative removal efficiencies of 89.4% (2 mg/L) and 85.5% (22 mg/L), respectively. Complementary FSS removal occurred in P_1 (21.4%), but then increased in P_2B_4 (7.1%). VSS increased in P_1 by a staggering 137.2% (expected!) and further 42.1% in P_2B_4 to 82 mg/L (Table 6.1, Table 6.3 and Figure 6.6).

Figure 6.6 - Column graphs of FSS and VSS median removal efficiencies for each unit and overall (RS = raw domestic sewage; P_1 = Pond 1; P_2B_4 = Pond 2; GRoF = Graded Rock Filter).

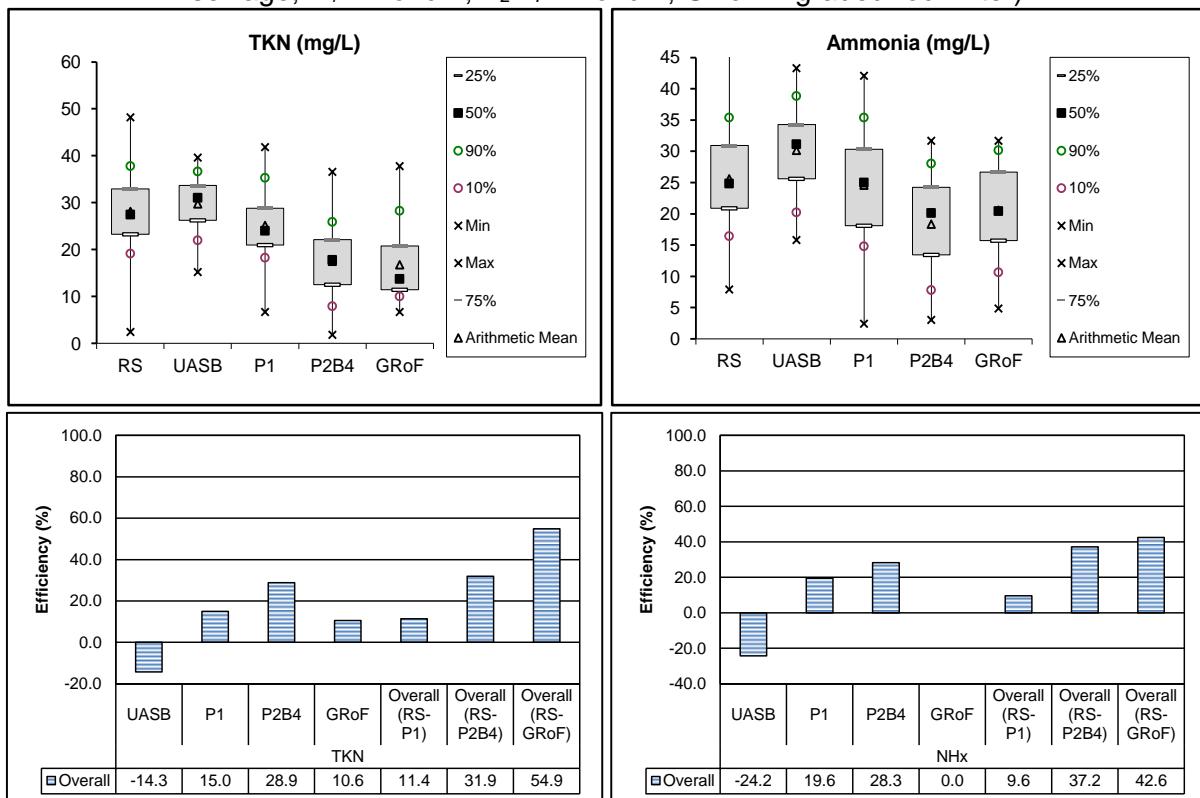


By substituting a full scale pond with a rock filter with decreasing grain size (GRoF), the concentration of organic matter and suspended solids were reduced substantially, making this new setup very attractive when a final effluent quality with low organic matter and suspended solids concentrations is required.

6.1.6. Total Kjeldahl Nitrogen (TKN) and Ammonia Nitrogen (Ammonia-N)

Figure 6.7 shows the concentrations and removal efficiencies for Total Kjeldahl Nitrogen (TKN) and Ammonia Nitrogen (Ammonia-N) in the raw sewage, each individual treatment unit and the overall cumulative removal efficiencies.

Figure 6.7 - Box-plot and column graphs of TKN and ammonia-N concentrations (top graphs) and median removal efficiencies (bottom graphs) for each unit and overall (RS = raw sewage; P₁ = Pond 1; P₂B₄ = Pond 2; GRoF = graded rock filter).



Ammonia made up most of TKN along the treatment units, with both constituents following a decreasing trend in concentration after exiting the UASB reactor. Ammonia increased slightly in concentration in the UASB concentration (Table 6.1 and Figure 6.7). All median concentrations of ammonia were lower than TKN concentrations (as expected because TKN = ammonia-N + organic N) in the treatment units except for the final effluent which was higher (TKN_{GRoF} = 14 mg/L and ammonia_{GRoF} = 19 mg/L). The mean concentration of ammonia-N, on the other hand, was lower than that of TKN. The median concentration of TKN decreased from 27 mg/L to 14 mg/L (RF – GRoF = 54.9%), with most of the removal occurring in the two ponds, especially in the 2nd pond. Ammonia-N median concentration decreased from 25 mg/L to 19 mg/L (RF – GRoF = 42.6%), again with most of the removal being achieved in the two ponds, particularly in the 2nd pond (Table 6.1, Table 6.3 and Figure 6.7). These results highlight the role of the shallow depth in the 2nd pond. This decrease in Ammonia and TKN concentration was important because it is not easily achievable in biological treatment systems and even more so in systems with reduced HRT. The main mechanisms for nitrogen removal in pond systems are reported to be: (i) ammonia volatilization, (ii) ammonia and nitrate assimilation by algae and consequent organic nitrogen sedimentation, followed by its retention

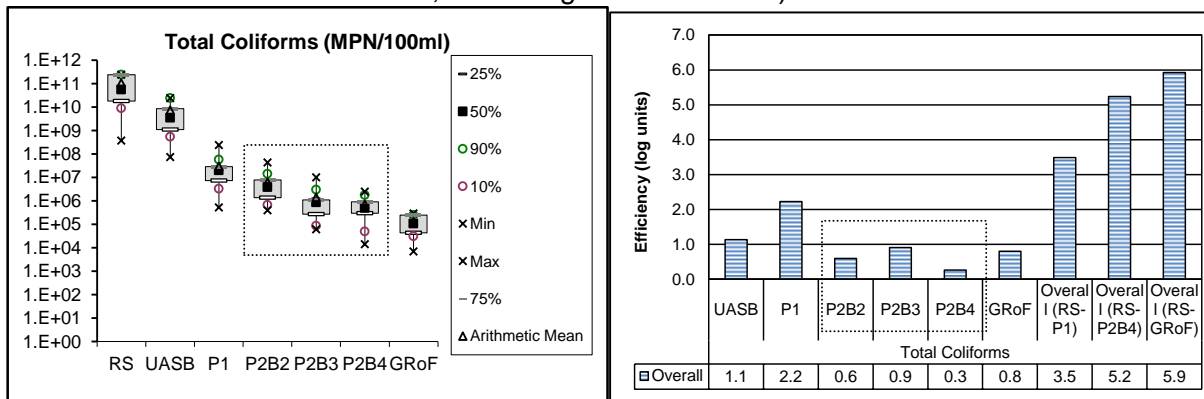
in the pond bottom sludge and (iii) nitrification–denitrification in the liquid column or sediment layer (Pano and Middlebrooks, 1982; Reed, 1985; Craggs, 2005; Camargo-Valero et al., 2010; Senzia et al., 2002; Ferrara and Avci, 1982; Assunção and von Sperling, 2013; Rodrigues *et al.*, 2015, 2016).

6.1.7. Total coliforms and *E. coli*

Maturation ponds in series have as their main objective the removal of pathogenic organisms (subsections 4.3, 4.4 and 4.9). Total coliforms and *E. coli* are a indicator bacteria for faecal contamination and potentially pathogenic organisms. Figure 6.8 and Figure 6.9 exhibits total coliform and *E. coli* counts and removal efficiencies, respectively, in the RS, individual treatment units and overall. Counts are discussed in geometric mean values and removal efficiencies are discussed in median values.

Total coliform removal was considered effectively removed (RS – GRoF = 5.9 log units), resulting in a final effluent count of $9.08 \times 10^{+04}$ MPN/100mL (Table 6.1, Table 6.3 and Figure 6.8).

Figure 6.8 - Box-plot and column graphs of total coliform concentration and median removal efficiencies for each unit and overall (RS = raw domestic sewage; P_1 = Pond 1; P_2B_4 = Pond 2; GRoF = graded rock filter).



Removal was mainly done in the 1st (2.2 log units) and 2nd (1.8 log units) ponds of the treatment system, with the central channel ($P_2B_2 - P_2B_3$) of the 2nd pond (Figure 5.7) contributing the most. The GRoF and UASB reactor performed complementary removal of total coliforms,

particularly in the UASB reactor. Overall, the system performed very efficiently in removing total coliforms, especially considering the low overall HRT of 6.7 days.

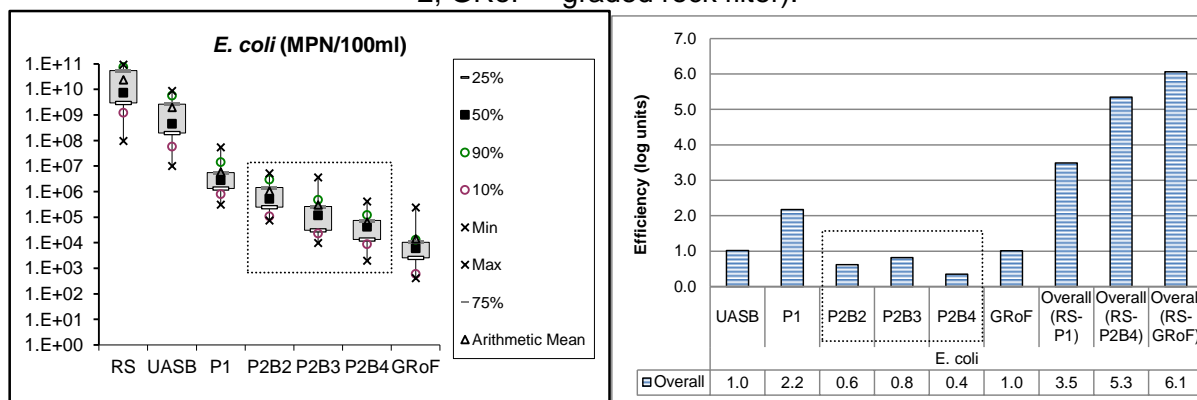
E. coli counts and removal efficiencies are shown in Figure 6.9. It is worth mentioning that during the monitoring period the RS counts of *E. coli* were strikingly high ($7.79 \times 10^{+09}$ MPN/100mL) compared with previous studies. A consistent decay in *E. coli* counts occurred throughout the treatment line with the highest removal efficiency taking place in the 1st pond (2.2 log units) (Table 6.1, Table 6.3 and Figure 6.9). The 2nd pond removed 1.8 log units, lower than the removal efficiency of P_1 , what was not expected, considering the shallow depth of P_2B_4 (Table 5.1) and the presence of longitudinal baffles. However, shallow depth also implies short HRT, which could have affected the removal rate. The highest removal efficiency of *E. coli* in the 2nd pond (0.8 log units) (Table 6.3 and Figure 6.9) took place in the middle channel (between P_2B_2 and P_2B_3 – Figure 5.7), here the highest increase in DO in the 2nd pond was also recorded. The pH value was already above the 8.5 level (Table 6.2 and Figure 6.10). The third channel did not increase disinfection further because most of it is in the shade and this was confirmed by the decrease in DO and temperature. The final effluent concentration of $4.81 \times 10^{+03}$ MPN/100mL (GRoF), was considered low for natural treatment system with a short HRT and complied with guidelines of the World Health Organization (WHO, 2006) for some practises of restricted and unrestricted irrigation (Table 6.1 and Figure 6.9). These practices are discussed in subsection 6.1.10.

The overall removal efficiency (RS – GRoF) of *E. coli* was remarkable with a median value of 6.1 log unit (Table 6.3 and Figure 6.9). This was almost 0.5 log unit above to the overall removal efficiency reported by Dias *et al.* (2014) in a treatment line comprised of three maturation ponds. The excellent overall removal efficiency was achieved with a very low theoretical HRT in $P_1 = 3.4$ days and $P_2B_4 = 1.8$ days (Table 5.1), totalling 5.2 days (Table 6.3 and Figure 6.9) resulting in 78% of the overall time needed. P_1 and P_2B_4 removed in total 4.0 log units, resulting in 66% of the total removal efficiency of the treatment system. *E. coli* removal in the 2nd pond was quite high, taking into account the short HRT and therefore highlighting the effect of the shallow depth and/or baffles (Table 5.1). This resulted in enhancing removal mechanisms based on solar irradiance (UV and PAR), pH and DO (Figure 6.10).

The excellent performance of the shallow ponds was compatible with the findings of von Sperling (2005b). The author investigated 186 facultative and maturation ponds around the

world for coliform disinfection and concluded that the coliform die-off coefficient was inversely related with pond depth. Shallow depths allow for an increase in the probability of a pathogenic organism being inactivated due sunlight when compared to deeper ponds. This is because UV penetration is limited due to the upper layers of a pond.

Figure 6.9 - Box-plot and column graphs of *E. coli* concentration and median removal efficiencies for each unit and overall (RS = raw domestic sewage; P_1 = Pond 1; P_2B_4 = Pond 2; GRoF = graded rock filter).



The UASB reactor and GRoF removed 1.0 and 1.1 log units (Table 6.3 and Figure 6.9), respectively, this also contributed for the high final effluent quality.

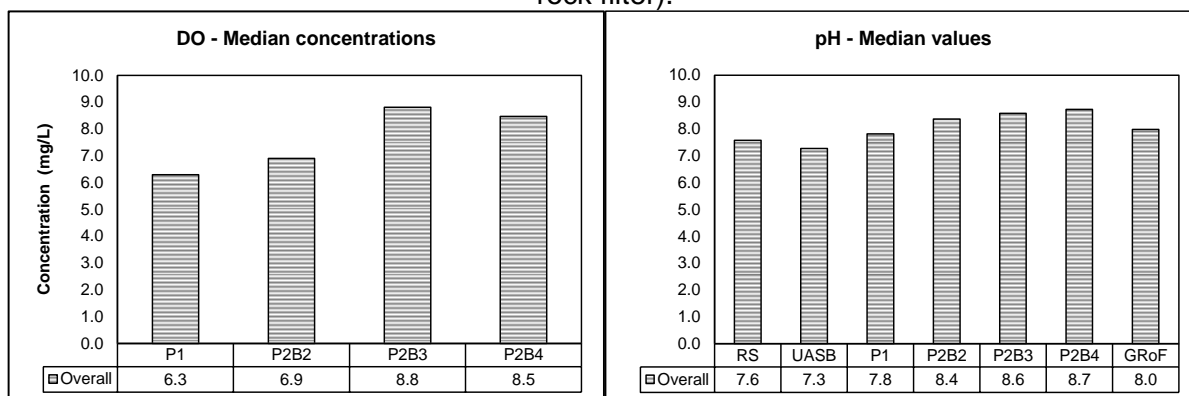
6.1.8. Environmental data

Environmental parameters are important to assess the “health” of each treatment unit. Anaerobic reactors are characterised for stabilising organic matter in the absence of dissolved oxygen (DO) and reducing pH values. Aerobic reactors usually have high concentrations of DO and pH, especially in ponds. Table 6.2 summarises the data for turbidity, DO, pH, oxidation/reduction potential (ORP), alkalinity and settleable solids (RS and UASB reactor) in each treatment unit. Figure 6.10 shows DO and pH levels in each treatment unit and intermediate points in the 2nd pond (P_2B_2 , P_2B_3 and P_2B_4).

Maturation ponds require high concentrations of DO and pH to create a favourable environment for pathogenic organism disinfection. As expected, DO concentration increased along the ponds, then decreasing in the GRoF due to the absence of direct solar radiation, i.e., essential for photosynthetic activity, and the consumption of DO from the oxidation of organic matter (Figure 6.10). pH values followed this tendency. Even with the 1st pond of the series receiving higher organic loads (similar to typical facultative pond – subsection 6.1.2), it was capable of

maintaining a high DO concentration of 6.3 mg/L, 1.54 mg/L under the 7.84 mg/L saturation point of water at 22.3 °C and 852 m in altitude (median temperature and altitude of the treatment line) (Pöpel, 1979; Qasim, 1985) (Table 6.2 and Figure 6.10). pH increased slightly to 7.8 in the 1st pond compared to the value in RS. This is normal of any 1st pond of any series as it receives the most incoming organic matter from primary treatment, therefore subjected to greater organic matter stabilisation. In the 2nd pond there was a greater increase in DO (from 7.8 to 8.7), with the middle channel ($P_2B_2 - P_2B_3$ - Figure 5.7) increasing DO from 6.9 mg/L to 8.8 mg/L (1.9 mg/L increase) (Table 6.2 and Figure 6.10), coinciding with the same tendency, but in the opposite direction of *E. coli* disinfection (Table 6.3 and Figure 6.9).

Figure 6.10 - Column graphs of dissolved oxygen and pH concentration in RS and each treatment unit (RS = raw domestic sewage; P_1 = Pond 1; P_2B_4 = Pond 2; GRoF = graded rock filter).



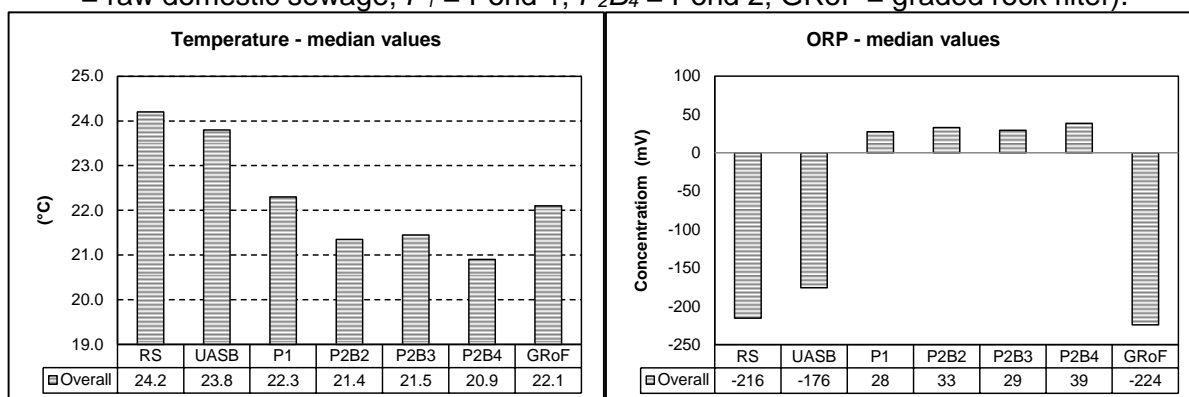
pH followed the same tendency with the greatest increase in the middle channel (0.2 value increase) and already above the desired value of 8.5. The highest increase of pH, from 7.8 to 8.4 occurred from P_1 to P_2B_2 (Figure 5.7, Table 6.2 and Figure 6.10).

The influent, the UASB effluent and the final effluent from the GRoF, all presented DO concentrations of 0 mg/L, indicating anaerobic conditions. This was endorsed by the negative oxidation/reduction potential (ORP) values in all the three effluents (Table 6.2 and Figure 6.11), with the GRoF presenting the highest negative value. The GRoF decreased pH by 0.7 unit, necessary for discharging the final effluent into waterbodies.

During the entire monitoring period the ponds were able to maintain aerobic conditions, i.e., high DO concentrations and positive ORP values (Table 6.2, Figure 6.10 and Figure 6.11) and no foul odours were ever detected in the vicinity.

Temperature in the treatment line decreased from 24.2 °C (RS) to 21.4 °C (P_2B_2), only increasing slightly (21.5 °C) at P_2B_3 and then decreasing again in the last channel (P_2B_4) (Figure 5.7, Table 6.2 and Figure 6.11). An increase in temperature was expected throughout the ponds due to high solar exposure, but only occurred again in the GRoF (Table 6.2 and Figure 6.11), probably due to reactions in stabilising reminiscent organic matter from the ponds. The 1st pond of the series exhibited a median temperature higher than the 2nd pond with a shallower depth, which was not expected.

Figure 6.11 - Column graphs of temperature and ORP values in RS and each treatment (RS = raw domestic sewage; P_1 = Pond 1; P_2B_4 = Pond 2; GRoF = graded rock filter).



6.1.9. Comparison of the final effluent with the previous treatment line setup

Table 6.4 shows a comparison between the final effluent quality of the actual treatment line and the previous treatment line used at CePTS before the current research (UASB reactor + 3 ponds in series with a rock filter in the final third of the third pond), which operated with a lower flow rate (Dias *et al.*, 2014).

A Wilcoxon-Mann-Whitney U test with confidence level of 95% was performed to compare the final effluent concentrations of the previous setup with the new one.

Table 6.4 – Comparison between final effluent concentrations of main constituents (mean/median) of the new treatment line and the previous treatment line studied by Dias *et al.* (2014).

Constituent	Previous line (Dias <i>et al.</i> , 2014) – Three ponds, rock filter in the final third of the third pond (2.0 to 2.5 m ² /inhab.)		New configuration with two ponds (2 nd pond baffled) and GRoF (1.5 m ² /inhab.)
BOD Total	<u>48/32</u>	>	16/17
BOD Particul.	<u>28/14</u>	>	3/2
BOD Filtered	<u>18/11</u>	>	14/14
COD Total	<u>103/97</u>	>	74/79
COD Particul.	42/44	<	<u>50/52</u>
COD Filtered	<u>58/51</u>	>	31/28
TSS	<u>39/33</u>	>	27/25
FSS	-	-	4/2
VSS	<u>32/27</u>	>	23/22
TKN	<u>18/16</u>	>	17/14
Ammonia N	12/10	<	<u>17/19</u>
Total coliforms*	1.80×10⁺⁴/2.40×10⁺⁴	<	<u>9.08×10⁺⁴/1.05×10⁺⁵</u>
<i>E. coli</i>*	4.50×10⁺²/6.20×10⁺²	<	<u>4.81×10⁺³/6.09×10⁺³</u>

Units: mg/L, except total coliforms and *E. coli* (MPN/100 mL); underlined = higher concentration; **significantly lower concentration**; * total coliforms and *E. coli*— geometric mean/median.

The effluent concentrations from the new treatment line are for the most part lower than the concentrations from the previous treatment line studied by Dias *et al.* (2014). Out of the thirteen constituents compared, only four were slightly higher than those of the previous setup, and six had significantly lower concentrations. Surprisingly, one of the constituents which was higher was particulate COD, which was not expected since the GRoF should reduce COD particulate to a lower level than the previous treatment line. The other constituents with higher concentrations (ammonia-N, total coliforms and *E. coli*) were expected since their reduction may only occur with the incorporation of a third pond, which would further promote ammonia removal (subsection 6.1.6) and coliform disinfection (subsections 4.4 and 6.1.7). Despite the previous comments, performance increased with the new configuration when compared to the previous one, requiring less area = 1.5 m²/inhabitant to treat wastewater and resulting in reduced land requirements of 0.5 to 1.0 m²/inhabitant when compared to the previous setup.

As mentioned before, influent counts of total coliforms and *E. coli* were unusually higher than those obtained by Dias *et al.* (2014). On the other hand, *E. coli* removal efficiency was 6.4 log units, considered excellent. Ammonia-N increased its concentration when compared to the previous setup, probably due to environment in the GRoF, which was essentially anaerobic.

6.1.10. Compliance with discharge goals and irrigation reuse

Compliance with discharge goals is very important to evaluate the final effluent to avoid overloading receiving waterbodies and therefore elude subsequent eutrophication and, most importantly, pollution overload leading to oxygen consumption. The final effluent was tested against the strict European Community Standards (Council for European Communities, 1991) for discharging stabilisation pond effluents. Reuse of wastewater effluent is a growing practise because of the scarcity of fresh water in arid and poor areas. There are different practises for wastewater effluent as defined by World Health Organisation (WHO, 2006), including unrestricted and restricted irrigation.

The European Community standards for discharging stabilisation pond effluents are shown in Table 6.5 (Council for European Communities, 1991) and compliance percentages. Compliances for bacteriological concentration in this case *E. coli* counts, and log unit reduction for different practises of irrigation (health-based targets) set by WHO (2006) are show in Table 6.6 and health protection measures in Figure 6.12.

Table 6.5 – Percentage of stabilisation pond effluent samples complying with standards for discharging in waterbodies. Official Journal of the European Communities No. L 135/40.

Parameter	Official Journal of the European Communities No. L 135/40
BOD₅ (filtered) ≤ 25 mg/L	100%
COD (filtered) ≤ 125 mg/L	100%
Total Suspended Solids ≤ 150 mg/L	100%

The final effluent complied (100%) with all three standards set by the Official Journal of the European Communities No. L 135/40 for discharging stabilisation pond effluent. This suggests that this system can be used, not only in developing countries, but is also suitable for developed countries from warm areas in Europe.

In terms of agricultural reuse and WHO guidelines, combining health protection measures used to accomplish health based targets are presented in Figure 6.12.

Health-based targets are achieved by different health protection measure combinations, as shown in Table 6.6. Pathogen reductions can be achieved by combining different wastewater treatment and other health protection control measures to accomplish health-based target of a disability adjusted life year (DALY) loss of $\leq 10^{-6}$ per person per year (Figure 6.12).

Figure 6.12 - Examples of options for the reduction of viral, bacterial and protozoan pathogens by different combinations of health protection measures that achieve the health-based target of $\leq 10^{-6}$ DALY per person per year (Source: WHO, 2006).

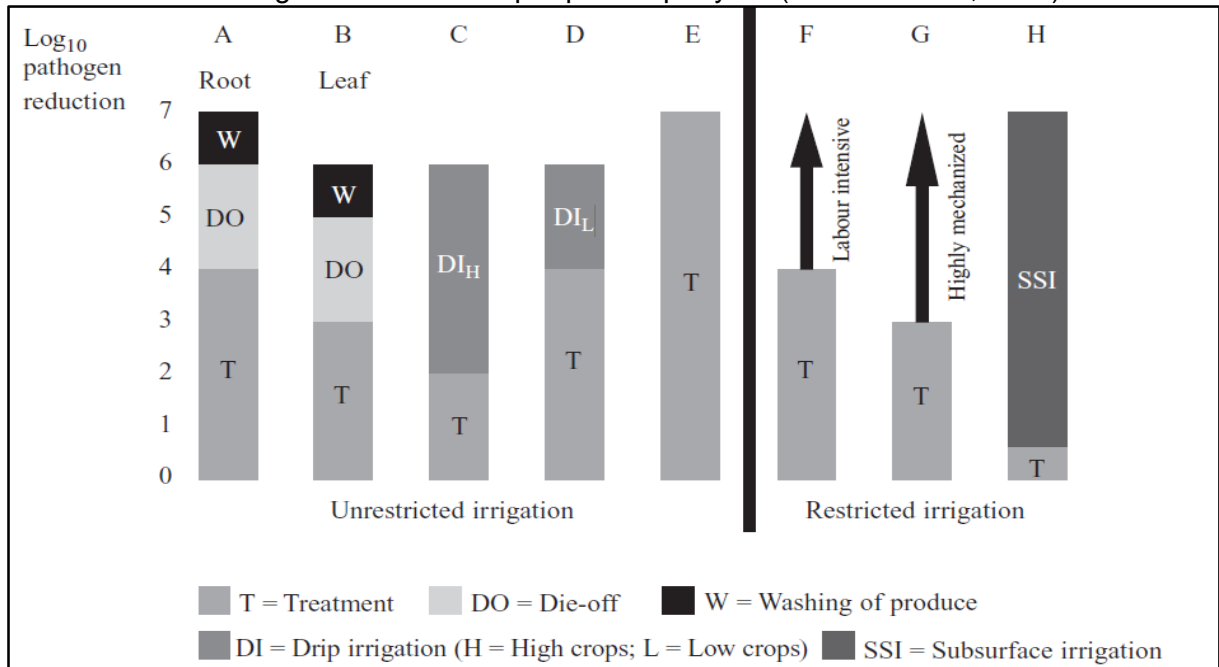


Table 6.6 - Verification monitoring^A (*E. coli* numbers per 100 mL of treated wastewater) for the various levels of wastewater treatment in Options A–G presented in Figure 6.12 (WHO, 2006).

Type of irrigation	Option (Figure 6.12)	Required pathogen reduction by treatment (log units)	Verification monitoring level (<i>E. coli</i> per 100 ml)	Notes
Unrestricted	A	4	$\leq 10^3$	Root crops
	B	3	$\leq 10^4$	Leaf crops
	C	2	$\leq 10^5$	Drip irrigation of high-growing crops
	D	4	$\leq 10^3$	Drip irrigation of low growing crops
	E	6 or 7	$\leq 10^1$ or $\leq 10^0$	Verification level depends on the requirements of the local regulatory agency
Restricted	F	3	$\leq 10^4$	Labour-intensive agriculture (protective of adults and children under 15 years of age)
	G	2	$\leq 10^5$	Highly mechanised agriculture
	H	0.5	$\leq 10^6$	Pathogen removal in a septic tank

^A “Verification monitoring” refers to what has previously been referred to as “effluent standards” or “effluent guideline” levels.

^B For example, for secondary treatment, filtration and disinfection: BOD₅ < 10 mg/l; turbidity < 2 NTU; Chlorine residual 1mg/l; pH = 6 – 9 mg/L; and faecal coliforms not detectable in 100 mL (State of California, 2001).

The final concentration of *E. coli*, $4.81 \times 10^{+03}$ MPN/100mL (geometric mean) (Table 6.1), implies that the effluent can be used for the following irrigation practises for values $\leq 10^{+04}$ (WHO, 2006):

Unrestricted irrigation

- **Option B:** lower degree of wastewater treatment than Option A (3 log units, rather than 4) combined with two post-treatment health protection control measures: a 2 log unit reduction due to die-off and a 1 log unit reduction due to washing the salad crops or vegetables with water prior to consumption. This option provides a 6 log unit pathogen reduction, and is suitable for irrigation of non-root salad crops (e.g. lettuce, cabbage) and vegetables eaten uncooked.
- **Option C:** combines an even lower degree of treatment (2 log units) with drip irrigation of high-growing crops (such as fruit trees, olives), which achieves the required remaining 4 log unit pathogen reduction.

Restricted irrigation

- **Option F:** labour-intensive restricted irrigation; the health based target of an additional disease burden of $\leq 10^{-6}$ DALY loss per person per year is achieved by a 4 log unit pathogen reduction.
- **Option G:** represents restricted irrigation using highly mechanized agricultural practices (e.g. tractors, automatic sprinklers, etc.); wastewater treatment to $10^5 - 10^6$ *E. coli* per 100 ml is required (i.e. a pathogen reduction of 3 log units).
- **Option H:** minimal treatment in a septic tank (0.5 log unit pathogen reduction) followed by subsurface irrigation via the soil absorption system for the septic tank effluent. There is no contact between the crop and the pathogens in the septic tank effluent, so the subsurface irrigation system is credited with the remaining 6.5 log unit pathogen reduction required for root crops.

6.2. Solar Radiation

Section 6.2.1 and 6.2.2 presents data for total solar radiation (TSI) for the entire monitoring period – APPENDIX II and Figure 6.13 – and seasonal variation for TSI – APPENDIX III, APPENDIX IV, Figure 6.14 and Figure 6.15 – measured onsite at the treatment plant (subsection 5.4.2). Comparison between median, mean, maximum and minimum values of TSI are shown in Figure 6.16, Figure 6.17 and Figure 6.18. Section 6.2.3 details data from UV-A, UV-B and PAR depth profiling, considered essential for bacterial disinfection in waste stabilisation ponds, shown in Figure 6.19, Figure 6.20, Figure 6.21, Figure 6.22, Figure 6.23 and Figure 6.24. Seasonal influence was analysed to assess different atmospheric conditions during the monitoring period. APPENDIX II, APPENDIX III, APPENDIX IV, APPENDIX V, APPENDIX VI, APPENDIX VII, APPENDIX VIII, APPENDIX IX and APPENDIX X presents the time of day divided in 10 minute intervals, sample numbers (n), arithmetic mean, median, maximum, minimum, 25% and 75% quartile and the coefficient of variation (CV) for the last year and four months. CV were used to compare the variability or dispersion of data of a sample of two or more variables. It is a dimensionless number (standard deviation divided by mean) and always positive. Distributions for $CV < 1$ are considered low-variance, and high-variance when $CV > 1$. CV values varied the least when close to mid-day. Section 6.2.4 presents equations for modelling sunlight attenuation coefficients. From October to February the time was -3 hours from UTC (Coordinated Universal Time) and from February to October it was -2 hours from UTC. This was accounted for in the results and the dataloggers were adjusted accordingly.

6.2.1. Overall total surface solar irradiance

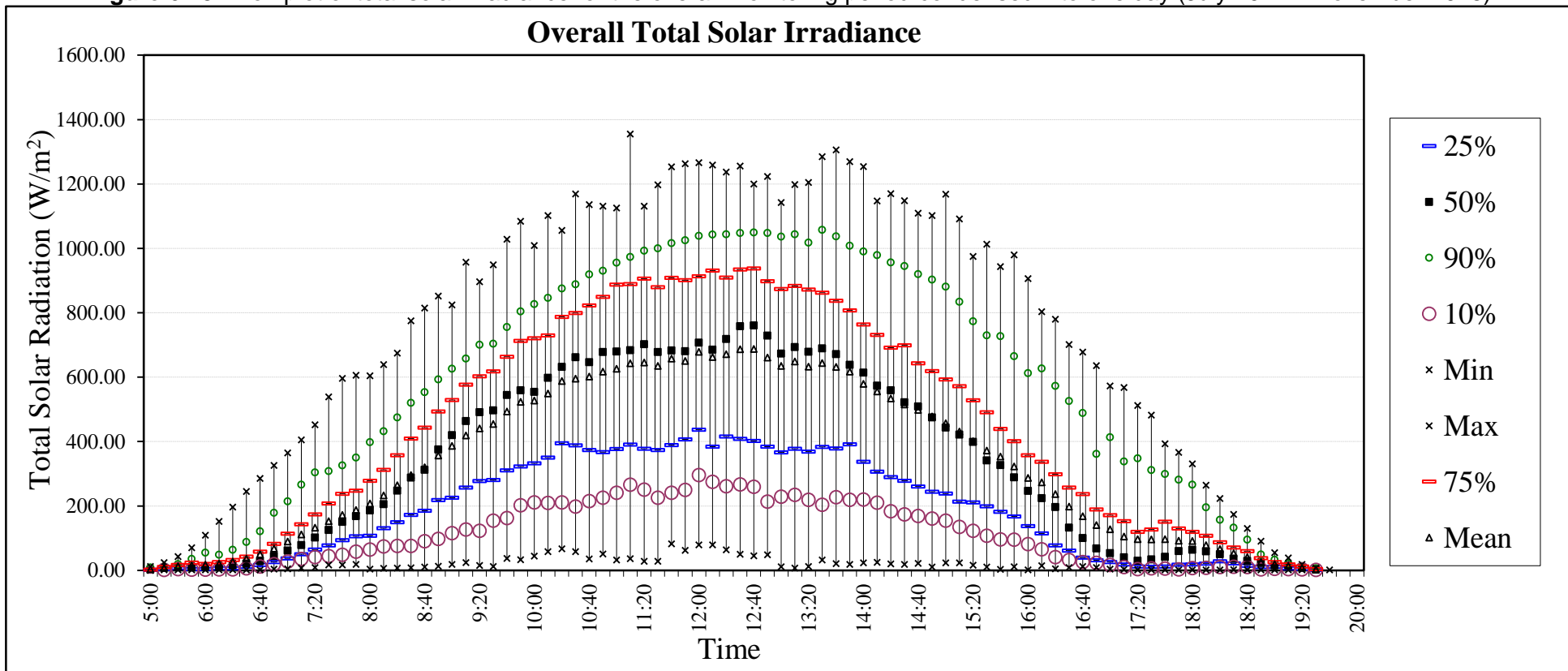
To understand the variability of total solar irradiance (TSI) reaching the surface, APPENDIX II presents a statistical analyses of the data. Figure 6.13 presents a box-plot of TSI for the overall monitoring period (July 2014 – November 2015) vs time. Since this was for the total monitoring period, sunrise and sunset changed over the year, but the objective is to show the TSI variation during the monitoring period. The greatest TSI amplitudes (maximum and minimum) between the lowest and highest recorded TSI occurred close to mid-day, which was expected because of stronger sunlight conditions compared to overcast conditions.

APPENDIX II and Figure 6.13 shows that, on average, the sun rose at 05:30:00 ($n = 9$) and 06:00:00 ($n = 60$) and set between 18:50:00 ($n = 87$) and 19:40:00 ($n = 17$) (Figure 6.16), with

the highest mean/median value for TSI recorded at 12:50:00 of 687.89/760.50 W.m⁻², usually when the sun was at its highest point in the sky (12:00:00 – 13:00:00). The maximum recorded TSI value was 1355.00 W.m⁻² at 11:20:00 and not at the same time of the highest mean/median value. The CV values presented in APPENDIX II are for the most part <1, with 72 time intervals considered low-variance and the other 14 time intervals are high-variance. TSI was affected between 06:00:00 and 06:50:00 and from 16:50:00 to 18:00:00 (CV >1). It was least affected between 07:00:00 and 16:50:00 (CV <1). From 7:00:00 to 12:10:00 the CV value decreased to as low as 0.41 and then increased until 16:50:00, i.e., TSI was more stable during this interval mainly because sunlight intensity was stronger, especially closer to noon. Subsection 6.3 presents *E. coli* disinfection in depth during two time intervals (08:00:00 – 12:00:00 and 12:00:00 – 16:00:00) as explained in section 5.5, therefore the CV values justified the two intervals used for *E. coli* disinfection because TSI varied the least and energy levels were more consistent.

The plotted data follows a bell-like-shape, increasing and decreasing with solar intensity during the day. The shape is typical of solar irradiance data.

Figure 6.13 - Box-plot of total solar irradiance for the overall monitoring period condensed into one day (July 2014 – November 2015).



6.2.2. Seasonal variation of total solar irradiance

Figure 6.14 and Figure 6.15 present box-plot graphs for two different seasons:

- Dry and Cool (April to September) – Figure 6.14;
- Wet and Warm (October to March) – Figure 6.15.

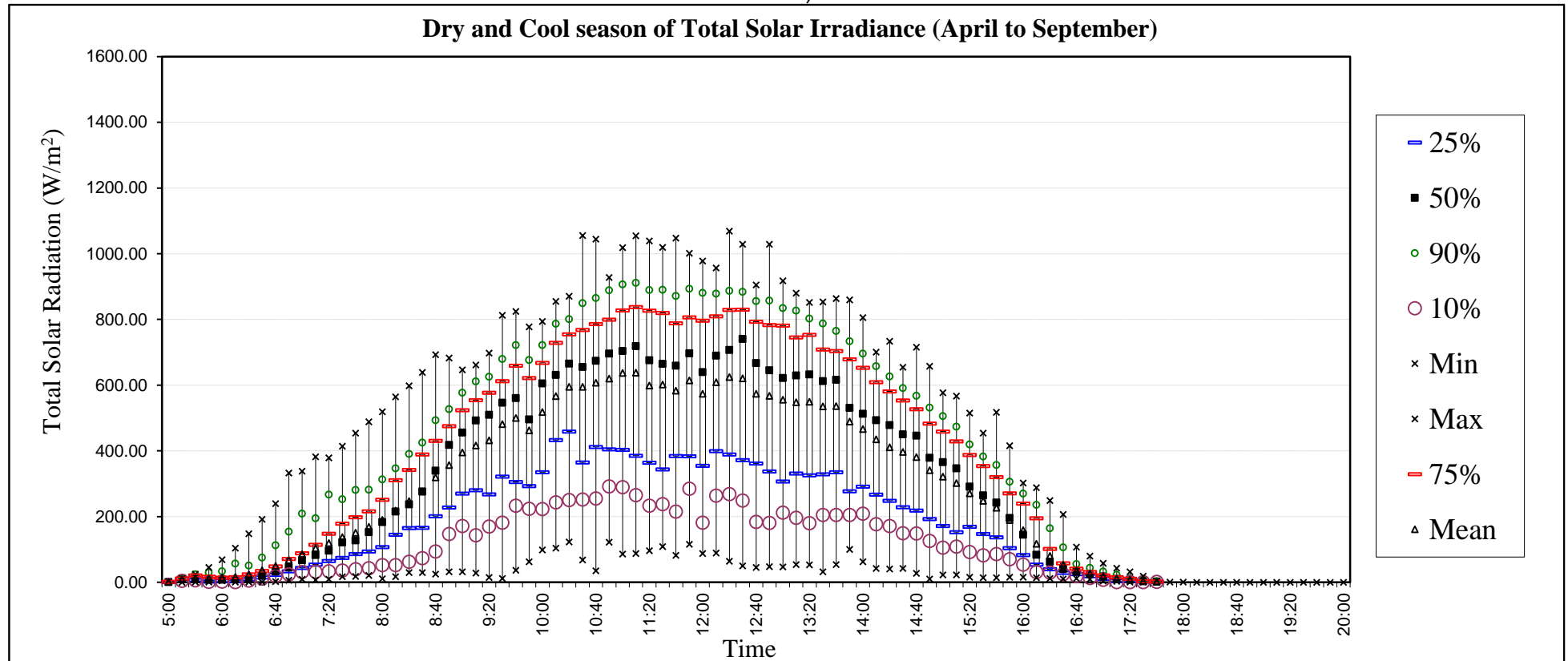
Discussion was based on analysis from Figure 6.14 and Figure 6.15, and data from APPENDIX III and APPENDIX IV for the dry and cool season and wet and warm season, respectively. In the state of Minas Gerais, there is daylight saving time (one-hour adjustment during some months of the year) and consequently the wet and warm period hours are affected by it.

6.2.2.1. Dry and Cool (April to September)

The highest median TSI value occurred at 12:50:00 and was 741.50 W.m^{-2} and the highest mean value was at 12:40:00 (624.60 W.m^{-2}). Maximum TSI during the dry and cool season was 1069.00 W.m^{-2} and occurred at 12:40:00 (Figure 6.16 and Figure 6.17) and coincided with the same time interval as the highest mean value of TSI. Maximum irradiance during this period was lower than the overall period, therefore the maximum value occurred during the wet and warm season (October – March). The median TSI values were closer to the 75% percentile than the TSI values during the overall period, but arithmetic mean and median were more distant than the overall period, therefore presenting an asymmetric data distribution (Figure 6.14). As expected, TSI variation varied less than for the overall period, presenting more stable values between the 25% and 75% percentiles. Sunrise was between 05:40:00 (n=3) and 06:30 (n=101) and increased until 11:30:00/12:40:00, slightly earlier than the overall period. Irradiance then decreased until sunset occurred between 17:30:00 (n=112) and 18:00:00 (n=2) (Figure 6.14 and APPENDIX III), much earlier than the overall period (Figure 6.16).

CV values varied between 1.32 and 0.36 with seven intervals > 1 (high-variance), again this occurred in the early hours of the morning, following the same tendency as the overall period (APPENDIX II). From 08:00:00 until 16:00:00 the CV varied between 0.36 and 0.63, similar to the overall period and showing a lower-variation of data during the season (APPENDIX III). Minimum solar irradiance values are greater than those presented during the overall period.

Figure 6.14 - Box-plot of solar irradiance for the dry and cool season during the monitoring period condensed into one day (July 2014 – November 2015).

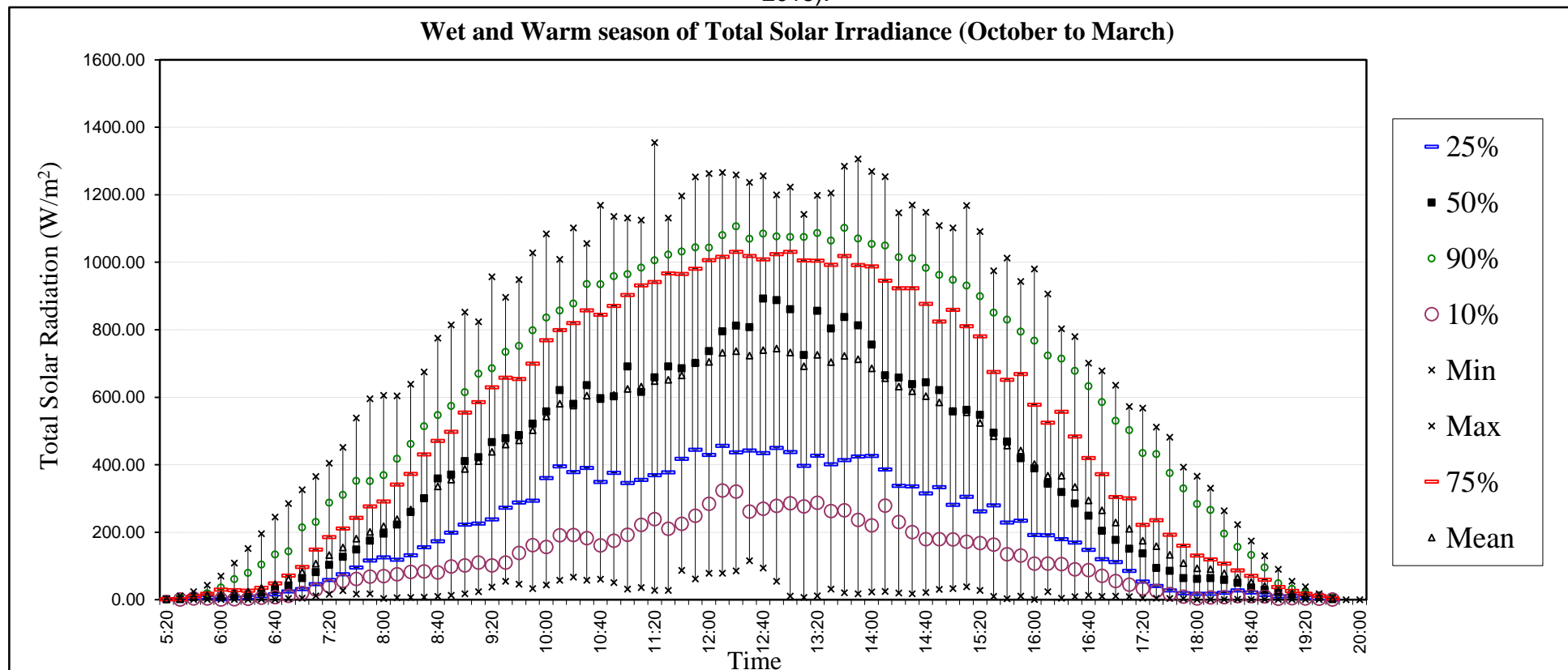


6.2.2.2. Wet and Warm season (October to March)

The highest median value was 892.50 W.m⁻² at 12:40:00 and the highest mean value was 744.57 W.m⁻² 10 minutes later. Maximum solar irradiance was 1355.00 W.m⁻² and recorded at 11:20:00 (same value as the overall period). Maximum solar irradiance was greater than during the dry and cool season and the highest mean/median values were as well (APPENDIX III, APPENDIX IV, Figure 6.14 and Figure 6.15). This was expected because TSI during the wet and warm period (summer) is usually higher, even though it is a rainy season. The median values are similar to the arithmetic mean values except between 12:00:00 and 14:00:00, but generally the values are the same (APPENDIX IV and Figure 6.15), contrary to the dry and cool season (APPENDIX III and Figure 6.15). The amplitude for this season (percentiles 25% - 75%) is greater than the dry and cool season and similar to the overall season (APPENDIX II, APPENDIX III, APPENDIX IV, Figure 6.13, Figure 6.14 and Figure 6.15).

The wet and warm season is better for bacterial disinfection because of higher insolation (Figure 6.16 and Figure 6.17). This was endorsed by the highest mean/median TSI being greater than in the dry and cool season, especially in the afternoon the difference was pronounced (Figure 6.16), again consolidating this season as more advantageous for pathogenic disinfection. Sunrise during this period was between 05:30:00 (n=9) and 06:10:00 (n=75) and TSI proceeded to increase until 11:20:00/13:50:00, i.e., a longer period at its strongest and once again showing the importance of this season for bacterial disinfection. Decrease in irradiance then proceeded until sunset, occurring between 18:30:00 (n=97) and 18:40:00 resulted in longer pond exposure to TSI compared with the dry and cool season. The CV values for this period varied between 1.20 and 0.41, 7 time intervals > 1 (early hours of the morning and late hours of the afternoon). The other 79 CV were lower than 1 (low-variance). From 08:00:00 to 16:00:00 TSI was at its strongest and further strengthens the time interval chosen for the experiments of *E. coli* disinfection profiling.

Figure 6.15 - Box-plot of solar irradiance for the warm and wet season during the monitoring period condensed into one day (July 2014 – November 2015).



6.2.2.3. Comparison between mean/median, maximum and minimum total solar irradiance values

Figure 6.16 presents a comparison between median and mean TSI values from both seasons, cold and dry (April to September) and wet and warm (October to March). Mean and median TSI during the morning for both seasons were virtually the same, exchanging places at 08:40:00 and again at 10:00:00 (median) with the cold and dry season exhibiting slightly higher irradiance. The mean values during the same period show the wet and warm season slightly higher than the dry and cold season during the morning. From 11:30:00 (mean and median), the wet and warm season started to distance itself from the cold and dry until sunset. Sunrise for both seasons happened at practically the same time.

The same tendency for maximum TSI did not happen, with the wet and warm season predominantly greater than the cold and dry season, even though during the morning the distance between both seasons is not as pronounced (Figure 6.17). The same conclusion was reached for sunlight-mediated disinfection for maximum TSI, and should be greater during the wet and warm season, especially in the afternoon. Sunrise for both seasons happened at virtually the same time while sunset for the dry and cold season was closer to 18:00:00 and for the wet and warm season at 19:30:00, consequently the same as for the mean/median values of TSI.

Figure 6.16 – Comparison between median and mean total solar irradiance of the dry and cold (April to September) and warm and wet (October to March) seasons.

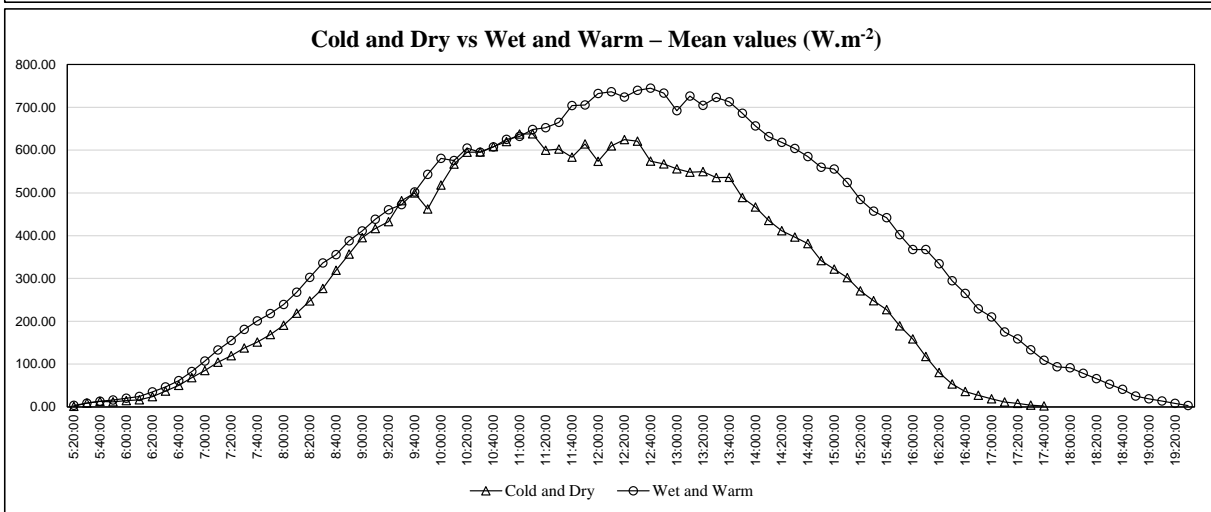
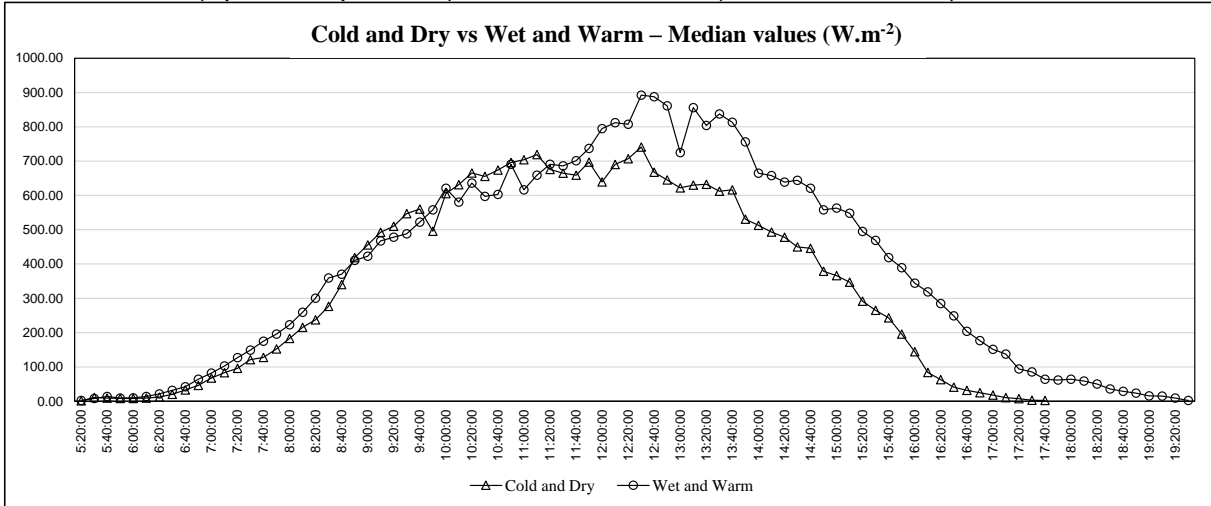


Figure 6.17 – Comparison between maximum total solar irradiance of the dry and cold (April to September) and warm and wet (October to March) seasons.

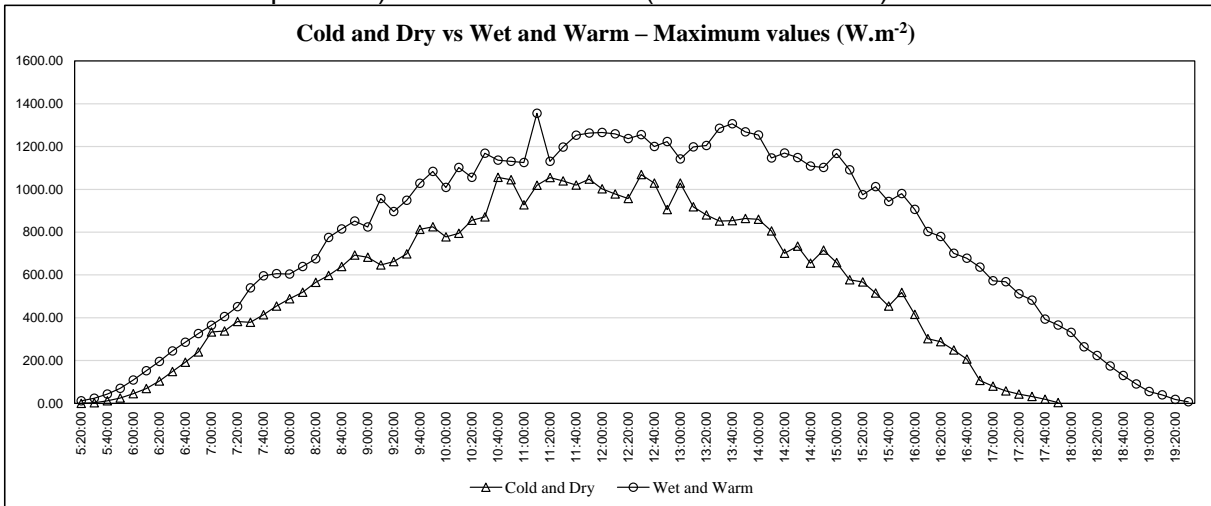
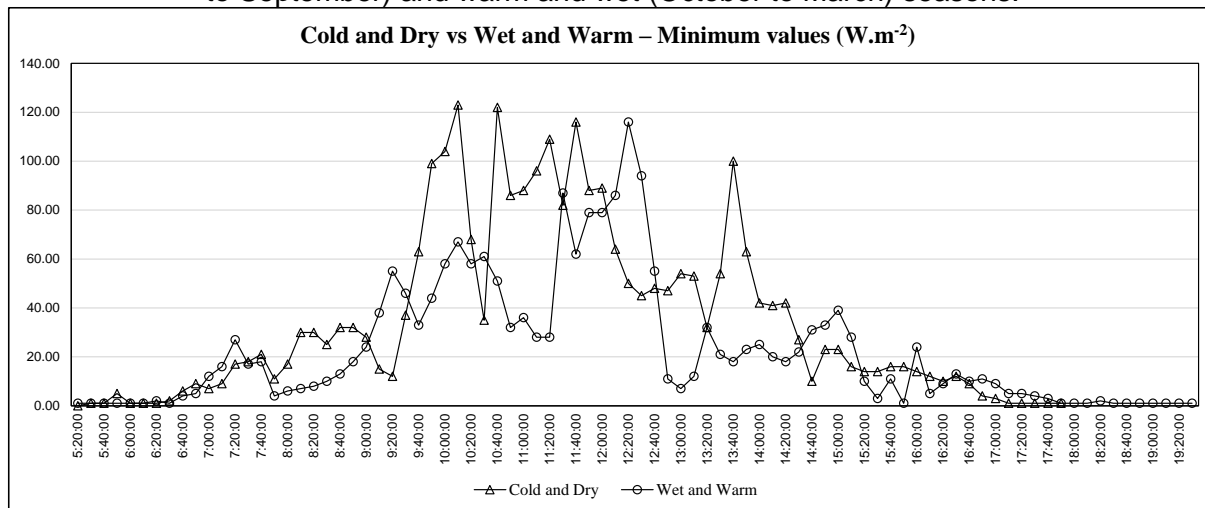


Figure 6.18 presents the minimum values for both seasons. An erratic behaviour is observed for both cold and dry and wet and warm seasons, therefore showing the influence of atmospheric conditions such as cloud cover on the amount of TSI arriving at the surface. Peak minimum values were around 120 W.m^{-2} , with sunrise occurring at roughly the same time and sunset for the wet and warm season occurring much later (nearly 2 hours later). Figure 6.18 does not give any indication which season's minimum values are better for sunlight-mediated disinfection.

Figure 6.18 – Comparison between minimum total solar irradiance of the dry and cold (April to September) and warm and wet (October to March) seasons.



6.2.3. Depth profiling of solar radiation

Radiation monitoring was conducted over lengthy periods of time at different depths in the 2nd pond from the 26/06/2014 to the 23/11/2015 and produced interesting results for penetration depths, attenuation rates and minimal amounts of solar irradiance reaching different depths during the overall period and both seasons. The two seasons followed the same criteria as in subsection 6.2.2, i.e., wet and warm (October – March), and dry and cold (April – September) for different depths. As shown in Table 5.2, solar irradiance depth profiling for UV-A, UV-B and PAR was performed at five different depths and each depth was monitored for at least one week in each month. PAR was detected at all depths and UV-A and UV-B were limited to 10 cm. Arithmetic mean and median values are shown in Figure 6.19 and APPENDIX V, and Figure 6.20 and APPENDIX VI measured at 5 cm and 10 cm, respectively. Figure 6.21 and APPENDIX VII presents arithmetic mean and median values from three different depths (15 cm, 20 cm and 30 cm) for only PAR. Additional monitoring points, 5 cm and 15 cm, guaranteed

more irradiance values in total, at least for the UV spectrum, therefore producing a better depth profile in the pond.

A summary of arithmetic mean/median, maximum (W.m^{-2}) and CV values is presented in APPENDIX V, APPENDIX VI and APPENDIX VII, for 5 cm, 10 cm and 15 cm, 20 cm and 30 cm from 08:00:00 to 16:00:00. Sample numbers (n) are also shown. Figure 6.19 and Figure 6.20 present graphs of mean and median values for the three different wavelengths at 5 cm (APPENDIX V) and 10 cm (APPENDIX VI), respectively. Figure 6.21 shows the plotted data of mean and median PAR from three different depths (15 cm, 20 cm and 30 cm).

Seasonal variation of solar irradiance depth profiling for the Dry and Cool (D&C – April to September) and Wet and Warm (W&W – October to March) are shown in Figure 6.20, Figure 6.22, Figure 6.24, APPENDIX VI, APPENDIX VIII and APPENDIX X. The analysis shows the differences encountered during the seasons with surprising results as depth increased.

Figure 6.25 and Figure 6.26 presents attenuation percentages regarding depths and between depths.

It is worth emphasising that long term solar radiation monitoring at different depths in treatment ponds were not found in the literature, therefore enhancing the importance of the present results.

6.2.3.1. 5 cm depth profile for the overall period

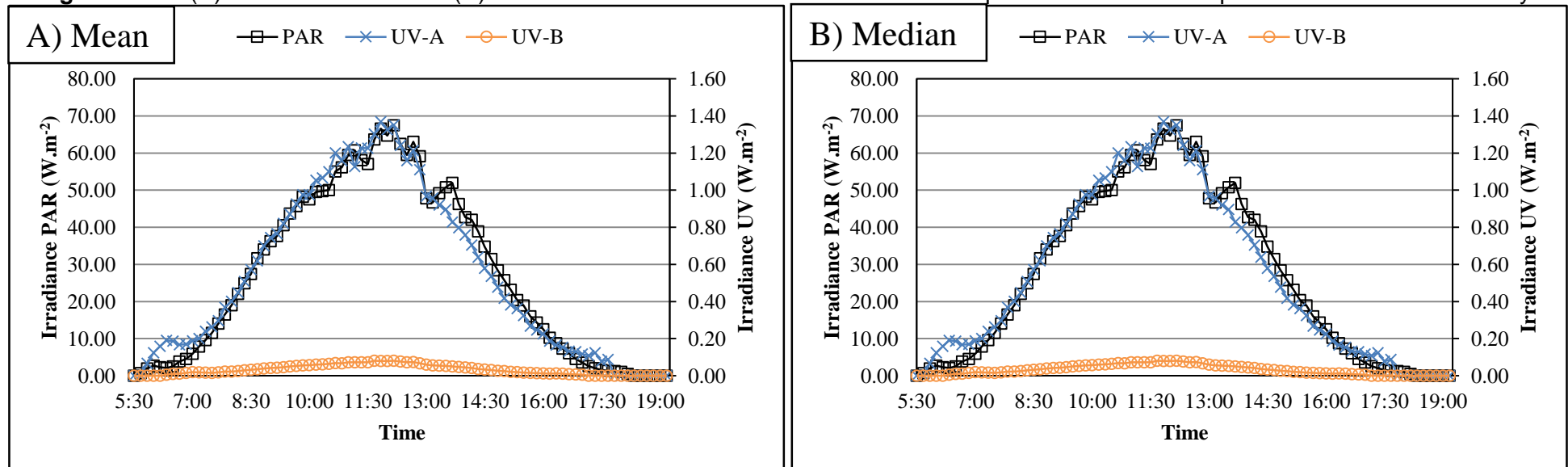
APPENDIX V shows UV-A, UV-B and PAR irradiance from 5 cm in depth in the 2nd maturation pond. Figure 6.19 presents arithmetic mean and median values during the monitoring period condensed into one day.

The highest arithmetic mean and median UV-A values were 1.37 W.m^{-2} (11:50:00) and 1.07 W.m^{-2} (12:10:00) (Figure 6.19), respectively. Both peaked at different times and maximum irradiance was 6.22 W.m^{-2} (11:10:00). The values were rather low when compared to the maximum values recorded during the monitoring period (APPENDIX V). Sample number varied from 2, in the early hours of the morning and late afternoon, to 65, at around midday. The Coefficient of Variation (CV) is much closer to the unit (APPENDIX V) than shown in APPENDIX II, probably due to strong light attenuation conditions in the 2nd pond affecting UV-A. 54 time intervals are low-variance and 18 time intervals are high-variance.

UV-B irradiance was recorded in relatively small doses when compared to UV-A and did not exceed the unit barrier, even at the maximum values (Figure 6.19 and APPENDIX V) and probably due to strong pond optics. The highest mean and median values were 0.081 W.m^{-2} (11:40:00) and 0.062 W.m^{-2} (12:10:00), respectively. The maximum value was 0.343 W.m^{-2} , at 11:10:00 (same time as UV-A). Sample numbers (n) varied from 1 (early hours of the morning and late afternoon) to 62 (closer to midday). CV values were similar to UV-A CV values, suggesting that UV-B varied just as much as UV-A. There are less time intervals for UV-B and it was only detected from 06:20:00 to 17:00:00 while UV-A was from 05:50:00 to 17:40:00 (APPENDIX V).

PAR is the strongest wavelength at this depth (APPENDIX V) and at other depths (APPENDIX VI and APPENDIX VII). Greater than UV-A and UV-B (Figure 6.19), mean and median values were 67.52 W.m^{-2} and 61.41 W.m^{-2} (12:10:00), respectively, coinciding with the same time interval as UV-A and UV-B (median values). Maximum PAR solar irradiance was 222.08 W.m^{-2} at 11:10:00, identical to the time interval of UV-A and UV-B (Figure 6.19 and APPENDIX V). Sample numbers varied from 2 to 76 (less samples associated to the early hours of the morning and afternoon). CV varied the least until 5 cm compared with the other two wavelengths (APPENDIX V). 71 time intervals are low-variance and 5 time intervals are high-variance (early hours of the morning – APPENDIX V), therefore demonstrating that it was the least PAR affected by pond optics. All wavelengths followed a bell-like-shape, increasing in the morning and decreasing in the afternoon, the same as TSI (Figure 6.13).

Figure 6.19 – (A) Arithmetic mean and (B) median of PAR and UV solar irradiance at a depth of 5 cm in the 2nd pond condensed into one day.



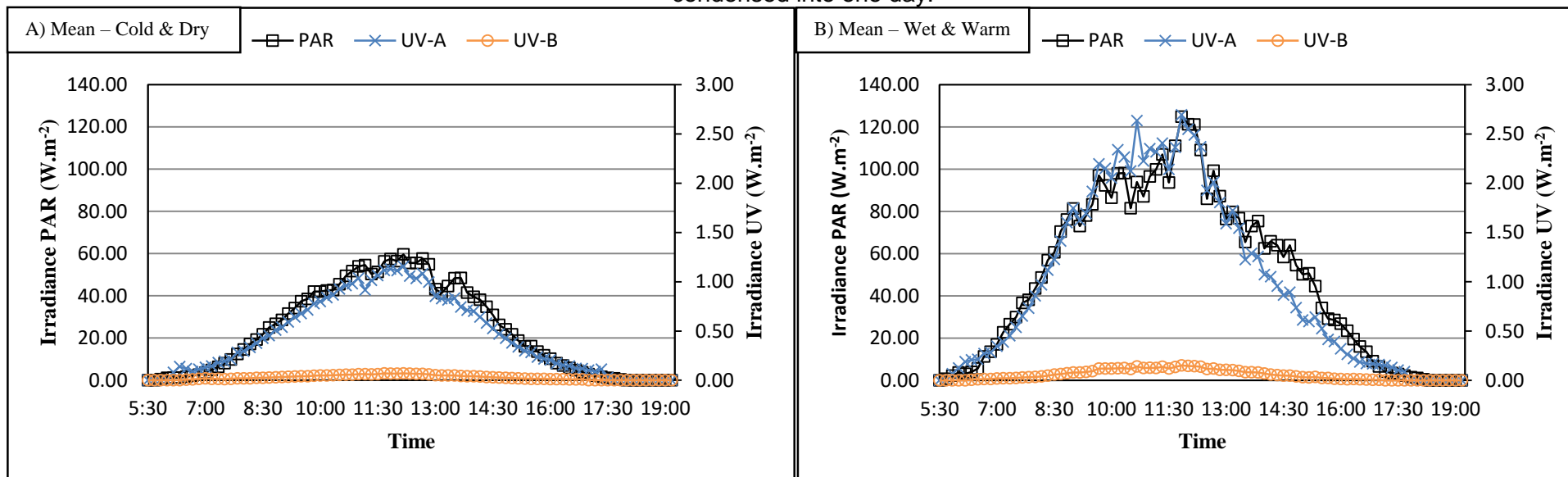
6.2.3.2. 5 cm depth profile for seasonal variation

Figure 6.20 presents arithmetic mean for UV-A, UV-B and PAR irradiance during the cold and dry (**A**) and wet and warm (**B**) seasons for the depth of 5 cm. Results are discussed for arithmetic mean and both mean and median values can be consulted in APPENDIX VI.

Double the amount of energy, i.e. solar irradiance, was present during the wet and warm season (W&W) compared to the cool and dry (C&D) season for all three waves (Figure 6.20 and APPENDIX VI). Although this was expected, but not to such a degree because the difference between mean and median TSI for seasonal variation (Figure 6.16) was not as pronounced as in the 2nd pond. Less energy could probably impact pathogenic bacteria disinfection rates, hence reducing solar-mediated disinfection influence and allowing for other disinfection mechanisms such as predation and sedimentation to play a more predominant role. The highest mean values during the C&D season (08:00:00 – 16:00:00) for UV-A, UV-B and PAR were 1.16 W.m⁻² (12:10:00), 0.071 W.m⁻² (11:40:00) and 59.61 W.m⁻² (12:10:00), respectively. The highest mean values for UV-A, UV-B and PAR during the W&W season (08:00:00 – 16:00:00) were 2.69 W.m⁻², 0.153 W.m⁻² and 124.89 W.m⁻², all at 11:50:00, respectively.

Naturally the sun in the hotter months (W&W) is stronger than during the cooler months (C&D), but the difference between irradiance was more pronounced than expected. TSI does not show the same difference, therefore only pond optics could reduce the energy of each wave (UV-A, UV-B and PAR) to virtually half at 5 cm (W&W=2×C&D). Note that all waves from both seasons maintained the same bell-like-shape as for the overall period (Figure 6.19). The W&W season presented some irregularities from 09:30 to 11:30, probably due to strong cloud cover during those time intervals.

Figure 6.20 – Arithmetic mean for cold and dry (A) and wet and warm (B) for PAR and UV solar irradiance at 5 cm in depth in the 2nd pond condensed into one day.



6.2.3.3. 10 cm depth profile for the overall period

APPENDIX VII presents UV-A, UV-B and PAR values from 10 cm in depth. UV-A, UV-B and PAR all dipped in energy and presented much lower values than at 5 cm (APPENDIX V). Figure 6.21 presents arithmetic mean and median values for the monitoring period condensed into one day.

The highest arithmetic mean and median values of UV-A were 0.268 W.m^{-2} (11:50:00) and 0.212 W.m^{-2} (17:10:00), respectively. The time interval for the median value is not on par with previous analyses showing that the highest values occurred close to midday. The peak values are probably caused by low turbidity at the time, therefore allowing more solar light to infiltrate. Consequently, UV-A at 10 cm was much distorted (scattering and absorption) compared to UV-A irradiance at 5 cm (Figure 6.19). The absence of an increase in irradiance in the morning and a decrease in the afternoon supports this conclusion by presenting a very irregular shape, i.e., no bell-like-shape was present. Maximum solar irradiance of UV-A was 2.48 W.m^{-2} at 11:50:00, similar time for UV-A at 5 cm in depth (APPENDIX V and APPENDIX VII). Sample numbers varied from 1 in the early hours of the morning and late afternoon, to 58, around midday. The CV (APPENDIX VII) presented 51 low-variance time intervals and 9 time intervals as high-variance. Note that UV-A was only detected at 7:50:00 whereas at 5 cm it was detected earlier (Figure 6.19, Figure 6.21, APPENDIX V and APPENDIX VII), therefore proving that in the early hours of the morning UV-A does not have the intensity to reach a 10 cm depth.

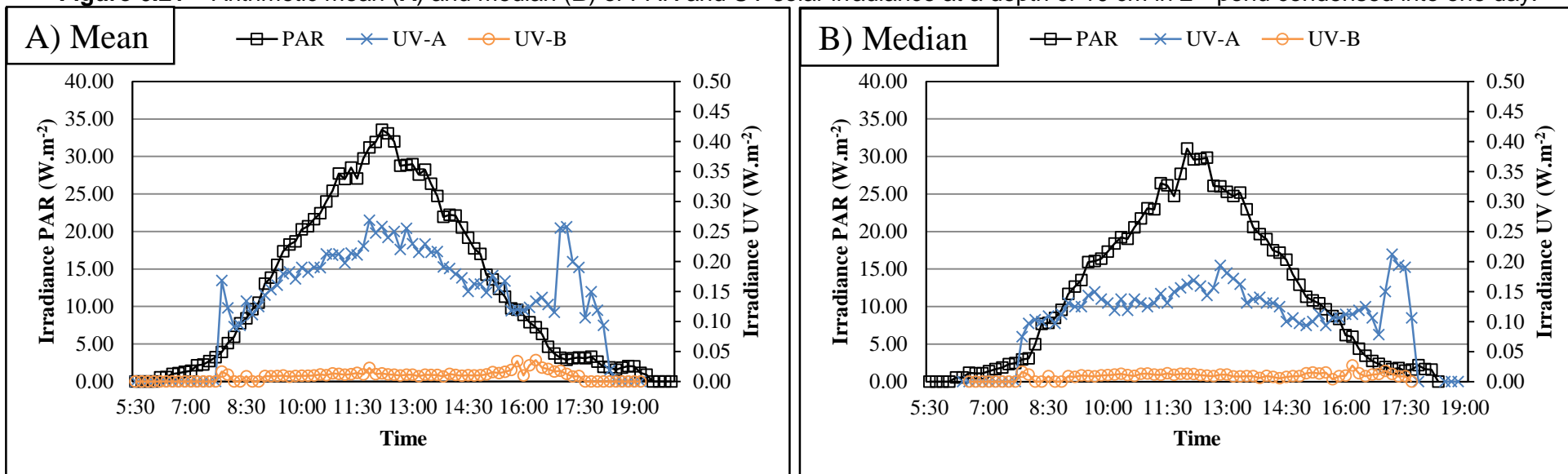
UV-B maximum peak value was 0.143 W.m^{-2} at 11:50:00 (Figure 6.21 and APPENDIX VII), the same time interval as UV-A. Figure 6.21 shows UV-B irradiance at 10 cm was also very irregular when compared at 5 cm (UV-A presented the same characteristics). UV-B follows the same trend as that of UV-A (10 cm), increasing and decreasing throughout the day, when finally attenuating completely an hour before UV-A. The highest arithmetic mean and median value of UV-B were 0.0355 W.m^{-2} (16:20:00) and 0.0268 W.m^{-2} (16:10:00), respectively (Figure 6.21 and APPENDIX VII). Sample number varied from 1 to 24, resulting in a drastic decrease compared at 5 cm (APPENDIX V and APPENDIX VII). This was further evidence that the UV spectrum was drastically affected by scattered matter and other substances in the ponds. UV-B varied less in energy compared to UV-A and is endorsed by lower CV values, however sample numbers could cause this. 43 time intervals are low-variance and 7 time intervals are high-

variance (APPENDIX VII). Just as with UV-A, UV-B radiation was detected at a later stage, even later than UV-A.

PAR irradiance strength was much greater than UV-A and UV-B, as shown in Figure 6.21, arithmetic mean and median reached 33.56 W.m^{-2} (12:10:00) and 31.03 W.m^{-2} (12:00:00), respectively (Figure 6.21 and APPENDIX VII). The bell-like-shape for PAR irradiance was still present at this depth, contrary to UV-A and UV-B. Maximum solar irradiance was 137.37 W.m^{-2} at 12:50:00, attenuating very little compared to 5 cm irradiance (APPENDIX V and APPENDIX VII). Sample numbers varied from 1 to 83 (lowest sample numbers associated to the early hours of the morning and late afternoon). PAR CV varied the least when compared with the other two wavelengths (APPENDIX VII): 65 time intervals are low-variance and 13 are high-variance.

The total sample numbers varied the most for the UV spectrum, therefore increasing the effect of suspended solids/algae/organic matter on attenuating UV-A and UV-B. PAR on the other hand was less or not affected by pond optics and presented a maximum of 83 samples, UV-A, 58 samples and UV-B, 24 samples for one time interval (APPENDIX VII). Both UV-A and UV-B, and in particular UV-B, presented difficulty in penetrating until 10 cm in depth. PAR irradiance presented a bell-like shape whereas UV-A and UV-B a distorted and irregular shape (Figure 6.21), not increasing and then decreasing, but instead a pulsating graph.

Figure 6.21 – Arithmetic mean (A) and median (B) of PAR and UV solar irradiance at a depth of 10 cm in 2nd pond condensed into one day.



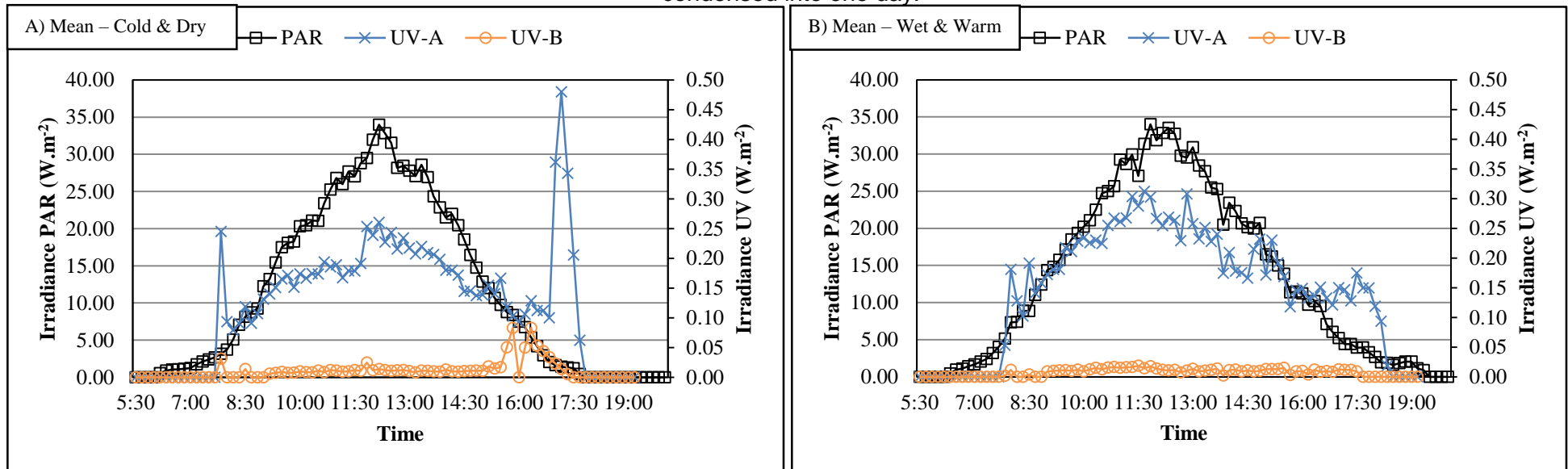
6.2.3.4. 10 cm depth profile for season variation

UV-A, UV-B and PAR irradiance during the cold and dry (C&D) (**A**) and wet and warm (W&W) (**B**) seasons are shown in Figure 6.22. As for the 5 cm profile, the results are discussed for arithmetic mean values, and median values are plotted in APPENDIX VIII to consult but are not discussed.

The same amount of solar irradiance was present during the wet and warm season (W&W) compared to the cool and dry (C&D) season for PAR and UV-B (Figure 6.22 and APPENDIX VIII). UV-A during the W&W was slightly higher than C&D at around midday and the discrepancy between C&D and W&W for PAR and UV-B mean values were not as great as 5 cm, but overall W&W presented higher mean values ((Figure 6.22 and APPENDIX VIII). Highest mean values during the C&D season (08:00:00 – 16:00:00) for UV-A, UV-B and PAR were 0.260 W.m^{-2} (12:10:00), 0.0830 W.m^{-2} (15:50:00) and 33.98 W.m^{-2} (12:10:00), respectively. The highest mean values for UV-A, UV-B and PAR during the W&W season (08:00:00 – 16:00:00) were 0.312 W.m^{-2} (11:40:00), 0.019 W.m^{-2} (11:30:00) and 34.01 W.m^{-2} (11:50:00), respectively. Both seasons presented similar highest mean values, but UV irradiance was very erratic. UV-A values during the C&D season were more erratic than during the W&W season. UV-B during both seasons showed similar trends, although more erratic during the C&D season. PAR during both seasons was very similar, both presenting comparable peak mean values, but with the sun setting later during the W&W season (Figure 6.22 and APPENDIX VIII).

Although hotter months (W&W) should present stronger irradiance values than during the cooler months (C&D), this was not generally observed at 10 cm. Pond optics reduced the energy of each wave (UV-A, UV-B and PAR) during both seasons to virtually the same values (W&W \approx C&D). Note that PAR from both seasons maintained the same bell-like-shape as for the 5 cm profiles (overall and season variation) and 10 cm overall period (Figure 6.19, Figure 6.20 and Figure 6.21).

Figure 6.22 – Arithmetic mean for cold and dry (A) and wet and warm (B) for PAR and UV solar irradiance at 10 cm in depth in the 2nd pond condensed into one day.

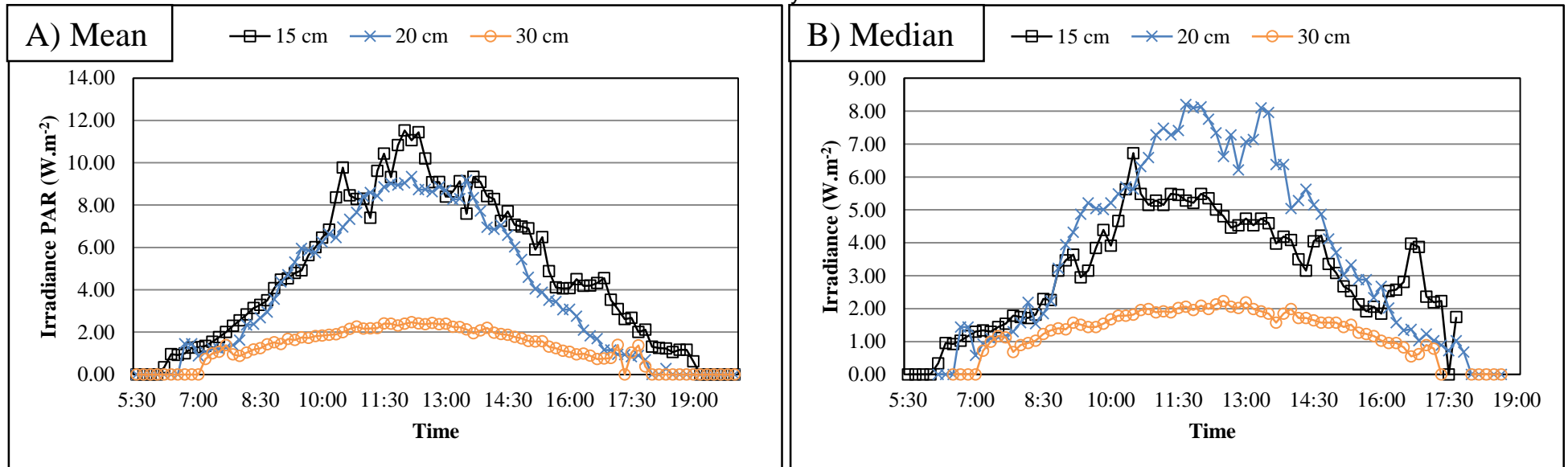


6.2.3.5. 15 cm, 20 cm and 30 cm depth profile for the overall period

PAR from 15 cm, 20 cm and 30 cm in depth in the 2nd maturation pond are shown in Figure 6.23 and APPENDIX IX. UV-A and UV-B are not shown because the waves extinguished somewhere between 10 cm and 15 cm and all PAR levels decreased in energy (Figure 6.19, Figure 6.23, APPENDIX V and APPENDIX IX). Figure 6.23 presents arithmetic mean and median values for the monitoring period condensed into one day. Only arithmetic mean values are discussed below because median values are less stable at 15 cm, as shown in Figure 6.23 and APPENDIX IX.

UV-A and UV-B were not perceptible at 15 cm depth, having completely attenuated between 10 and 15 cm. PAR was able to penetrate deeper and reached 30 cm in depth with little trouble (subsection 4.2), which is important for bacterial disinfection (subsection 6.3). The highest mean values (and median) at 15, 20 and 30 cm were 11.52 W.m⁻² (12:00:00), 9.34 W.m⁻² (12:10:00) and 2.48 W.m⁻² (12:10:00), respectively. PAR maintained its bell-like-shape (Figure 6.23) at 15 and 20 cm, but more flattened at 30 cm and finally showing that pond optics affected PAR. Maximum solar irradiance was 54.51 W.m⁻² (12:20:00) at 15 cm, 26.98 W.m⁻² (13:50:00) at 20 cm and 8.10 W.m⁻² (12:30:00) at 30 cm. Note how irradiance at 15 cm was detected earlier than at 20 and 30 cm, and 20 cm was detected earlier than 30 cm. At sunset the same happened inversely, irradiance was last detected at 15 cm (APPENDIX IX). The pond optics were less affected at 15 cm than at 20 cm and 30 cm as shown in Figure 6.13.

Figure 6.23 – Arithmetic mean (A) and median (B) of PAR solar irradiance at 15 cm, 20 cm and 30 cm in depth in the 2nd pond condensed into one day.



6.2.3.6. 20 cm and 30 cm depth profile for season variation

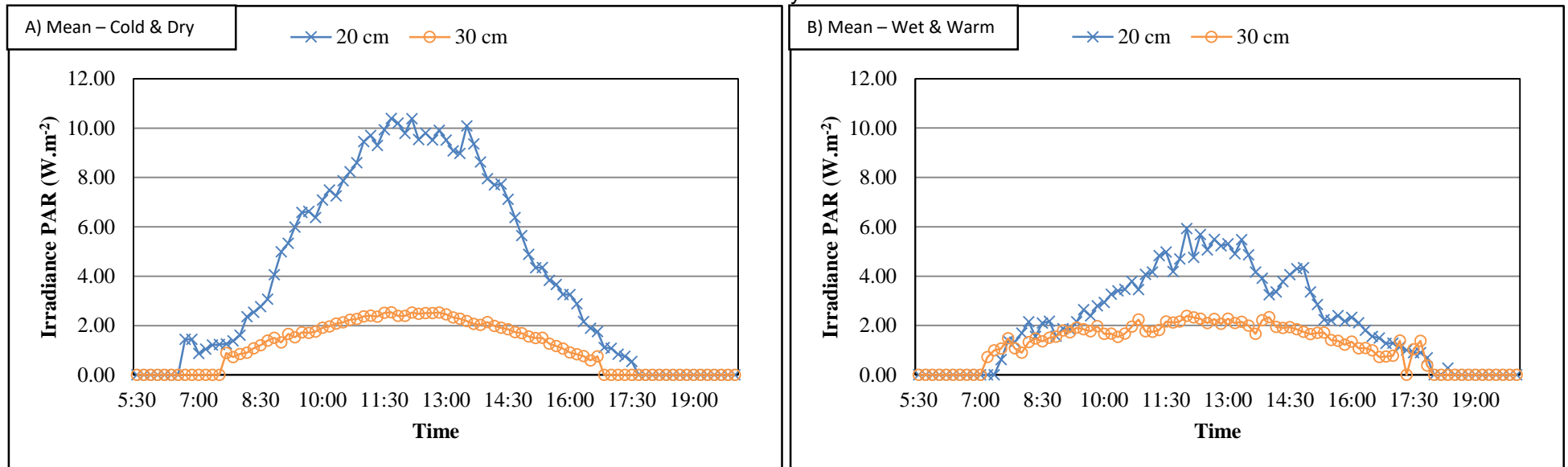
PAR irradiance at 20 cm and 30 cm during the cold and dry (C&D) (A) and wet and warm (W&W) (B) seasons are shown in Figure 6.24. 15 cm is not plotted because there were not enough samples for the C&D season to draw conclusions (subsection 6.2.3.5). APPENDIX X presents all arithmetic mean and median values during both seasons. Median values were not plotted.

PAR irradiance (20 cm) during the cool and dry (C&D) was generally greater than during the wet and warm season (W&W), resulting in $W\&W < C\&D$ (Figure 6.24 and APPENDIX X), contrary to results for 5 cm ($W\&W > C\&D$) and 10 cm ($W\&W = C\&D$) (Figure 6.20 and Figure 6.22). Irradiance at 30 cm during both seasons was practically the same. The results are interesting in a way that, during the W&W season, higher mean irradiance values decreased as the depth increased, becoming equal at 10 cm and then the C&D season gained leadership with stronger irradiance at 20 and 30 cm. PAR at 30 cm during the W&W season was even more erratic than during the C&D season (Figure 6.20, Figure 6.22 and Figure 6.24 – subsections 6.2.3.2/4). The highest mean values during the C&D season (08:00:00 – 16:00:00) at 20 cm and 30 cm were 10.32 W.m^{-2} and 2.54 W.m^{-2} both at 11:40:00, respectively. During the W&W the highest mean values at 20 cm and 30 cm were (08:00:00 – 16:00:00) were 5.92 W.m^{-2} and 2.39 W.m^{-2} both at 12:00:00, respectively.

Although hotter months (W&W) should present stronger irradiance values than during the cooler months (C&D), this was not observed at 20 cm and 30 cm. Pond optics, with increasing algal concentrations reduced irradiance (due to scattering and reflecting) during the W&W season, compared to the C&D season ($C\&D > W\&W$). Even though it still maintained the same bell-like-shape for both depths (overall and season variation) (Figure 6.19, Figure 6.20, Figure 6.21, Figure 6.22 and Figure 6.23).

PAR could penetrate further into the pond, as shown by Bolton *et al.* (2011a), and reach the bottom (44 cm), but because the sensors are 15 cm in height, the amount of solar radiation could not be measured at floor level.

Figure 6.24 – Arithmetic mean for cold and dry (**A**) and wet and warm (**B**) for PAR at 20 cm and 30 cm in depth in the 2nd pond condensed into one day.



6.2.3.7. Attenuation percentages of solar irradiance (PAR, UV-A, UV-B) between depths

Figure 6.25 and Figure 6.26 presents attenuation percentages and plotted data for UV-A, UV-B and PAR between the various irradiances measured at each depth every 30 minutes, divided up in 10cm/5cm (UV-A, UV-B and PAR) and PAR (10cm/5cm; 20cm/10cm; 30cm/20cm; 30cm/10cm; 30cm/5 cm). Percentages relate to the amount of attenuated irradiance between two depths, i.e., the percentage of irradiance that diminished between two depths. Figure 6.27 displays the behaviour of mean solar irradiance values from APPENDIX V, APPENDIX VII and APPENDIX IX for each time interval and depth profile.

Figure 6.25 shows UV-B and UV-A attenuated roughly the same from 09:00:00 to around 12:00:00 between 10 cm and 5 cm. UV-B from 12:00:00 attenuated more compared to UV-A until 13:30:00 and was then overtaken by UV-A as the most attenuated wave. A maximum 85% of UV-B was attenuated and lost between 5 cm and 10 cm and a maximum of 83% was attenuated for UV-A. UV-B attenuated on average the most for virtually all time intervals between the 10 cm and 5 cm.

PAR between 10 cm and 5 cm attenuated less compared to the two other waves, losing as much as 73% (08:00:00) in the morning between 5 cm to 10 cm. At midday, PAR only attenuated 51% between 10 cm and 5 cm (Figure 6.26). Between 10 and 5 cm, PAR demonstrated a constant decrease in attenuation percentages, resulting in less attenuation when approaching the end of the day. Attenuation percentages between 20/10 cm, 30/20 cm and 30/10 cm presented the same trend as UV-A and UV-B, all three increased until 12:00:00 and then decreased in percentage, therefore indicating that attenuation between the depths during the day increased until midday and then proceeded to decrease.

PAR attenuation for 30/5 cm presented a more stable tendency throughout the day, an indication that attenuation percentages, and consequently rates, throughout the day are quite stable, but there was still a slight increase in the attenuation percentage (1%) and then a slight decrease when approaching the end of the day (Figure 6.26). Maximum attenuation occurred around midday with 96% of PAR measured at 5 cm attenuating at 30 cm.

As expected, the highest irradiance values are perceptible around noon for all depths (Figure 6.19, Figure 6.21 and Figure 6.23) because the sun is at the highest point in the sky. Around

noon was when the waves attenuated the most due to pond optics (subsection 6.2.4) in the form of algae.

Bolton *et al.* (2011a) findings suggested that UV-B penetration was limited to the first 8 cm in a facultative pond, here, UV-B was still detected at 10 cm, 2 cm deeper than their findings. UV-A, on the other hand, was not detected at a 15 cm depth as in Bolton *et al.* (2011a) findings. These results showed that UV-B could penetrate in maturation ponds as much as UV-A, although the amount of energy that each wave carried was very different.

Figure 6.25 – Mean attenuation percentages between 10 cm and 5 cm for UV-A and UV-B over one day.

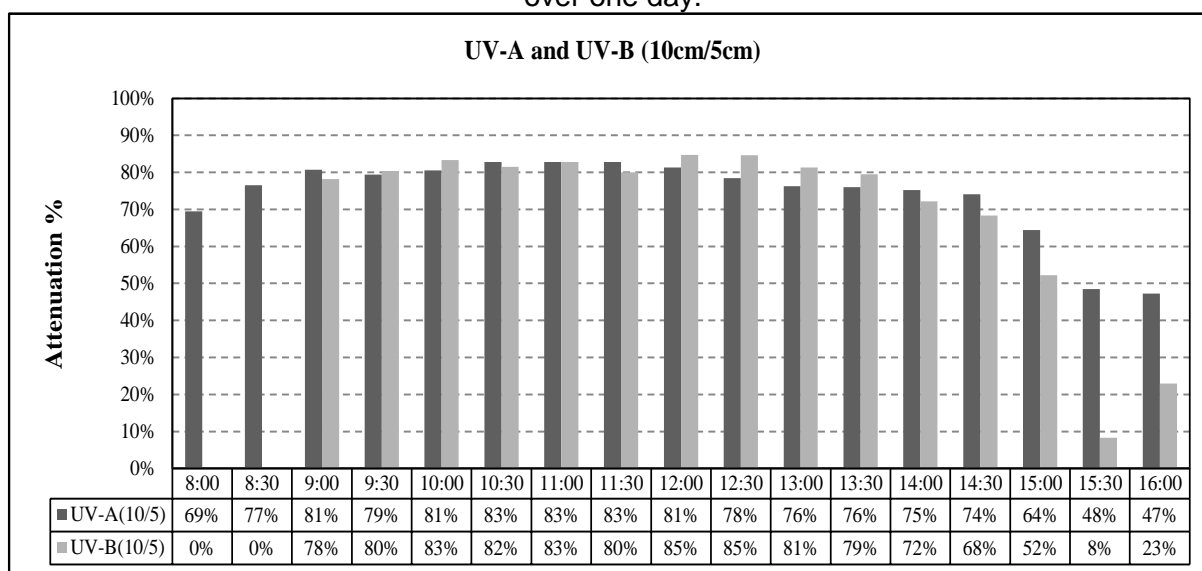


Figure 6.26 – Mean attenuation percentages between 10cm/5cm, 20cm/10cm, 30cm/20cm, 30cm/10cm and 30cm/5 cm for PAR over one day.

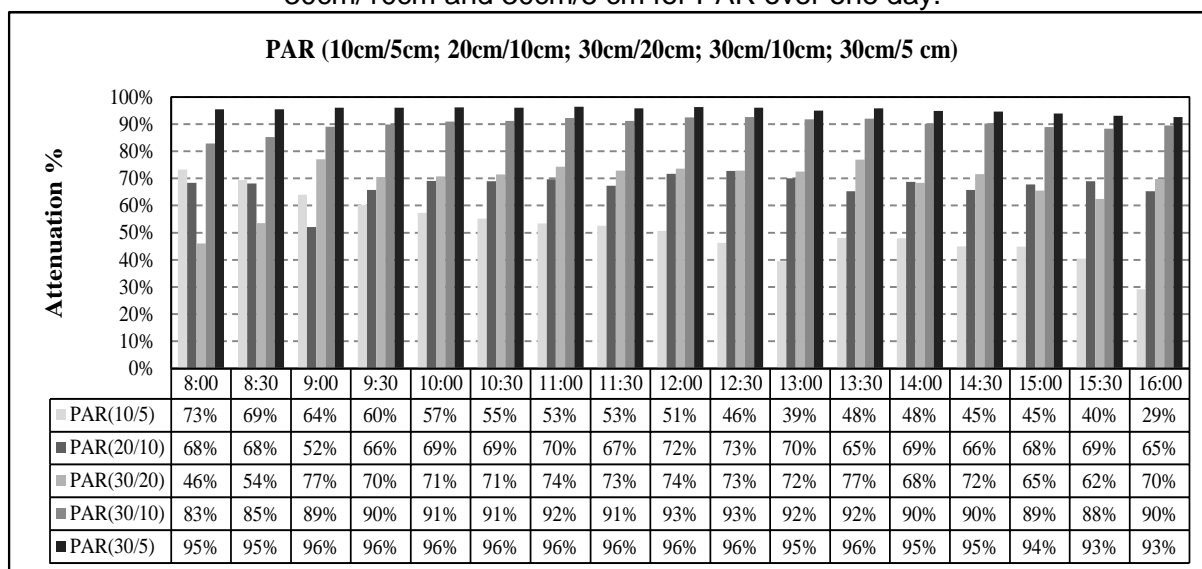
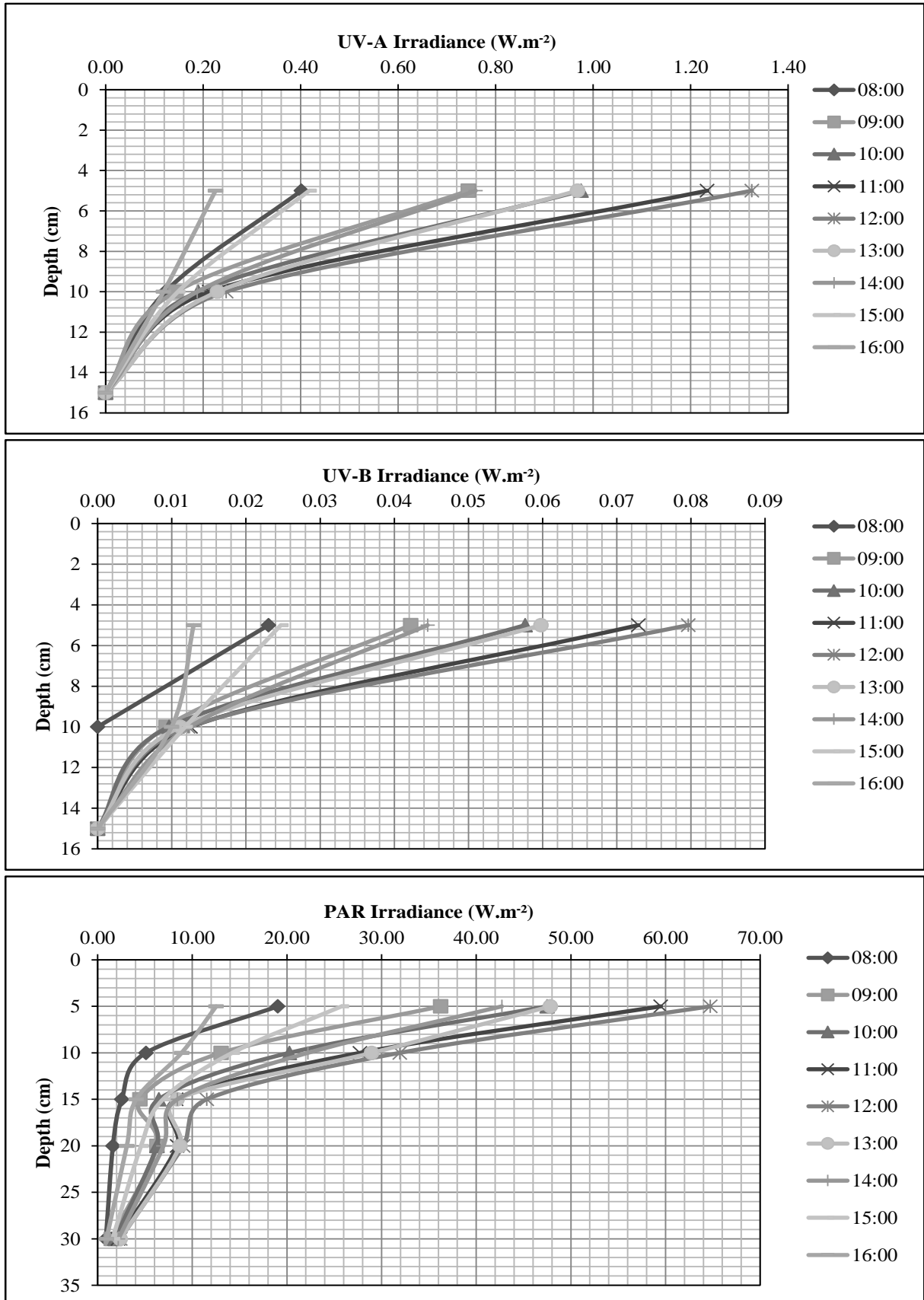


Figure 6.27 presents UV-A, UV-B and PAR mean irradiance for every hour at different depths. UV-A and UV-B both presented similar attenuation behaviour as depth increased, i.e., sharper attenuation between 5 cm and 10 cm closer to midday, and slower attenuation between 10 cm and 15 cm. PAR behaved very differently from the other two waves, penetrating more in the liquid column with a sharp decrease in irradiance between 5 cm and 15 cm, and a slower decrease from 15 cm to 30 cm. Most energy was lost in the upper layers of the pond (UV-A and UV-B: first 5 cm; and PAR: first 15 cm). The lowest mean irradiance for all waves was detected at 08:00:00 and 16:00:00 and the highest at 12:00:00 and then 11:00:00, 13:00:00.

Figure 6.27 – Summary of UV-A, UV-B and PAR median irradiance in relation to depth and time.



6.2.4. Modelling attenuation coefficients for sunlight penetration

Since PAR, UV-A and UV-B were not measured at the pond's surface, but only inside the pond, two approaches are presented in this subsection concerning modelling attenuation coefficients for sunlight penetration. The first scenario took into account the percentages recommended by Shilton (2005) at noon (PAR = 50%; UV-A = 5%; and UV-B = 0.2%) to estimate the amount of surface PAR, UV-A and UV-B from total solar irradiance (TSI) – subsection 6.2.4.1 and 6.2.4.2. The second scenario considered the value estimates by the SMARTS programme for PAR, UV-A and UV-B in pristine conditions (no cloud cover) – subsection 6.2.4.3 and 6.2.4.4. Attenuation models are compared with each other and the reason to present two different methods estimating surface UV-A, UV-B and PAR was to conclude on the best method to predict attenuation rates. Mean turbidity values until each depth profile (10 cm, 20 cm and 30 cm) over the course of the experiment are presented in Table 6.7 and Figure 6.28, and based on APPENDIX XI. All attenuation coefficients regard arithmetic mean irradiance values.

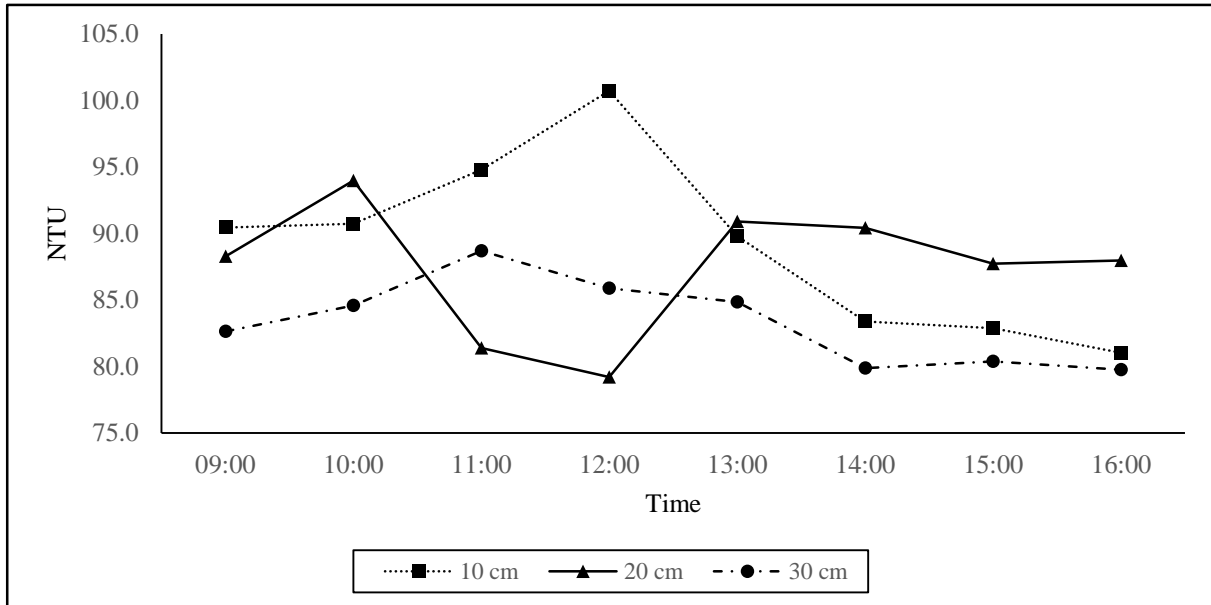
Table 6.7 – Mean nephelometric turbidity units (NTU) for each depth (10 cm, 20 cm and 30 cm) and overall depth during each time frame.

Depth/Time	09:00:00	10:00:00	11:00:00	12:00:00	13:00:00	14:00:00	15:00:00	16:00:00
10 cm	90.5	90.7	94.8	100.7	89.8	83.4	82.9	81.0
20 cm	88.3	94.0	81.4	79.2	90.9	90.4	87.7	88.0
30 cm	82.6	84.6	88.7	85.9	84.9	79.9	80.4	79.8
Overall mean*	86.0	88.5	87.3	87.7	88.5	84.6	83.7	82.9

*Mean values were calculated based on all turbidity values for the three depths during each time interval – APPENDIX XI.

The time interval used was from 09:00 to 16:00 and overall mean turbidity (NTU) varied little (82.9 – 88.5 NTU) (Table 6.7). Turbidity at 10 cm and 30 cm followed the same trend, both increased until 11:00/12:00 and then proceeded to decrease, with a sharper decrease for turbidity in the first 10 cm layer and a more subtle decrease for 30 cm (Table 6.7 and Figure 6.28). Turbidity at 20 cm presented a more erratic behaviour, increasing and decreasing during the day and then finally balancing out. This was probably due to algae shifting between layers as sunlight intensity increased and decreased in order to find an equilibrium of just the right amount of sunlight needed to carry out photosynthesis and not to get damaged. Or, other hydrodynamic phenomenons could explain it (subsection 6.3.7). This was seen between 10:00 and 13:00 with turbidity decreasing (10 cm increased and 30 cm increased slightly).

Figure 6.28 - Plotted mean values of turbidity for the different depth profiles at each time interval.



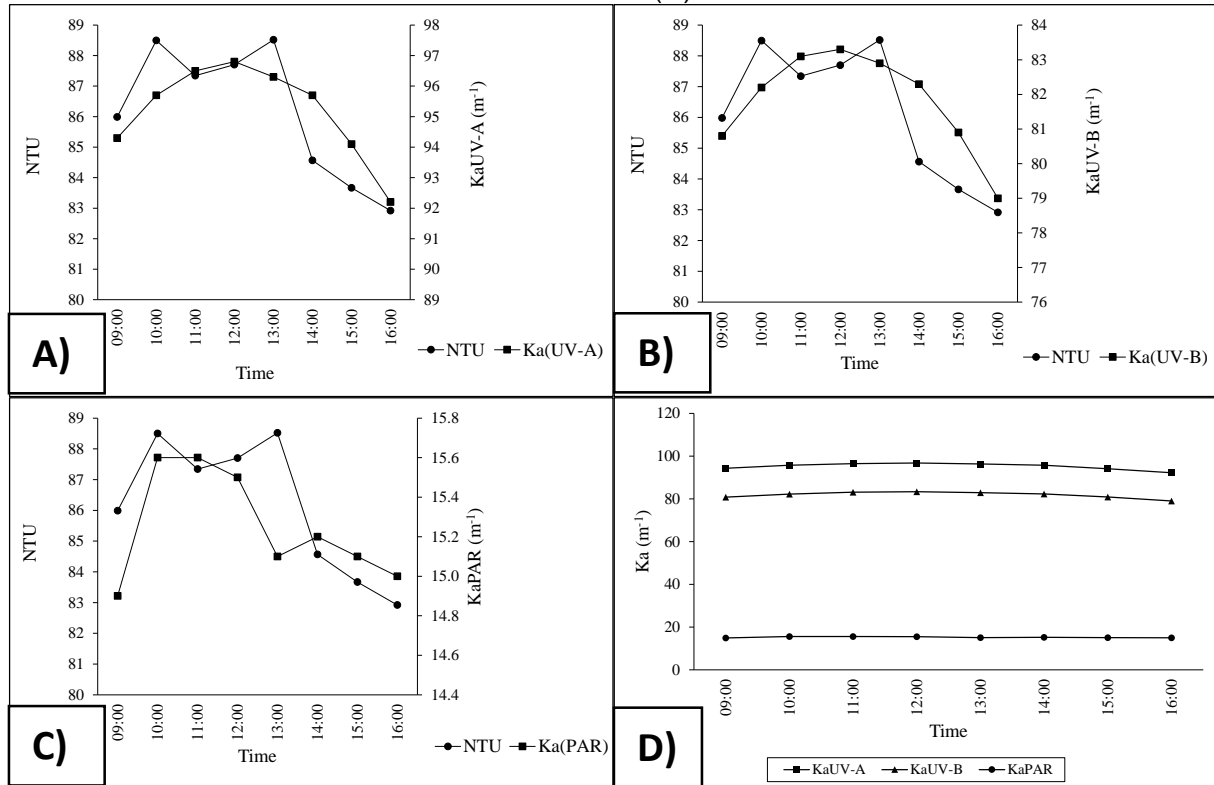
6.2.4.1. Attenuation coefficients for UV-A, UV-B and PAR using percentages

Figure 6.29 shows the behaviour of attenuation coefficient (K_a) values for UV-A, UV-B and PAR, and turbidity during the different time intervals. K_a values were calculated based on Equation 4.36 in subsection 4.8 and used irradiances from APPENDIX V, APPENDIX VII, APPENDIX IX and APPENDIX XII which are presented in APPENDIX XII. The time period used was also between 9:00 and 16:00.

Turbidity values in all three graphs in Figure 6.29 (A, B and C) are the same. Turbidity overall presented an erratic tendency, increasing from 09:00:00 to 10:00:00, but between 10:00:00 and 13:00:00 it dipped in value. Attenuation rate (K_a) values for UV-A and UV-B increased during the same period and then decreased together with turbidity from 13:00:00 until 16:00:00, therefore showing that the waves were affected by turbidity values. During sampling, and on a general basis, turbidity during the morning increased with increasing solar intensity (algal activity), then decreased at end of the afternoon. PAR K_a values followed the same erratic tendency as the NTU (Figure 6.29 C) and increased from 09:00 to 10:00, stabilising between 10:00 and 12:00. At 13:00 a sharp decrease for K_a PAR occurred, contrasting with the sharp increase of NTU, but at 14:00 the K_a PAR increased slightly (probably as a result of an increase in turbidity at 13:00), but then decreased following the same trend as turbidity. The graphs showed that UV and PAR are affected differently by pond optics, as suggested by Curtis *et al.*

(1994), and penetration varied for each wavelength due to the algal mass by producing different light attenuation effects.

Figure 6.29 - K_a UV-A vs NTU (A); K_a UV-B vs NTU (B); K_a PAR vs NTU (C) considering Shilton (2005) percentages for estimating surface irradiance; and K_a values for UV-A, UV-B and PAR (D).



Attenuation rates (K_a) of UV-A, UV-B and PAR shown in Figure 6.29 (D) did not follow the trends previously documented in literature because UV-A attenuated the most (higher K_a values) throughout the day. This was not expected because UV-B is considered the weaker wave and should have attenuated more, but both waves presented the same behaviour throughout the day (Figure 6.29 A and B, and APPENDIX XII). PAR attenuated the least (expected) and the difference was substantial (Figure 6.29 D), therefore justifying why it can penetrate beyond 30 cm.

6.2.4.2. Modelling attenuation coefficients for PAR using surface irradiance percentages

Due to the vast amount of PAR irradiance measured at different depths, Equation (4.36), with its traditional structure was used (reproduced in Equation (6.1)), with the calculated value of the attenuation rate (K_a). K_a for PAR was calculated using the Solver tool in Excel, minimising the sum of the squared errors. Two other equations were investigated (Equations (6.2) and (6.3)), on the basis that turbidity as such (TUR) or expressed as its \log_{10} (LOG(TUR)) influence

the attenuation coefficient. All equations are for a timeline from 09:00 – 16:00. Table 6.8 shows the estimated K_a values for all three equations, as well as the resulting Coefficient of Determination (CD). Figure 6.30 (A, B and C) shows the goodness of fit for the observed results vs calculated results for the CD values.

$$I = I_0 \cdot e^{-24.73 \cdot Z} \quad (6.1)$$

$$I = I_0 \cdot e^{-0.278 \cdot TUR \cdot Z} \quad (6.2)$$

$$I = I_0 \cdot e^{-12.66 \cdot \text{LOG}_{10}(TUR) \cdot Z} \quad (6.3)$$

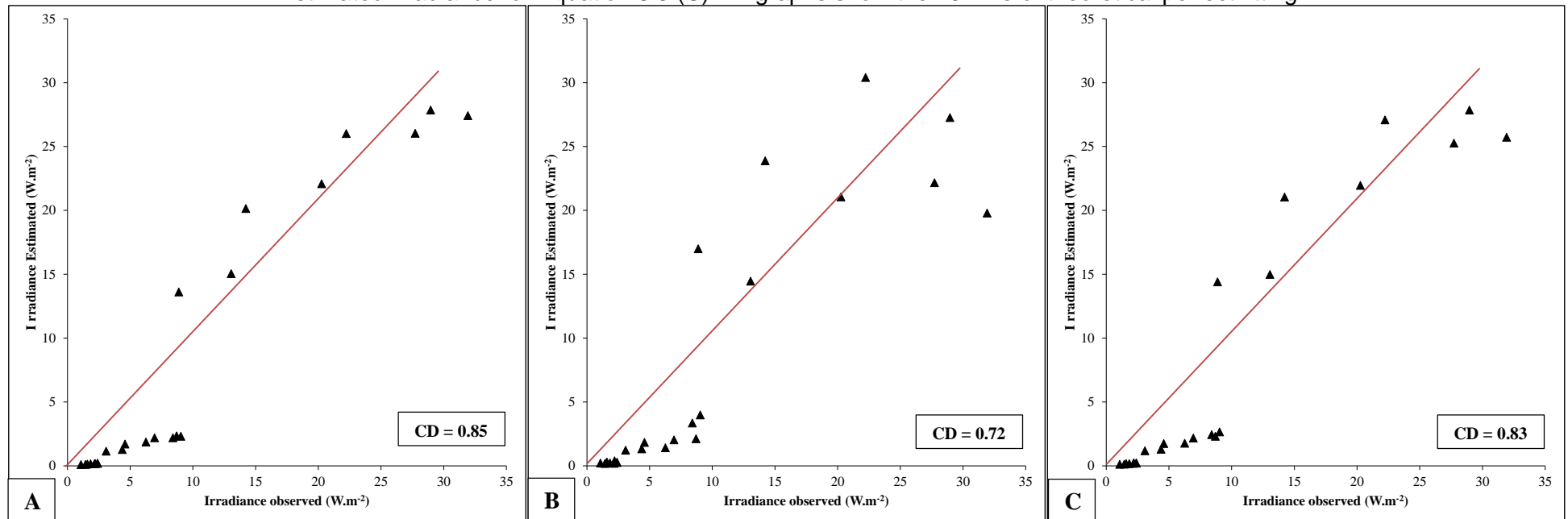
where,

- I – PAR irradiance at depth z ($\text{W} \cdot \text{m}^{-2}$);
- I_0 – PAR irradiance at the pond surface ($\text{W} \cdot \text{m}^{-2}$);
- TUR – turbidity (NTU);
- Z – Depth from surface or reference point (m).

Table 6.8 - K_a values, Coefficient of Determination and K_a units for Equations 6.1, 6.2 and 6.3.

Equation	K_a	CD	K_a unit
6.1	24.73	0.85	m^{-1}
6.2	0.278	0.72	$\text{m}^{-1} \cdot \text{NTU}^{-1}$
6.3	12.66	0.83	$\text{m}^{-1} \cdot \text{LOG}_{10}(\text{NTU}^{-1})$

Figure 6.30 - Observed and Estimated Irradiance for Equation 6.1 (A); Observed and Estimated Irradiance for Equation 6.2 (B) and; Observed and Estimated Irradiance for Equation 6.3 (C). All graphs show the 45° line of theoretical perfect fitting.



Equation 6.1, with the simpler structure, produced the best fit after analysing observed irradiance versus estimated irradiance (Figure 6.30-A) because $CD = 0.85$ (Table 6.8), indicating a good fit. Equations 6.2 and 6.3 presented a CD of 0.72 and 0.83, respectively, being the latter very similar to the CD for Equation 6.1 and suggesting that $LOG(TUR)$ could be included in the model for irradiance attenuation. Figure 6.30-B corresponds to the plotted observed and estimated data from Equation 6.2, and it is clear that using turbidity did not produce as good a fit as the other two equations, although the CD value was still high. By applying the logarithm of turbidity (Figure 6.30-C), as Bolton *et al.* (2011a) did, the observed and estimated values follow a more linear trend, virtually imitating that of Figure 6.30-A and resulting in a better CD . In fact, as suggested by Bolton *et al.* (2011a), turbidity could indeed be a good attenuation indicator and also a simple parameter to measure in any pond system. However, all CD values can be considered high and each model can be used to predict irradiance at different depths with good confidence. Notice that in Table 6.8 the attenuation coefficients are presented in different units and cannot be compared directly with each other. When planning to apply these equations for other pond systems, it should be noted that the pond is shallow and turbidity did not change substantially along the depth (Table 5.1, Table 6.7 and Figure 6.28).

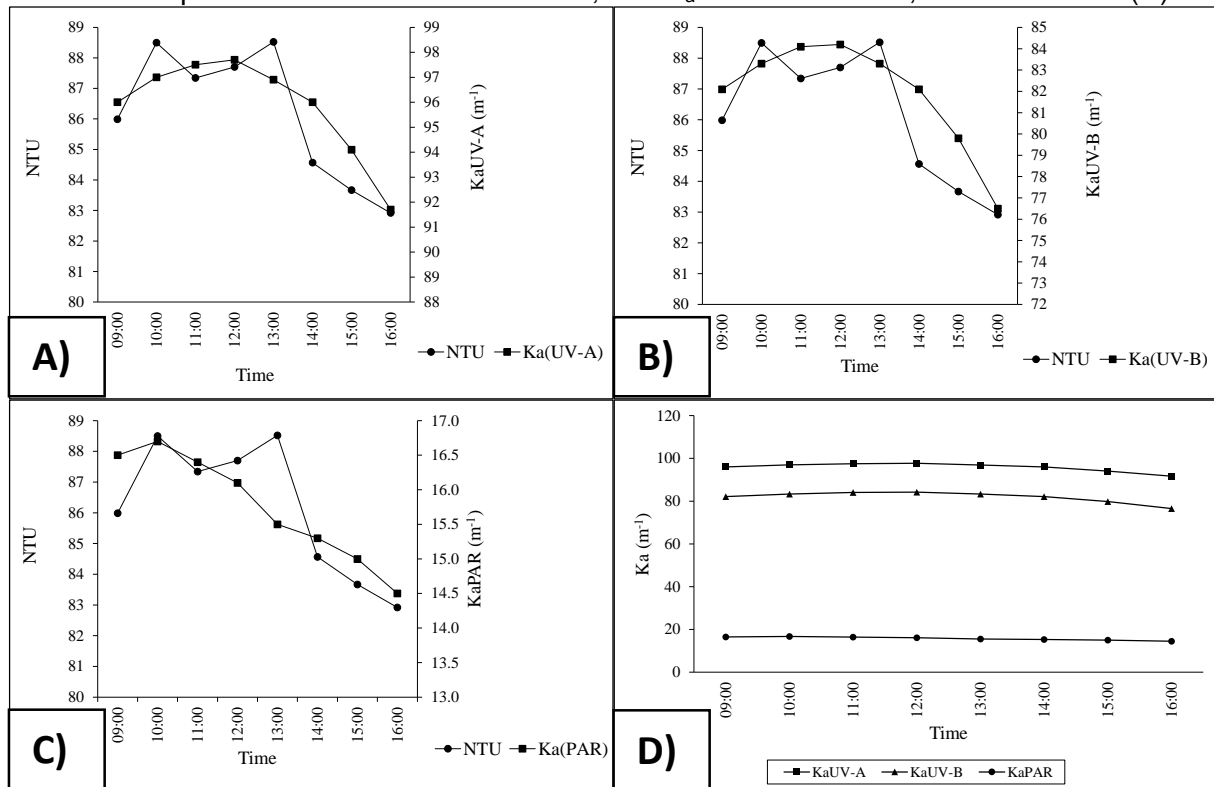
6.2.4.3. Attenuation coefficients for UV-A, UV-B and PAR using SMARTS

This subsection presents a similar evaluation as in subsection 6.2.4.1, but instead of considering Shilton (2005) percentages for determining surface irradiance of UV-A, UV-B and PAR, these were estimated by the Simple Model of the Atmospheric Radiative Transfer of Sunshine (SMARTS) by Gueymard (1995 and 2001). UV-A, UV-B and PAR attenuation coefficients (K_a) and turbidity during the different time intervals are presented in Figure 6.31. K_a values were calculated based on irradiances from APPENDIX V, APPENDIX VII, APPENDIX IX and APPENDIX XIII and are presented in APPENDIX XIII. The time period was the same, between 9:00 and 16:00. Turbidity is the same as in Table 6.7 and Figure 6.28, therefore comments on turbidity were presented in subsection 6.2.4.1.

Attenuation rate (K_a) values for UV-A and UV-B (Figure 6.31 **A** and **B**) followed the same tendency as in Figure 6.29 (**A** and **B**) and also decreased together with turbidity from 13:00:00 until 16:00:00. The same conclusion was implied about the waves being related with turbidity values. UV-A and UV-B K_a values calculated from the irradiance values predicted by the SMARTS programme were generally greater than UV-A and UV-B K_a values estimated from

the percentages recommended by Shilton (2005). The attenuation coefficient for UV-B continued less than the attenuation coefficient of UV-A (Figure 6.29 D, Figure 6.31 D, APPENDIX XII and APPENDIX XIII). This was not expected, but in both models this tendency presented itself and by quite a difference (more than 10 m^{-1}). PAR K_a values decreased from morning to afternoon even with erratic turbidity (NTU) behaviour (Figure 6.31 C) and only increased from 09:00 to 10:00. As with subsection 6.2.4.1 the graphs showed that UV and PAR are affected differently by pond optics as suggested by Curtis *et al.* (1994).

Figure 6.31 - K_a UV-A vs NTU (A); K_a UV-B vs NTU (B); K_a PAR vs NTU (C) considering SMARTS prediction for surface irradiance; and K_a values for UV-A, UV-B and PAR (D).



6.2.4.4. Modelling attenuation coefficients for PAR using surface SMARTS

Equation (4.36) was reproduced in Equation (6.4), with the calculated value of the attenuation rate (K_a) considering surface irradiance predicted by the SMARTS programme. K_a was also estimated using the Solver tool in Excel, minimising the sum of the squared errors. Equation (6.5) and Equation (6.6) were also estimated considering that turbidity (TUR) and the \log_{10} of turbidity ($\text{LOG}(\text{TUR})$) influenced the attenuation coefficient. As in subsection 6.2.4.2, all equations are for a timeline from 09:00 – 16:00. Table 6.9 presents the estimated K_a values for all three equations, CD values. Figure 6.32 (A, B and C), as in subsection 6.2.4.2 shows the goodness-of-fit for the observed irradiance vs calculated irradiance for the CD values.

$$I = I_0 \cdot e^{-27.66.Z} \quad (6.4)$$

$$I = I_0 \cdot e^{-0.305.TUR.Z} \quad (6.5)$$

$$I = I_0 \cdot e^{-14.10.LOG10(TUR).Z} \quad (6.6)$$

where,

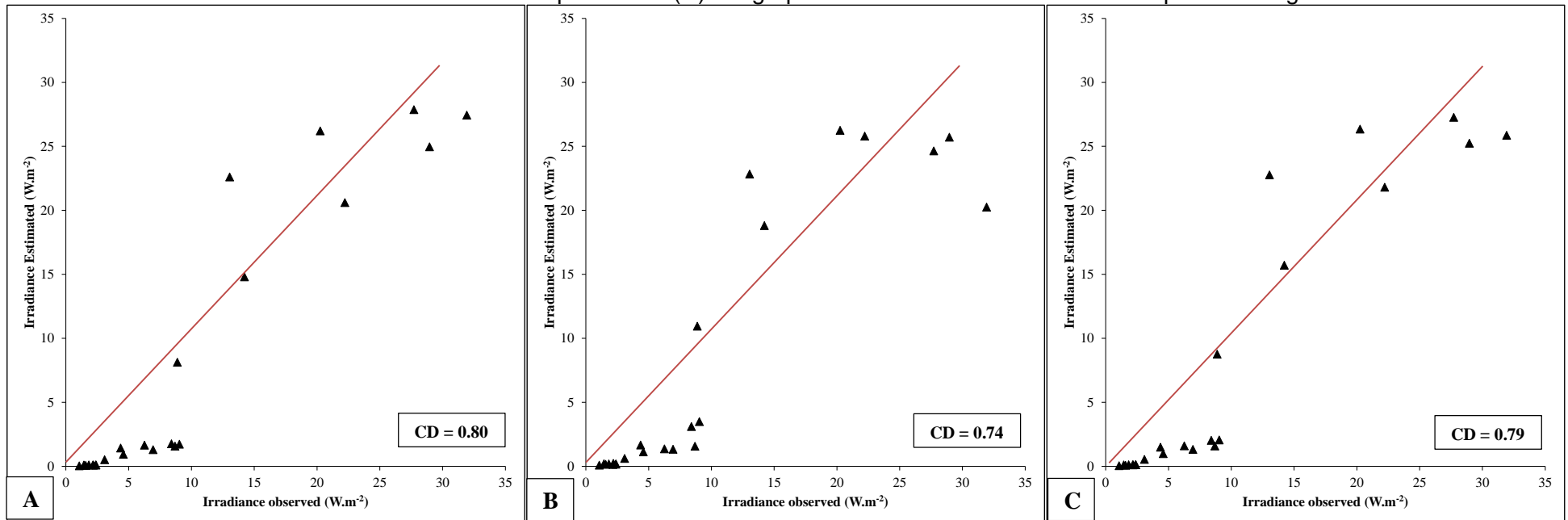
- I – PAR irradiance at depth z (W.m⁻²);
- I₀ – PAR irradiance at the pond surface (W.m⁻²);
- TUR – turbidity (NTU);
- Z – Depth from surface or reference point (m).

Table 6.9 - K_a values, Coefficient of Determination and K_a units for Equations 6.4, 6.5 and 6.6.

Equation	K_a	CD	K_a unit
6.4	27.66	0.80	m ⁻¹
6.5	0.305	0.74	m ⁻¹ .NTU ⁻¹
6.6	14.10	0.79	m ⁻¹ .LOG10(NTU ⁻¹)

Equation 6.4 produced the best fit, just as Equation 6.1 in subsection 6.2.4.2, however the CD is lower than the CD for Equation 6.1 (Table 6.8, Figure 6.30 **A**, Table 6.9 and Figure 6.32 **A**). Equations 6.5 and 6.6 presented a CD of 0.74 and 0.79, respectively, the latter being virtually the same to the CD for Equation 6.4, but lower than Equation 6.3 (CD = 0.83) (Table 6.8, Figure 6.30 **B** and **C**, Table 6.9 and Figure 6.32 **B** and **C**). Equation 6.5 on the other hand presented a higher CD value than Equation 6.2, therefore indicating that only this equation proved to produce better results when using the SMARTS program. The other two equations produced lower CD values and consequently indicated that the percentages used to multiply TSI proposed by Shilton (2005) are probably closer to reality. However, all CD values from both methods (percentages and SMARTS) can be considered high and each model can be used to predict irradiance at different depths with a good confidence. As mentioned for Equations 6.1, 6.2 and 6.3 when planning to apply these equations for other pond systems, it should be noted that the pond is shallow and turbidity did not change substantially along the depth (Table 5.1, Table 6.7 and Figure 6.28).

Figure 6.32 - Observed and Estimated Irradiance for Equation 6.4 (A); Observed and Estimated Irradiance for Equation 6.5 (B) and; Observed and Estimated Irradiance for Equation 6.6 (C). All graphs show the 45o line of theoretical perfect fitting.



6.2.4.5. TSI divided into UV-A, UV-B and PAR

Table 6.10 presents the median percentages between irradiance values of UV-A, UV-B and PAR estimated by SMARTS and the measured TSI (UV-A/TSI; UV-B/TSI and; PAR/TSI). Interestingly, the overall mean/median percentages are very similar to the percentages proposed by Shilton (2005) for midday (UV-A = 6%; UV-B = 0.2% and; PAR = 50%). Therefore, it is possible to conclude that Shilton's (2005) percentages or the overall percentages (Table 6.10) multiplied by TSI provided accurate irradiance values for UV-A, UV-B and PAR between 09:00:00 and 16:00:00.

Table 6.10 - Percentage ratio between UV-A, UV-B and PAR irradiance estimated by SMARTS and total solar irradiance measured from the meteorological station.

Time/Wave	UV-A/TSI	UV-B/TSI	PAR/TSI
09:00:00	11%	0.29%	86%
10:00:00	8%	0.26%	63%
11:00:00	8%	0.26%	60%
12:00:00	7%	0.24%	55%
13:00:00	7%	0.22%	52%
14:00:00	6%	0.18%	48%
15:00:00	6%	0.10%	48%
16:00:00	4%	0.02%	40%
Overall MEAN/MEDIAN	7%/7%	0.20%/0.23%	57%/54%
Ratios proposed by Shilton (2005) for midday	5%	0.20%	50%

6.3. *E. coli* disinfection throughout the depth in a shallow maturation pond

As shown in subsection 4.3 there is an array of mechanisms affecting *E. coli* disinfection with prominent contribution from sunlight-mediated disinfection. Subsection 6.3.1 and 6.3.2 focuses on disinfection coefficients (K_b) and dark disinfection/repair coefficients (K_d) in the medium (depth profiling) for *in situ* temperature and for a standardised temperature of 20°C. Disinfection efficiencies (log units) vs depth and statistical comparisons between K_b , K_d and log units removed from experiments conducted in the test tube vessels for different depths and periods of the day (morning and afternoon) are also presented. Data for subsections 6.3.1 and 6.3.2 are shown in APPENDIX XIV and APPENDIX XV. Subsection 6.3.3 shows the influence of some environmental variables: dissolved oxygen (DO), pH and temperature measured from the effluent used in the test tube vessels regarding disinfection coefficients (K_b), dark disinfection/repair coefficients (K_d) and removal efficiencies (log units). Subsection 6.3.4 presents statistical tests and comparisons between K_b , K_d , log units and environmental variables

pertaining to depth and period of the day from the test tube experiments. Subsection 6.3.5 shows applied and received doses for the overall period of solar irradiance (UV-A, UV-B and PAR) at different depths that caused *E. coli* disinfection. Modelling *E. coli* disinfection (K_b) regarding environmental variables is shown in subsection 6.3.6 and a comparison between the two phases and vertical hydrodynamic profiling is presented in subsection 6.3.7.

6.3.1. Disinfection coefficient (K_b)

The disinfection coefficients (K_b) are necessary in all models for the estimating disinfection efficiency in reactors. In this case, disinfection coefficients were calculated based on the batch flow hydraulic regime (the same as plug flow hydraulic regime), subsection 4.7, because the effluent inside the test tube vessels did not alter its identity horizontally, but rather vertically. As explained in subsection 5.5, three different depths in the 2nd maturation pond were trialled for *E. coli* disinfection during the morning and afternoon periods. The depths were **10 cm = 0 cm – 10 cm**, **20 cm = 10 cm – 20 cm** and **30 cm = 20 cm – 30 cm** and their mean overall K_b values are presented in Figure 6.33 for the morning and afternoon. Each K_b value was then standardised for a temperature of 20 °C (Equation 4.12) to compare with values reported in literature (Figure 6.34). The sample numbers (n) for each profile and period were 15, totalling 86 samples for the experiment (except for 20 cm and 30 cm afternoon, $n = 13$ samples each). APPENDIX XIV shows the observed K_b values and estimated $K_{b20^\circ C}$. Subsection 6.3.4 presents the nonparametric variance analysis of K_b and $K_{b20^\circ C}$.

K_b values were obtained based on the time the liquid in the vessels were subjected to sunlight (4 hours for each experiment) and are expressed in hour⁻¹ (h⁻¹). Figure 6.33 shows, as expected, the disinfection coefficient decreasing in value as depth increased and this tendency was observed in the morning and afternoon, with the latter presenting similar values for 20 cm and 30 cm (0.28 h⁻¹). Morning values decreased from 0.45 h⁻¹ (10 cm), to 0.39 h⁻¹ (20 cm) and reached a minimum of 0.31 h⁻¹. The maximum disinfection coefficient was 0.48 h⁻¹ (10 cm) and occurred during the afternoon, slightly higher than the K_b value for the 10 cm profile in the morning. Interestingly enough, the minimum mean K_b value obtained was during the afternoon (0.28 h⁻¹) at the 30 cm profile and not during the morning (0.31 h⁻¹) at the same depth and this was not expected. The same 0.28 h⁻¹ K_b value was also observed at 20 cm during the afternoon period and the morning K_b value was 0.39 h⁻¹ (20 cm), also presenting a higher disinfection rate which was also not expected. Even with higher DO, pH and temperature values (Table 6.11)

during the afternoon for every profile, only the K_b value for the 10 cm profile was greater. DO, pH and temperature values were from the two litre sample from the 30 cm profile in P_1 and characterise the liquid column profile as a composite sample of the three depths.

Table 6.11 – Summary of range and (*mean*) values for environmental variables during the *E. coli* disinfection test tubes experiment for morning and afternoon periods for each depth profile. Ouali *et al.* (2014) DO, pH and temperature results.

Parameter	Depth	Morning	Afternoon	Ouali <i>et al.</i> (2014)
DO	10 cm	1.47 – 5.59 (3.98)	2.94 – 14.32 (9.85)	1.2 – 8.19
	20 cm	2.01 – 10.97 (4.21)	4.51 – 14.49 (9.56)	
	30 cm	2.72 – 8.18 (4.81)	8.19 – 15.68 (11.45)	
pH	10 cm	7.53 – 8.04 (7.77)	7.65 – 8.41 (7.79)	5.16 – 12.07
	20 cm	7.57 – 8.12 (7.70)	7.63 – 8.75 (7.97)	
	30 cm	7.63 – 8.44 (7.84)	7.66 – 8.50 (8.00)	
Temperature	10 cm	18.40 – 25.90 (22,40)	20.50 – 27.90 (24.01)	14 – 28.9
	20 cm	19.10 – 25.20 (21.93)	21.20 – 29.00 (24.52)	
	30 cm	18.60 – 24.50 (21.87)	20.10 – 27.60 (24.10)	

Ouali *et al.* (2014) studied *E. coli* disinfection in a pilot size laboratory maturation pond (very shallow depth of 2 cm) under controlled pH, temperature and DO conditions (Table 6.11) with UV-A, UV-B and PAR irradiance varying between 0.12 and 25 W.m⁻². K_b values were calculated using the batch flow equation (Figure 4.20) and varied from 0.04 to 0.43 h⁻¹. The highest value was comparable to the K_b values from the 10 cm profile (morning and afternoon), and the morning 20 cm profile value was also very similar to the author's. The DO values from Ouali *et al.* (2014) experiment were slightly lower than the measured values from this experiment, while temperature was about the same and pH values had a bigger range (Table 6.11). The K_b values were not standardised for a temperature of 20 °C. Disinfection for the 10 cm profile during both morning and afternoon periods was always greater than in the subsequent profiles (Figure 6.33), highlighting the effects of UV-A and UV-B (subsection 6.2.3) and solar-mediated mechanisms 1 and 2. Greater disinfection during the morning could have occurred because of the larger differences in temperature between the night and the morning than the morning and afternoon, therefore having a more pronounced effect on cells.

Figure 6.34 shows the K_b values standardised for a temperature of 20 °C using Equation 4.12. The disinfection coefficients can be compared with K_b values from the literature and future experiments in this area. On average, all K_b values decreased when converting to the standard temperature because the temperature in the test tubes rarely went below 20 °C, with the

exception from the morning profiles, which explains the slight decline in K_b for each profile compared to the afternoon profiles (Table 6.11). These values are still within the range presented by Ouali *et al.* (2014). Disinfection at 20 cm and 30 cm, in the absence of UV radiation, still occurred and confirmed that PAR participates in disinfection through the 2nd and 3rd sunlight-mediated mechanism until 30 cm. The 2nd and 3rd sunlight-mediated mechanism (although it was not clear which mechanism contributed more) disinfected *E. coli* to a significant degree, as shown in Figure 6.34. The 2nd mechanism uses shortwaves (UV-A and UV-B) absorbed by endogenous photosensitisers and react with oxygen to form ROS that cause damage to internal targets (DNA and DNA repair mechanisms). The 3rd mechanism uses the whole UV (290–400 nm) and PAR range (400–700 nm) and are absorbed by external photosensitisers found on the outside of the microorganism's cells. External photosensitisers react with oxygen to form highly ROS and cause damage to cell membranes. This is in line with Davies-Colley *et al.* (1999) conclusions on the 3rd mechanism. UV-B radiation during the morning can be considered to have insignificant effects as suggested by Kadir and Nelson (2014) when comparing the 10 cm profiles with the 20 cm and 30 cm ones, knowing that UV radiation is fully attenuated before 15 cm. UV could also be less important because of the high disinfection coefficients obtained at 20 and 30 cm, suggesting that PAR plays a large role in disinfection during the morning, but not as much during the afternoon.

It should be noted that these K_b values should not be compared with overall K_b values available in the literature, obtained in continuous-flow ponds. The latter is usually calculated assuming a certain hydraulic model, and those obtained here are intrinsic kinetic coefficients for batch experiments (which coincide with idealised plug-flow reactors). Furthermore, the K_b obtained here is for specific depth ranges, whereas those obtained in existing ponds take into account their full depth and hydraulic retention time. Finally, one needs to pay attention to the fact that the time unit here is hour, while in most publications the time unit is day. To convert K_b expressed in h^{-1} to K_b expressed in d^{-1} , one needs simply to multiply the former by 24 h/d.

Figure 6.33 – Summary of overall mean K_b values (h^{-1}) for the morning and afternoon period at 10 cm = 0 - 10 cm, 20 cm = 10 - 20 cm and 30 cm = 20 - 30 cm profiles in the 2nd maturation pond.

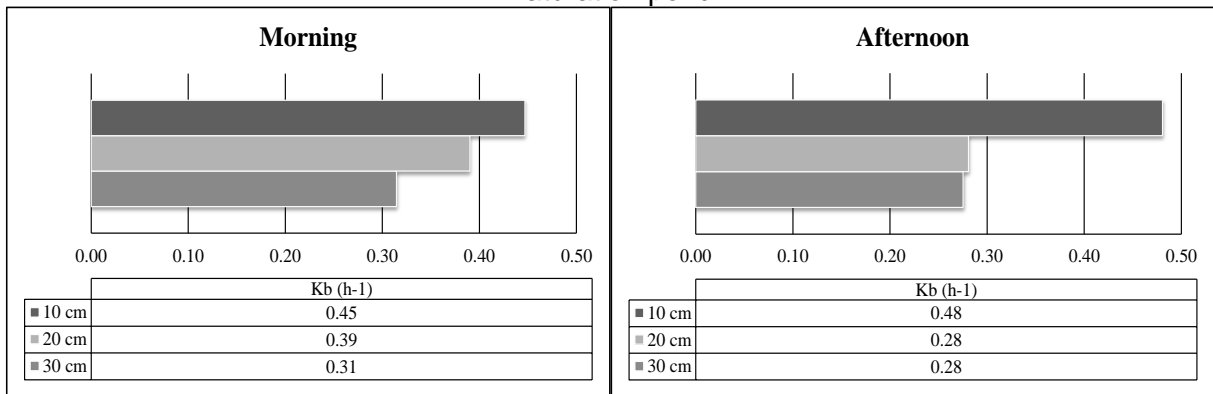
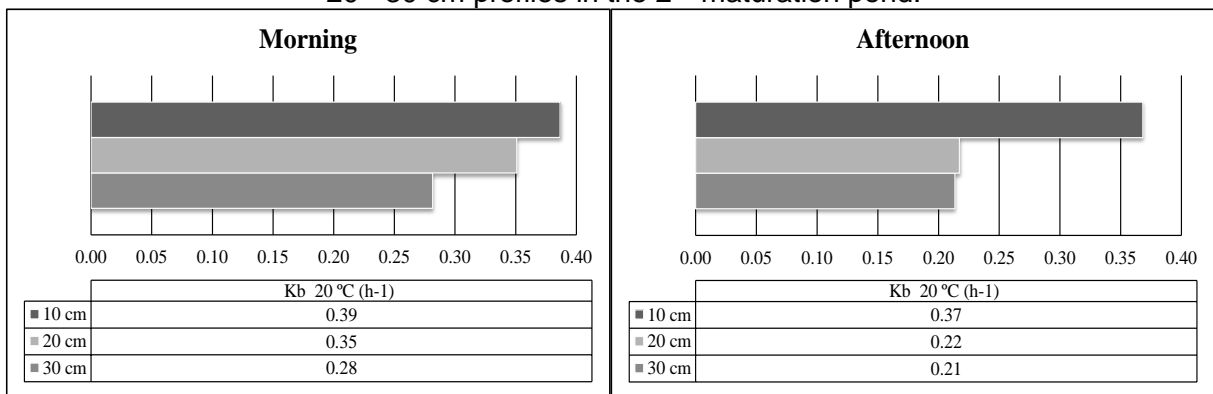


Figure 6.34 – Summary of mean K_b values (h^{-1}) standardised for a temperature of 20 °C during the morning and afternoon period at 10 cm = 0 - 10 cm, 20 cm = 10 - 20 cm and 30 cm = 20 - 30 cm profiles in the 2nd maturation pond.



6.3.2. Dark disinfection or repair coefficient (K_d)

The dark disinfection or repair coefficient (K_d) has been at the centre of controversy since researchers have tried to understand its nature. Researchers are not sure if repair or damage occurs to *E. coli* bacteria, some claim that disinfection (Mayo, 1989 and Maiga *et al.*, 2009a) and others claim that repair (Harm (1968) and Davies-Colley *et al.*, 1999) takes place, and other researchers consider it to have little contribution to overall results (Sinton *et al.*, 2002 and Kadir and Nelson, 2014). The K_d coefficients (Figure 6.35) were calculated based on the batch flow hydraulic regime (subsection 4.7) and at the same depths as mentioned in subsection 5.5. Each value was also standardised for a temperature of 20 °C (Equation 4.12 - $K_{d20^{\circ}C}$) to compare with values reported in literature (Figure 6.36). The sample numbers (n) varied between 12 and 13 for each profile and period, totalling 76 samples in total for the experiment. APPENDIX XV shows the observed K_d values and estimated $K_{d20^{\circ}C}$. Subsection 6.3.4 shows the nonparametric variance analysis of K_d and $K_{d20^{\circ}C}$.

On average, dark disinfection occurred during both morning and afternoon periods, decreasing with depth (Figure 6.35), just as with sunlight-mediated disinfection. Morning and afternoon disinfection for the 10 cm profiles were practically the same (0.137 h⁻¹ and 0.138 h⁻¹, respectively), but for the other 20 cm and 30 cm depths, disinfection in dark conditions was greater during the morning period. Both 10 cm and 20 cm profiles during the morning period presented also very similar disinfection rates (0.137 h⁻¹ and 0.126 h⁻¹, respectively). During the afternoon period, the same was observed for the 20 cm and 30 cm, also presenting similar disinfection rates (0.045 h⁻¹ and 0.043 h⁻¹, respectively). The results for K_d are in line with the results from K_b with higher disinfection rates occurring in the morning at the 20 cm and 30 cm profiles and lower disinfection rates during the afternoons 20 cm and 30 cm profiles (Figure 6.33), which is nonetheless an interesting observation. K_d values were rather low compared to K_b values, resulting in 13% (1/8) to 23% (1/4) of the overall disinfection in the experiments, similar to Craggs *et al.* (2004) 1/5 to a 1/3.

APPENDIX XV shows that probably both groups of researchers were right because dark repair and dark disinfection occurred throughout the ponds depth, especially during the morning period and due to lower concentrations of oxygen, pH, and temperature (Table 6.11), as well as the absence of sunlight. This is interesting because sunlight-mediated disinfection was also greater during the morning period for all profiles. i.e., morning 10 cm profile was very similar

to the afternoon 10 cm profile (Figure 6.33). Although its overall influence was not as pronounced as sunlight-mediated disinfection, dark disinfection still accounts for *E. coli* disinfection performance and its contribution is not as small as some authors stated (Sinton *et al.*, 2002 and Kadir and Nelson, 2014), and can be as high as 0.55 h^{-1} (APPENDIX XV).

Figure 6.36 presents the standardised K_d values for a temperature of $20 \text{ }^\circ\text{C}$ calculated using Equation 4.12. Just as with $K_{b20^\circ\text{C}}$, the $K_{d20^\circ\text{C}}$ values also decreased because most of the time the measured temperatures were higher than $20 \text{ }^\circ\text{C}$. The morning period presented lower temperatures than the afternoon period, therefore $K_{d20^\circ\text{C}}$ in the morning period decreased less compared to the afternoon period (APPENDIX XV).

Figure 6.35 – Summary of mean K_d values during the morning and afternoon period at 10 cm = 0 - 10 cm, 20 cm = 10 - 20 cm and 30 cm = 20 - 30 cm profiles in the 2nd maturation pond.

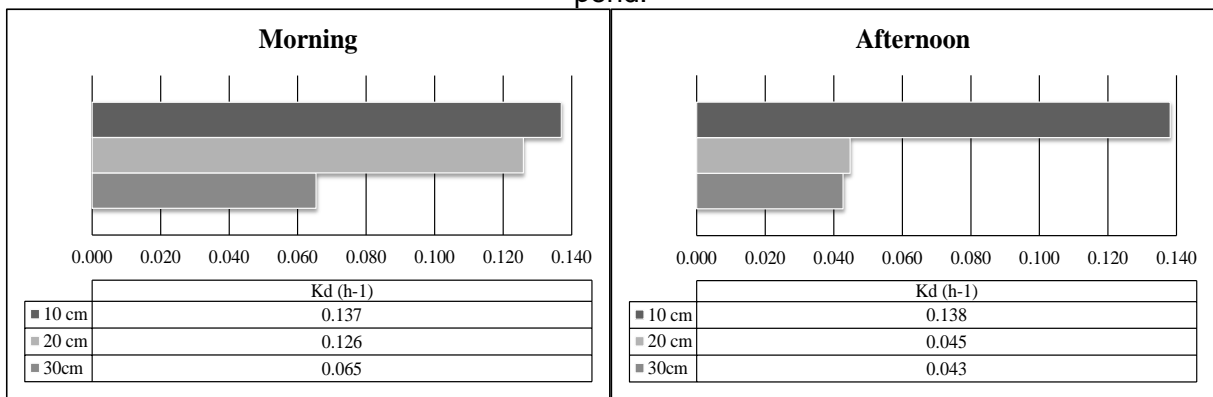


Figure 6.36 – Summary of mean $K_{d20^\circ\text{C}}$ values standardised for a temperature of $20 \text{ }^\circ\text{C}$ during the morning and afternoon period at 10 cm = 0 - 10 cm, 20 cm = 10 - 20 cm and 30 cm = 20 - 30 cm profiles in the 2nd maturation pond.

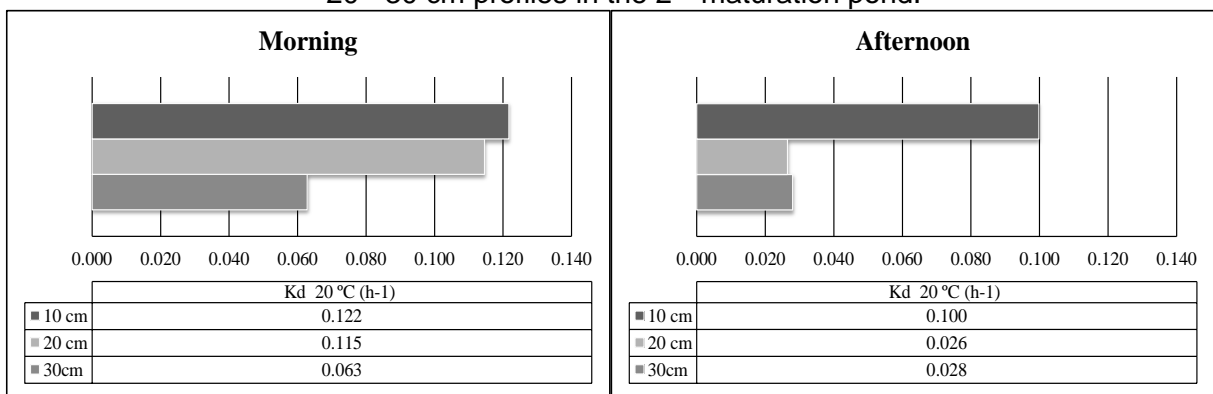


Table 6.12 shows the difference between the K_b and the K_d coefficients, therefore and showing the real influence of solar-mediated disinfection. The the difference between the coefficients for the morning and the afternoon follow the same trend as for the K_b and the K_d coefficients, solar-mediated influence is still very strong.

Table 6.12 - The difference between the K_b and the K_d coefficients for the different periods and depths.

$K_b - K_d$	Morning (h^{-1})	Afternoon (h^{-1})
10 cm	0.313	0.342
20 cm	0.265	0.235
30 cm	0.245	0.237

6.3.3. Log units removed at different depths and time periods associated with environmental parameters

Literature has shown that *E. coli* is disinfected by various mechanisms, including the influence of environmental variables such as pH, DO and temperature. This section is divided up into the different environmental variables and their influence on *E. coli* disinfection presented in log unit removed during the test tube experiments (removal during four hours of each experiment). Table 6.13 presents the mean (and *median*) *E. coli* disinfection efficiencies and environmental values measured in the effluent used for the test tube experiments and based on the values in APPENDIX XVI.

Table 6.13 - Summary of mean (*median*) values and percentages of removal efficiencies, DO concentrations, pH and temperature values for the different depth profiles and periods for the 4 hour experiment in the test tubes.

	Morning			Afternoon		
	10 cm	20 cm	30 cm	10 cm	20 cm	30 cm
<i>E. coli</i> removal (log units)	0.77 (0.81)	0.67 (0.61)	0.54 (0.53)	0.82 (0.81)	0.49 (0.44)	0.48 (0.59)
<i>E. coli</i> removal (%)	83.0 (84.5)	78.6 (75.5)	71.2 (70.5)	84.9 (84.5)	67.6 (63.7)	66.7 (74.3)
DO ($mg.L^{-1}$)	3.98 (4.53)	4.21 (3.08)	4.81 (4.56)	9.85 (9.45)	9.28 (9.12)	11.42 (11.13)
pH	7.77 (7.78)	7.70 (7.66)	7.84 (7.78)	7.99 (8.01)	7.98 (7.91)	8.02 (8.05)
Temperature ($^{\circ}C$)	22.40 (22.70)	21.93 (22.30)	21.87 (22.20)	24.01 (23.90)	24.55 (25.00)	23.95 (24.60)

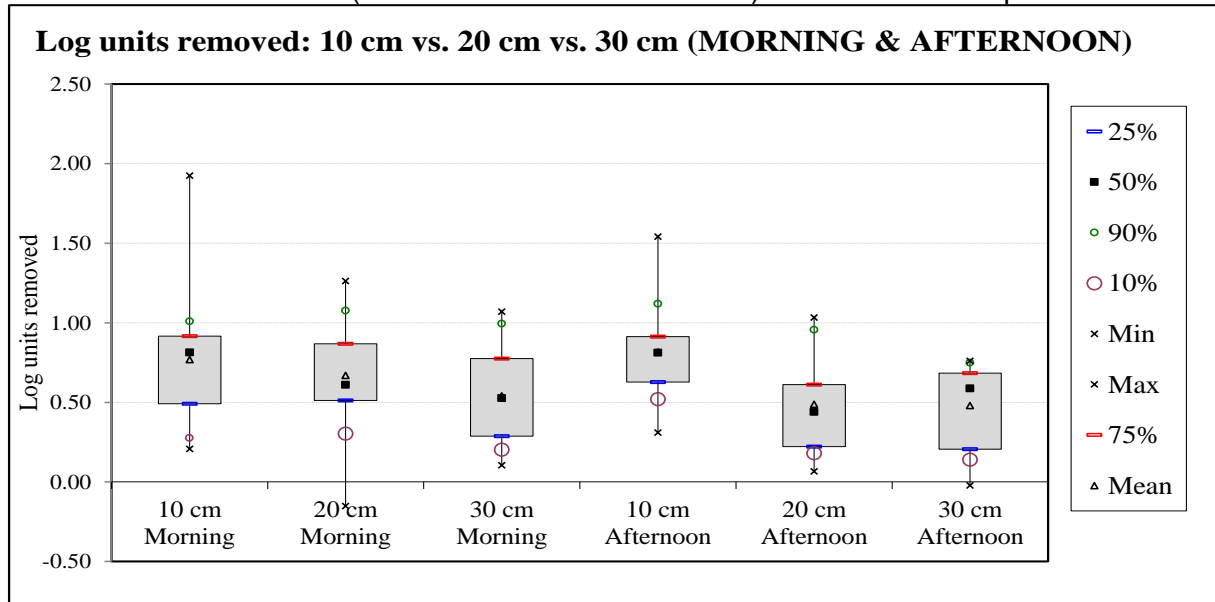
6.3.3.1. Overall *E. coli* log reduction for each depth profile and period of the day

Figure 6.37 and APPENDIX XVI presents removal efficiencies during the two different periods at the three different depths after 4 hours of exposure in the 2nd pond (see subsection 5.5). Subsection 6.3.4 presents nonparametric variance analysis of log reduction.

The 10 cm profile produced the best removal efficiencies for *E. coli* as shown in section 6.3.1. As expected, removal efficiencies are in line with the K_b values presented in subsection 6.3.1 and were greater nearer the surface of the pond (10 cm profile) during the afternoon and slightly less during the morning. The morning period produced better removal efficiencies for the 20 cm and 30 cm profile and as mentioned above this was not expected and could be because of temperature differences between morning and night.

On average, four hours was not enough time for 90% disinfection efficiency ($t_{90\%}$) to take place for all depths and time periods (although the 10 cm depth profiles were close on average), although some samples were inactivated above 90% for all depths and periods, except 30 cm in the afternoon (Table 6.13, Figure 6.37 and APPENDIX XVI). However, the results showed better removal efficiencies compared with Mayo (1995) best results, $t_{90\%} = 21$ hours at 15 cm from the surface in batch experiments with plastic bottles. Results from an experiment in Burkina Faso with mesocosms operating at different depths showed that *E. coli* can be inactivated within hours in shallow mesocosms (9 hours – 1.5 to 2.5 log reduction in the summer months), according to Maïga *et al.* (2009a).

Figure 6.37 – *E. coli* log units removed: 10 cm = 0 – 10 cm vs. 20 cm = 10 – 20 cm vs. 30 cm = 20 – 30 cm (MORNING and AFTERNOON) over 4 hours of exposure.



6.3.3.2. Dissolved oxygen (DO) influence on *E. coli* log reduction for each depth profile and period of the day

Figure 6.38 and Figure 6.39 refer to dissolved oxygen (DO) concentrations measured from the medium used in the test tube experiments and log unit removal efficiencies based on the tables in APPENDIX XVI.

DO concentrations during the afternoon were higher than in the morning but did not seem to have influenced directly the removal efficiencies. This was verified during all experiments with the test tubes. When DO concentrations were lower than 8.0 mg.L⁻¹, i.e., morning conditions, the removal efficiency (log units) of *E. coli* were generally greater than the removal efficiencies with higher DO concentrations (Figure 6.38, Figure 6.39 and Table 6.13). DO is important for the 2nd and 3rd sunlight-mediated mechanism (subsection 4.3.4), but as results suggested there is no need for high concentrations for disinfection through these mechanisms to occur, in fact low concentrations (morning) occurred together with greater disinfection. This is because DO in combination with photosensitisers to produce ROS which are detrimental towards *E. coli* and not DO on its own. The only time that high DO concentrations influenced removal efficiencies was at 30 cm depth profile compared to 20 cm depth profile, both in the afternoon (Figure 6.38 and Figure 6.39).

Figure 6.38 - Box plot of DO concentrations at different depths and during different periods of the day (morning and afternoon) measured in the test tubes.

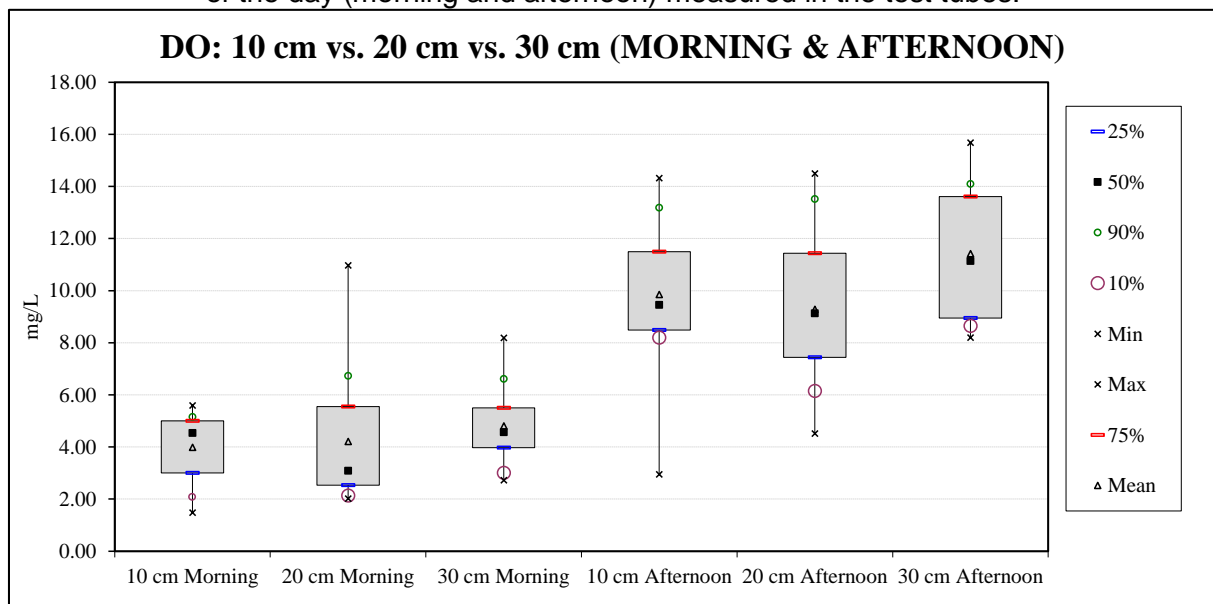
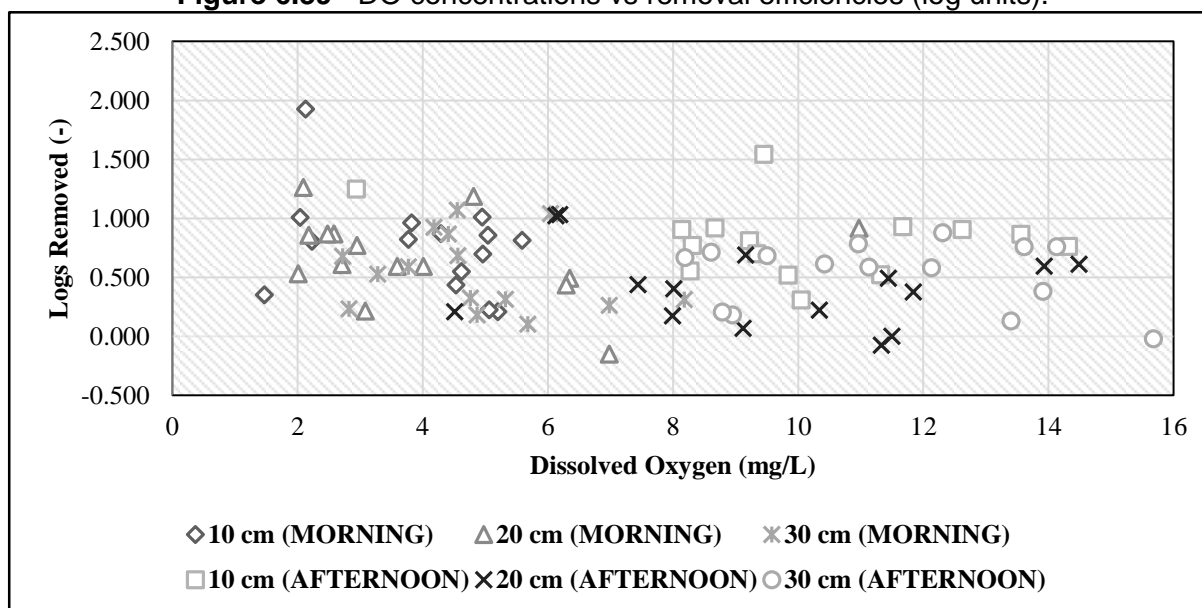


Figure 6.39 - DO concentrations vs removal efficiencies (log units).



6.3.3.3. pH influence on *E. coli* log reduction for each depth profile and period of the day

As in the previous subsection, Figure 6.40 and Figure 6.41 displays pH levels measured from the liquid used in the test tube experiments and removed log units based on the tables in APPENDIX XVI.

pH values varied between 7.53 and 8.75. During the morning the pH levels were lower than in the afternoon was expected because DO increases with photosynthesis and consequently so does pH (Figure 6.40, Figure 6.41 and Table 6.13). pH levels were below the 9.3 recommended to cause adverse effects on *E. coli* bacteria (Parhad and Rao, 1974; Smallman, 1986; and Pearson *et al.*, 1987b), but still enhanced disinfection for the deeper profile (30 cm) for morning and afternoon, although this was not as clear as for DO. It is only in the presence of high concentrations of DO and pH in combination with high insolation that removal efficiencies are increased (Davies-Colley *et al.*, 1999), but low values also aided disinfection, as shown in Figure 6.41.

Figure 6.40 - Box plot of pH values at different depths and during different periods of the day (morning and afternoon) measured in the test tubes.

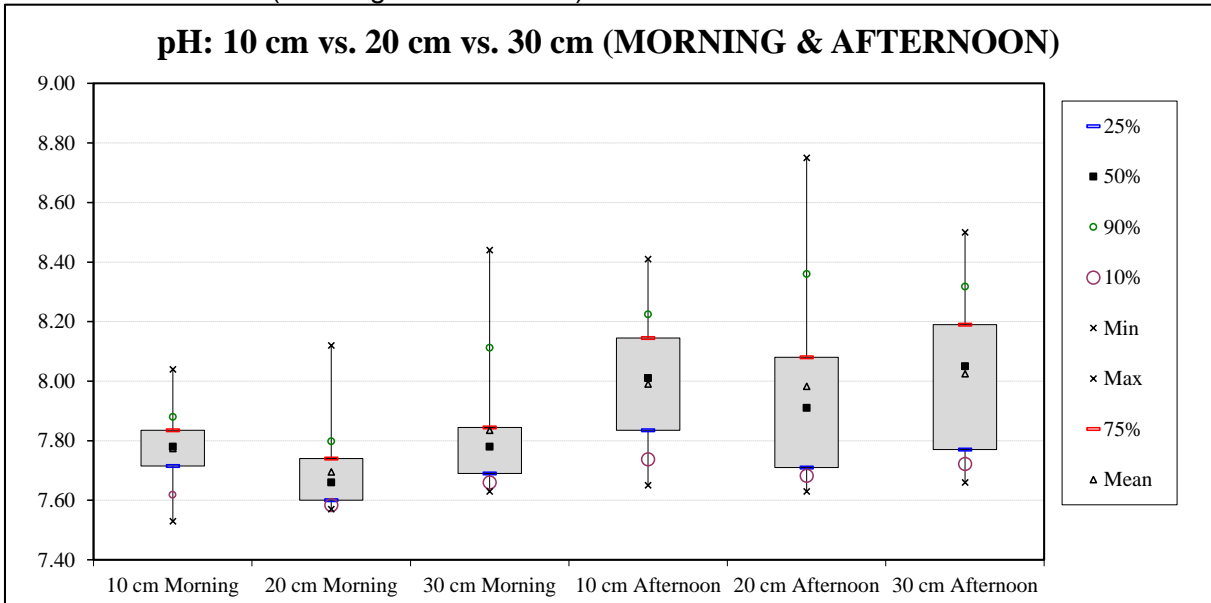
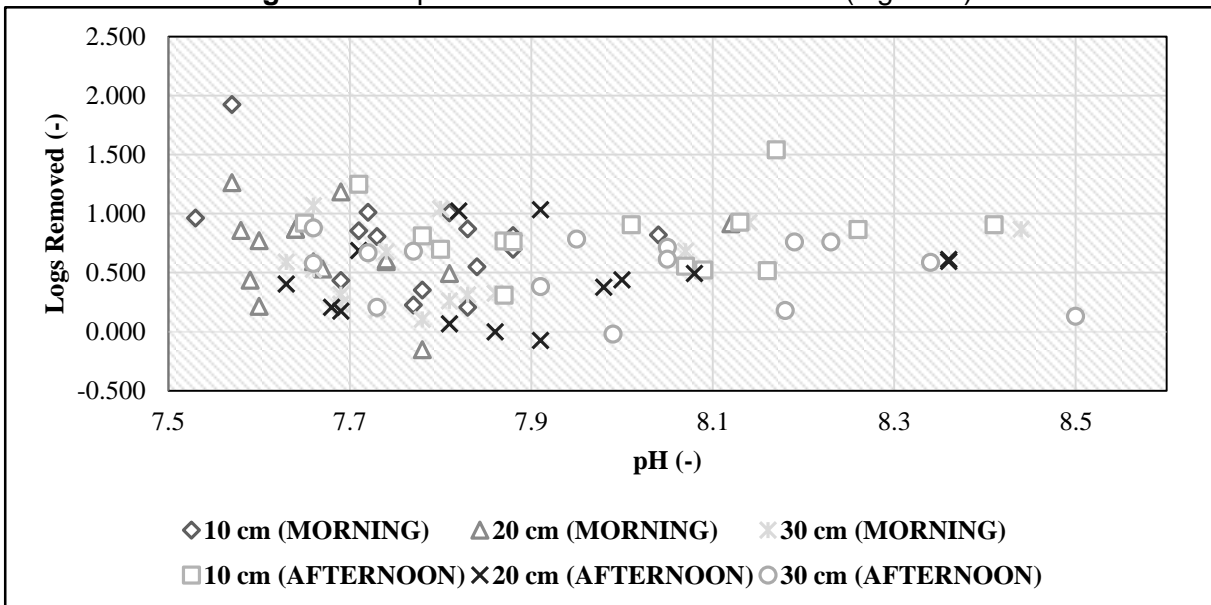


Figure 6.41 - pH value vs removal efficiencies (log units).



6.3.3.4. Temperature influence on *E. coli* log reduction for each depth profile and period of the day

Figure 6.42 shows temperature from different depth profiles and periods of the day used in the test tubes and Figure 6.43 presents the effect of temperature on *E. coli* removal efficiency. The figures were plotted based on the table in APPENDIX XVI.

Temperature during the morning period was lower than temperature during the afternoon period, which was expected because insolation increased and consequently water temperature

rose (Figure 6.42 and Table 6.13). Analysing Figure 6.43 it is possible to conclude that temperature had no apparent association with *E. coli* bacteria disinfection, because even in the presence of lower or higher temperatures for the same depth profile, similar removal efficiency levels occurred.

Figure 6.42 - Box plot of temperature values at different depths and during different periods of the day (morning and afternoon) measured in the test tubes.

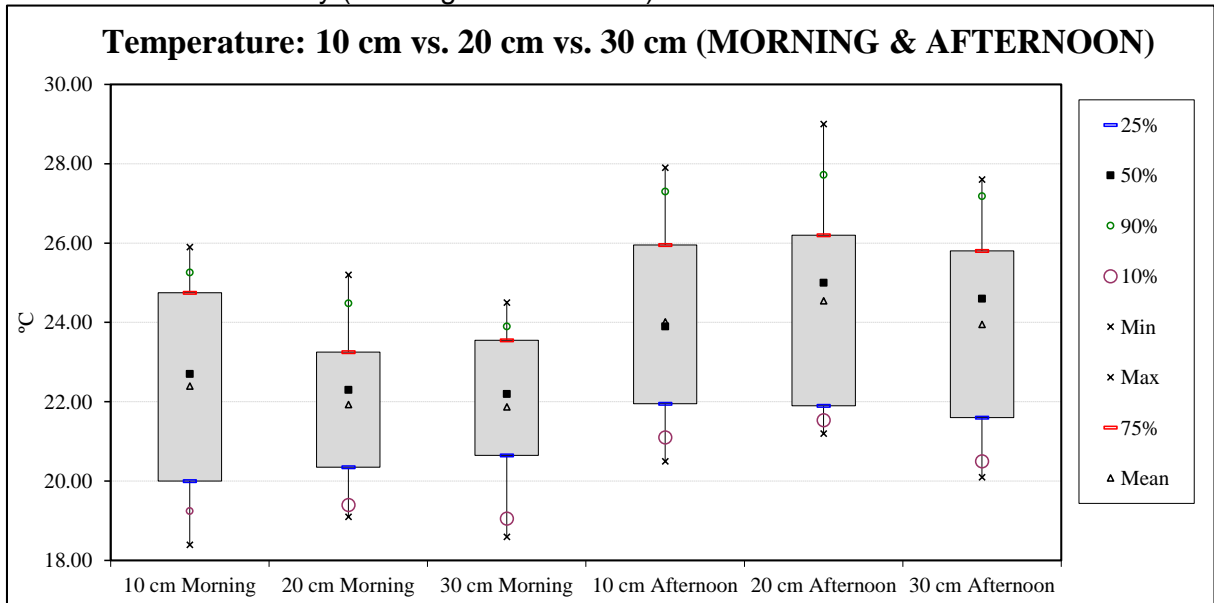
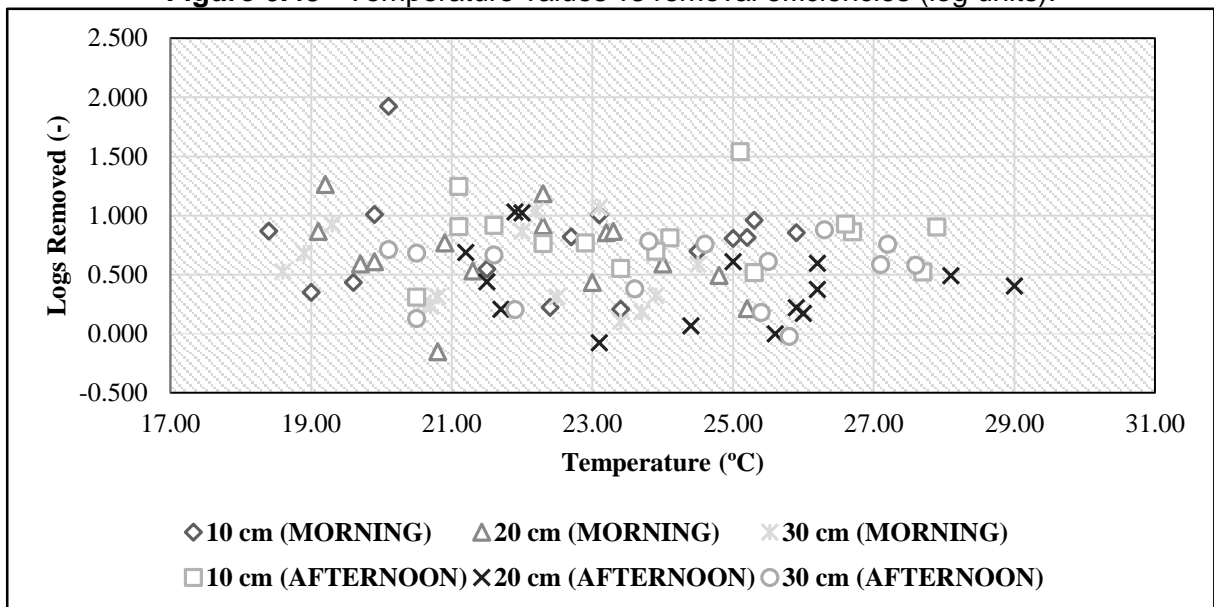


Figure 6.43 - Temperature values vs removal efficiencies (log units).



6.3.4. Nonparametric variance analysis of K_b , K_d , log unit values and environmental parameters between depths and periods (Kruskal-Wallis)

The results from the Kruskal-Wallis test with a confidence of 95% ($\alpha = 0.05$) were calculated in each of the following subsections, and if there was a possibility of significant difference the results were calculated based on the multiple comparisons of mean ranks for all groups (Statistica[®] program) and are presented in Table 6.14 for each depth/period.

6.3.4.1. Disinfection rate (K_b)

For this test the following hypotheses were used:

H₀: the disinfection rates (K_b) are the same for any depth and period of the day; as opposed to

H_a: the disinfection rates (K_b) are different for each depth and period.

The Kruskal-Wallis statistical test ($H = 13.81$) presented a value of $p = 0.017$, less than $\alpha (0.05)$, consequently rejecting H₀ and resulting in a significant difference between median K_b values for the three different depths and two different periods of the day, therefore requiring a multiple comparison test to identify the differences between pairs (Table 6.14). The statistical test used the values from APPENDIX XIV.

Table 6.14 shows that there were no significant differences from the multiple comparison test for the K_b values from different depths and periods of the day. Even though all the comparisons were not significantly different, the difference between Afternoon 10 cm and both Afternoon 20 cm and 30 cm came very close to a different conclusion, therefore showing that the difference is large between the three different disinfection rates, but not significantly so.

6.3.4.2. Standardised disinfection rate ($K_{b20^{\circ}C}$)

As in the previous test the following hypotheses were made:

H₀: the standardised disinfection rates ($K_{b20^{\circ}C}$) are the same for any depth and period of the day;

as opposed to H_a: the standardised disinfection rates ($K_{b20^{\circ}C}$) are different for each depth and period.

The statistical test ($H = 12.25$) presented a value of $p = 0.0316$, less than $\alpha (0.05)$, therefore rejecting H₀ and resulting in significant differences between median $K_{b20^{\circ}C}$ for the three different

depths and two different periods of the day. Just as for subsection 6.3.4.1, a multiple comparison test was performed to identify the differences between pairs (Table 6.14) based on the values in APPENDIX XIV. The results from the multiple comparison test for $K_{b20^{\circ}C}$ values are shown in Table 6.14, verifying there were no significant differences for different depths and periods of the day.

Results showed no significant differences in Table 6.14, and it is possible to note the decrease in observed differences for the Afternoon 10 cm and Afternoon 20 cm and 30 cm. Other comparisons increased the observed difference, namely when comparing morning and afternoon because temperatures were fairly different between the two periods (Table 6.11).

6.3.4.3. E. coli removal efficiency (log units removed)

The following hypotheses were made for the Kruskal-Wallis test:

H₀: removal efficiencies (log units) are the same for any depth and period of the day; as opposed to H_a: removal efficiencies (log units) are different for each depth and period.

The Kruskal-Wallis statistical test produced $H = 12.42$ and presented $p = 0.0295$, less than $\alpha = 0.05$, consequently rejecting H₀ and resulting in significant differences between median removal efficiencies for the three different depths and two different periods of the day. A multiple comparison test was performed to identify the differences between pairs (Table 6.14), just as for subsection 6.3.4.2. No significant differences were observed in Table 6.14, but as with the previous comparison tests, the closest pairs for significant differences were afternoon between the 10 cm, 20 cm and 30 cm, as well as between the afternoon 10 cm and 20 cm with the morning 10 cm and 30 cm.

6.3.4.4. Dark disinfection/repair (K_d)

The following hypotheses were made:

H₀: the dark disinfection/repair rates (K_d) are the same for any depth and period of the day; as opposed to H_a: the dark disinfection/repair rates (K_d) are different for each depth and period.

The value of $p = 0.803$ was greater than $\alpha (0.05)$ for the statistical test ($H = 2.32$), therefore accepting H₀ and resulting in no significant difference between median K_d for the three different

depths and both periods of the day. The values used are shown in APPENDIX XV. No multiple comparison test was needed.

6.3.4.5. Standardised dark disinfection/repair ($K_{d20^{\circ}C}$)

For the Kruskal-Wallis test, the following hypotheses were made:

H_0 : the dark disinfection/repair rates ($K_{d20^{\circ}C}$) are the same for any depth and period of the day; as opposed to H_a : the dark disinfection/repair rates ($K_{d20^{\circ}C}$) are different for each depth and period.

The value of $p = 0.743$ was greater than $\alpha (0.05)$ for the statistical test ($H = 2.72$), therefore also accepting H_0 and resulting in no significant difference between median $K_{d20^{\circ}C}$ at the three different depths and both periods of the day. APPENDIX XV shows the values used for the statistical test. As for dark disinfection/ repair, no multiple comparison test was needed.

6.3.4.6. Temperature values

The following hypotheses were made for the Kruskal-Wallis test:

H_0 : temperature values are the same for any depth and period of the day; as opposed to H_a : temperature values are different for each depth and period.

The H test value was 13.45 and p value was 0.0195, less than 0.05 (α), consequently rejecting H_0 and resulting in significant differences between median temperature values for the three different depths and two different periods of the day. A multiple comparison test was performed to detect the differences between pairs (Table 6.14) based on temperature readings in APPENDIX XVI. No significant differences were observed for temperature values, although some of the values were close to being statistically different.

6.3.4.7. Dissolved oxygen (DO) concentrations

The following hypotheses were made:

H_0 : dissolved oxygen (DO) concentrations are the same for any depth and period of the day; as opposed to H_a : dissolved oxygen (DO) concentrations are different for each depth and period.

The Kruskal-Wallis statistical test ($H = 53.71$) presented a very low p value = 2.41×10^{-10} , much less than α (0.05) and as a result rejecting H_0 and resulting in a significant difference between median DO concentrations for the three different depths and two different periods of the day, thus requiring a multiple comparison test to identify the differences between pairs (Table 6.14). DO concentrations are shown in APPENDIX XVI. There are significant differences between morning and afternoon DO concentrations at all depths. DO concentrations are much higher during the afternoon than the morning, as covered in subsection 6.3.3.2 (Figure 6.38), and Figure 6.39 which shows DO could influence *E. coli* disinfection at deeper depths.

6.3.4.8. pH values

This test considered the following hypotheses:

H_0 : pH values are the same for any depth and period of the day; as opposed to H_a : pH values are different for each depth and period.

$H = 23.78$ and $p = 0.000239$, also much lower than the α (0.05) value, therefore rejecting H_0 and resulting in significant differences between median pH values for the different depth profiles and both periods of the day, therefore requiring a multiple comparison test to identify the differences (Table 6.14). pH values are shown in APPENDIX XVI. Table 6.14 showed that there were significant differences between the afternoon 10 cm, 20 cm and 30 cm and the morning 20 cm profile only. This was endorsed by subsection 6.3.3.3 showing pH values on average were the lowest for the morning 20 cm profile.

Table 6.14 - Summary of the multiple comparison test (p-values) for K_b , $K_{b20^\circ C}$, removal efficiency, temperature, DO and pH considering a confidence level of 95%.

Compared factors (depths and periods)	K_b	$K_{b20^\circ C}$	Removal efficiency (log units)	Temp	DO	pH
Morning 10 cm - Morning 20 cm	1.0	1.0	1.0	1.0	1.0	1.0
Morning 10 cm - Morning 30 cm	1.0	1.0	1.0	1.0	1.0	1.0
Morning 10 cm - Afternoon 10 cm	1.0	1.0	1.0	1.0	0.0002	0.331
Morning 10 cm - Afternoon 20 cm	0.529	0.420	0.616	0.661	0.0027	1.0
Morning 10 cm - Afternoon 30 cm	0.431	0.465	0.526	1.0	0.000009	0.366
Morning 20 cm - Morning 30 cm	1.0	1.0	1.0	1.0	1.0	0.671
Morning 20 cm - Afternoon 10 cm	1.0	1.0	1.0	0.469	0.0002	0.0001
Morning 20 cm - Afternoon 20 cm	1.0	0.443	1.0	0.159	0.0024	0.0249
Morning 20 cm - Afternoon 30 cm	1.0	0.490	1.0	0.691	0.000008	0.0015
Morning 30 cm - Afternoon 10 cm	0.358	1.0	0.528	0.448	0.0038	0.713
Morning 30 cm - Afternoon 20 cm	1.0	1.0	1.0	0.151	0.029	1.0
Morning 30 cm - Afternoon 30 cm	1.0	1.0	1.0	0.662	0.0002	0.758
Afternoon 10 cm - Afternoon 20 cm	0.094	0.240	0.158	1.0	1.0	1.0
Afternoon 10 cm - Afternoon 30 cm	0.073	0.268	0.131	1.0	1.0	1.0
Afternoon 20 cm - Afternoon 30 cm	1.0	1.0	1.0	1.0	1.0	1.0

Differences; significantly different

The statistical tests analyse each variable separately, but literature suggests that they act simultaneously and complement each other when acting on *E. coli*.

6.3.5. Applied and received UV and PAR doses

Literature usually only reports one type of dose, either applied dose or received dose of UV and/or PAR. This can be considered a gap in research because only one of the doses is reported. Therefore, results for overall applied surface doses based on the irradiances estimated by the SMARTS programme and received doses at different depths during the whole monitoring period are presented in Table 6.15. Results are shown for both morning (08:00 – 12:00) and afternoon (12:00 – 16:00) periods, 4 hours or 14400 seconds for each period. The mean solar irradiance value during each period for surface and depth were multiplied by the exposure time (Equation 6.7) and the irradiance from the whole monitoring period was taken into account instead of irradiance on just the days of the test tube experiments. Table 6.16 and Table 6.17 shows mean *E. coli* disinfection coefficients (K_b) and removal efficiencies (%) for received mean irradiance doses (UV-A, UV-B and PAR) over the whole monitoring period for the different depth profiles and periods of the day. Dose is usually expressed as milliwatt second per square centimetre.

$$D = I \times t \quad (6.7)$$

where,

- D – dose, mJ.cm^2 ($\text{mJ.cm}^2 = \text{mW.s.cm}^2$);
- I – Intensity or irradiance (mW.cm^2);
- t – exposure time (s).

The applied surface doses for all three waves in the morning were higher than in the afternoon, which was not expected (Table 6.15). The tendency maintained at 5 cm in depth, with mean morning received doses superior to mean afternoon received doses for all three waves, indicating that morning disinfection until 5 cm should be greater. At 10 cm in depth, the scenario changed for UV-A and PAR with the afternoon received dose now greater than the morning received dose. UV-B dose in the morning was greater than UV-B dose in the afternoon, but only slightly (Table 6.15). From 20 cm (including 30 cm) the afternoon overall received

dose was greater than the morning overall received dose, but slightly. This indicated that afternoon disinfection of *E. coli* should be greater from 10 cm in depth onwards.

Table 6.15 - Applied surface doses and received doses at different depths for morning and afternoon periods (4 hours each) during the whole monitoring period.

Depth/Wave		Doses (mW.s.cm ⁻²)					
		UV-A (Morning)	UV-B (Morning)	PAR (Morning)	UV-A (Afternoon)	UV-B (Afternoon)	PAR (Afternoon)
cm	Surface (Applied dose)	72001	2180	555657	56080	1562	439986
	5 (Received dose)	1362	81	65614	1088	67	58343
	10 (Received dose)	282	18	27790	295	17	31353
	20 (Received dose)	-	-	8711	-	-	9702
	30 (Received dose)	-	-	2740	-	-	2865

Tarrán (2002) concluded that for a 1 log and 2 log reduction, *E. coli* should be exposed to a UV strength of 3 mW.s.cm⁻² and 6.6 mW.s.cm⁻², respectively, but from the ideal wavelength of 254 nm (UV-C). Chernicharo *et al.* (2003) observed with UV lamps a 4 to 5 log unit reduction with dosages of 13.6 mW.s.cm⁻² and 50.7 mW.s.cm⁻², corresponding to 40 and 150 seconds, respectively. Even with 20 second doses (6.7 mW.s.cm⁻²), *E. coli* was inactivated by 3 log units. Again, with UV lamps (UV-C) and in a confined environment disinfection is optimised, while in natural treatment systems like ponds, the probability of an *E. coli* organism staying in contact with constant dosages is not the same. Another factor is that surface UV is confined to 280 nm to 400 nm wavelengths, not the most bactericidal range, as shown in subsection 4.2, while UV-C lamps emit a constant wavelength of 254 nm, ideal for disinfection (subsection 4.2).

Removal efficiencies for the 10 cm profile during morning and afternoon periods (Table 6.16 and Table 6.17) were 83% ($K_b = 0.45 \text{ h}^{-1}$) and 84.9% ($K_b = 0.48 \text{ h}^{-1}$) for 4 hours of exposure, respectively. This profile was the only one that received UV-A and UV-B, while PAR was received at every depth. 1 log removal of *E. coli* corresponds to 90% removal efficiency, but none of the profiles on average presented a 90% removal efficiency, therefore much lower than the results presented by Tarrán (2002) and Chernicharo *et al.* (2003). As mentioned the UV spectrum was not detected from 15 cm and therefore did not participate in disinfection for the other depth profiles (Table 6.16 and Table 6.17), however disinfection still occurred for the 20 cm and 30 cm depth profiles. The 20 cm profile presented removal efficiencies of 78.6% ($K_b =$

0.39 h⁻¹) and 67.6% ($K_b = 0.28$ h⁻¹) for the morning and afternoon respectively. Interestingly, removal efficiency was greater during the morning than in the afternoon, even though the received PAR dose was higher on average during the afternoon (~ 1000 mW.s.cm⁻²). The same tendency was observed for the 30 cm profile, with higher removal efficiencies during the morning (71.2%) than the afternoon (66.7%), but received dose was higher by over 100 mW.s.cm⁻², lower than the 20 cm profile.

Results for the 10 cm profile during the morning and afternoon were similar probably because of the presence of UV-A and UV-B with virtually the same average strength (Table 6.16 and Table 6.17), and the differences between morning and afternoon periods for the 20 cm and 30 cm profile were probably because of turbidity values. The K_b values are for the *in situ* temperature and not a standardised temperature of 20°C.

Table 6.16 – Overall morning irradiance dose (UV-A, UV-B and PAR) received and *E. coli* removal efficiency and disinfection coefficients for different depth profiles.

MORNING Profile (cm)	UV-A (mW.s.cm ⁻²)	UV-B (mW.s.cm ⁻²)	PAR (mW.s.cm ⁻²)	Removal efficiency (%)	Disinfection coefficient K_b (h ⁻¹)
10 (Received dose)	282	18	27790	83.0%	0.45
20 (Received dose)	-	-	8711	78.6%	0.39
30 (Received dose)	-	-	2739	71.2%	0.31

Table 6.17 – Overall afternoon irradiance dose (UV-A, UV-B and PAR) received and *E. coli* removal efficiency and disinfection coefficients for different depth profiles.

AFTERNOON Profile (cm)	UV-A (mW.s.cm ⁻²)	UV-B (mW.s.cm ⁻²)	PAR (mW.s.cm ⁻²)	Removal efficiency (%)	Disinfection coefficient K_b (h ⁻¹)
10 (Received dose)	295	17	31352	84.9%	0.48
20 (Received dose)	-	-	9701	67.6%	0.28
30 (Received dose)	-	-	2864	66.7%	0.28

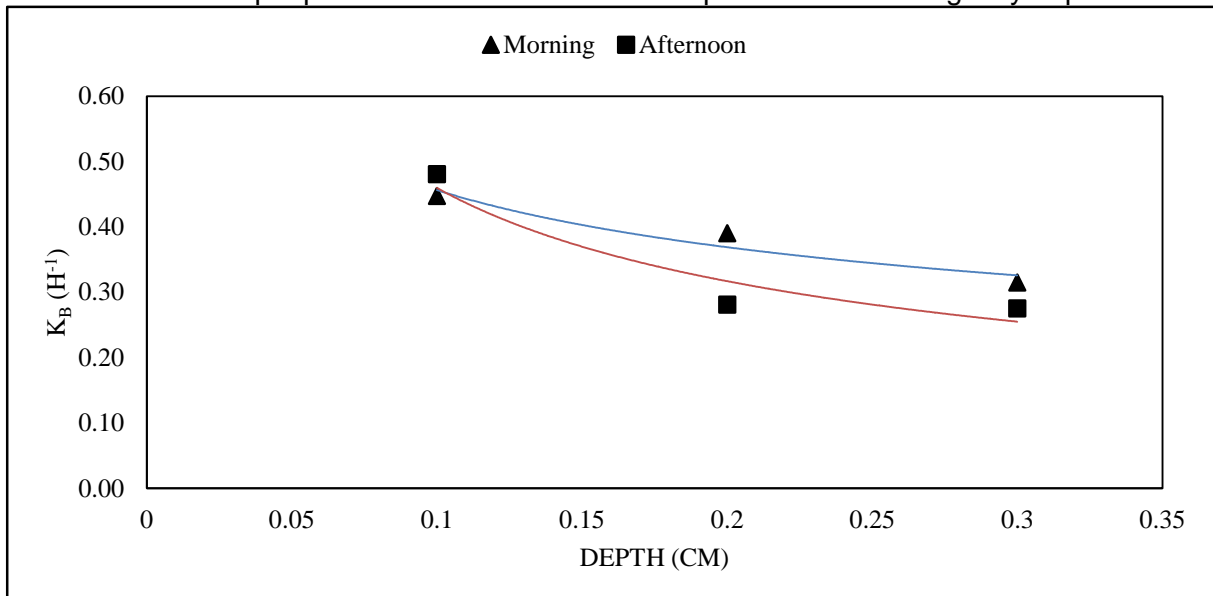
6.3.6. Modelling *E. coli* disinfection coefficient (K_b)

Modelling the disinfection coefficient is important to estimate efficiency of a pond and can be as simple as just adopting a fixed value or considering depth (H) and HRT (von Sperling (1999); von Sperling (2005b); von Sperling, Bastos and Kato (2005)) or just H. Other models are more complex, considering an array of different variables such as pH, DO, solar radiation, H, K_d and

temperature (Mayo, 1995, Sarikaya and Saatçi, 1987 and Ouali *et al.*, 2014). Modelling was based on the K_b models presented by these authors as well as tweaking some models using the data acquired from the depth profiling experiment with the test tubes. When using these equations, the designer must bear in mind that they are for a very shallow maturation pond ($H = 44$ cm) treating wastewater in a tropical climate.

Figure 6.44 presents plotted data considering disinfection rates for each depth profile during both morning and afternoon periods and are represented by Equations 6.8 and 6.9 respectively. The equations used the mean K_b values for *in situ* temperatures measured throughout the monitoring period and condensed into one day (Figure 6.33). Both equations considered depth as the varying variable, similar to von Sperling (1999) - Equation 4.13 - and von Sperling (2005b) - Equation 4.16. Equation 6.10 represents the model for the mean overall K_b value (*in situ* temperatures as well) (08:00 – 16:00) considering all depths and periods. The coefficient of determination (R^2) was high for all equations, the highest was for the overall Equation 6.10 ($R^2 = 0.99$). The high R^2 values were expected for all equations because there are only three depth profiles analysed. Two separate equations (6.8 and 6.9) allow for estimating maximum and minimum disinfection coefficients, and all three are a simple means of predicting K_b values for tropical countries.

Figure 6.44 – Mean K_b values during the morning (blue line) and afternoon (red line) for the different depth profiles and disinfection rate equations considering only depth.



Morning (08:00 – 12:00) – ($R^2 = 0.92$)

$$K_b = 0.225 \cdot Z^{-0.307} \quad (6.8)$$

Afternoon (12:00 – 16:00) – ($R^2 = 0.89$)

$$K_b = 0.134 \cdot Z^{-0.536} \quad (6.9)$$

Overall (08:00 – 16:00) – ($R^2 = 0.99$)

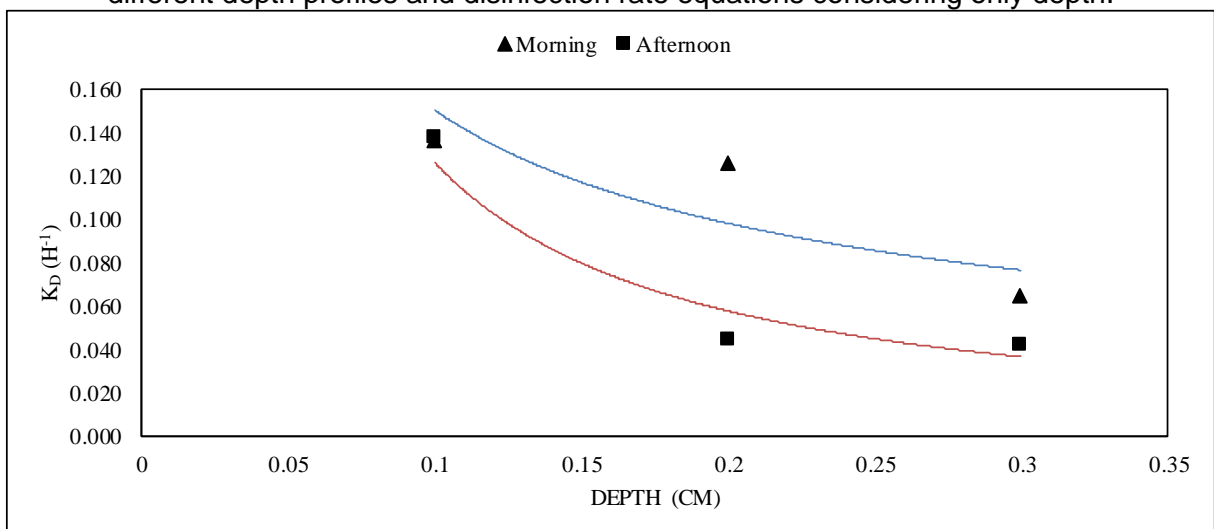
$$K_b = 0.175 \cdot Z^{-0.421} \quad (6.10)$$

where,

- Z – depth from surface (m).

Equations 6.11 and 6.12 are for the dark disinfection/repair coefficient during the morning and afternoon period, as well as the same three depths (Figure 6.45). The morning and afternoon periods presented R^2 , 0.71 and 0.89 respectively. Equation 6.13 presents the model for the mean overall K_d coefficient (08:00 – 16:00), and also presented a high $R^2 = 0.98$ considering all depths and periods.

Figure 6.45 – Mean K_d values during the morning (blue line) and afternoon (red line) for the different depth profiles and disinfection rate equations considering only depth.



Morning K_d (08:00 – 12:00) – ($R^2 = 0.71$)

$$K_d = 0.0365 \cdot Z^{-0.614} \quad (6.11)$$

Afternoon K_d (12:00 – 16:00) – ($R^2 = 0.89$)

$$K_d = 0.0094 \cdot Z^{-1.129} \quad (6.12)$$

Overall K_d (08:00 – 16:00) – ($R^2 = 0.98$)

$$K_b = 0.021 \cdot Z^{-0.836} \quad (6.13)$$

where,

- Z – depth from surface (m).

Equations 6.15 and 6.16 are based on Mayo (1995) - Equation 6.14, considering total solar irradiance (TSI), depth (H) and pH, and temperature (T), respectively. Not very good fittings were observed, as shown by the low CD values and the 45° line in Figure 6.46 for observed vs estimated K_b values. pH showed to have very little or no influence when estimating K_b values, with the solver programme always disregarding its weight in the equations. Therefore, only two equations are presented and the others were not considered because of low CD values and similarities to Equation 6.16. Just as Mayo (1995) found, DO was not well correlated with K_b .

$$K_b = K_{20} \cdot \theta^{(T-20)} + \frac{k_s \cdot S_0}{K \cdot H} + k_{pH} \cdot pH \quad (6.14)$$

TSI, H and pH (08:00 – 16:00) (CD = 0.069)

$$K_b = \frac{1.57 \times 10^{-4} \cdot TSI}{11.683 \cdot H} + 0.038064 \cdot pH \quad (6.15)$$

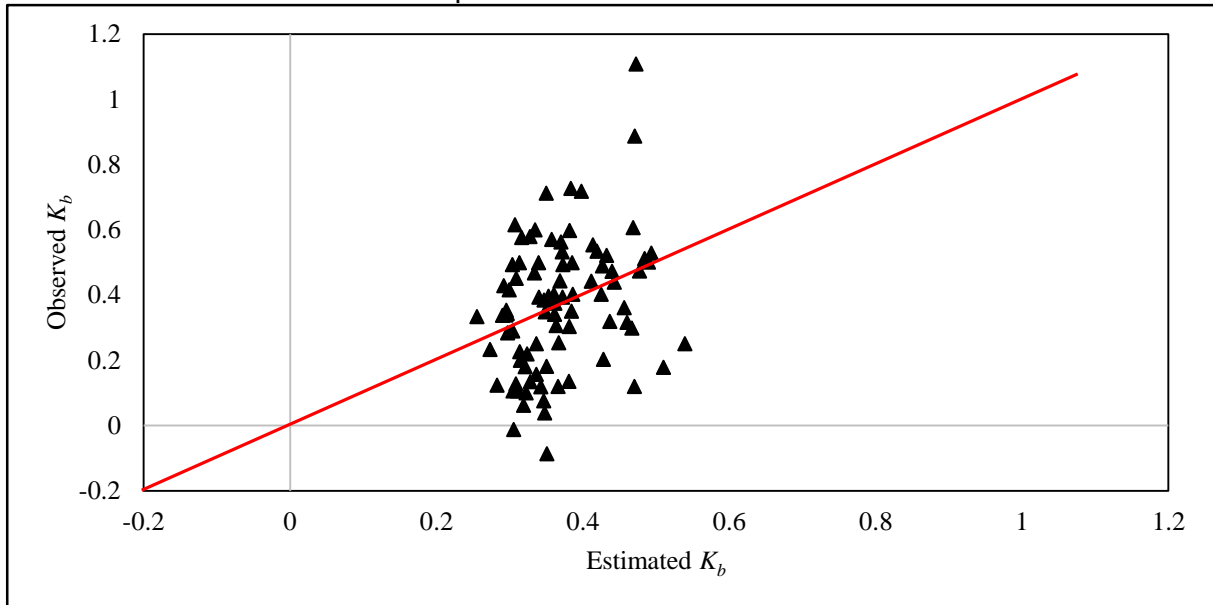
TSI, H and T (08:00 – 16:00) (CD = 0.097)

$$K_b = 0.332 \cdot [0.962]^{(T-20)} + \frac{1.67 \times 10^{-4} \cdot TSI}{11.71 \cdot H} \quad (6.16)$$

where,

- TSI – total solar irradiance (W.m^{-2});
- H – depth (m);
- pH – pH value (-);
- T – temperature ($^{\circ}\text{C}$).

Figure 6.46 - Observed K_b values vs Estimated K_b values considering Mayo (1995) equation. Equation 6.16 – CD = 0.097.



Equation 6.18 was based on Sarikaya and Saatçi (1987) - Equation 6.17 for estimating the disinfection coefficient. Again the fitting was not good (CD = 0.042) as shown in Figure 6.47 with the 45° line for observed vs estimated K_b values. In contrast to other equations above, Sarikaya and Saatçi (1987) accounts for dark disinfection which can correspond up until 1/4 of total *E. coli* disinfection (subsection – 6.3.2).

$$K_b = K_d + \frac{k_s S_0 (1 - e^{-K.H})}{K.H} \quad (6.17)$$

K_d , TSI and H (08:00 – 16:00) (CD = 0.04)

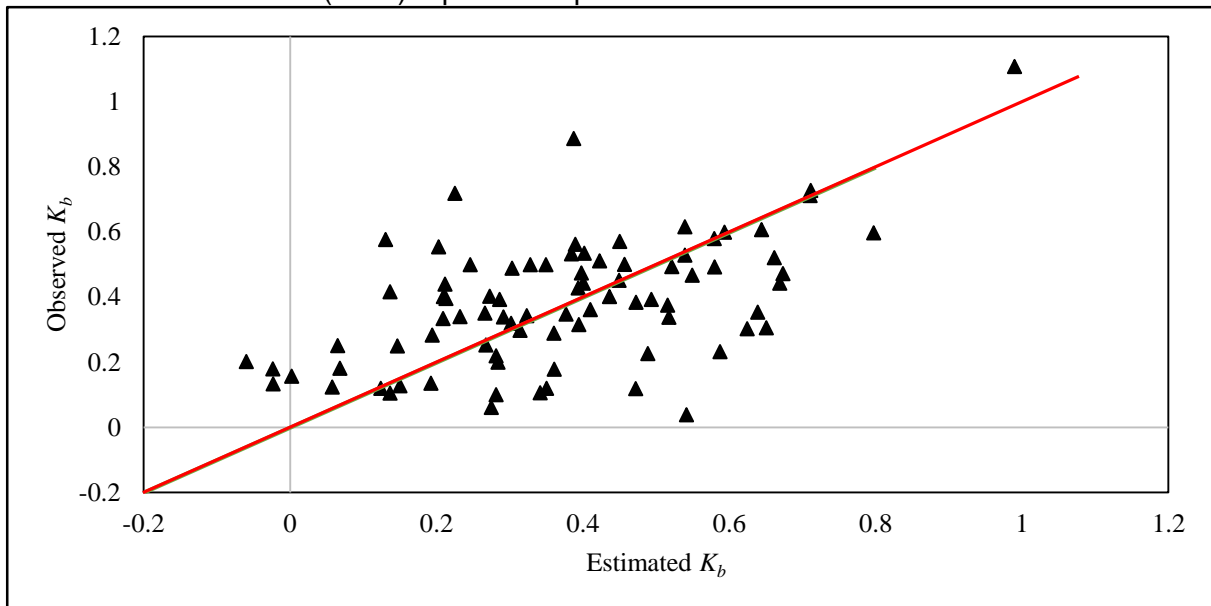
$$K_b = K_d + \frac{4.95 \times 10^{-3} \cdot \text{TSI}}{4.39 \times 10^{-2} \cdot H} \cdot e^{-4.39 \times 10^{-2} \cdot H} \quad (6.18)$$

where,

- K_d - first order *E. coli* disinfection coefficient in dark conditions (h^{-1});

- TSI – total solar irradiance (W.m^{-2});
- H – depth (m).

Figure 6.47 - Observed K_b values vs Estimated K_b values considering Sarikaya and Saatçi (1987) equation. Equation 6.18 – CD = 0.04.



Finally, Ouali *et al.* (2014) proposed Equation 6.19 to estimate K_b values. The equation is simpler than the previous ones and only consists in adding parameters which are multiplied by their coefficients. Three equations, Equation 6.20, 6.21 and 6.23 are presented based on Ouali *et al.* (2014), modifying some parts of the original Equation 6.22. Note that the solver programme in Excel excluded the weight of total surface irradiance from the equations to produce a better fit for the observed K_b values vs estimated K_b value (Figure 6.48). The goodness of the fit is shown by the 45°.

$$K_b = (K_d + K_{pH} \cdot pH + K_{DO} \cdot DO + K_I \cdot I) \cdot \theta^{(T-20)} \quad (6.19)$$

K_d , pH, DO and T (CD = 0.31)

$$K_b = (K_d + 0.368 \cdot pH + 0.011325 \cdot DO) \cdot 0.934^{(T-20)} \quad (6.20)$$

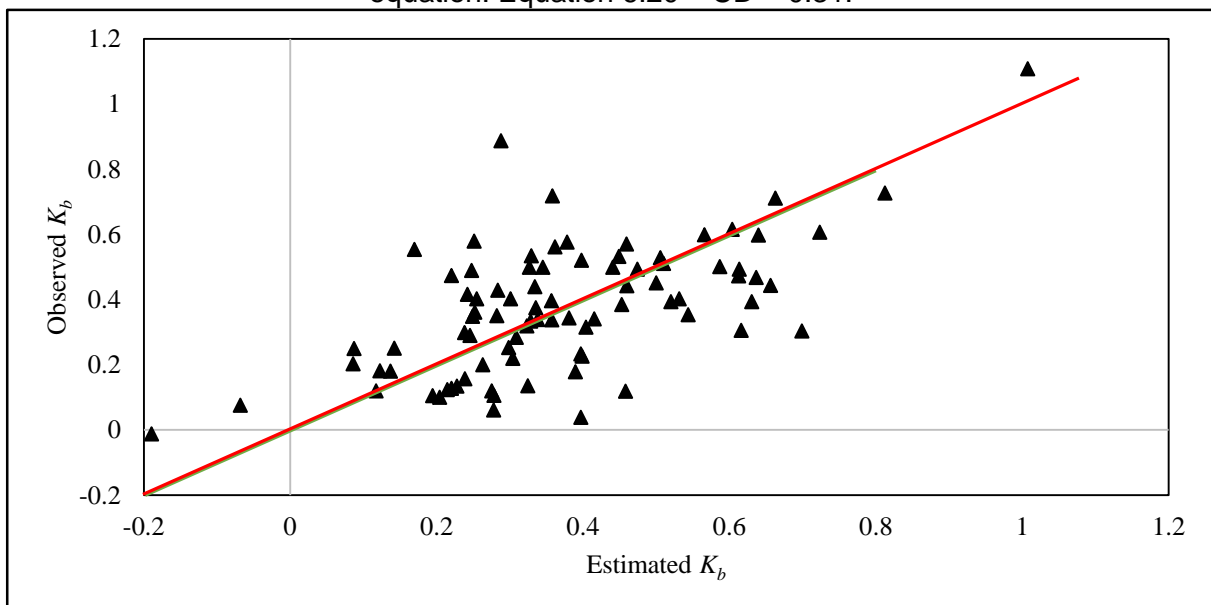
where,

- K_d - first order *E. coli* disinfection coefficient in dark conditions (h^{-1});
- pH – pH value (-);
- DO – dissolved oxygen (mg.L^{-1});

- T – medium temperature (°C).

Compared with the previous models presented by the authors, this one so far has produced the best fit [not accounting for von Sperling (1999 and 2005b) equations], requiring only three environmental variables (pH, DO and T). Again including K_d is important for dark disinfection because it considers disinfection that is not directly related to solar radiation. Although TSI was rejected when modelling Equation 6.20, temperature prevailed and can be considered an indirect parameter for quantifying TSI.

Figure 6.48 - Observed K_b values vs Estimated K_b values considering Ouali *et al.* (2014) equation. Equation 6.20 – CD = 0.31.



K_d , pH, DO, TSI, TUR and T (CD = 0.32)

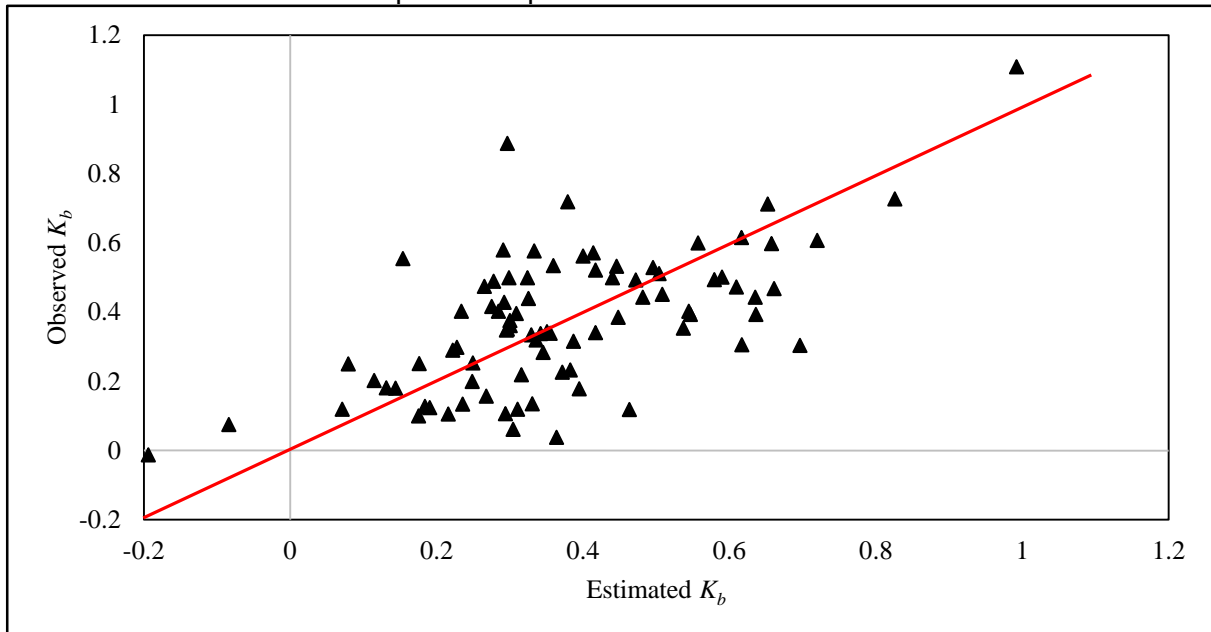
$$K_b = (K_d + 0.027 \cdot pH + 0.0112 \cdot DO + 1.44 \times 10^{-6} \cdot TSI + 0.001 \cdot TUR) \cdot 0.937^{(T-20)} \quad (6.21)$$

where,

- K_d - first order *E. coli* disinfection coefficient in dark conditions (h^{-1});
- pH – pH value (-);
- DO – dissolved oxygen (mg.L^{-1});
- TSI – total solar surface irradiance (W.m^{-2});
- T – medium temperature (°C).

Equation 6.21 was based on Ouali *et al.* (2014) Equation 4.35 but included a new parameter, turbidity (TUR). Compared with the previous Equation 6.20, Equation 6.21 included TSI and turbidity, consequently increasing the CD value slightly to 0.32. The goodness of the fit is shown in Figure 6.49, and even though the CD value increased, it can still be considered low.

Figure 6.49 - Observed K_b values vs Estimated K_b values considering Ouali *et al.* (2014) equation. Equation 6.21 – CD = 0.32.



$$K_b = (K_{Kd} \cdot K_d + K_{pH} \cdot pH + K_{DO} \cdot DO + K_I \cdot I) \cdot \theta^{(T-20)} \quad (6.22)$$

K_d , pH, DO and Temperature (CD = 0.55)

$$K_b = (0.66 \cdot K_d + 0.044 \cdot pH + 4.62 \times 10^{-4} \cdot DO) \cdot 0.955^{(T-20)} \quad (6.23)$$

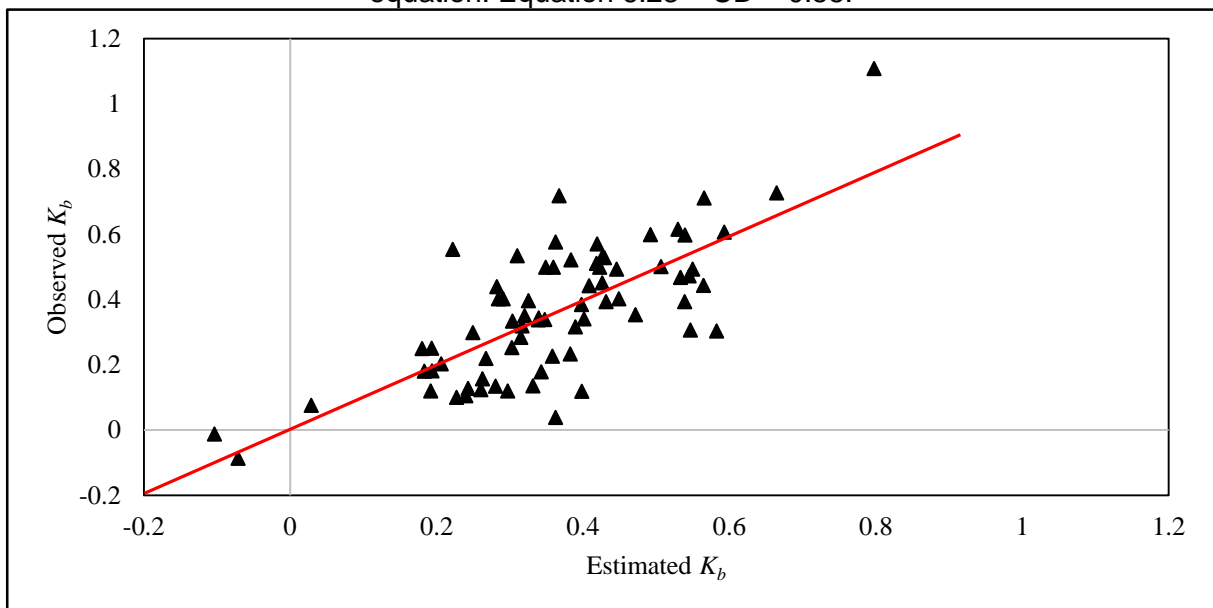
where,

- K_d – first order *E. coli* disinfection coefficient in dark conditions (h^{-1});
- pH – pH value (-);
- DO – dissolved oxygen ($mg \cdot L^{-1}$);
- T – medium temperature ($^{\circ}C$).

Equation 6.23 was also based on Ouali *et al.* (2014) – Equation 6.22 – and included a new coefficient proposed here, K_{Kd} , to reduce the influence of dark disinfection by 33%, therefore resulting in a better CD of 0.55, much higher than any of the other previous models presented

above [not including von Sperling (1999 and 2005b)]. The model again rejected the TSI variable, but maintained the T which can be considered an indirect variable of solar radiation. The goodness of the fit is shown in Figure 6.50 and it was the best fit compared to the previous equations and considered good. Strangely, the best fit was observed considering DO and pH levels, but as shown in subsections 6.3.3.2, 6.3.3.3, 6.3.4.7 and 6.3.4.8 it seemed that they had very little influence on *E. coli* disinfection. On the other hand, Liu, Hall and Champagne (2015) concluded that indicator organism disinfection is driven by a combination of mechanisms and factors, especially temperature, pH and DO play an important role. In fact, Mendonca *et al.* (1994) considered that high temperatures and pH levels increased disinfection, and was therefore well correlated between each other (Liu, Hall and Champagne, 2015). To a certain degree these parameters influenced disinfection as shown in literature, as well as temperature, but pH needs to be high and DO needs to react with sunlight to cause detrimental effects.

Figure 6.50 - Observed K_b values vs Estimated K_b values considering Ouali *et al.* (2014) equation. Equation 6.23 – CD = 0.55.



Of all the equations proposed by the authors, only von Sperling (1999 and 2005b) and a slightly modified version of Ouali *et al.* (2014) produced good fits, therefore aiding the estimation of the *E. coli* disinfection coefficient with confidence for shallow maturation ponds operating in tropical environments. Better fits were not observed since modelling is usually based on experiments done in laboratories with controlled conditions, or considering a pond as a “black-box” and only accounting for variables entering and exiting the unit. Here, monitoring was done in depth over of the course of a year and considered a variety of changing variables, which

proved challenging to produce a robust model. However, the model produced using Ouali *et al.* (2014) equation is satisfactory and gives an idea of what could be an observed K_b value (Equation 6.23). Equations 6.8, 6.9, 6.10, 6.11 and 6.12 account for only depth (H), and are ideal for designing shallow ponds. The goodness of the fit for these three equations was excellent as expected because they only considered three different depths, and as depth increased, K_b values decreased, therefore fitting perfectly with the potential equations presented by von Sperling (1999 and 2005b). For better modelling and better fits when applying more complicated equations, more samples from depth profiling are probably needed and longer term monitoring as well.

6.3.7. Modelling *E. coli* disinfection based on two different approaches and applied in the dispersed flow regime

Once more it is important to emphasise that the K_b values obtained in subsection 6.3.6 are for batch experiments in closed vessels, therefore representing the true intrinsic kinetic coefficient. Most of the K_b values available in the literature were based on measured values of influent and effluent concentrations in continuous flow reactors, and therefore incorporate, not only the kinetic component, but also the imperfections of adopting one idealised hydraulic regimen (complete mix or plug flow). Dispersed flow models, which take into account dispersion inside the pond, are likely to better approach the existing hydrodynamics in the ponds, therefore leading to a K_b coefficient that is closer to the kinetic value obtained here. But this requires a good estimation of the dispersion coefficient d .

Based on the kinetic coefficients obtained here, it was investigated whether they could be incorporated into the dispersed flow model and lead to good estimations of the effluent *E. coli* concentration. Since the disinfection coefficients have been obtained from Pond 2, this pond was firstly used in the modelling exercise. After that, Pond 1 (unbaffled) was used for validation purposes.

Two approaches were adopted:

- Single disinfection coefficient for the whole liquid column (traditional approach of having one kinetic coefficient and the utilisation of the dispersed flow model for the whole pond);

- Multi-layer approach, with one disinfection coefficient for each vertical layer within the pond depth, utilisation of the dispersed flow model for each layer, and calculation of the overall effluent concentration based on all the layers.

Since K_b and K_d values from different depth profiles had been obtained, i.e., 0 to 10 cm, 10 to 20 cm and 20 to 30 cm, it was possible to estimate K'_b and K'_d values for the full depth of the ponds. This was done for the first and second pond, assuming that the relationship of the disinfection coefficients with depth is the same in both ponds. The simple potential equation with a structure similar to that proposed by von Sperling (1999 and 2005b) is shown in Equation 6.24 for the sunlight disinfection coefficient (K'_b) and Equation 6.25 for the dark disinfection/repair coefficient (K'_d). A simplifying assumption was made that each fluid element, i.e., including coliforms and *E. coli*, have an equal probability of staying in each vertical layer for the same time because of horizontal mixing and daily cycles of vertical mixing (Passos *et al.*, 2015, 2016). Consequently, the K_b and K_d values were a weighted average regarding the thickness of each layer (10 cm), which, in this case, is equal to the calculated arithmetic mean K'_b and K'_d values, since the thicknesses of each layer are equal (Equation 6.24 and Equation 6.25).

$$K'_b = a.Z^{-b} \quad (6.24)$$

$$K'_d = c.Z^{-d} \quad (6.25)$$

where,

- K'_b – average sunlight disinfection coefficient considering different depths (h^{-1});
- K'_d – average dark disinfection/repair coefficient considering different depths (h^{-1});
- a and b – coefficients for K'_b ;
- c and d – coefficients for K'_d ;
- Z – depth from surface (cm).

The average K'_b and K'_d values for the second pond (equation derived from measured data) and first pond (assuming the same behaviour of the second pond in terms of depth) are shown in Equation 6.26 (which is the same as Equation 6.10 shown before) and 6.27, respectively:

$$K'_b = 0.175.Z^{-0.421} \quad (6.26)$$

$$K'_d = 0.021 \cdot Z^{-0.836} \quad (6.27)$$

For the second approach (multi-layer approach), in order to have a profile of coliform decay throughout depth, the first and second ponds' depths were divided into twenty layers (a high number that ensured a smooth profile over depth), and the mean K'_b and K'_d were estimated considering the depth of each layer (total depth divided by 20 layers) using Equations 6.26 and 6.27, as shown in Table 6.18. First pond = 0.77 m (layer thickness = 0.77m/20 = 0.039 m); second pond = 0.44 m (layer thickness = 0.44m/20 = 0.022 m).

Table 6.18 - Depth from the surface and resulting K'_b and K'_d in each of the 20 vertical layers of the first and second ponds based on Equations 6.27 and 6.28, including the final weighted mean for K'_b and K'_d in both ponds.

Layers	First pond			Second Pond		
	Depth from surface: Z (m)	K'_b (h ⁻¹)	K'_d (h ⁻¹)	Depth from surface: Z (m)	K'_b (h ⁻¹)	K'_d (h ⁻¹)
-	0	-	-	0	-	-
1	0.039	0.688	0.315	0.022	0.870	0.503
2	0.077	0.514	0.177	0.044	0.650	0.282
3	0.116	0.433	0.126	0.066	0.548	0.201
4	0.154	0.384	0.099	0.088	0.486	0.158
5	0.193	0.350	0.082	0.11	0.442	0.131
6	0.231	0.324	0.071	0.132	0.410	0.113
7	0.270	0.303	0.062	0.154	0.384	0.099
8	0.308	0.287	0.056	0.176	0.363	0.089
9	0.347	0.273	0.050	0.198	0.345	0.080
10	0.385	0.261	0.046	0.22	0.331	0.073
11	0.424	0.251	0.042	0.242	0.318	0.068
12	0.462	0.242	0.040	0.264	0.306	0.063
13	0.501	0.234	0.037	0.286	0.296	0.059
14	0.539	0.227	0.035	0.308	0.287	0.056
15	0.578	0.220	0.033	0.33	0.279	0.052
16	0.616	0.214	0.031	0.352	0.271	0.050
17	0.655	0.209	0.030	0.374	0.264	0.047
18	0.693	0.204	0.028	0.396	0.258	0.045
19	0.732	0.199	0.027	0.418	0.252	0.043
20	0.770	0.195	0.026	0.440	0.247	0.041
	Weighted mean:	0.301	0.071	Weighted mean:	0.380	0.113

Note: since the thickness of each layer is the same, the mean weighted by the layer thicknesses is equal to the arithmetic mean

A simple form of estimating the overall K_b was by calculating the weighted mean of K'_b (h⁻¹) and K'_d (h⁻¹) as shown in Table 6.18 for the first and second ponds. Note that the values are different for each pond. Based on the radiation profiles in subsection 6.2.1 and APPENDIX II, overall sunlight conditions were 13.7 hours long (06:00 – 19:40) and night conditions were 10.3 hours long (19:40 – 06:00) for one day (24 hours). The final average K_b , expressed in the usual unit of d⁻¹, and applied in the dispersed flow model, is presented in Equation 6.28 and considers

the weighted mean values of K'_b (h^{-1}) and K'_d (h^{-1}) multiplied by the mean values of measured hours of sunlight (13.7 hours per day) and dark time at night (10.3 hours per day), respectively:

$$K_b = K'_b \cdot 13.7 \frac{\text{hours with sunlight}}{\text{day}} + K'_d \cdot 10.3 \frac{\text{hours without sunlight}}{\text{day}} \quad (6.28)$$

where,

- K_b – overall average disinfection coefficient considering sunlight and night conditions for all depths (d^{-1});
- K'_b – average sunlight disinfection coefficient considering different depths (h^{-1});
- K'_d – average dark disinfection/repair coefficient considering different depths (h^{-1}).

Therefore, from Table 6.18, the overall K_b value used in the traditional approach (whole liquid column) considering sunlight and night conditions in the first and second ponds at liquid temperature was (Equation 6.29 and Equation 6.30):

First pond

$$K_b = 0.301 \times 13.7 + 0.071 \times 10.3 = 4.846 \text{ d}^{-1} \quad (6.29)$$

Second pond

$$K_b = 0.380 \times 13.7 + 0.113 \times 10.3 = 6.372 \text{ d}^{-1} \quad (6.30)$$

Equation 6.31 was then used for estimating the final concentration of coliforms/*E. coli* considering the dispersed flow regimen:

$$N = N_0 \cdot \frac{4 \cdot a \cdot e^{1/2 \cdot d}}{(1+a)^2 \cdot e^{a/2 \cdot d} - (1-a)^2 \cdot e^{-a/2 \cdot d}} \quad (6.31)$$

where,

- N – *E. coli* concentration in the effluent (MPN/100 mL);
- N_0 – *E. coli* concentration in the influent (MPN/100 mL);
- d – dispersion number (-);
- K_b – *E. coli* disinfection coefficient (d^{-1});

- t – hydraulic retention time (d);
- $a = \sqrt{1 + 4 \cdot K_b \cdot t \cdot d}$

The dispersion number (d) for the first and second pond was obtained by Passos *et al.* (2015, 2016) through tracer tests, and even though d in the second pond was considered high (not expected because the second pond had baffles and this intervention should have reduced d), it was used in Equation 6.32. This was justified because of short-circuiting occurring in the second pond (Table 6.19). Influent geometric mean concentrations of *E. coli* (N_0) and HRT (t) from the monitoring period during the first phase for the first and second ponds are also shown in Table 6.19, as well as the calculated K_b values for both ponds. The observed influent and effluent concentrations were sampled using the core sampler until 0.30 m in depth, representing the liquid column in the ponds, and have been also presented in Table 6.1.

Table 6.19 - N_0 , K_b (whole liquid column approach), t and dispersion number (d) (Passos *et al.*, 2015; 2016) in the first and second pond.

	<i>First pond</i>	<i>Second pond</i>
Observed influent concentration N_0 (MPN/100mL)	$5.95 \times 10^{+08}$	$2.89 \times 10^{+06}$
Dispersion number d (-)	0.28	0.30
Overall K_b (d^{-1}) (estimated)	4.85	6.37
Hydraulic retention time t (days)	3.5	1.8

The final estimated concentration (N) (Equation 6.31) for both ponds based on the whole liquid column approach for calculating K_b from Equation 6.29 and 6.30 and considering the influent concentrations and dispersion numbers from Table 6.19 are shown in Table 6.20. Final observed geometric mean concentrations (taken from Table 6.1) are also presented to compare with the estimated concentrations.

Table 6.20 - Observed N vs estimated N in the first and second pond for the dispersed model considering a simpler form of estimating K_b .

	<i>First pond</i>	<i>Second pond</i>
Observed N	$2.89 \times 10^{+06}$	$3.55 \times 10^{+04}$
Estimated N	$7.22 \times 10^{+05}$	$1.66 \times 10^{+04}$

The estimated effluent *E. coli* concentrations were relatively close to the geometric mean of the measured effluent concentrations (observed values), especially in the second pond.

With the multi-layer approach, a different way of estimating the final concentration also using the dispersed model was by calculating each individual overall K_b value based on Equation 6.28 using the K'_b and K'_d values estimated from Equation 6.26 and 6.27 (Table 6.18) for each

different vertical layer in the ponds, as shown in Table 6.21. The dispersed flow model was used for each layer, keeping the same input values of N_0 , d and t shown in Table 6.19. The hydraulic retention time in each layer was the same as the overall retention time, considering that each of the 20 layers represented 1/20 of the pond volume and received 1/20 of the total inflow. Each layer, situated at a different depth from the surface, presented a different effluent *E. coli* concentration and then a weighted mean *E. coli* concentration was calculated, in order to obtain the overall effluent concentration. This value represented the mean concentration throughout the depth, and can be compared with effluent samples collected with a column sampler, as was the case in this research in the first and second ponds. This method was somewhat more complex and laborious compared to the previous method, but provided a much better estimation of the final effluent *E. coli* concentration for both ponds, and allowed for vertically profiling *E. coli* concentrations over depth (Figure 6.51 and Figure 6.52).

Table 6.21 - K_b in each layer and estimated N for each individual layer in the first and second pond for *E. coli*, as well as their respective weighted mean. Estimated mean *E. coli* concentration from the effluent of the first pond and second pond.

Layers	First pond			Second Pond		
	Depth from surface: Z (m)	K_b (d ⁻¹)	N estimated (MPN/100mL)	Depth from surface: Z (m)	K_b (d ⁻¹)	N estimated (MPN/100mL)
-	0	0	-	0	0	-
1	0.039	12.67	$4.62 \times 10^{+03}$	0.022	17.11	$2.55 \times 10^{+02}$
2	0.077	8.86	$4.03 \times 10^{+04}$	0.044	11.81	$1.56 \times 10^{+03}$
3	0.116	7.23	$1.17 \times 10^{+05}$	0.066	9.58	$3.78 \times 10^{+03}$
4	0.154	6.28	$2.32 \times 10^{+05}$	0.088	8.28	$6.65 \times 10^{+03}$
5	0.193	5.64	$3.80 \times 10^{+05}$	0.11	7.41	$9.95 \times 10^{+03}$
6	0.231	5.16	$5.55 \times 10^{+05}$	0.132	6.77	$1.36 \times 10^{+04}$
7	0.270	4.80	$7.53 \times 10^{+05}$	0.154	6.28	$1.74 \times 10^{+04}$
8	0.308	4.50	$9.70 \times 10^{+05}$	0.176	5.89	$2.14 \times 10^{+04}$
9	0.347	4.26	$1.20 \times 10^{+06}$	0.198	5.56	$2.55 \times 10^{+04}$
10	0.385	4.05	$1.45 \times 10^{+06}$	0.22	5.28	$2.97 \times 10^{+04}$
11	0.424	3.88	$1.71 \times 10^{+06}$	0.242	5.05	$3.39 \times 10^{+04}$
12	0.462	3.72	$1.98 \times 10^{+06}$	0.264	4.84	$3.82 \times 10^{+04}$
13	0.501	3.59	$2.26 \times 10^{+06}$	0.286	4.66	$4.25 \times 10^{+04}$
14	0.539	3.46	$2.55 \times 10^{+06}$	0.308	4.50	$4.67 \times 10^{+04}$
15	0.578	3.36	$2.85 \times 10^{+06}$	0.33	4.36	$5.10 \times 10^{+04}$
16	0.616	3.26	$3.15 \times 10^{+06}$	0.352	4.23	$5.53 \times 10^{+04}$
17	0.655	3.17	$3.45 \times 10^{+06}$	0.374	4.11	$5.96 \times 10^{+04}$
18	0.693	3.08	$3.76 \times 10^{+06}$	0.396	4.00	$6.38 \times 10^{+04}$
19	0.732	3.01	$4.08 \times 10^{+06}$	0.418	3.90	$6.81 \times 10^{+04}$
20	0.770	2.94	$4.39 \times 10^{+06}$	0.440	3.81	$7.23 \times 10^{+04}$
	Estimated weighted mean:		$1.80 \times 10^{+06}$	Estimated weighted mean:		$3.31 \times 10^{+04}$

Note: since the thickness of each layer is the same, the mean weighted by the layer thicknesses is equal to the arithmetic mean

As mentioned before, the dispersion number (d) for the first and second pond was obtained by Passos *et al.* (2015, 2016) through tracer tests. Initial geometric mean concentrations of *E. coli*

and HRT (t) from the monitoring period during the first phase for the first and second ponds are shown in Table 6.19, and the estimated weighted mean K_b value for both ponds based on the multi-layer method are shown in Table 6.22 and compared with the observed concentrations.

The difference in the multilayer method lies on the individual K_b values for each layer and effluent concentrations. The difference between having a single overall K_b and several K_b values for each depth are because the estimation of the effluent concentration N is not directly related to K_b , but rather to the square root of K_b , imbedded in the parameter a in the dispersed flow equation (Equation 6.31). The multilayer approach led to a very good estimation of the *E. coli* effluent concentration, as shown in Table 6.22.

Table 6.22 - Observed N vs estimated N in the first and second pond for the dispersed model using the dispersed flow model applied with the multilayer approach.

	<i>First pond</i>	<i>Second pond</i>
Observed N	$2.89 \times 10^{+06}$	$3.55 \times 10^{+04}$
Estimated N	$1.80 \times 10^{+06}$	$3.31 \times 10^{+04}$

Both methods (whole liquid column and multilayer) proved to produce an excellent estimation of the final effluent concentration compared to the observed final effluent *E. coli* concentration, with the latter, more complex methodology producing the best results. The first method could be used to have an initial idea of the performance of the pond, while the second method allowed to estimate *E. coli* concentrations for every vertical layer in the pond (Table 6.21) and the overall estimation was closer to the observed results. Note how *E. coli* concentrations increased with depth because of sunlight attenuation (subsection 6.2.3) (Figure 6.51 and Figure 6.52), therefore exemplifying the influence of depth and sunlight penetration in ponds. This also reinforces the indication provided in the literature that effluent from maturation ponds should be withdrawn close to the pond surface, where concentrations are lower (Shilton, 2005; Moumouni, 2015).

Figure 6.51 - Estimated *E. coli* concentration vs pond height in the first pond [Black vertical line demonstrates the geometric mean concentration of *E. coli* in the 30 cm liquid column ($1.80 \times 10^{+06}$ MPN/100 mL)].

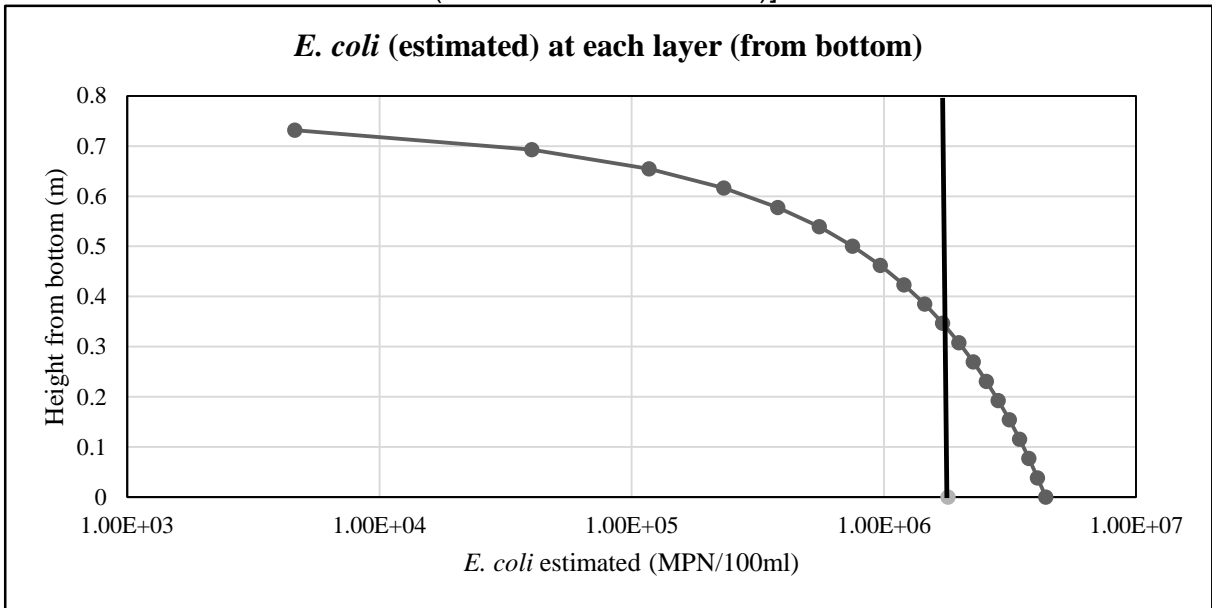
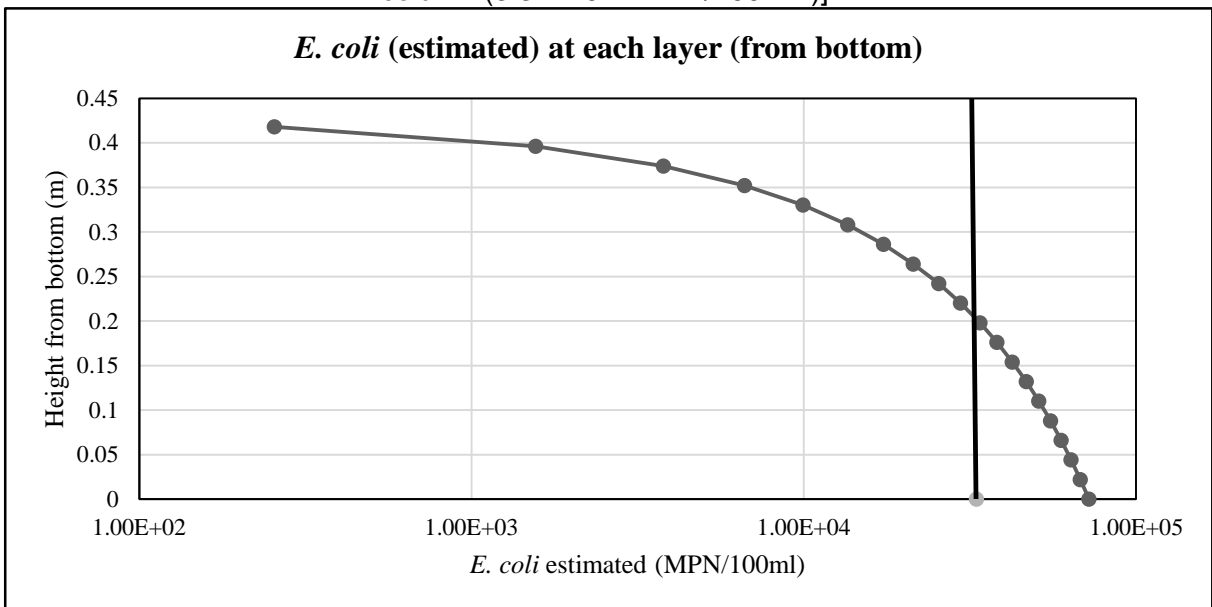


Figure 6.52 - Estimated *E. coli* concentration vs pond height in the second pond [Black vertical line demonstrates the geometric mean concentration of *E. coli* in the 30 cm liquid column ($3.31 \times 10^{+04}$ MPN/100 mL)].



6.3.8. Vertical hydrodynamic profiling and comparison between the two hydraulic phases (without and with vertical baffles)

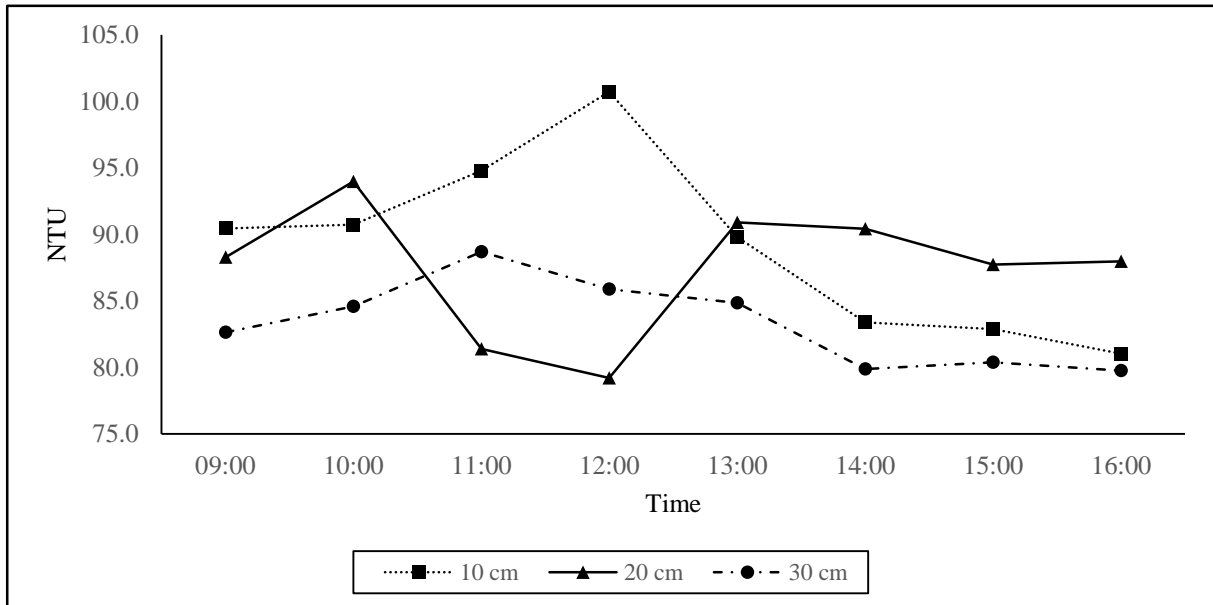
This section focuses on the vertical hydrodynamic profiling and then a comparison between the two different phases in the 2nd pond (without and with vertical baffles).

As shown by Passos *et al.* (2015, 2016), vertical mixing occurs in both ponds of the series at CePTS in a daily cyclic form, where 56% (13 hours of the day) of the time the ponds are stratified and 44% (11 hours of the day) of the time they are in completely mixed conditions. Stratification in the 2nd pond begins at around 08:00 hours, reaching the largest temperature difference at 13:00 hours, and then mixing starts at 21:00 hours. This was observed on a regular basis every day that monitoring took place. The thermocline is located roughly in the middle of the 2nd pond depth (22.5 cm) and this is supported by turbidity data already shown in subsection 6.2.4 and again shown in Figure 6.53. Note that at 09:00 hours the 10 cm and 20 cm profile presented similar turbidity values. At 10:00 hours turbidity for the 20 cm profile increased and the 10 cm profile stayed the same. From 10:00 hours turbidity dipped for the 20 cm profile and increased in both the 10 cm and 30 cm profile, therefore indicating a migration of mobile algae to the surface to seek out strong solar conditions to perform photosynthesis and settling of other material (probably organic matter) to the bottom of the pond. It is known that some algae can move on their own account, but the increase of turbidity is nearly 25% in one hour, therefore indicating stratification had taken place. This was also supported by the increase in turbidity in the 30 cm profile, indicating that stratification also directed material to the bottom of the pond. From 12:00 o'clock, turbidity for the 10 cm profile decreased and the 20 cm profile increased, suggesting that algae now fled from the strong sun at noon to deeper depths, but not passing the 20 cm barrier. The 30 cm profile remained with virtually the same turbidity value.

These are important findings because *E. coli* cells can also follow this pattern due to stratification, with some remaining below 22.5 cm, therefore reducing disinfection, while others will stay above the 22.5 cm thermocline and consequently be inactivated at a faster rate. *E. coli* organisms are also known to attach themselves to other objects in pond systems (algae, organic matter, etc.), therefore with stratification some organisms, are sent to the bottom of the pond and do not undergo sunlight-mediated disinfection. The probability of an *E. coli* cell remaining in a certain profile depends on its mobility and the stratification/destratification cycles in the pond, therefore there is a 50% chance of it remaining above the thermocline and 50% chance

of it floating below the thermocline. When destratification takes place, the vertical mixing is responsible to approximate complete mixed conditions in the vertical column, and bacteria that were in the lower layers have now the possibility of receiving more radiation closer to the surface.

Figure 6.53 - Plotted mean values of turbidity for the different depth profiles at each time interval.



Therefore, if the bottom layer of the stratified pond could be forced to flow to the surface layers of the pond, in theory this should increase disinfection. Inserting the three vertical baffles in the first channel of the 2nd pond (subsection 5.6.2) aimed to partially break stratification in the pond at its stratified stage and thus increase disinfection. Results for *E. coli* disinfection (removed log units) and concentrations in each unit are shown in Table 6.23 and are compared with the *E. coli* concentrations and disinfection from the 1st phase. Due to problems with the pump that fed the treatment line, only 7 (n) samples for each unit were collected, but results are promising. A Wilcoxon-Mann-Whitney U test with confidence level of 95% was performed to compare removal efficiencies from the overall 1st phase (without vertical baffles; n = 28; 11/06/2014 – 16/09/2015) and 2nd phase (with vertical baffles; n = 7; 30/09/2015 – 19/04/2016) (Table 6.23).

Table 6.23 - Summary of mean/median removal efficiencies (log units) and geometric means for the treatment line during the overall 1st and 2nd phases.

Parameter/Unit	Raw Sewage	UASB	Pond 1	1 st channel <i>P₁ - P₂B₂</i>	2 nd and 3 rd channels <i>P₂B₂ - P₂B₄</i>	GRoF
Mean/median Overall 1 st phase (log units removed)	-	1.21/1.05	2.31/2.16	0.51/0.53	<u>1.31/1.28</u>	0.88/0.98
Mean/median 2 nd phase (log units removed)	-	0.70/0.85	2.36/2.29	<u>1.30/1.32</u>	0.86/0.85	1.0/1.05
Geometric mean 1 st phase (MPN.100mL ⁻¹)	7.79×10 ⁺⁰⁹	5.95×10 ⁺⁰⁸	2.89×10 ⁺⁰⁶	5.54×10 ⁺⁰⁵	3.55×10 ⁺⁰⁴	4.81×10 ⁺⁰³
Geometric mean 2 nd phase (MPN.100mL ⁻¹)	4.81×10 ⁺⁰⁹	9.62×10 ⁺⁰⁸	4.19×10 ⁺⁰⁶	2.09×10 ⁺⁰⁵	2.90×10 ⁺⁰⁴	2.91×10 ⁺⁰³

Underlined: significantly higher removal efficiency (log units); P₁ = Pond 1; P₂B₂, P₂B₃ and P₂B₄ = Pond 2, end of each baffle and outlet; GRoF = graded rock filter (effluent).

Table 6.23 shows that the insertion of the vertical baffles increased disinfection by twofold in the first compartment of the second pond (*P₁ - P₂B₂*) compared with the overall 1st phase, endorsed by the statistically better removal efficiency and therefore impacted the final concentration in the 2nd pond. *P₂B₂ - P₂B₄* in the first phase presented statistically better removal efficiency, compensating for the lower removal rate occurring before and probably because the pond unit was balancing out removal efficiencies based on the kinetics (higher concentrations, high disinfection rate; lower concentrations, low disinfection rate). This was confirmed during the second phase with the first compartment (vertical baffles) presenting higher removal efficiencies, and then lower removal efficiencies from *P₂B₂ - P₂B₄*, indicating that because there was a lower concentration of *E. coli*, removal rates were reduced. Note that the effluent concentration before entering the second pond was higher in the 2nd phase compared to the 1st phase, further endorsing the vertical baffles and confirmed by the lower final effluent from the 2nd phase for *E. coli* concentration.

The 2nd phase was also compared to the same period in the year during the 1st phase (n = 14; 25/09/2014 – 23/04/2015) (Table 6.24) and a Wilcoxon-Mann-Whitney U test with confidence level of 95% was performed to compare removal efficiencies. Results showed that only *P₁ - P₂B₂* was able to reach a statistically higher removal efficiency, again highlighting the application of the vertical baffles in the first channel of the 2nd pond. Final concentration of the 2nd phase was still lower than the 1st phase considering the same period.

Table 6.24 - Summary of mean/median removal efficiencies (log units) and geometric means for the treatment line during the same period of the 1st (25/09/2014 – 23/04/2015) and 2nd (30/09/2015 – 19/04/2015) phases.

Parameter/Unit	Raw Sewage	UASB	Pond 1	1 st channel <i>P₁ - P₂B₂</i>	2 nd and 3 rd channels <i>P₂B₂ - P₂B₄</i>	GROF
Mean/median same period 1 st phase (log units removed)	-	1.36/1.28	2.20/2.11	0.53/0.55	1.38/1.38	0.70/0.93
Mean/median 2 nd phase (log units removed)	-	0.70/0.85	2.36/2.29	<u>1.30/1.32</u>	0.86/0.85	1.0/1.05
Geometric mean 1 st phase (MPN.100mL ⁻¹)	1.10×10 ⁺¹⁰	4.49×10 ⁺⁰⁸	2.92×10 ⁺⁰⁶	7.50×10 ⁺⁰⁵	3.21×10 ⁺⁰⁴	6.62×10 ⁺⁰³
Geometric mean 2 nd phase (MPN.100mL ⁻¹)	4.81×10 ⁺⁰⁹	9.62×10 ⁺⁰⁸	4.19×10 ⁺⁰⁶	2.09×10 ⁺⁰⁵	2.90×10 ⁺⁰⁴	2.91×10 ⁺⁰³

Underlined: significantly higher removal efficiency (log units).

Even though these initial results are promising, more monitoring and sample collections are needed to confirm that the insertion of vertical baffles resulted in reducing stratification in the 2nd pond and consequently increased disinfection. It is recommended that inserting another 6 vertical baffles, three in each channel, should create a greater impact on disinfection in the 2nd pond and overall treatment line by forcing mixed conditions in the pond.

7. CONCLUSIONS

The overall treatment system composed of a UASB reactor, two shallow maturation ponds (unbaffled and baffled) and a graded rock filter (GRoF) produced excellent results, highlighting high organic matter removal (BOD, COD and SS) and limited TKN and ammonia-N removal. Total coliforms and *E. coli* removal was excellent. The monitoring period lasted two years and three months of sampling and analysis (24/01/2014 to 19/04/2016). The median final effluent concentrations and cumulative removal efficiencies of the treatment setup for total BOD, total COD and TSS were 17 mg/L (92.6%), 79 mg/L (79.4%) and 25 mg/L (86.9%), respectively. Particulate BOD, particulate COD and VSS concentrations were 2 mg/L, 52 mg/L and 22 mg/L, correspondingly, emphasising the low concentrations in a very short overall hydraulic retention time (6.7 days), and also the important role of the graded rock filter. TKN and ammonia-N removal was considered satisfactory because it is not easily achieved in natural treatment lines. Cumulative overall disinfection of the treatment line for *E. coli* was 6.1 log units, considered excellent when working with a low total HRT (6.7 days). Major contributions in the disinfection came from the first and second ponds due to their aerobic nature (high levels of pH and DO) and explicit disinfection mechanisms associated with radiation. The final effluent of the proposed setup was polished and complied with strict discharge regulations and consequently are likely to pollute less waterbodies if discharged into them, while requiring only 1.5 m².inhab.⁻¹ to do so. Compliances for bacteriological concentration allowed for different practises of restricted and unrestricted irrigation set by the WHO (2006).

Overall total solar irradiance (TSI) reaching the pond's surface varied widely, even more so during the two different seasons. TSI over the course of the day presented a distinct bell-like-shape, increasing in the morning and decreasing in the afternoon. This shape was expected because the highest peaks of total solar radiation occur when the sun is highest in the sky (around noon), and the lowest values are during sunrise and sunset. Mean total solar irradiance during the wet and warm (October to March) season was generally greater than during the mildly cold and dry (April to September) season, but only visible with some significance during the afternoon period. Overall, the wet and warm period was better for disinfection, considering solely the sunlight-mediated mechanism because of higher surface insolation.

Vertical depth profiling of UV-A, UV-B and photosynthetically active radiation (PAR) undertaken inside pond 2 was limited for the UV spectrum because of pond optics and seasonal

variation. Overall, UV-A and UV-B were able to penetrate to a maximum of 10 cm, both extinguishing somewhere between 10 cm and 15 cm and probably impacting overall disinfection. As expected, PAR was able to reach 30 cm in depth, therefore confirming to be the more energised wave. All waves were able to maintain the bell-like-shape at the 5 cm depth profile, therefore confirming little influence from the ponds optics in attenuation rates. Seasonal variation at 5 cm showed on average that the wet and warm season presented double the irradiance value for all three waves compared with the cold and dry season. At 10 cm irradiance values for all three waves during both seasons were effectively the same. At 20 cm PAR during the cold and dry season was greater than during the wet and warm season, and at 30 cm both seasons presented effectively the same irradiance. This partly confirmed that sunlight attenuation was affected by optical conditions as depth increased, affecting all three waves during different seasons (first hypothesis). The attenuation coefficient along the pond depth for photosynthetically active radiation (PAR) was calculated using three different models (without turbidity, with turbidity, with \log_{10} of turbidity) and considering two different methods for estimating surface UV-A, UV-B and PAR. The simpler model, that considered fixed percentages for estimating surface PAR as a function of total irradiance, produced the best equations. Turbidity showed to influence the attenuation coefficient (K_a).

Based on experiments with closed vessels immersed inside the second pond at different depths, the *E. coli* disinfection coefficient (K_b) was greater during the first 10 cm profile and decreased as depth increased. Disinfection occurred at deeper depths where only photosynthetically active radiation (PAR) was present and this confirmed the hypothesis that PAR contributes for *E. coli* disinfection. The dark repair/disinfection coefficient (K_d) on average showed little influence for overall disinfection and only accounted for 1/8 to 1/4 of total disinfection, decreasing also as depth increased. However, results showed that dark disinfection and repair occurred at any depth, with repair being more significant at deeper depths, but disinfection dominated on average. This confirmed the second hypothesis that both repair and disinfection occurred in dark conditions.

The synergy of dissolved oxygen (DO), pH and solar radiation influencing *E. coli* disinfection was not evident, but maybe influenced disinfection at deeper depths (especially DO). The model that produced the best fit for the disinfection coefficient included pH, DO and temperature (T), and did not include directly total solar irradiance (TSI). These results rejected the third

hypothesis that stated that an array of environmental variables could produce a better model for estimating the *E. coli* disinfection coefficient. Temperature can be considered a secondary effect from solar radiation and therefore used instead of total solar irradiance (TSI). Modelling the disinfection coefficient considering only depth (H) produced the best fitting, because one varying parameter was more easily correlated than a magnitude of fluctuating variables (DO, TSI, pH, temperature, etc.). When applying the kinetic coefficients obtained in the in-pond vessels to the dispersed flow model, and considering different vertical layers inside the pond produced excellent results for estimating the final effluent concentration from ponds 1 (unbaffled) and 2 (baffled).

To the author's knowledge, for the first time, applied and received doses were presented concerning *E. coli* disinfection for all three waves and not only waves from the UV spectrum (natural sunlight). The amount of dose needed to inactivate *E. coli* at different depth profiles, even for the 10 cm profile, were much higher than those reported in literature, which are mainly based on UV-C emitted by lamps.

Studies on the vertical profile produced promising results, based on work carried out together with another PhD student (Ricardo Gomes Passos) in the second pond. Stratification occurred in the second pond and produced two distinct layers. This was endorsed by differences in turbidity from the three different depth profiles, explicitly showing the separation of the layers. Three vertical baffles were later installed in the first channel of the second pond, and produced the desired results by creating mixed conditions and further promoting disinfection by increasing *E. coli* exposure from the bottom layers to the top layers and therefore to UV-A and UV-B. In fact, results with the vertical baffles improved significantly and impacted on overall treatment results for the treatment line. This confirmed the fifth hypothesis that stratification influences disinfection in ponds, and consequently the sixth hypothesis that vertical baffles would assist in destratifying the liquid layer and enhancing disinfection.

After extensive monitoring of the treatment line, solar irradiance depth profiling, *E. coli* disinfection depth profiling and upgrading hydrodynamics in two phases, the interventions were beneficial for the overall treatment line. Depth profiling of *E. coli* disinfection opened new insights on the influence that depth and daily periods (morning and afternoon) had, as well as the applied and received doses of solar irradiance (UV-A, UV-B and PAR) from different depths, which until now had not been reported.

8. RECOMMENDATIONS

For future research, it is recommended to:

1. Monitor different depths and if possible all depths at the same time, this way guaranteeing that all samples receive the same amount of solar radiation and possess the same pH and DO levels;
2. Carry out depth profiling of disinfection considering the additional removal mechanism of predation, by filtering samples and thus removing higher-order organisms;
3. Further investigate the hydrodynamics of ponds to increase disinfection by altering established flow patterns, horizontally and vertically;
4. Insert more vertical baffles in strategic points in the second pond to evaluate the true overall effect of them in terms of breaking stratification and improving disinfection.

9. REFERENCES

- ADAM, J. M. Investigation of Rock Filters in Northwestern Illinois. *In the 7th Annual Conference, Illinois Water Pollution Control Association*, June 24-26, 1986.
- AGUNWAMBA, J. C. Simplified optimal design of wastewater stabilization pond. *Wat. Air, Soil, Pollu.* **59**(3/4), 299-309, 1991.
- AGUNWAMBA J. C.; EGBUNIWE N.; ADEMILUYI J.O. Prediction of the Dispersion Number in Waste Stabilization Ponds. *Water Research* **21**(1), p. 85±89, 1992.
- AL-JUBOORI, R., ARAVINTHAN, V. and YUSAF, T. A review of Common and Alternative Methods for Disinfection of Microorganisms in Water. In: *Proceedings of the 2010 Southern Region Engineering Conference (SREC 2010)*. Engineers Australia, p. F3-1, 2010.
- ALMASI, A. and PESCOD M. B. Pathogen removal mechanisms in anoxic waste stabilization ponds. *Wat. Sci. Tech.* **33**(7), 133 – 140, 1996.
- ANSA, E. D. O., LUBBERDING, H. J., AMPOFO, J. A., and GIJZEN, H. J. The role of algae in the removal of *Escherichia coli* in a tropical eutrophic lake. *Ecological Engineering*, **37**(2), 317–324, 2011.
- APHA. AWWA. WEF. *Standard methods for the examination of water and wastewater*. Washington, D.C.: American Public Health Association. American Water Works Association, Water Pollution Control Federation, 2005.
- ARAÚJO, F., LIMA, W. R. de, BECKER, V., ARAÚJO, A. L. C. & CAMARGO-VALERO M. A. Occurrence of cyanobacteria and microcystins in waste stabilization ponds in northeast of Brazil. In: *11th IWA Specialist Group Conference on Wastewater Pond Technologies*, University of Leeds, Leeds, England, United Kingdom, 21 – 23 March, 2016.
- ACHER, A., FISCHER, E., TURNHEIM, R. and MANOR, Y. Ecologically friendly wastewater disinfection techniques. *Water research*, **31**(6), 1398-1404, 1997.
- ASSUNÇÃO, F. A. L. & VON SPERLING, M. Importance of the ammonia volatilization rates in shallow maturation ponds treating UASB reactor effluent. *Water Sci. Technol.* **66**(6), 1239–1246, 2012.
- ATLAS, R. M. and BARTHA, R. *Microbial ecology: Fundamentals and applications*. Addison-Wesley Publishers Co. London, 1981, 560p.
- AUER, M. T. and NIEHAUS, S. L. Modelling faecal coliform bacteria: Part I - Field and laboratory determination of loss kinetics. *Wat. Res.* **27**(4), 693-701, 1993.
- AWUAH, E. *Pathogen removal mechanisms in macrophyte and algal waste stabilization ponds*. 2006. 147 p. PhD dissertation (PhD in Sanitation) UNESCO-IHE, Delft, The Netherlands, 2006.
- BALOGH, V.K., NÉMETH, B., and VÖRÖS, L. Specific attenuation coefficients of optically active substances and their contribution to the underwater ultraviolet and visible light climate in shallow lakes and ponds. *Hydrobiologia*, v. 632, n. 1, p. 91–105, 2009.
- BARZILY, A. and KOTT, Y. Survival of pathogenic bacteria in an adverse environment. *Water Science and Technology*. **24**(2), 395-400, 1991.

- BASTOS, R. K. X., CALIJURI, M. L., BEVILACQUA, P. D., RIOS, E. N., DIAS, E. H. O., CAPELETE, B. C., and MAGALHÃES, T. B. Post-treatment of UASB reactor effluent in waste stabilization ponds and in horizontal flow constructed wetlands: a comparative study in pilot scale in Southeast Brazil. *Water science and technology*, **61**(4), p. 995–1002, 2010.
- BASTOS, R. K. X., RIOS, E. N., BEVILACQUA, P. D., and ANDRADE, R. C. UASB-polishing ponds design parameters: contributions from a pilot scale study in southeast Brazil. *Water science and technology : a journal of the International Association on Water Pollution Research*, **63**(6), p. 1276–81, 2011.
- BITTON, G. *Wastewater microbiology*. Second Edition. New York: Wiley-Liss, 1999. 781 p.
- BLANCHETOT, A., HAJNSDORF, E., and FAVRE, A. Metabolism of transfer-Rna in near-ultraviolet illuminated *Escherichia-coli* – the transfer-Rna repair hypothesis. *European Journal of Biochemistry*. 139, 547-552, 1984.
- BLAUSTEIN, R. A., PACHEPSKY, Y., HILL, R. L., SHELTON, D. R., and WHELAN, G. *Escherichia coli* survival in waters: temperature dependence. *Water Research*, **47**(2), 569–78, 2013.
- BOLTON, N.F., CROMAR, N.J., HALLSWORTH, P., and FALLOWFIELD, H.J. A Review of the Factors Affecting Sunlight Inactivation of Micro-Organisms in Waste Stabilisation Ponds: Preliminary Results for Enterococci. *Water Science and Technology*, **61**(4), p. 885–90, 2010.
- BOLTON, N. F., CROMAR, N. J., BUCHANAN, N. A., and FALLOWFIELD, H. J. Variations in Sunlight Attenuation in Waste Stabilisation Ponds and Environmental Waters. In: *9th IWA Specialist Conference on Waste Stabilisation Ponds* Adelaide, South Australia, Australia, 1-3 August 2011a.
- BOLTON, N.; CROMAR, N.; BUCHANAN, A.; FALLOWFIELD, H.J. Mechanisms of sunlight inactivation of common microbial indicators in Waste Stabilisation Ponds. In: *9th IWA Specialist Group Conference on Waste Stabilization Pond - International Water Association*, Adelaide, South Australia, Australia, 1-3 August 2011b.
- BOSSHARD, F., RIEDEL, K., SCHNEIDER, T., GEISER, C., BUCHELI, M. and EGLI, T. Protein oxidation and aggregation in UVA irradiated *Escherichia coli* cells as signs of accelerated cellular senescence. *Environmental Microbiology*. 12, 2931-2945, 2010.
- BOWLES, D. S., MIDDLEBROOKS, E. J. and REYNOLDS, J. H. Coliform decay rates in waste stabilization ponds. *Journal of Water Pollution Control Federation*. **51**(1), 87-99. 1979.
- BRACHO, N. R, LLOYD, B. and ALDANA, G. J. Plug flow can be induced in maturation ponds by increasing the l/w ratio. In: *8th IWA Specialist Group Conference on Waste Stabilization Ponds - International Water Association*, Belo Horizonte, Minas Gerais, Brazil, 26-30 April 2009.
- BRACHO, N.R; LLOYD, B.; ALDANA, G.J. Optimisation of hydraulic performance to maximise faecal coliform removal in maturation ponds. *Water Research*, **40**(8) p. 1677–1685, 2006.
- BUCHANAN, A., CROMAR, N., BOLTON, N. and FALLOWFIELD, H.J. The *E.coli* Removal Performance of Two Waste Stabilisation Ponds in the Barossa Valley region of South Australia. In: *9th IWA Specialist Group Conference on Waste Stabilization Pond - International Water Association*, Adelaide, South Australia, Australia, 1-3 August 2011.

- CAMARGO-VALERO, M. A., MARA, D. D. and NEWTON, R. J. Nitrogen removal in maturation waste stabilisation ponds via biological uptake and sedimentation of dead biomass. *Water Sci. Technol.* **61**(4), 1027–1034, 2010.
- CASLAKE, L. F., CONNOLLY, D. J., MENON, V., DUNCANSON, C. M., ROJAS, R. and TAVAKOLI, J. Disinfection of contaminated water by using solar irradiation. *Applied and Environmental Microbiology*, **70**(2), 1145-1151, 2004.
- CHERNICHARO C. A. L., CASTRO J. C. S., ZERBINI A. M. and GODINHO V. M. Inactivation of *E. coli* and helminthes eggs in aerobic and anaerobic effluents using UV radiation. *Water Science Technology* 47: 185-192, 2003.
- CHERNICHARO, C. A. L. *Anaerobic Reactors*. 1st ed. Belo Horizonte: International Water Association, 2007. p. 188.
- CHENG, L., KELLOGG, E.W. and PACKER, L. Photoinactivation of catalase. *Photochemistry and Photobiology*. **34**, 125-129, 1981.
- COUNCIL OF EUROPEAN COMMUNITIES. Council Directive of 21st May 1991 concerning urban waste water treatment (91/271/EEC). Official Journal of the European Communities, No. L 135/40, 1991.
- CRAGGS, R. J., ZWART, A., NAGELS, J. W. and DAVIES-COLLEY, R. J. Modelling sunlight disinfection in a high rate pond, *Ecological Engineering*. **22**, 113–122, 2004.
- CRAGGS, R. Chapter 5: Nutrients. In: Shilton, A. (Ed.), *Pond Treatment Technology*. IWA Publishing, London, 2005. p. 496.
- CRITES, R. W., MIDDLEBROOKS, E. J, BASTIAN, R. K. and REED, S. C. 2nd edition. *Natural Wastewater Treatment Systems*. CRC Press, 2014. p. 549.
- CURTIS T. P. *The mechanisms of removal of faecal coliforms from waste stabilization ponds*. 1990. PhD. thesis, University of Leeds, 1990.
- CURTIS, T. P., MARA, D. D., DIXO, N. G. H. and SILVA, S.A. Light Penetration in Waste Stabilization Ponds. *Water Research*, **28**(5), p. 1031–1038, 1994.
- CURTIS T. P., MARA D. D., and SILVA S. A. Influence of pH, oxygen, and humic substances on ability of sunlight to damage faecal coliforms in waste stabilization pond water. *Applied Environmental Microbiology*. 58, 1335-1343. 1992a.
- CURTIS, T. P., MARA, D. D., SILVA, S. A. The Effect of Sunlight on Faecal Coliforms in Ponds: Implications for Research and Design. *Water Science & Technology*, **26**(7-8), p. 1729–1738, 1992b.
- DA COSTA, R. H. R., GOMES, M. C. R. L. and FILHO, P. B. Maturation Pond and Rock Filter For Post-Treatment of Facultative Pond Treating Piggery Wastewater. In: *9th IWA Specialist Group Conference on Waste Stabilisation Ponds – International Water Association*, Adelaide, SA, Australia, 1-3 August 2011.
- DAVIES, C. M. and BAVOR, H. J. The fate of stormwater-associated bacteria in constructed wetland and water pollution control pond systems. *Journal of Applied Microbiology*, **89**(2), 349-360, 2000.
- DAVIES, C. M. and EVISON, L. M. Sunlight and the survival of enteric bacteria in natural waters. *Journal of Applied Microbiology*, **70**, 265-274, 1991.

- DAVIES-COLLEY R.J., SPEED, D.J., ROSS, C.M. and NAGELS, J.W. Inactivation of faecal indicator micro-organisms in waste stabilisation ponds: interactions of environmental factors with sunlight. *Water Research*, **33**(5) p. 1220–1230, 1999.
- DAVIES-COLLEY, R. J., DONNISON, A. M., and SPEED, D. J. Towards a mechanistic understanding of pond disinfection. *Water Science and Technology*, **42**(10), p. 149–158, 2000.
- DE LANGE, H. J. The attenuation of ultraviolet and visible radiation in Dutch inland waters. *Aquatic Ecology*, **34**, 215–226, 2000.
- DIAS, D. F. C., POSSMOSER-NASCIMENTO, T. E., RODRIGUES, V. A. J., and VON SPERLING, M. Overall performance evaluation of shallow maturation ponds in series treating UASB reactor effluent: Ten years of intensive monitoring of a system in Brazil. *Ecological Engineering*, **71**, 206–214, 2014.
- DIAS, D. F. C., PASSOS, R. G., RODRIGUES, V. A. J., MARTINS, L. J., and VON SPERLING, M. Desempenho de sistema de tratamento de esgoto para pequenas comunidades composto por reator UASB, lagoas de polimento em série (lagoa sem chicana e lagoa com chicana) e filtro grosseiro de pedra. In: *28th Congresso Brasileiro de Engenharia Sanitária e Ambiental – Associação Brasileira de Engenharia Sanitária (ABES)*, Rio de Janeiro, RJ, Brazil, 4-8 October 2015.
- EISENSTARK, A., SCANDALIOS, J. G., WRIGHT, T. R. F., and SCANDALIOS, J.G. Bacterial genes involved in response to near-ultraviolet radiation. In: *Advances in Genetics*. Academic Press, 1989.
- FADEL, R., BARAKAT, R. M. and FADEL, H. A. The Egyptian experience in dealing with waste stabilization ponds. In: *9th IWA Specialist Group Conference on Waste Stabilization Ponds*. Adelaide, Australia, 1 - 3 August 2011.
- FAVRE, A., HAJNSDORF, E., THIAM, K. and DEARAUJO, A.C. Mutagenesis and growth delay induced in *Escherichia coli* by near-ultraviolet radiations. *Biochimie* **67**, 335-342, 1985.
- FEACHEM, R. G., BRADLEY, D. J., GARELICK, H. and MARA, D. D. *Sanitation and Disease: Health Aspects of Excreta and wastewater management*. Published for the World Bank by John Wiley and Sons, U.K, 1983.
- FERNANDEZ, A., TEJEDOR, C. and CHORDI, A. Influence of pH on the elimination of faecal coliform bacteria in waste stabilization ponds. *Water Air Soil Pollution*. **63**(3-4), 317-320, 1992a.
- FERNANDEZ, A., TEJEDOR, C., and CHORD, A. Effect of different factors on the die-off of faecal bacteria in a stabilization pond purification plant. *Water Research*. **26**(8), 1093-1098, 1992b.
- FERRARA, R. A. AND HARLEMAN, D. R. F. Dynamic nutrient cycle model for waste stabilization ponds. *Journal of Environmental Engineering Division. ASCE 107(EE4)*, 817-830, 1981.
- FERRARA, R. A., and AVCI, C. B. Nitrogen dynamics in waste stabilization ponds. *Journal of Water Pollution Control Federation*. **4**(54), 361–369, 1982.
- FLETCHER M. M. *Bacteria Adhesion: molecular and ecological diversity*. New York: Wiley-Liss Inc, 1996. p. 371.

- FUJIOKA, R. S., HASHIMOTO, H. H., SIWAK, E. B., and YOUNG, R. H. F. Effect of sunlight on survival of indicator bacteria in seawater. *Applied Environmental Microbiology* **41**, 690-696, 1981.
- FURTADO, A. L. F. F., DO CARMO CALIJURI, M., LORENZI, A. S., HONDA, R. Y., GENUÁRIO, D. B. & FIORE, M. F. Morphological and molecular characterization of cyanobacteria from a Brazilian facultative wastewater stabilization pond and evaluation of microcystin production. *Hydrobiologia*, **627**(1), 195-209, 2009.
- GAMESON, A. L. H. and GOULD, D. J. *Investigation of Sewage Discharges to some British Coastal Waters*. Chapter 8 Bacterial Mortality, Part II. Water Research Centre Technical Report No. 222, Steven age, U.K, 1985.
- GANN, J. D., COLLIER, R. E. and LAWRENCE C. H. Aerobic bacteriology of waste stabilisation ponds. *Journal of Water Pollution Control Federation*. **40**(2), 185-191, 1968.
- GANNON, J. J., BUSSE, M. K. and SCHILLINGER, J. E. Faecal coliform disappearance in a river impoundment. *Water Research*, **17**(11), 1595-1601, 1983.
- GARCIA-PICHEL, F. A model for internal self-shading in planktonic organisms and its implications for the usefulness of ultraviolet sunscreens. *Association for the Sciences of Limnology and Oceanography*, **39**,1704–1717, 1994.
- GERSBERG, R., BRENNER, R., LYON, S., and ELKINS B. Survival of bacteria and viruses in municipal wastewater applied to artificial wetlands. In: Reddy K and Smith W (eds.) *Aquatic plants for wastewater treatment using artificial wetlands*. Orlando Florida: Magnolia, 1987. p. 237-245.
- GLOYNA, E. F. *Waste Stabilization Ponds*, Monograph Series No. 60, World Health Organization, Geneva, Switzerland, 1971.
- GODINHO, V. M., NASCIMENTO, F. M., SILVA, S. Q., VON SPERLING, M. Characterization of pathogenic bacteria in a UASB- polishing pond system using molecular techniques. *Water Science and Technology*, **61**(3), p. 813-9, 2010.
- GONÇALVES, H. R. R, SILVEIRA, D. A, MONTEGGIA, L. O, BASSEGGIO, G., and MIRANDA, L. A. Análise do desempenho de sistema integrado, enfatizando lagoa de polimento, tratando efluentes domésticos em condições de variações de temperatura. In: *8th IWA Specialist Group Conference on Waste Stabilization Ponds*, Belo Horizonte, Brazil, 26 – 30 Abril 2009.
- GRACY, R. W., TALENT, J. M., KONG, Y. and CONRAD, C. C. Reactive oxygen species: the unavoidable environmental insult? *Mutation Research*. **428**, 17–22, 1999.
- GRIMASON, A. M., SMITH, H. V., YOUNG, G. and THITAI, W. N. Occurrence and removal of *Ascaris sp.* Ova by waste stabilization ponds in Kenya. *Water Science and Technology*. **33**(7), 75-82, 1996a.
- GRIMASON, A. M., WIANDT, S., BALEUX, B., THITAI, W. N., BONTOUX, J. and SMITH, H. V. Occurrence and removal of *Giardia sp.* cysts by Kenyan and French waste stabilization pond systems. *Water Science and Technology*. **33**(7), 83-89, 1996b.
- GUEYMARD, C. (2001). Parameterized Transmittance Model for Direct Beam and Circumsolar Spectral Irradiance. *Solar Energy* (71:5); pp. 325–346, 2001.

- GUEYMARD, C. *SMARTS, A Simple Model of the Atmospheric Radiative Transfer of Sunshine: Algorithms and Performance Assessment*. Professional Paper FSEC-PF-270-95. Florida Solar Energy Center, 1679 Clearlake Rd., Cocoa, FL 32922, 1995.
- HAAG, W. R. and HOIGNE, J. Singlet oxygen in surface waters. 3. Photochemical formation and steady-state concentrations in various types of waters. *Environmental Science and Technology*. **17**(2), 65–71, 1986.
- HAAS. C. N. Wastewater disinfection and infectious disease risks. *CRC Critical Reviews in Environmental Control*, **17**, 1-20, 1986.
- HARM W. Dark repair of photorepairable UV lesions in *Escherichia coli*. *Mutation Research*. **6**, 25-35, 1968.
- HARTLEY, W. R., and WEISS C.M. Light intensity and the vertical distribution of algae in tertiary oxidation ponds. *Water Research* **4**(11): 751-763, 1970.
- HAWLEY, A. L. and FALLOWFIELD, H. J. Inclusion of pond walls to enhance solar exposure and pathogen removal. In: *11th IWA Specialist Group Conference on Wastewater Pond Technologies*, University of Leeds, Leeds, England, United Kingdom, 21 – 23 March, 2016.
- HOERTER, J.D., ARNOLD, A.A., KUCZYNSKA, D.A., SHIBUYA, A., WARD, C.S., SAUER, M.G., GIZACHEW, A., HOTCHKISS, T.M., FLEMING, T.J., JOHNSON, S. Effects of sublethal UVA irradiation on activity levels of oxidative defense enzymes and protein oxidation in *Escherichia coli*. *Journal of Photochemistry and Photobiology B: biology* **81**, 171-180, 2005.
- HOLZINGER, A., and LÜTZ, C. Algae and UV irradiation: effects on ultrastructure and related metabolic functions. *Micron*, **37**(3), 190–207, 2006.
- IMLAY, J. A. Pathways of oxidative damage. In: *Annual Review of Microbiology*, **57**, 395-418, 2003.
- ISO 21348. Definitions of Solar Irradiance Spectral Categories. Environment, (section 5), 6–7.
- JACK, U.; DE SOUZA, P.; SNYMAN, H. Waste stabilisation ponds Management, Operations and Maintenance Tools. In: *8th IWA Specialist Group Conference on Waste Stabilization Ponds*, Belo Horizonte, Brazil, 26 – 30 April 2009.
- JAGGER, J. *Solar-UV Action on Living Cells*. New York: Praeger, 1985. pp. 202.
- JAMES, A. An Alternative Approach to the Design of Waste Stabilization Ponds. *Water Science and Technology*, **19**(12), p. 213 – 218, 1988.
- JOUX F., JEFFREY W. H., LEBARON P., and MITCHELL D. L. Marine bacterial isolates display diverse responses to UV-B radiation. *Applied Environmental Microbiology*, **65**, 3820–3827, 1999.
- KADIR, K., and NELSON, K. L. Sunlight mediated inactivation mechanisms of *Enterococcus faecalis* and *Escherichia coli* in clear water versus waste stabilization pond water. *Water Research*, **50**, 307–17, 2014.
- KANEKO, M. Virus removal by domestic wastewater treatment system. *Water Science Technology*. **35** (11/12), 187-195, 1997.
- KAYOMBO, S., MBWETTE, T. S. A., MAYO, A. W., KATIMA, J. H. Y. and JORGENSEN, S. E. Diurnal cycles of variation of physical–chemical parameters in waste stabilization ponds. *Ecol. Eng.* **18**(3), 287–291, 2002.

- KILANI, J.S and OGUNROMBI, J.A. Effects of Baffles on the Performance of Model Waste Stabilization Ponds. *Water Research*, **18**(8), p. 941–944, 1984.
- KIRK, J. T. O. *Light and Photosynthesis in Aquatic Ecosystems*, Second Edition, Cambridge Univ. Press, 1994, 509 p.
- KLOCK, J. W. Survival of coliform bacteria in wastewater lagoons. *Journal of Water Pollution Control Federation*. **50**(11), 2071-2083, 1971.
- KOHN, T. and NELSON, K.L. Sunlight-mediated inactivation of MS2 coliphage via exogenous singlet oxygen produced by sensitizers in natural waters. *Environmental science and Technology*, **41**(1), p. 192–7, 2007.
- KOHN, T., GRANDBOIS, M., MCNEILL, K. and NELSON, K. L. Association with natural organic matter enhances the sunlight-mediated inactivation of MS2 coliphage by singlet oxygen. *Environmental Science and Technology*, **41**(13), 4626–32, 2007.
- KOTUT, K., BALLOT, A., WIEGAND, C. and KRIENITZ, L. Toxic cyanobacteria at Nakuru sewage oxidation ponds—a potential threat to wildlife. *Limnologica-Ecology and Management of Inland Waters*, **40**(1), 47-53, 2010.
- LARSEN, M. N. and ROEPSTORFF, A. Seasonal variation in development and survival of *Ascaris suum* and *Trichuris suis* eggs on pastures. *Parasitology*. **119**, 209-220, 1999.
- LEITE, V.D., ATHAYDE JR, G.B., DE SOUSA, J.T., LOPES, W.S. and HENRIQUE, I.N. Treatment of domestic wastewater in shallow waste stabilization ponds for agricultural irrigation reuse. *Journal of Urban and Environmental Engineering*, **3**(2), 2009.
- LEGENDRE, P., BALEUX, B. and TROUSSELLIER, M. Dynamics of pollution-indicator and heterotrophic bacteria in sewage treatment lagoons. *Applied Environmental Microbiology*. **48**, 486-593, 1984.
- LILTVED, H. and LANDFOLD, B. Influence of liquid holding recovery and photoreactivation on survival of ultraviolet-irradiated fish pathogenic bacteria. *Water Research*. **30**, 1109-1114, 1996.
- LIU, L., HALL, G. and CHAMPAGNE, P. Effects of Environmental Factors on the Disinfection Performance of a Wastewater Stabilization Pond Operated in a Temperate Climate. *Water*, **8**(1), 5, 2015.
- LLOYD, B. J., VORKAS, C. A. and GUGANESHARAJAH, R. K. Reducing hydraulic short-circuiting in maturation ponds to maximize pathogen removal using channels and wind breaks. *Water Science and Technology*, **48**(2), p. 153–62, 2003.
- MAÏGA, Y.; DENYIGBA, K.; WETHE, J.; OUATTARA, A.S. Sunlight Inactivation of *Escherichia coli* in Waste Stabilization Microcosms in a Sahelian Region (Ouagadougou, Burkina Faso). *Journal of Photochemistry and Photobiology*, **94**(2) p. 113–9, 2009a.
- MAÏGA, Y.; WETHE, J.; DENYIGBA, K.; OUATTARA, A.S. The Impact of Pond Depth and Environmental Conditions on Sunlight Inactivation of *Escherichia coli* and Enterococci in Wastewater in a Warm Climate. *Canadian Journal of Microbiology*, **55**, p. 1364–1374, 2009b.
- MANAGE, P. M., KAWABATA, Z., NAKANO, S. and NISHIBE, Y. Effect of heterotrophic nanoflagellates on the loss of virus-like particles in pond water. *Ecological Research*, **17**, 473-479, 2002.

- MARA D. D., ALABASTER G. P., PEARSON H. W. and MILLS S. W. *Waste Stabilization Ponds: a Design Manual for Eastern Africa*. Lagoon Technology International, Leeds, 1992.
- MARA, D. D. Waste stabilization ponds: Effluent quality requirements and implications for process design. *Water Science and Technology*, **33**(7), p. 23–31, 1996.
- MARA, D. D. and PEARSON, H. W. Artificial freshwater environments: waste stabilization ponds. In: *Biotechnology*, ed. W. Schoernborn, 1986. p. 177-206.
- MARA, D. D. *Domestic wastewater treatment in developing countries*. London: Earthscan, 2003. p. 293.
- MARAIS, G. V. R. Faecal bacterial kinetics in stabilisation ponds. *Journal of the Environmental Engineering*. Division ASCE 115: p. 119 – 139, 1974.
- MARAIS, G. V. R. and SHAW, V. A. A rational theory for the design of sewage stabilization ponds in central and South Africa. *Transactions of the South African Institution of Civil Engineering*. **13**(11), 205-227, 1961.
- MATALLANA-SURGET, S., MEADOR, J. A., JOUX, F., and DOUKI, T. Effect of the GC content of DNA on the distribution of UVB-induced bipyrimidine photoproducts. *Photochemical and Photobiological Science*. **7**, 794–801, 2008.
- MAYNARD, H. E., OUKI, S. K., and WILLIAMS S. C. Tertiary Lagoons: A review of removal mechanisms and performance. *Water Research*. **33**, 1 – 13, 1999.
- MAYO, A. W. Effect of Pond Depth on Bacterial Mortality Rate. *Environmental Engineering*, **115**(5), p. 964–977, 1989.
- MAYO, A. Modelling Coliform Mortality in Waste Stabilization Ponds. *Journal of Environmental Engineering*, **121**(2), p. 140–152, 1995.
- MAYO, A. W., and NOIKE, T. Response of mixed cultures of *Chlorella vulgaris* and heterotrophic bacteria to variation of pH. *Water, Science and Technology*. **30**(8), 285-294, 1994.
- MAYO, A. W., and NOIKE, T. (1996). Effects of temperature and pH on the growth of heterotrophic bacteria in waste stabilization ponds. *Water Research*. **30**, 447-455, 1996.
- MENDONCA, A. F., AMOROSO, T. L. AND KNABEL, S. J. Destruction of gram-negative food-borne pathogens by high pH involves disruption of the cytoplasmic membrane. *Applied and Environmental Microbiology*, **60**(11), 4009–4014, 1994.
- METCALF and EDDY, Inc. *Wastewater Engineering: Treatment and Resource Recovery*. 5th Edition. New York: Mc Graw-Hill, 2013. p. 2048.
- MEZRIOUI, N., and BALEUX, B. Effet de la température du pH et du rayonnement solaire sur la vie de différentes bactéries d'intérêt sanitaire dans une eau usée épurée par lagunage (Effect of temperature pH and solar radiation on sanitary bacteria in wastewater treated by waste stabilization pond), *Rev. Science and Water*. **5**, 573–591, 1992.
- MEZRIOUI N. E., OUDRA B., OUFDOU K., HASSANI L., LOUDIKI M. and DARLEY J. Effect of micro-algae growing on wastewater batch culture on *Escherichia coli* and *Vibrio cholerae* survival. *Water, Science and Technology*. **30**(8), 295-302, 1994.
- MEZRIOUI, N., OUFDOU, K. and BALEUX, B. Dynamics of non-01 *Vibrio cholerae* and faecal coliforms in experimental stabilization ponds in the arid region of Marrakesh, Morocco, and the effect of pH, temperature, and sunlight on their experimental survival. *Canadian Journal of Microbiology*. **41**(6), 489-498, 1995.

- MEZRIOUI N. E. and OUDRA B. Dynamics of picoplankton and microplankton flora in the experimental wastewater stabilization ponds of the arid region of Marrakech, Morocco and cyanobacteria effects on *Escherichia coli* and *Vibrio cholerae* survival. In: *Wastewater treatment with algae*, Wong Y-S and Tam N. F. Y. (eds). Springer-Verlag and Landes Bioscience, 1998, pp. 234.
- MIDDLEBROOKS, E. J. Review of rock filters for the upgrade of lagoon effluents. *Journal of Water Pollution Control Federation*, 60, 1657-1662, 1988.
- MILLS, S. W., AÇABASTER, G. P., MARA, D. D., PEARSON, H. W. and THITAI, W. N. Efficiency of Faecal Bacterial Removal in Waste Stabilisation Ponds in Kenya. *Water, Science and Technology*. **26**(7-8), 1739-1748, 1992.
- MITCHELL, R. *Environmental microbiology*. New York: Wiley-liss Inc, 1992. p. 411.
- MOELLER, J. R. AND CALKINS, J. Bactericidal agents in wastewater lagoons and lagoon design. *Journal Water Pollution Control Federation*, 2442-2451, 1980.
- MOUMOUNI, D. A., ANDRIANISA, H. A., KONATÉ, Y., NDIAYE, A. and MAÏGA, A. H. Inactivation of *Escherichia coli* in a baffled pond with attached growth: treating anaerobic effluent under the Sahelian climate. *Environmental technology*, 1-11, 2015.
- MUELA, A.; GARCÍA-BRINGAS, J.M.; SECO, C.; ARANA, I.; BARCINA, I. Participation of oxygen and role of exogenous and endogenous sensitizers in the photoinactivation of *Escherichia coli* by photosynthetically active radiation, UV-A and UV-B. *Microbial Ecology*, **44**(4), 354–64, 2002.
- NELSON, K. L., KADIR, K., FISHER, M. B., and LOVE, D. New insights into sunlight disinfection mechanisms in waste stabilization ponds. In: *8th IWA Specialist Group Conference on Waste Stabilization Ponds*, Belo Horizonte, Brazil, 26 – 30 Abril 2009.
- NGUYEN, M. T., JASPER, J. T., BOEHM, A. B. and NELSON, K. L. Sunlight inactivation of fecal indicator bacteria in open-water unit process treatment wetlands: Modeling endogenous and exogenous inactivation rates. *Water research*, **83**, 282-292, 2015.
- NOBLE, R. T., LEE, I. M. and SCHIFF, K. C. Inactivation of indicator micro-organisms from various sources of faecal contamination in seawater and freshwater. *Journal of Applied Microbiology*. **96**, 464-472, 2004.
- NOYOLA, A.; PADILLA-RIVERA, A.; MORGAN-SAGASTUME, J. M.; GUERECA, L. P. AND HERNANDEZ-PADILLA, F. Typology of municipal wastewater treatment technologies in Latin America. *Clean – Soil, Air, Water*, **40**(9), 926–932, 2012.
- OLUKANNI, D. O. and DUCOSTE, J. J. Optimization of Waste Stabilization Pond Design for Developing Nations using Computational Fluid Dynamics. *Ecological Engineering*, **37**(11), p. 1878–1888, 2011.
- ORAGUI J. I., CURTIS T. P., SILVA S. A. and MARA D. D. The Removal of excreted bacteria and viruses in deep waste stabilization ponds in Northeast Brazil. *Water, Science and Technology*. **18** (7/8), 31-35, 1986.
- ORAGUI J. I., CURTIS T., SILVA S. A. and MARA D. D. The removal of faecal coliforms in experimental waste stabilization pond systems with different geometries and configuration. *Water, Science and Technology*. **19** (3/4), 569-573, 1987.
- ORLOB, G. T. Viability of sewage bacteria in seawater. *Sewage and Industrial Wastes* **28**, 1147-1167, 1956.

- OUFDOU, K., MEZRIOUI, N., OUDRA, B., LOUDIKI, M., BARAKATE, M. and SBUYA, B.. Bioactive compounds from Pseudanabaena species (Cyanobacteria). *Microbios*, **106**, 21-29, 2001.
- OUALI, A., JUPSIN, H., GHRABI, A. & VASEL, J. L. Removal kinetic of *Escherichia coli* and *enterococci* in a laboratory pilot scale wastewater maturation pond. *Water Science and Technology*. **69**(4), 755–9, 2014.
- PAERL, H.W. & HUISMAN, J. Blooms like it hot. *Science* (80-.). **320**, 57–58, 2008.
- PAERL, H. W. & OTTEN, T. G. Harmful cyanobacterial blooms: causes, consequences, and controls. *Microbial Ecology*, **65**(4), 995-1010, 2013.
- PAERL H. W., BLAND P. T., DEAN BOWLES N. and HAIBACH M. E. Adaptation to high intensity, low wavelength light among surface blooms of the cyanobacterium *Microcystis aeruginosa*. *Applied Environmental Microbiology*. **49**, 1046-1052, 1985.
- PACHEPSKY, Y. A., BLAUSTEIN, R. A., WHELAN, G., and SHELTON, D. R. Comparing temperature effects on *Escherichia coli*, *Salmonella*, and *Enterococcus* survival in surface waters. *Letters in Applied Microbiology*, **59**(3), 278–83, 2014.
- PALMER, C. M. A composite rating of algae tolerating organic pollution. *Journal of Phycology*. **5**, 78-82, 1969.
- PANO, A. and MIDDLEBROOKS, E.J. Ammonia nitrogen removal in facultative wastewater stabilisation ponds. *Journal Water Pollution Control Federation* **54**: 344 – 351, 1982.
- PAPADOPOULOS, F. H., TSIHRINTZIS, V. A. and ZDRAGAS, A. G. Removal of faecal bacteria from septage by treating it in a full-scale duckweed-covered pond system. *Journal of Environmental Management*, **92**(12), 3130–5, 2011.
- PARHAD, N. M., and RAO, N. U. Effect of pH on survival of *Escherichia-coli*. *Water Pollution Control Federation*, **56**(5), 980-986, 1974.
- PASSOS, R. G. and VON SPERLING, M. Avaliação da ocorrência de estratificação térmica em lagoas de polimento rasas para pequenas comunidades. In: *28th Congresso Brasileiro de Engenharia Sanitária e Ambiental – Associação Brasileira de Engenharia Sanitária (ABES)*, Rio de Janeiro, Rio de Janeiro, Brazil, 4-8 October 2015.
- PASSOS, R. G., DIAS, D. F. C., RODRIGUES, V. A. J. and VON SPERLING, M. Thermal stratification and destratification in shallow maturation ponds with different operational configurations and periods of the year. Submitted to *Ecological Engineering*, 2016.
- PEARSON, H. W., MARA D. D., MILLS S. W. and SMALLMAN D. J. Factors determining algal populations in waste stabilization ponds and influence on algae pond performance. *Water, Science and Technology*. **19**(12), 131-140, 1987a.
- PEARSON, H. W., MARA, D. D., MILLS, S. W., and SMALLMAN, D. J. Physico-chemical parameters influencing faecal bacterial survival in waste stabilization ponds. *Water Science and Technology*. **19**(12), 145-152, 1987b.
- PEARSON, H. W., MARA, D. D. and ARRIDGE, H. A. The influence of Pond Geometry and Configuration on Facultative and Maturation Waste Stabilisation Pond Performance and Efficiency. *Water Science and Technology*. **31**(12), 129-139, 1995.

- PEARSON H. W., MARA D. D., CAWLEY L. R., ARRIDGE H. M. and SILVA S. A. The performance of an innovative tropical experimental waste stabilization pond system operating at high organic loadings. *Water Science and Technology*. **33**(7), 63 – 73, 1996.
- POLPRASERT, C., DISSANAYAKE, M. G. and THANH, N. C. Bacterial die-off kinetics in waste stabilisation ponds. *Journal of Water Pollution Control Federation*. **55**, 285-296, 1983.
- POLPRASERT, C. and BHATTARAI, K. K. Dispersion Model for Waste Stabilisation Ponds. *Journal of Environmental Engineering Division, ASCE*, **111**, p.45, 1985.
- PÖPEL, H. J. *Aeration and gas transfer*. 2nd ed. Delft, Delft University of Technology, 1979, p. 169.
- PORTIER, R., and PALMER, S. Wetlands microbiology: Form, function, process. In: *Constructed wetlands for wastewater treatment: Municipal, industrial and agricultural*. Hammer DA (ed). Chelsea, Michigan: Lewis publishers, 1989. p. 89-106.
- POSSMOSER-NASCIMENTO, T. E., RODRIGUES, V. A. J., VON SPERLING, M.. Acumulação e Distribuição Espacial do Lodo em um Sistema de Lagoas de Polimento em Série (Spatial Distribution and Accumulation of Sludge in a System of Polishing Ponds in Series). In: *27th Congresso Brasileiro de Engenharia Sanitária e Ambiental*, 15–19 September 2013, ABES—Associação Brasileira de Engenharia Sanitária, Goiânia, 2013.
- POSSMOSER-NASCIMENTO, T. E., RODRIGUES, V. A. J., VON SPERLING, M., VASEL, J. L. Sludge accumulation in shallow maturation ponds treating UASB reactor effluent: results after 11 years of operation. *Water Science and Technology*. **70**(2), 321–328, 2014.
- PRATT, R. and FONG, J. Studies on *Chlorella vulgaris*: Further evidence that *Chlorella* cells form a growth inhibiting substance. *American Journal of Botany*. **27**, 431-436, 1940.
- QASIM, S. R. *Wastewater treatment plants: planning, design and operation*. Holt, Rinehart and Winston, New York, 1985.
- QIANG, F. Radiation (Solar). *Elsevier Science*, 1859–1863, 2003.
- QIN, D., BLISS, P. J., BARNES, D. and FITZGERALD, P.A. Bacterial (Total Coliform) Die-Off in Maturation Ponds. *Water Science and Technology*, **23**(7-9) p. 1525 – 1534, 1991.
- RANGEBY M., JOHANSSON P. and PERNRUP M. Removal of faecal coliforms in a waste stabilization pond system in Mindelo, Cape Verde. *Water Science and Technology*. **34** (11), 149 – 157, 1996.
- REED, S.C. Nitrogen Removal in Wastewater Stabilization Ponds. *Journal of the Water Pollution Control Federation*, **57**(1), p. 39-45, 1985.
- REED, R. H. Solar inactivation of faecal bacteria in water: the critical role of oxygen. *Letters in Applied Microbiology*. **24**, 276–280, 1997.
- RODRIGUES, V. A. J., POSSMOSER-NASCIMENTO, T. E., DIAS, D. F. C., PASSOS, R. G., VON SPERLING, M., VASEL, J. L. Performance comparison between two equal stabilization ponds operating with and without sludge layer. *Water Science and Technology*, **71**(6), 929 – 937, 2015.
- RODRIGUES, V. A. J. *Sediment contribution in the removal of nitrogen from domestic sewage in polishing ponds*. p. 190. PhD thesis in sanitation. Post graduated programme in Sanitation, Environment and Water Resources. Federal University of Minas Gerais. Belo Horizonte, Minas Gerais, Brazil, 2016. (In Portuguese).

- RODRÍGUEZ-CHUECA, J., POLO-LÓPEZ, M. I., MOSTEO, R., ORMAD, M. P., and FERNÁNDEZ-IBÁÑEZ, P. Disinfection of real and simulated urban wastewater effluents using a mild solar photo-Fenton. *Applied Catalysis B: Environmental*, **150-151**, 619–629, 2014.
- RUDOLPH, K-U., WEIL S. and FUCHS, L. Solar Radiation - Driver of Innovations in Pond Design and Process Technologies. In: *11th IWA Specialist Group Conference on Wastewater Pond Technologies*, University of Leeds, Leeds, England, United Kingdom, 21 – 23 March, 2016.
- RYER, A. D. *Light measurement handbook*. 2nd ed. Newburyport: Technical Publications International Light Inc., 1997. 64 p.
- SAIDAM, M. Y., RAMADAN, S. A., and BUTLER, D. Upgrading waste stabilization pond effluent by rock filter. *Water Science and Technology*, **31**(12), 369-378, 1995.
- SANTOS, A. B., MOTA, S., BEZERRA, F. M., and AQUINO, B.F. Fruits Produced with Wastewater Treated in Stabilization Ponds systems : Evaluation in a Quality Prospective In: *8th IWA Specialist Group Conference on Waste Stabilization Ponds*, Belo Horizonte, Brazil, 26 – 30 Abril 2009.
- SANTOS, A. L., OLIVEIRA, V., BAPTISTA, I., HENRIQUES, I., GOMES, N. C. M., ALMEIDA, A. and CUNHA, Â. Wavelength dependence of biological damage induced by UV radiation on bacteria. *Archives of Microbiology*, **195**(1), 63–74, 2013.
- SAQQAR, M. M. and PESCOD, M. B. Modelling Coliform Reduction in Wastewater Stabilization Ponds. *Water Science and Technology*, **26**(7-8), p. 1667–1677, 1992a.
- SAQQAR M. M. and PESCOD M. B. Modelling nematode egg elimination in wastewater stabilization ponds. *Water Science and Technology*. **26**(7-8), 1659-1665, 1992b.
- SARIKAYA, H. and SAATÇI, A. Bacterial Die-off in Waste Stabilization Ponds. *Journal of Environmental Engineering*, **113**(2), 366–382, 1987.
- SARIKAYA, H., SAATÇI, A. and ABDULFATTAH, A. Effect of Pond Depth on Bacterial Die-Off. *Journal of Environmental Engineering*, **113**(6), 1350–1362, 1987.
- SENZIA, M. A., MAYO, A. W., MBWETTE, T. S. A., KATIMA, J. H. Y. and JORGENSEN, S. E. Modelling nitrogen transformation and removal in primary facultative ponds. *Ecological Modelling*. 154, 207–215, 2002.
- SHILTON, A. *Studies into the Hydraulics of Waste Stabilisation Ponds*. 2001. p. 280. Thesis (PhD in Environmental Engineering) – Turitea Campus, Massey University, New Zealand, 2001.
- SHILTON, A. (Ed. 4). *Pond treatment technology*. IWA publishing, 2005. p. 496.
- SHILTON, A. and HARRISON, J. Integration of coliform decay within a CFD model of a waste stabilisation pond. *Water Science and Technology*. **48**(2), 205-210, 2003.
- SILVERMAN, A. I., PETERSON, B. M., BOEHM, A. B., MCNEILL, K., and NELSON, K. L. Sunlight inactivation of human viruses and bacteriophages in coastal waters containing natural photosensitizers. *Environmental Science and Technology*. **47**(4), 1870–8, 2013
- SILVERMAN, A. I., NGUYEN, M. T., SCHILLING, I. E., WENK, J., and NELSON, K. L.. Sunlight inactivation of viruses in open-water unit process treatment wetlands: modeling endogenous and exogenous inactivation rates. *Environmental science and technology*, **49**(5), 2757-2766, 2015.

- SINTON, L. W., HALL, C. H., LYNCH, P. A. and DAVIES-COLLEY, R. J. Sunlight Inactivation of Fecal Indicator Bacteria and Bacteriophages from Waste Stabilization Pond Effluent in Fresh and Saline Waters. *Applied and Environmental Microbiology*. **68**(3), 1122–1131, 2002.
- SMALLMAN, D. J. *An Ecological Appraisal of Waste Stabilization Pond Performance*. 1986. PhD thesis, School of Civil Engineering, University of Leeds, Leeds, 1986.
- STATE OF CALIFORNIA. *California Code of Regulations, Title 22, Division 4, Chapter 3: Water recycling criteria (Sections 60301–60357)*. Sacramento, CA, Office of Administrative Law, 2001.
- SUTHERLAND, J. C. and GRIFFIN, K. P. Absorption-spectrum of DNA for wavelengths greater than 300-Nm. *Radiation Research*. **86**, 399-410, 1981.
- SWEENEY, D. G., NIXON, J. B., CROMAR, N. J. and FALLOWFIELD, H. J. Temporal and spatial variations of physical, biological and chemical parameters in a large waste stabilisation pond, and the implications for WSP modelling. *Water Science and Technology*. **55**(11), 1–9, 2007.
- TARRÁN E. P. Desinfección por luz ultravioleta. *Revista Água Latinoamérica 2*: p.28- 35, 2002.
- THACKSTON, E. L., SHIELDS, D. and SCHROEDER, P. R. Residence Time Distributions of Shallow Basins. *Journal of Environmental Engineering*, **113**(6), 1319–1332, 1987.
- TOMS, I. P., OWENS, M., HALL J. A. and MINDENHALL, M. J. Observations on the performance of polishing lagoons at a large regional works. *Water Pollution Control*. **74**, 383-401, 1975.
- TORTORA, G. J., FUNKE, B. R. and CASE, C. L. *Microbiology: An introduction*. California: 8th Edition. Benjamin/Cumming Press, 2003. p. 944.
- TROUSSELLIER M., LEGENDRE P. and BALEUX B. Modelling of the evolution of bacterial densities in an eutrophic ecosystem (sewage lagoons). *Microbial Ecology*. **12**, 355-379, 1986.
- USEPA. *Design Manual: Municipal Wastewater Stabilization Ponds*, EPA 625/1-83-015, Center for Environmental Research Information, U.S. Environmental Protection Agency, Cincinnati, OH, 1983.
- VAN DER STEEN, P., BRENNER, A., SHABTAI, Y. & ORON, G. Improved faecal coliform decay in integrated duckweed and algal ponds. *Water Science and Technology*. **42** (10/11), 363-370, 2000.
- VASCONCELOS, V. M. and PEREIRA, E. Cyanobacteria diversity and toxicity in a wastewater treatment plant (Portugal). *Water Research*. **35**(5), 1354-1357, 2001.
- VERBYLA, M. E., and MIHELICIC, J. R. A review of virus removal in wastewater treatment pond systems. *Water research*, **71**, 107-124, 2015.
- VISSER, P. M., POOS, J. J., SCHEPER, B. B., BOELEN, P. and VAN DUUYL, F. C. Diurnal variations in depth profiles of UV-induced DNA damage and inhibition of bacterioplankton production in tropical coastal waters. *Marine Ecology Progress Series*. **228**, 25–33, 2002.
- VITAL, M., HAMMES, F. and EGLI, T. (2012). Competition of *Escherichia coli* O157 with a drinking water bacterial community at low nutrient concentrations. *Water research*, **46**(19), 6279-6290, 2012.

- VON SPERLING, M., BASTOS, R. K. X. and KATO, M. T. Removal of *E. coli* and helminth eggs in UASB: Polishing pond systems in Brazil. *Water Science and Technology*, **51**(12), 91–7, 2005.
- VON SPERLING, M. and DE ANDRADA, J.G.B. Simple wastewater treatment (UASB reactor, shallow polishing ponds, coarse rock filter) allowing compliance with different reuse criteria. *Water Science and Technology*, **54**(11), 199, 2006.
- VON SPERLING, M., DORNELAS, F. L., ASSUNÇÃO, F. A. L., DE PAOLI, A. C., and MABUB, M. O. A. Comparison between polishing (maturation) ponds and subsurface flow constructed wetlands (planted and unplanted) for the post- treatment of the effluent from UASB reactors. *Water Science and Technology*, **61**(5), 1201 – 1209, 2010.
- VON SPERLING, M., and MASCARENHAS, L. C. Performance of very shallow ponds treating effluents from UASB reactors. *Water Science and Technology*, **51**(12), p. 83–90, 2005.
- VON SPERLING, M. Performance evaluation and mathematical modelling of coliform die-off in tropical and subtropical waste stabilization ponds. *Water Research*, **33**(6), 1435–1448, 1999.
- VON SPERLING, M. *Introdução à qualidade das águas e ao tratamento de esgotos*. 3ª ed. Belo Horizonte: Departamento de Engenharia Sanitária e Ambiental – UFMG, 2005a. p. 452.
- VON SPERLING, M. *Waste Stabilisation Ponds*. Belo Horizonte: 1st. ed. International Water Association, 2007. p. 175.
- VON SPERLING, M. Modelling of coliform removal in 186 facultative and maturation ponds around the world. *Water Research*, **39**(20) p. 5261–73, 2005b.
- VON SPERLING, M. *Wastewater Characteristics, Treatment and Disposal*. Belo Horizonte: 1st. ed. International Water Association, 2008a. p. 304
- VON SPERLING, M. *Basic principles of wastewater treatment*. Belo Horizonte: 1st. ed. International Water Association, 2008b. p. 104
- VON SPERLING, M., DORNELAS, F. L., ASSUNÇÃO, F. A. L., DE PAOLI, A. C., and MABUB, M. O. A. Comparison between polishing (maturation) ponds and subsurface flow constructed wetlands (planted and unplanted) for the post- treatment of the effluent from UASB reactors. *Water Science & Technology*, **61**(5), 1201 – 1209, 2010.
- WEAVER, L., WEBBER, J., KARKI, N., THOMAS, K., MACKENZIE, M., LIN, S., INGLIS, A. and WILLIAMSON, W. Optimising wastewater ponds for effective pathogen removal. In: *11th IWA Specialist Group Conference on Wastewater Pond Technologies*, University of Leeds, Leeds, England, United Kingdom, 21 – 23 March, 2016.
- WHO. *International Programme on Chemical Safety Environmental Health: Criteria 160 Ultraviolet Radiation*. WHO, Geneva, 1994.
- WHO. *Global Solar UV Index - A Practical Guide*, WHO, Geneva, 2002.
- WHO (World Health Organisation). *Guidelines for the Safe Use of Wastewater, Excreta and Greywater*. Geneva: Volume 2: Wastewater Use in Agriculture. WHO, Geneva, 2006. p. 213.
- WILKINSON J., JENKIN A., WYER M. and KAY D. Modelling of faecal coliforms dynamics in streams and rivers. *Water Research*. **3**, 847-855, 1994.
- WHITMAN, R. L., PRZYBYLA-KELLY, K., SHIVELY, D. A., NEVERS, M. B., and BYAPPANAHALLI, M. N.. Sunlight, season, snowmelt, storm, and source affect *E. coli*

populations in an artificially ponded stream. *The Science of the Total Environment*, **390**(2-3), 448–55, 2008.

WHITLAM G. C. and CODD G. A. Damaging effects of light on microorganisms, *Spec. Publ. Soc. Gen. Microbiol.* 17, 129 – 169, 1986.

WU, S. and KLEIN, D. A. Starvation effect on *Escherichia coli* and aquatic bacteria to nutrient addition and secondary warming stresses. *Journal of Applied Environmental Microbiology*. **31**, 216-220, 1976.

YANEZ F. *Lagunas de estabilización. Teoría, diseño y mantenimiento*. Cuenca: ETAPA, Ecuador, 1993. p. 421.

ZEPP, R. G. Environmental photoprocesses involving natural organic matter. In: *Humic substances and their role in environments*. Frimmel FH and Christian RF (eds) Wiley Publishers, New York, 1988, pp. 193-214.

APPENDIX I

Parameter	Input	Unit
Site pressure	Varied for each hour and day	millibar
Altitude	0.852	km
Height	0	km
Atmosphere*	Tropical standard	
Water vapour	Calculated from reference atmosphere and altitude	
Columnar ozone abundance	Default from reference atmosphere	
Gaseous absorption and pollution	Default from reference atmosphere	
Carbon dioxide	370	ppmv
Extra-terrestrial spectrum*	Gueymard 2004	
Aerosol model*	Shettle & Fenn Urban	
Atmospheric turbidity	130	
Regional albedo	Meteorological range (km)	
Tilted surface and local albedo	Dry grass	
Spectral range	Bypass tilt calculations	
Solar constant	280 – 700	nm
Circumsolar calculations	1367	W.m-2
Extra scanning/smoothing	Bypass	
Extra illuminance calculations	Bypass	
Extra UV calculations	UV-A and UV-B	
Solar position	Latitude: - 19.9245	
	Longitude: - 43.9352	

*Recommended by SMARTS

APPENDIX II

Descriptive statistical analysis of overall total solar irradiance from July 2014 to November 2015.

Time	n	Arithmetic Mean (W.m ⁻²)	Median (W.m ⁻²)	Maximum (W.m ⁻²)	Minimum (W.m ⁻²)	25% quartile (W.m ⁻²)	75% quartile (W.m ⁻²)	CV
05:20:00	0	-	-	-	-	-	-	-
05:30:00	9	3.44	2.00	12.00	1.00	1.00	2.00	1.13
05:40:00	20	7.60	7.50	24.00	1.00	4.25	10.00	<u>0.74</u>
05:50:00	30	12.70	12.00	43.00	1.00	7.25	17.00	<u>0.64</u>
06:00:00	60	15.17	9.00	70.00	1.00	4.00	24.25	<u>0.95</u>
06:10:00	101	17.92	10.00	109.00	1.00	4.00	20.00	1.16
06:20:00	169	21.20	12.00	152.00	1.00	6.00	26.00	1.22
06:30:00	235	26.93	15.00	196.00	1.00	6.00	32.00	1.27
06:40:00	281	36.12	21.00	245.00	1.00	11.00	43.00	1.19
06:50:00	290	50.11	29.00	285.00	4.00	17.00	58.00	1.06
07:00:00	290	67.91	44.00	326.00	5.00	26.00	82.00	<u>0.94</u>
07:10:00	291	89.43	61.00	365.00	7.00	37.00	114.00	<u>0.84</u>
07:20:00	291	111.13	78.00	405.00	9.00	50.00	143.00	<u>0.78</u>
07:30:00	291	132.22	102.00	452.00	17.00	64.50	173.50	<u>0.71</u>
07:40:00	291	153.09	125.00	539.00	17.00	77.50	207.50	<u>0.67</u>
07:50:00	291	172.20	150.00	596.00	18.00	94.00	238.00	<u>0.63</u>
08:00:00	292	187.80	168.00	606.00	4.00	105.50	247.25	0.62
08:10:00	292	207.53	186.00	604.00	6.00	107.50	278.00	0.60
08:20:00	292	232.87	205.50	639.00	7.00	130.75	312.50	0.58
08:30:00	292	264.70	247.50	675.00	8.00	149.25	357.75	0.56
08:40:00	292	296.11	288.00	775.00	10.00	171.75	409.00	0.56
08:50:00	292	319.97	312.50	815.00	13.00	185.25	443.25	0.53
09:00:00	292	356.83	375.00	852.00	18.00	218.00	493.00	0.51
09:10:00	292	386.66	419.50	824.00	24.00	225.75	529.25	0.49
09:20:00	292	418.93	463.50	957.00	15.00	257.00	577.00	0.48
09:30:00	292	440.65	491.00	896.00	12.00	277.00	603.00	0.47
09:40:00	292	454.43	497.00	949.00	37.00	280.75	618.25	0.46
09:50:00	292	493.08	544.50	1028.00	33.00	310.75	663.25	0.45
10:00:00	291	523.60	559.00	1084.00	44.00	322.50	712.50	0.44
10:10:00	290	526.97	554.00	1009.00	58.00	332.50	720.75	0.45
10:20:00	290	549.42	597.50	1102.00	67.00	350.25	729.50	0.43
10:30:00	291	587.84	632.00	1056.00	58.00	395.00	787.00	0.43
10:40:00	291	595.01	662.00	1169.00	35.00	388.00	799.50	0.44
10:50:00	291	601.92	646.00	1136.00	51.00	373.50	823.00	0.45
11:00:00	290	617.39	677.50	1131.00	32.00	367.00	849.25	0.44
11:10:00	290	626.42	679.50	1125.00	36.00	376.50	887.75	0.44
11:20:00	290	643.33	683.50	1355.00	28.00	390.75	888.75	0.43
11:30:00	291	645.84	702.00	1131.00	28.00	378.00	906.00	0.44
11:40:00	290	635.24	678.00	1197.00	82.00	374.00	879.25	0.46
11:50:00	291	657.87	683.00	1253.00	62.00	389.00	908.50	0.43
12:00:00	291	650.06	680.00	1263.00	79.00	407.00	901.50	0.45
12:10:00	291	678.87	707.00	1266.00	79.00	437.00	913.00	0.41
12:20:00	291	662.70	685.00	1259.00	64.00	384.00	931.00	0.46
12:30:00	291	671.60	718.00	1237.00	50.00	415.50	909.50	0.43
12:40:00	291	687.07	758.00	1256.00	45.00	408.50	934.00	0.43
12:50:00	290	687.89	760.50	1200.00	48.00	402.25	937.75	0.43
13:00:00	289	660.67	729.00	1223.00	11.00	384.00	898.00	0.46
13:10:00	289	635.22	673.00	1142.00	7.00	366.00	874.00	0.48
13:20:00	289	648.72	693.00	1198.00	12.00	378.00	883.00	0.47

13:30:00	288	632.72	679.00	1205.00	32.00	368.75	871.75	<u>0.47</u>
13:40:00	288	643.67	689.00	1285.00	21.00	383.25	862.25	<u>0.48</u>
13:50:00	287	631.37	671.00	1306.00	18.00	378.50	837.50	<u>0.47</u>
14:00:00	288	616.85	638.50	1269.00	23.00	391.50	807.00	<u>0.47</u>
14:10:00	288	579.24	614.00	1254.00	25.00	337.00	764.00	<u>0.48</u>
14:20:00	288	555.63	573.50	1147.00	20.00	306.50	731.50	<u>0.50</u>
14:30:00	288	533.84	559.00	1170.00	18.00	289.75	691.25	<u>0.52</u>
14:40:00	287	515.29	522.00	1148.00	22.00	278.00	699.00	<u>0.54</u>
14:50:00	287	498.24	509.00	1109.00	10.00	260.00	643.00	<u>0.53</u>
15:00:00	287	477.75	475.00	1102.00	23.00	244.50	619.00	<u>0.55</u>
15:10:00	287	457.33	443.00	1168.00	23.00	238.50	592.50	<u>0.56</u>
15:20:00	287	431.09	421.00	1091.00	16.00	213.00	571.50	<u>0.58</u>
15:30:00	289	401.33	399.00	975.00	10.00	211.00	528.00	<u>0.57</u>
15:40:00	289	372.30	341.00	1013.00	3.00	199.00	491.00	<u>0.60</u>
15:50:00	289	353.43	327.00	943.00	11.00	182.00	439.00	<u>0.62</u>
16:00:00	287	322.89	289.00	980.00	1.00	167.00	401.50	<u>0.65</u>
16:10:00	286	286.63	246.50	906.00	14.00	137.00	357.75	<u>0.68</u>
16:20:00	287	273.10	224.00	803.00	5.00	115.00	337.50	<u>0.75</u>
16:30:00	286	236.48	196.00	780.00	9.00	77.50	298.50	<u>0.82</u>
16:40:00	286	198.03	132.50	701.00	12.00	61.00	256.75	<u>0.92</u>
16:50:00	283	168.41	100.00	678.00	9.00	39.50	236.50	1.03
17:00:00	284	140.50	67.50	636.00	4.00	31.00	189.50	1.11
17:10:00	281	127.33	53.00	573.00	3.00	26.00	171.00	1.20
17:20:00	279	104.77	40.00	568.00	1.00	18.00	153.00	1.30
17:30:00	266	96.73	30.00	512.00	1.00	12.00	119.75	1.39
17:40:00	220	95.65	34.00	482.00	1.00	11.00	126.50	1.29
17:50:00	172	96.66	42.00	393.00	1.00	12.00	151.25	1.16
18:00:00	144	92.34	59.50	366.00	1.00	17.75	129.75	1.09
18:10:00	122	91.34	64.00	331.00	1.00	18.00	119.25	<u>0.97</u>
18:20:00	108	78.31	59.00	264.00	1.00	21.00	107.25	<u>0.90</u>
18:30:00	97	65.90	50.00	223.00	2.00	28.00	87.00	<u>0.86</u>
18:40:00	92	52.76	36.00	174.00	1.00	21.75	71.00	<u>0.85</u>
18:50:00	87	41.00	29.00	130.00	1.00	14.50	59.50	<u>0.80</u>
19:00:00	82	25.39	23.50	90.00	1.00	10.25	38.00	<u>0.74</u>
19:10:00	64	18.98	15.50	55.00	1.00	11.00	26.00	<u>0.66</u>
19:20:00	49	13.47	15.00	39.00	1.00	6.00	18.00	<u>0.63</u>
19:30:00	33	8.24	9.00	18.00	1.00	5.00	12.00	<u>0.54</u>
19:40:00	17	2.94	2.00	7.00	1.00	1.00	4.00	<u>0.76</u>
19:50:00	0	-	-	-	-	-	-	-
20:00:00	0	-	-	-	-	-	-	-

CV: High-variance; Low-variance; Coefficient of Variation during the monitoring period for the proposed time interval for *E. coli* inactivation. CV: Coefficient of variation

APPENDIX III

Descriptive statistical analysis of total solar irradiance during the cold and dry season from July 2014 to November 2015.

Time	n	Arithmetic Mean (W.m ⁻²)	Median (W.m ⁻²)	Maximum (W.m ⁻²)	Minimum (W.m ⁻²)	25% quartile (W.m ⁻²)	75% quartile (W.m ⁻²)	CV
05:20:00	0	-	-	-	-	-	-	-
05:30:00	0	-	-	-	-	-	-	-
05:40:00	3	1.33	1.00	2.00	1.00	1.00	1.50	<u>0.43</u>
05:50:00	5	9.20	11.00	12.00	1.00	10.00	12.00	<u>0.51</u>
06:00:00	13	12.62	9.00	25.00	5.00	7.00	21.00	<u>0.62</u>
06:10:00	26	12.04	8.00	45.00	1.00	2.25	17.25	1.00
06:20:00	53	14.49	8.00	69.00	1.00	5.00	14.00	1.06
06:30:00	101	16.37	9.00	104.00	1.00	3.00	16.00	1.32
06:40:00	129	24.02	12.00	148.00	2.00	9.00	24.00	1.19
06:50:00	131	36.80	20.00	192.00	6.00	15.00	34.50	1.11
07:00:00	131	50.17	33.00	240.00	9.00	23.00	48.50	1.00
07:10:00	132	68.27	46.00	333.00	7.00	34.00	71.50	<u>0.94</u>
07:20:00	132	85.06	67.50	338.00	9.00	43.75	88.25	<u>0.83</u>
07:30:00	132	104.42	83.00	382.00	17.00	53.75	114.25	<u>0.77</u>
07:40:00	132	119.55	96.00	379.00	18.00	64.75	148.25	<u>0.71</u>
07:50:00	132	137.48	121.00	414.00	21.00	74.75	178.50	<u>0.65</u>
08:00:00	132	151.44	127.50	454.00	11.00	86.00	198.25	<u>0.63</u>
08:10:00	132	169.05	152.50	489.00	17.00	94.00	216.25	<u>0.59</u>
08:20:00	132	190.49	183.00	519.00	30.00	107.50	251.25	<u>0.55</u>
08:30:00	132	218.83	215.50	565.00	30.00	145.00	311.25	<u>0.52</u>
08:40:00	132	247.32	237.50	598.00	25.00	165.50	342.00	<u>0.52</u>
08:50:00	132	276.59	276.50	639.00	32.00	166.00	389.00	<u>0.51</u>
09:00:00	132	319.13	340.00	693.00	32.00	201.50	430.50	<u>0.48</u>
09:10:00	132	356.94	418.50	683.00	28.00	227.50	475.00	<u>0.43</u>
09:20:00	132	395.53	456.00	647.00	15.00	270.00	524.00	<u>0.41</u>
09:30:00	132	416.73	492.50	662.00	12.00	280.00	554.75	<u>0.42</u>
09:40:00	132	432.66	510.00	698.00	37.00	267.50	577.25	<u>0.42</u>
09:50:00	132	481.95	547.00	813.00	63.00	321.50	612.25	<u>0.39</u>
10:00:00	132	500.02	560.50	825.00	99.00	305.75	659.25	<u>0.39</u>
10:10:00	132	462.54	495.50	778.00	104.00	293.25	621.50	<u>0.40</u>
10:20:00	132	518.30	605.50	794.00	123.00	335.25	668.00	<u>0.38</u>
10:30:00	132	567.33	631.50	855.00	68.00	432.75	728.75	<u>0.38</u>
10:40:00	132	594.80	665.50	871.00	35.00	459.00	755.00	<u>0.36</u>
10:50:00	132	595.34	655.50	1056.00	122.00	365.00	768.00	<u>0.39</u>
11:00:00	131	608.01	674.00	1045.00	86.00	412.00	786.00	<u>0.38</u>
11:10:00	131	619.95	696.00	928.00	88.00	405.00	799.50	<u>0.36</u>
11:20:00	131	637.35	704.00	1019.00	96.00	403.00	827.50	<u>0.37</u>
11:30:00	132	637.98	719.00	1055.00	109.00	385.00	838.00	<u>0.38</u>
11:40:00	131	599.44	676.00	1039.00	82.00	364.00	827.00	<u>0.44</u>
11:50:00	132	602.34	665.00	1020.00	116.00	343.75	819.75	<u>0.42</u>
12:00:00	132	583.46	659.00	1048.00	88.00	384.50	789.00	<u>0.43</u>
12:10:00	132	614.39	697.00	1002.00	89.00	383.50	806.50	<u>0.39</u>
12:20:00	132	573.86	639.50	978.00	64.00	354.50	796.75	<u>0.45</u>
12:30:00	133	609.59	690.00	957.00	50.00	399.00	810.00	<u>0.39</u>
12:40:00	133	624.60	707.00	1069.00	45.00	389.00	829.00	<u>0.40</u>
12:50:00	133	620.98	741.00	1029.00	48.00	372.00	830.00	<u>0.41</u>
13:00:00	132	574.40	667.50	905.00	47.00	362.00	793.50	<u>0.44</u>
13:10:00	132	567.52	645.00	1029.00	54.00	337.75	783.25	<u>0.45</u>

13:20:00	132	556.38	622.00	918.00	53.00	306.75	781.25	<u>0.45</u>
13:30:00	132	548.12	630.00	880.00	32.00	331.00	745.25	<u>0.45</u>
13:40:00	132	549.80	632.50	852.00	54.00	325.50	753.00	<u>0.43</u>
13:50:00	132	535.88	612.50	854.00	100.00	329.00	708.75	<u>0.41</u>
14:00:00	133	536.22	616.00	864.00	63.00	335.00	704.00	<u>0.39</u>
14:10:00	133	489.24	531.00	860.00	42.00	277.00	679.00	<u>0.43</u>
14:20:00	133	467.06	513.00	806.00	41.00	291.00	653.00	<u>0.43</u>
14:30:00	133	435.50	493.00	701.00	42.00	267.00	609.00	<u>0.44</u>
14:40:00	132	411.44	478.50	734.00	27.00	248.50	580.75	<u>0.45</u>
14:50:00	132	396.70	450.00	655.00	10.00	228.75	554.00	<u>0.44</u>
15:00:00	132	381.48	446.00	716.00	23.00	218.25	527.00	<u>0.45</u>
15:10:00	132	341.63	379.00	658.00	23.00	192.25	483.25	<u>0.47</u>
15:20:00	132	321.76	366.00	577.00	16.00	171.50	458.75	<u>0.48</u>
15:30:00	132	302.13	347.00	567.00	14.00	152.75	429.00	<u>0.49</u>
15:40:00	132	271.27	291.50	515.00	14.00	168.75	387.25	<u>0.47</u>
15:50:00	132	247.87	265.00	454.00	16.00	147.00	354.00	<u>0.48</u>
16:00:00	130	227.02	243.00	518.00	16.00	136.75	320.50	<u>0.47</u>
16:10:00	130	189.35	196.00	416.00	14.00	104.25	271.00	<u>0.49</u>
16:20:00	130	158.69	144.50	302.00	12.00	83.25	239.75	<u>0.53</u>
16:30:00	129	117.57	84.00	288.00	10.00	54.00	195.00	<u>0.67</u>
16:40:00	129	80.34	63.00	249.00	12.00	40.00	102.00	<u>0.67</u>
16:50:00	129	53.24	41.00	207.00	9.00	29.00	58.00	<u>0.72</u>
17:00:00	130	35.79	32.00	107.00	4.00	25.00	41.75	<u>0.50</u>
17:10:00	127	26.98	25.00	80.00	3.00	19.00	31.00	<u>0.52</u>
17:20:00	125	18.56	18.00	58.00	1.00	11.00	21.00	<u>0.60</u>
17:30:00	112	11.50	10.50	43.00	1.00	4.75	15.25	<u>0.76</u>
17:40:00	66	8.02	7.50	32.00	1.00	5.00	10.75	<u>0.70</u>
17:50:00	20	3.90	3.00	19.00	1.00	2.00	3.00	1.07
18:00:00	2	2.00	2.00	3.00	1.00	1.50	2.50	<u>0.71</u>
18:10:00	0	-	-	-	-	-	-	-
18:20:00	0	-	-	-	-	-	-	-
18:30:00	0	-	-	-	-	-	-	-
18:40:00	0	-	-	-	-	-	-	-
18:50:00	0	-	-	-	-	-	-	-
19:00:00	0	-	-	-	-	-	-	-
19:10:00	0	-	-	-	-	-	-	-
19:20:00	0	-	-	-	-	-	-	-
19:30:00	0	-	-	-	-	-	-	-
19:40:00	0	-	-	-	-	-	-	-
19:50:00	0	-	-	-	-	-	-	-
20:00:00	0	-	-	-	-	-	-	-

CV: High-variance; Low-variance; Coefficient of Variation during the monitoring period for the proposed time interval for *E. coli* inactivation. CV: Coefficient of variation

APPENDIX IV

Descriptive statistical analysis of total solar irradiance during the wet and warm season from July 2014 to November 2015.

Time	n	Arithmetic Mean (W.m ⁻²)	Median (W.m ⁻²)	Maximum (W.m ⁻²)	Minimum (W.m ⁻²)	25% quartile (W.m ⁻²)	75% quartile (W.m ⁻²)	CV
05:20:00	-	-	-	-	-	-	-	-
05:30:00	9	3.44	2.00	12.00	1.00	1.00	2.00	1.13
05:40:00	17	8.71	8.00	24.00	1.00	5.00	10.00	<u>0.62</u>
05:50:00	25	13.40	14.00	43.00	1.00	7.00	18.00	<u>0.64</u>
06:00:00	47	15.87	9.00	70.00	1.00	2.00	30.00	1.00
06:10:00	75	19.96	10.00	109.00	1.00	5.00	28.50	1.14
06:20:00	116	24.26	14.00	152.00	1.00	7.00	27.00	1.20
06:30:00	134	34.89	21.50	196.00	2.00	11.00	35.75	1.13
06:40:00	152	46.39	31.50	245.00	1.00	16.00	49.00	1.08
06:50:00	159	61.07	42.00	285.00	4.00	24.50	72.00	<u>0.97</u>
07:00:00	159	82.52	64.00	326.00	5.00	32.00	97.50	<u>0.85</u>
07:10:00	159	107.00	82.00	365.00	12.00	46.50	149.00	<u>0.74</u>
07:20:00	159	132.78	103.00	405.00	16.00	58.50	185.50	<u>0.70</u>
07:30:00	159	155.30	127.00	452.00	27.00	75.50	211.00	<u>0.64</u>
07:40:00	159	180.92	149.00	539.00	17.00	96.00	242.50	<u>0.60</u>
07:50:00	159	201.03	175.00	596.00	18.00	116.50	276.50	<u>0.57</u>
08:00:00	160	217.79	196.00	606.00	4.00	125.75	291.25	<u>0.57</u>
08:10:00	160	239.28	223.00	604.00	6.00	118.75	341.75	<u>0.56</u>
08:20:00	160	267.83	259.50	639.00	7.00	131.75	373.00	<u>0.54</u>
08:30:00	160	302.55	300.50	675.00	8.00	156.00	431.00	<u>0.54</u>
08:40:00	160	336.37	359.00	775.00	10.00	173.50	470.75	<u>0.53</u>
08:50:00	160	355.75	370.50	815.00	13.00	198.75	498.00	<u>0.52</u>
09:00:00	160	387.93	410.50	852.00	18.00	222.75	555.25	<u>0.51</u>
09:10:00	160	411.18	422.50	824.00	24.00	225.75	585.75	<u>0.52</u>
09:20:00	160	438.24	467.00	957.00	38.00	238.50	629.50	<u>0.51</u>
09:30:00	160	460.39	478.50	896.00	55.00	273.00	658.25	<u>0.50</u>
09:40:00	160	472.39	488.00	949.00	46.00	288.25	654.50	<u>0.49</u>
09:50:00	160	502.27	522.00	1028.00	33.00	293.50	699.50	<u>0.49</u>
10:00:00	159	543.18	558.00	1084.00	44.00	361.00	769.50	<u>0.47</u>
10:10:00	158	580.79	621.00	1009.00	58.00	395.25	799.00	<u>0.45</u>
10:20:00	158	575.42	580.50	1102.00	67.00	378.50	820.25	<u>0.46</u>
10:30:00	159	604.86	636.00	1056.00	58.00	390.50	857.50	<u>0.46</u>
10:40:00	159	595.19	597.00	1169.00	61.00	349.50	845.00	<u>0.50</u>
10:50:00	159	607.39	603.00	1136.00	51.00	376.50	871.00	<u>0.49</u>
11:00:00	159	625.13	691.00	1131.00	32.00	346.00	903.50	<u>0.48</u>
11:10:00	159	631.75	616.00	1125.00	36.00	355.50	932.00	<u>0.49</u>
11:20:00	159	648.26	659.00	1355.00	28.00	369.00	941.50	<u>0.48</u>
11:30:00	159	652.36	691.00	1131.00	28.00	378.00	967.50	<u>0.49</u>
11:40:00	159	664.74	686.00	1197.00	87.00	417.50	966.00	<u>0.47</u>
11:50:00	159	703.97	701.00	1253.00	62.00	445.00	981.00	<u>0.43</u>
12:00:00	159	705.35	737.00	1263.00	79.00	429.50	1006.50	<u>0.44</u>
12:10:00	159	732.41	795.00	1266.00	79.00	456.00	1016.50	<u>0.41</u>
12:20:00	159	736.45	812.00	1259.00	86.00	437.00	1031.00	<u>0.43</u>
12:30:00	158	723.80	807.50	1237.00	116.00	442.50	1018.50	<u>0.44</u>
12:40:00	158	739.65	892.50	1256.00	94.00	434.50	1009.00	<u>0.44</u>
12:50:00	157	744.57	888.00	1200.00	55.00	450.00	1024.00	<u>0.43</u>
13:00:00	157	733.21	861.00	1223.00	11.00	438.00	1031.00	<u>0.44</u>
13:10:00	157	692.14	725.00	1142.00	7.00	397.00	1006.00	<u>0.47</u>

13:20:00	157	726.36	856.00	1198.00	12.00	427.00	1005.00	<u>0.44</u>
13:30:00	156	704.30	804.00	1205.00	32.00	401.25	993.00	<u>0.45</u>
13:40:00	156	723.10	837.50	1285.00	21.00	414.00	1018.50	<u>0.47</u>
13:50:00	155	712.69	813.00	1306.00	18.00	425.00	992.00	<u>0.47</u>
14:00:00	155	686.03	756.00	1269.00	23.00	426.00	988.00	<u>0.47</u>
14:10:00	155	656.47	665.00	1254.00	25.00	386.00	945.50	<u>0.47</u>
14:20:00	155	631.62	658.00	1147.00	20.00	338.00	923.00	<u>0.50</u>
14:30:00	155	618.23	639.00	1170.00	18.00	336.00	923.50	<u>0.51</u>
14:40:00	155	603.72	644.00	1148.00	22.00	315.00	877.00	<u>0.52</u>
14:50:00	155	584.70	621.00	1109.00	31.00	333.50	825.00	<u>0.51</u>
15:00:00	155	559.74	558.00	1102.00	33.00	281.00	859.50	<u>0.53</u>
15:10:00	155	555.86	563.00	1168.00	39.00	305.50	811.00	<u>0.51</u>
15:20:00	155	524.19	548.00	1091.00	28.00	262.00	781.00	<u>0.53</u>
15:30:00	157	484.73	495.00	975.00	10.00	280.00	675.00	<u>0.52</u>
15:40:00	157	457.24	469.00	1013.00	3.00	229.00	652.00	<u>0.55</u>
15:50:00	157	442.18	419.00	943.00	11.00	234.00	669.00	<u>0.56</u>
16:00:00	157	402.27	389.00	980.00	1.00	192.00	578.00	<u>0.59</u>
16:10:00	156	367.71	344.00	906.00	24.00	191.50	525.00	<u>0.60</u>
16:20:00	157	367.83	319.00	803.00	5.00	180.00	557.00	<u>0.62</u>
16:30:00	157	334.18	285.00	780.00	9.00	170.00	484.00	<u>0.62</u>
16:40:00	157	294.74	249.00	701.00	13.00	148.00	420.00	<u>0.66</u>
16:50:00	154	264.88	204.00	678.00	10.00	120.25	372.50	<u>0.69</u>
17:00:00	154	228.88	177.00	636.00	11.00	112.00	304.75	<u>0.72</u>
17:10:00	154	210.09	151.50	573.00	9.00	85.25	300.25	<u>0.78</u>
17:20:00	154	174.75	137.50	568.00	5.00	54.00	222.25	<u>0.86</u>
17:30:00	154	158.71	94.00	512.00	5.00	41.00	236.25	<u>0.94</u>
17:40:00	154	133.21	85.50	482.00	4.00	28.00	192.50	<u>0.98</u>
17:50:00	152	108.87	64.00	393.00	3.00	19.00	160.50	1.05
18:00:00	142	93.61	61.50	366.00	1.00	18.00	131.25	1.07
18:10:00	122	91.34	64.00	331.00	1.00	18.00	119.25	0.97
18:20:00	108	78.31	59.00	264.00	1.00	21.00	107.25	<u>0.90</u>
18:30:00	97	65.90	50.00	223.00	2.00	28.00	87.00	<u>0.86</u>
18:40:00	92	52.76	36.00	174.00	1.00	21.75	71.00	<u>0.85</u>
18:50:00	87	41.00	29.00	130.00	1.00	14.50	59.50	<u>0.80</u>
19:00:00	82	25.39	23.50	90.00	1.00	10.25	38.00	<u>0.74</u>
19:10:00	64	18.98	15.50	55.00	1.00	11.00	26.00	<u>0.66</u>
19:20:00	49	13.47	15.00	39.00	1.00	6.00	18.00	<u>0.63</u>
19:30:00	33	8.24	9.00	18.00	1.00	5.00	12.00	<u>0.54</u>
19:40:00	17	2.94	2.00	7.00	1.00	1.00	4.00	<u>0.76</u>
19:50:00	0	-	-	-	-	-	-	-
20:00:00	0	-	-	-	-	-	-	-

CV: High-variance; Low-variance; Coefficient of Variation during the monitoring period for the proposed time interval for *E. coli* inactivation. CV: Coefficient of variation

APPENDIX V

Descriptive statistical analysis of mean/median and maximum values of UV-A, UV-B and PAR irradiance at 5 cm and respective CV values.

Time	UV-A (5 cm): n= 3-65			UV-B (5 cm): n= 1-62			PAR (5 cm): n= 2-76		
	Mean/Med (W.m ⁻²)	Max. (W.m ⁻²)	CV	Mean/Med (W.m ⁻²)	Max. (W.m ⁻²)	CV	Mean/Med (W.m ⁻²)	Max. (W.m ⁻²)	CV
05:10:00	-	-	-	-	-	-	-	-	-
05:20:00	-	-	-	-	-	-	-	-	-
05:30:00	-	-	-	-	-	-	-	-	-
05:40:00	-	-	-	-	-	-	0.74/0.62	1.17	<u>0.50</u>
05:50:00	0.07/0.06	0.09	<u>0.38</u>	-	-	-	1.95/2.09	2.61	<u>0.38</u>
06:00:00	0.12/0.14	0.15	<u>0.23</u>	-	-	-	2.75/3.36	4.05	<u>0.50</u>
06:10:00	0.16/0.16	0.24	<u>0.41</u>	-	-	-	2.32/1.30	6.25	<u>0.84</u>
06:20:00	0.19/0.19	0.30	<u>0.49</u>	0.006/0.006	0.006	-	2.11/1.37	6.86	<u>0.89</u>
06:30:00	0.19/0.19	0.39	<u>0.71</u>	0.010/0.009	0.012	<u>0.15</u>	2.51/1.72	8.86	<u>0.90</u>
06:40:00	0.17/0.09	0.50	<u>0.94</u>	0.012/0.013	0.015	<u>0.37</u>	3.87/2.13	21.97	1.31
06:50:00	0.17/0.11	0.55	<u>0.92</u>	0.015/0.015	0.020	<u>0.22</u>	4.54/2.81	25.68	1.29
07:00:00	0.19/0.13	0.70	<u>0.92</u>	0.020/0.019	0.026	<u>0.23</u>	5.95/3.50	33.98	1.17
07:10:00	0.20/0.13	0.81	<u>0.97</u>	0.018/0.018	0.032	<u>0.52</u>	7.85/5.15	39.68	1.12
07:20:00	0.24/0.16	0.95	<u>0.92</u>	0.017/0.012	0.040	<u>0.69</u>	9.62/5.97	47.09	1.08
07:30:00	0.26/0.18	1.07	<u>0.95</u>	0.015/0.010	0.048	<u>0.84</u>	11.58/7.35	53.00	1.00
07:40:00	0.30/0.21	1.25	<u>0.98</u>	0.018/0.012	0.054	<u>0.78</u>	14.03/9.41	61.24	<u>0.97</u>
07:50:00	0.37/0.25	2.05	1.09	0.023/0.014	0.137	1.07	16.47/13.87	72.97	<u>0.87</u>
08:00:00	0.40/0.29	1.90	1.06	0.023/0.015	0.097	0.93	19.03/15.34	83.27	0.88
08:10:00	0.45/0.31	2.10	1.04	0.025/0.016	0.116	0.93	22.10/19.36	88.83	0.81
08:20:00	0.51/0.33	2.30	1.04	0.029/0.018	0.130	0.93	24.88/19.77	97.76	0.82
08:30:00	0.57/0.41	2.57	0.99	0.033/0.022	0.146	0.92	27.44/24.10	109.91	0.78
08:40:00	0.62/0.41	2.84	1.04	0.036/0.024	0.166	0.94	31.63/26.77	118.35	0.78
08:50:00	0.70/0.41	3.40	1.08	0.039/0.026	0.188	1.00	34.04/26.43	133.73	0.83
09:00:00	0.74/0.45	3.39	1.06	0.042/0.026	0.198	0.97	36.25/28.01	132.97	0.80
09:10:00	0.77/0.47	3.68	0.98	0.043/0.030	0.212	0.95	37.64/32.54	144.51	0.72
09:20:00	0.82/0.58	3.18	0.91	0.046/0.032	0.223	0.91	40.56/35.22	123.43	0.68
09:30:00	0.87/0.58	3.83	1.01	0.050/0.035	0.234	0.95	43.67/39.85	139.91	0.70
09:40:00	0.92/0.55	4.43	1.10	0.053/0.036	0.242	1.03	45.72/38.92	176.36	0.80
09:50:00	0.97/0.58	4.45	1.08	0.056/0.037	0.248	1.01	48.21/40.98	164.62	0.77
10:00:00	0.98/0.55	4.46	1.05	0.058/0.034	0.245	0.98	47.49/36.25	160.92	0.78
10:10:00	1.05/0.57	5.05	1.10	0.060/0.035	0.275	1.08	49.51/38.92	187.48	0.81
10:20:00	1.07/0.57	4.71	1.05	0.062/0.036	0.259	1.05	49.73/38.51	168.12	0.79
10:30:00	1.10/0.63	5.17	1.05	0.064/0.039	0.269	1.03	50.00/38.92	158.03	0.75
10:40:00	1.20/0.72	5.59	1.10	0.069/0.042	0.308	1.08	55.03/43.46	175.54	0.74
10:50:00	1.16/0.63	5.82	1.08	0.067/0.040	0.324	1.05	56.15/46.75	208.76	0.76
11:00:00	1.23/0.66	5.64	1.04	0.073/0.041	0.276	0.97	59.50/51.35	178.97	0.75
11:10:00	1.13/0.70	6.22	1.10	0.072/0.046	0.343	1.00	60.74/50.56	222.08	0.74
11:20:00	1.23/0.72	4.87	0.99	0.072/0.046	0.278	0.98	58.09/46.17	173.68	0.76
11:30:00	1.23/0.81	4.79	0.91	0.072/0.051	0.271	0.88	57.02/51.08	170.25	0.68
11:40:00	1.30/0.87	4.77	0.93	0.081/0.054	0.269	0.90	63.67/54.99	166.13	0.73
11:50:00	1.37/0.99	5.92	0.94	0.080/0.055	0.340	0.94	66.54/56.02	215.49	0.73
12:00:00	1.33/1.00	5.84	0.94	0.080/0.061	0.339	0.88	64.72/61.41	220.37	0.71
12:10:00	1.35/1.07	4.94	0.85	0.081/0.064	0.288	0.81	67.52/55.95	180.14	0.66
12:20:00	1.24/0.92	5.65	0.90	0.077/0.063	0.324	0.83	62.49/55.95	214.87	0.70
12:30:00	1.16/0.84	5.24	0.92	0.072/0.056	0.300	0.85	59.51/52.07	203.07	0.69
12:40:00	1.21/0.94	5.35	0.92	0.073/0.056	0.294	0.85	63.02/57.77	189.75	0.67
12:50:00	1.11/0.84	4.66	0.92	0.067/0.052	0.250	0.82	59.14/55.40	171.42	0.68
13:00:00	0.97/0.71	4.79	0.98	0.060/0.041	0.276	0.88	47.82/43.04	181.30	0.74
13:10:00	0.96/0.63	4.40	0.93	0.056/0.040	0.245	0.88	46.69/36.80	182.47	0.77
13:20:00	0.92/0.69	4.05	0.87	0.055/0.043	0.225	0.84	49.21/42.49	182.47	0.73
13:30:00	0.90/0.68	3.80	0.91	0.054/0.040	0.212	0.81	50.77/44.42	158.58	0.71
13:40:00	0.83/0.62	3.72	0.93	0.050/0.039	0.208	0.83	51.95/54.10	158.10	0.70

13:50:00	0.80/0.62	3.47	<u>0.82</u>	0.047/0.040	0.189	<u>0.75</u>	46.30/43.94	153.23	<u>0.68</u>
14:00:00	0.76/0.61	3.14	<u>0.77</u>	0.044/0.037	0.172	<u>0.71</u>	42.71/39.99	144.58	<u>0.65</u>
14:10:00	0.70/0.53	2.74	<u>0.81</u>	0.042/0.035	0.147	<u>0.73</u>	42.06/38.31	133.94	<u>0.65</u>
14:20:00	0.64/0.50	2.66	<u>0.77</u>	0.037/0.029	0.140	<u>0.69</u>	38.87/37.21	130.57	<u>0.65</u>
14:30:00	0.58/0.43	2.36	<u>0.79</u>	0.033/0.025	0.123	<u>0.71</u>	34.76/31.58	119.86	<u>0.70</u>
14:40:00	0.54/0.44	2.13	<u>0.79</u>	0.030/0.023	0.109	<u>0.74</u>	31.48/27.22	110.87	<u>0.74</u>
14:50:00	0.48/0.39	1.78	<u>0.73</u>	0.027/0.023	0.087	<u>0.63</u>	28.39/26.12	95.29	<u>0.74</u>
15:00:00	0.42/0.32	1.39	<u>0.72</u>	0.025/0.020	0.067	<u>0.57</u>	25.78/18.43	83.82	<u>0.80</u>
15:10:00	0.38/0.32	1.42	<u>0.73</u>	0.022/0.019	0.069	<u>0.61</u>	23.19/16.17	84.03	<u>0.81</u>
15:20:00	0.36/0.27	2.33	<u>0.94</u>	0.019/0.016	0.101	<u>0.83</u>	20.37/16.00	99.06	<u>0.84</u>
15:30:00	0.32/0.26	1.70	<u>0.83</u>	0.017/0.015	0.073	<u>0.71</u>	18.95/12.22	79.15	<u>0.85</u>
15:40:00	0.27/0.22	1.10	<u>0.74</u>	0.016/0.013	0.048	<u>0.62</u>	15.99/12.63	59.79	<u>0.82</u>
15:50:00	0.25/0.18	1.00	<u>0.75</u>	0.015/0.012	0.041	<u>0.64</u>	14.36/11.88	54.30	<u>0.82</u>
16:00:00	0.23/0.17	0.70	<u>0.66</u>	0.013/0.011	0.030	<u>0.59</u>	12.52/10.61	48.40	<u>0.75</u>
16:10:00	0.19/0.15	0.62	<u>0.68</u>	0.012/0.010	0.025	<u>0.52</u>	10.27/8.38	40.02	<u>0.78</u>
16:20:00	0.17/0.13	0.54	<u>0.67</u>	0.012/0.011	0.021	<u>0.41</u>	8.76/7.79	31.78	<u>0.73</u>
16:30:00	0.15/0.12	0.47	<u>0.60</u>	0.011/0.011	0.018	<u>0.40</u>	7.29/6.66	29.31	<u>0.73</u>
16:40:00	0.13/0.11	0.39	<u>0.64</u>	0.009/0.009	0.013	<u>0.35</u>	6.08/4.81	21.08	<u>0.72</u>
16:50:00	0.13/0.11	0.36	<u>0.56</u>	0.008/0.010	0.011	<u>0.61</u>	4.57/3.64	18.47	<u>0.71</u>
17:00:00	0.12/0.11	0.29	<u>0.56</u>	0.005/0.005	0.005	-	3.54/2.88	13.04	<u>0.66</u>
17:10:00	0.11/0.11	0.22	<u>0.62</u>	-	-	-	2.56/2.33	7.07	<u>0.48</u>
17:20:00	0.12/0.11	0.22	<u>0.35</u>	-	-	-	2.03/1.72	6.73	<u>0.57</u>
17:30:00	0.08/0.08	0.16	<u>0.63</u>	-	-	-	1.51/1.24	5.22	<u>0.73</u>
17:40:00	0.09/0.08	0.09	<u>0.10</u>	-	-	-	1.35/1.10	3.50	<u>0.61</u>
17:50:00	-	-	-	-	-	-	1.25/1.17	2.33	<u>0.48</u>
18:00:00	-	-	-	-	-	-	1.08/1.10	1.44	<u>0.25</u>
18:10:00	-	-	-	-	-	-	0.48/0.48	0.62	<u>0.40</u>

CV: High-variance; Low-variance; **Coefficient of Variance during the monitoring period for the proposed time interval for *E. coli* inactivation.** Mean: Arithmetic mean; *Med*: Median; Max: Maximum; CV: Coefficient of variation

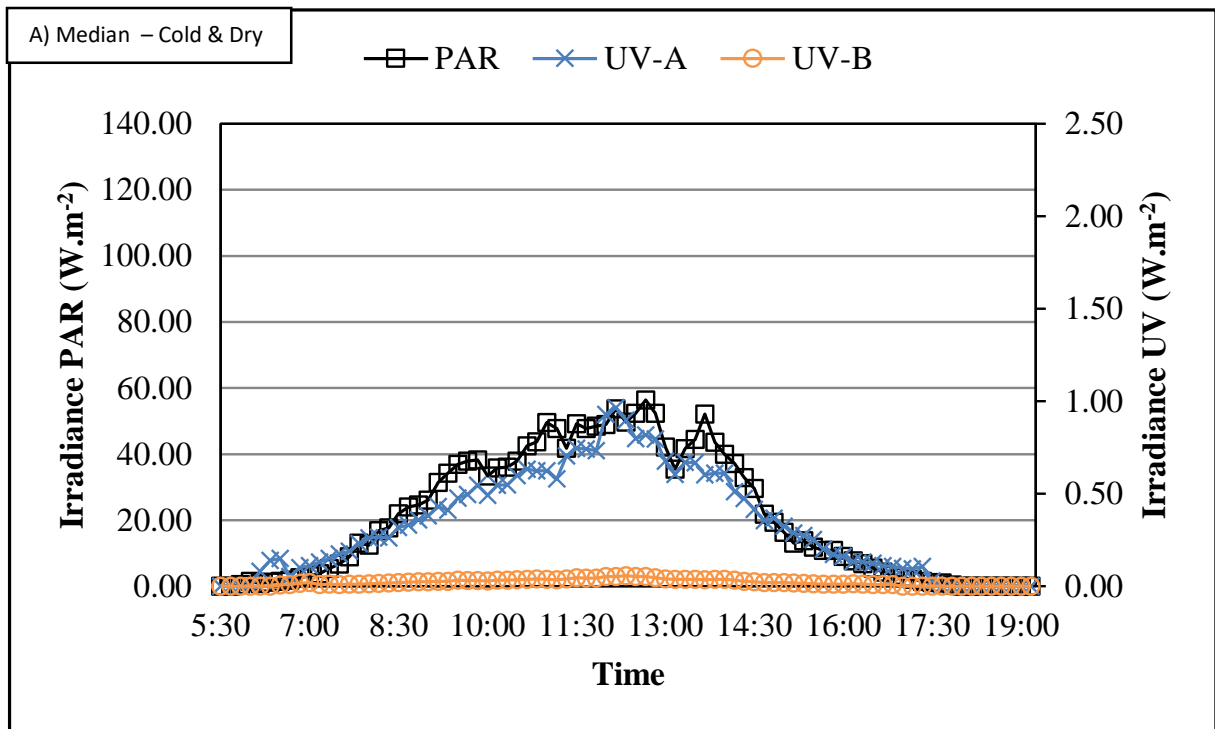
APPENDIX VI

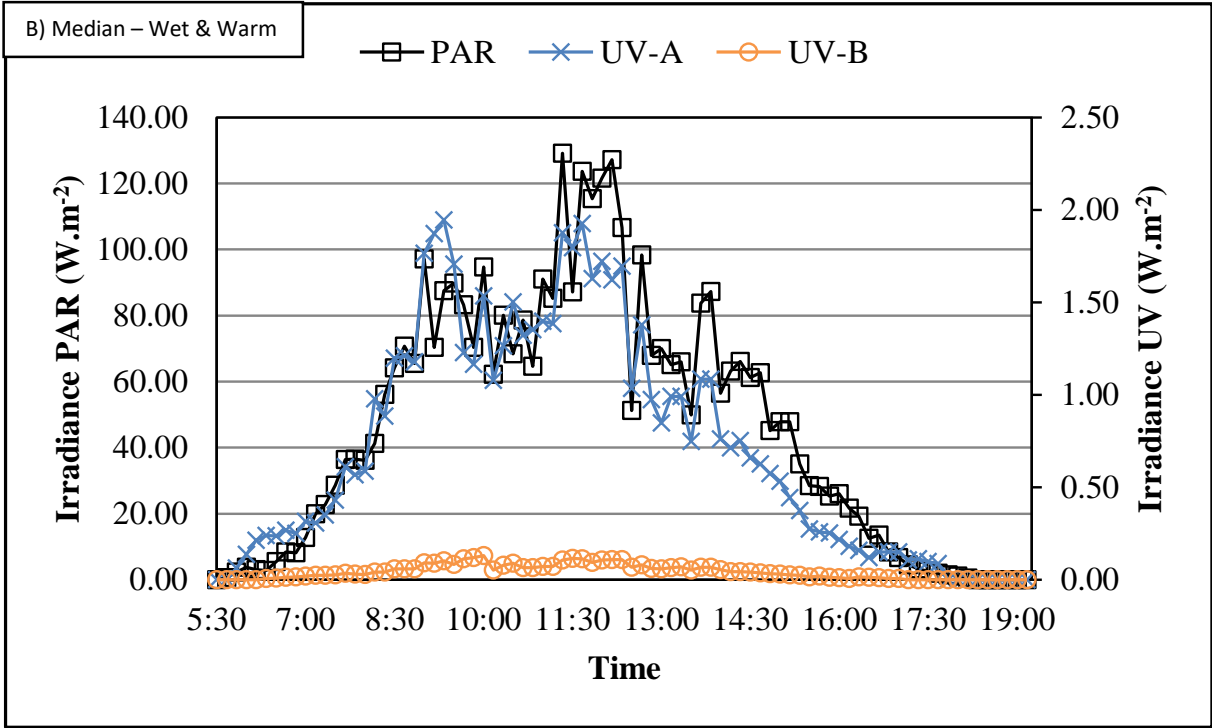
Descriptive statistical analysis of mean/median of UV-A, UV-B and PAR irradiance at 5 cm for cold and dry (C&D) and wet and warm (W&W) conditions.

	UV-A (5 cm)		UV-B (5 cm)		PAR (5 cm)	
	C&D – Mean/Med (W.m ⁻²)	W&W – Mean/Med (W.m ⁻²)	C&D – Mean/Med (W.m ⁻²)	W&W – Mean/Med (W.m ⁻²)	C&D – Mean/Med (W.m ⁻²)	W&W – Mean/Med (W.m ⁻²)
05:10:00	-	-	-	-	-	-
05:20:00	-	-	-	-	-	-
05:30:00	-	-	-	-	-	-
05:40:00	-	-	-	-	-	0.74/0.62
05:50:00	-	0.07/0.06	-	-	0.55/0.55	2.22/2.27
06:00:00	-	0.12/0.14	-	-	1.19/1.44	3.69/3.78
06:10:00	0.08/0.08	0.19/0.21	-	-	1.25/0.93	3.18/2.99
06:20:00	0.14/0.14	0.21/0.24	-	0.006/0.006	1.33/1.20	3.95/2.81
06:30:00	0.12/0.15	0.21/0.24	0.008/0.008	0.010/0.010	1.67/1.51	5.58/5.49
06:40:00	0.09/0.05	0.27/0.27	0.009/0.009	0.013/0.013	2.16/1.89	11.35/8.44
06:50:00	0.11/0.10	0.28/0.25	0.015/0.015	0.015/0.015	2.68/2.54	13.51/8.17
07:00:00	0.13/0.11	0.35/0.31	0.020/0.020	0.019/0.019	3.65/3.23	17.02/12.77
07:10:00	0.14/0.13	0.39/0.31	0.014/0.008	0.022/0.024	4.94/3.84	22.71/19.91
07:20:00	0.18/0.15	0.45/0.35	0.014/0.011	0.021/0.023	6.40/5.42	26.56/22.72
07:30:00	0.19/0.17	0.54/0.43	0.011/0.010	0.023/0.026	8.09/6.76	30.01/28.63
07:40:00	0.21/0.19	0.65/0.61	0.013/0.011	0.029/0.035	9.88/8.89	36.70/36.38
07:50:00	0.28/0.23	0.73/0.57	0.020/0.012	0.031/0.030	12.50/13.01	38.14/36.45
08:00:00	0.30/0.26	0.86/0.59	0.019/0.015	0.035/0.028	14.61/12.49	43.55/36.11
08:10:00	0.33/0.26	0.97/0.98	0.020/0.015	0.041/0.041	17.22/16.85	48.69/41.26
08:20:00	0.38/0.26	1.12/0.89	0.024/0.017	0.048/0.041	19.28/17.64	56.96/56.09
08:30:00	0.43/0.32	1.23/1.20	0.026/0.019	0.059/0.059	21.75/21.93	60.59/64.19
08:40:00	0.45/0.32	1.41/1.21	0.029/0.021	0.063/0.058	24.95/24.06	70.47/70.71
08:50:00	0.51/0.36	1.60/1.18	0.030/0.024	0.073/0.059	26.81/24.61	76.11/65.42
09:00:00	0.54/0.38	1.75/1.76	0.033/0.025	0.082/0.091	28.61/26.02	81.43/97.07
09:10:00	0.59/0.43	1.62/1.87	0.035/0.028	0.080/0.088	31.64/31.44	73.09/70.30
09:20:00	0.64/0.41	1.69/1.95	0.038/0.028	0.085/0.101	34.22/34.26	78.00/87.46
09:30:00	0.68/0.48	1.92/1.71	0.041/0.033	0.095/0.084	37.47/36.90	83.36/89.86
09:40:00	0.71/0.50	2.20/1.23	0.042/0.031	0.121/0.113	38.49/37.83	97.07/83.27
09:50:00	0.78/0.55	2.15/1.17	0.046/0.031	0.121/0.120	42.01/38.27	92.25/70.30
10:00:00	0.80/0.49	2.05/1.53	0.048/0.028	0.119/0.130	42.01/33.43	86.42/94.74
10:10:00	0.84/0.55	2.34/1.08	0.049/0.032	0.124/0.053	42.58/35.77	98.03/62.20
10:20:00	0.87/0.55	2.27/1.27	0.051/0.033	0.126/0.077	42.82/36.11	98.11/80.05
10:30:00	0.93/0.60	2.12/1.50	0.055/0.035	0.116/0.090	45.51/37.89	81.47/68.44
10:40:00	0.96/0.63	2.63/1.32	0.056/0.038	0.142/0.066	49.47/42.56	93.94/78.67
10:50:00	0.98/0.62	2.23/1.35	0.057/0.040	0.126/0.066	51.73/43.73	87.09/64.67
11:00:00	1.04/0.62	2.35/1.40	0.063/0.038	0.128/0.071	53.95/49.60	96.51/91.10
11:10:00	0.92/0.58	2.32/1.38	0.062/0.035	0.126/0.072	54.55/47.78	99.94/85.19
11:20:00	1.01/0.70	2.41/1.88	0.060/0.041	0.139/0.107	50.38/41.81	106.93/129.20
11:30:00	1.06/0.75	2.14/1.80	0.064/0.047	0.121/0.115	51.33/49.15	93.68/87.19
11:40:00	1.11/0.74	2.36/1.93	0.071/0.044	0.137/0.112	56.30/47.78	111.10/123.64
11:50:00	1.13/0.73	2.69/1.63	0.067/0.043	0.153/0.094	57.49/48.50	124.89/115.40
12:00:00	1.11/0.93	2.55/1.72	0.068/0.054	0.146/0.107	56.39/48.95	121.20/121.58
12:10:00	1.16/0.97	2.49/1.62	0.070/0.053	0.145/0.109	59.61/53.75	121.09/127.21
12:20:00	1.06/0.90	2.37/1.70	0.067/0.057	0.139/0.110	55.63/49.70	109.03/106.68
12:30:00	1.03/0.80	1.93/1.03	0.065/0.054	0.114/0.068	55.61/52.31	85.91/51.28
12:40:00	1.08/0.82	2.01/1.38	0.065/0.053	0.121/0.081	57.68/56.43	99.24/98.31
12:50:00	1.00/0.79	1.80/0.97	0.060/0.046	0.106/0.061	54.99/52.31	87.24/67.89
13:00:00	0.85/0.68	1.59/0.85	0.052/0.040	0.107/0.059	43.14/42.08	76.36/69.99
13:10:00	0.83/0.60	1.72/0.99	0.048/0.038	0.105/0.066	41.28/35.49	79.74/65.11
13:20:00	0.82/0.67	1.54/0.99	0.048/0.037	0.095/0.069	44.68/41.60	76.81/65.97
13:30:00	0.84/0.67	1.23/0.75	0.048/0.038	0.082/0.053	48.36/44.42	65.48/49.94
13:40:00	0.74/0.60	1.29/1.08	0.044/0.036	0.083/0.067	48.50/52.17	73.02/83.72

13:50:00	0.71/0.61	1.26/1.08	0.041/0.038	0.080/0.068	41.51/43.66	75.47/87.25
14:00:00	0.70/0.61	1.07/0.76	0.040/0.037	0.068/0.054	39.52/39.99	62.49/56.50
14:10:00	0.64/0.51	1.05/0.71	0.038/0.032	0.060/0.043	38.21/37.21	65.90/63.19
14:20:00	0.58/0.47	0.96/0.75	0.034/0.027	0.053/0.044	34.83/32.92	63.93/66.04
14:30:00	0.53/0.41	0.87/0.66	0.030/0.024	0.049/0.040	30.95/29.59	58.37/61.24
14:40:00	0.47/0.36	0.89/0.63	0.027/0.020	0.049/0.037	26.24/21.86	63.99/62.71
14:50:00	0.43/0.37	0.74/0.57	0.025/0.020	0.039/0.033	24.16/19.36	54.60/45.17
15:00:00	0.38/0.32	0.61/0.53	0.023/0.020	0.032/0.031	21.84/16.30	50.20/47.78
15:10:00	0.34/0.29	0.60/0.44	0.020/0.018	0.031/0.026	18.75/13.04	50.70/47.81
15:20:00	0.30/0.27	0.64/0.37	0.016/0.016	0.034/0.023	16.07/13.83	44.60/35.08
15:30:00	0.28/0.25	0.52/0.27	0.015/0.015	0.025/0.016	16.23/11.81	34.29/28.42
15:40:00	0.24/0.20	0.42/0.26	0.014/0.012	0.024/0.019	13.63/10.85	29.25/28.28
15:50:00	0.22/0.17	0.39/0.25	0.013/0.012	0.017/0.014	11.82/10.88	28.63/25.26
16:00:00	0.21/0.16	0.32/0.22	0.012/0.011	0.014/0.012	10.21/9.03	26.86/25.98
16:10:00	0.17/0.13	0.26/0.18	0.012/0.013	0.011/0.007	8.14/7.65	23.49/21.66
16:20:00	0.15/0.13	0.22/0.16	0.012/0.011	0.014/0.014	7.03/6.86	19.50/19.19
16:30:00	0.14/0.12	0.19/0.12	0.010/0.010	0.012/0.012	5.87/5.46	16.09/12.56
16:40:00	0.12/0.11	0.17/0.15	0.008/0.009	0.010/0.011	4.76/4.32	13.60/13.56
16:50:00	0.12/0.11	0.17/0.15	0.010/0.010	0.007/0.007	3.76/3.30	9.14/8.34
17:00:00	0.10/0.10	0.16/0.15	-	0.005/0.005	2.88/2.75	6.66/6.73
17:10:00	0.09/0.09	0.15/0.11	-	-	2.21/2.13	4.18/4.46
17:20:00	0.11/0.11	0.13/0.11	-	-	1.69/1.51	3.55/3.23
17:30:00	0.03/0.03	0.10/0.10	-	-	1.14/1.10	2.94/2.54
17:40:00	-	0.09/0.09	-	-	0.91/0.96	2.28/1.99
17:50:00	-	-	-	-	0.48/0.41	1.48/1.51
18:00:00	-	-	-	-	-	1.08/1.10
18:10:00	-	-	-	-	-	0.48/0.48

Median cold and dry (A) and wet and warm (B) for PAR and UV solar irradiance at 5 cm in depth over the length of the day.





APPENDIX VII

Descriptive statistical analysis of mean/median and maximum values of UV-A, UV-B and PAR irradiance at 10 cm and respective CV values.

Time	UV-A (10 cm): n= 1-58			UV-B (10 cm): n=1-24			PAR (10 cm): n= 1-83		
	Mean/Med (W.m ⁻²)	Max. (W.m ⁻²)	CV	Mean/Med (W/m ²)	Max. (W.m ⁻²)	CV	Mean/Med (W.m ⁻²)	Max. (W.m ⁻²)	CV
05:40:00	-	-	-	-	-	-	-	-	-
05:50:00	-	-	-	-	-	-	-	-	-
06:00:00	-	-	-	-	-	-	-	-	-
06:10:00	-	-	-	-	-	-	0.55/0.55	0.55	-
06:20:00	-	-	-	-	-	-	0.60/0.55	1.17	<u>0.56</u>
06:30:00	-	-	-	-	-	-	1.00/1.17	1.72	<u>0.44</u>
06:40:00	-	-	-	-	-	-	1.10/1.10	2.40	<u>0.47</u>
06:50:00	-	-	-	-	-	-	1.28/1.10	3.09	<u>0.47</u>
07:00:00	-	-	-	-	-	-	1.43/1.37	3.78	<u>0.51</u>
07:10:00	-	-	-	-	-	-	1.86/1.65	6.32	<u>0.56</u>
07:20:00	-	-	-	-	-	-	2.25/1.85	8.44	<u>0.63</u>
07:30:00	-	-	-	-	-	-	2.71/2.33	9.75	<u>0.61</u>
07:40:00	-	-	-	-	-	-	3.23/2.47	12.49	<u>0.67</u>
07:50:00	0.168/0.075	0.64	1.58	-	-	-	3.94/2.95	12.43	<u>0.71</u>
08:00:00	0.123/0.097	0.26	<u>0.56</u>	-	-	-	5.10/3.09	46.89	<u>1.16</u>
08:10:00	0.091/0.103	0.16	<u>0.48</u>	-	-	-	5.94/4.98	20.66	<u>0.70</u>
08:20:00	0.094/0.100	0.19	<u>0.52</u>	-	-	-	7.75/7.69	25.19	<u>0.64</u>
08:30:00	0.134/0.109	0.38	<u>0.74</u>	-	-	-	8.40/7.83	28.08	<u>0.66</u>
08:40:00	0.106/0.094	0.24	<u>0.57</u>	-	-	-	9.62/8.48	31.44	<u>0.70</u>
08:50:00	0.125/0.112	0.29	<u>0.58</u>	-	-	-	10.50/9.54	41.81	<u>0.76</u>
09:00:00	0.144/0.131	0.31	<u>0.51</u>	0.0092/0.0092	0.0092	-	13.05/11.67	43.18	<u>0.65</u>
09:10:00	0.153/0.125	0.35	<u>0.63</u>	0.0087/0.0077	0.0123	<u>0.37</u>	13.83/12.63	44.69	<u>0.64</u>
09:20:00	0.161/0.125	0.41	<u>0.69</u>	0.0090/0.0104	0.0123	<u>0.46</u>	15.56/13.52	50.53	<u>0.64</u>
09:30:00	0.180/0.143	0.45	<u>0.65</u>	0.0098/0.0096	0.0123	<u>0.13</u>	17.35/15.93	52.38	<u>0.63</u>
09:40:00	0.183/0.150	0.49	<u>0.66</u>	0.0080/0.0084	0.0115	<u>0.38</u>	18.25/16.06	58.35	<u>0.63</u>
09:50:00	0.171/0.137	0.55	<u>0.80</u>	0.0089/0.0104	0.0123	<u>0.38</u>	18.68/16.37	63.02	<u>0.67</u>
10:00:00	0.190/0.131	0.58	<u>0.75</u>	0.0096/0.0107	0.0138	<u>0.33</u>	20.26/17.30	67.69	<u>0.68</u>
10:10:00	0.182/0.118	0.62	<u>0.86</u>	0.0096/0.0115	0.0138	<u>0.39</u>	20.68/18.40	69.41	<u>0.65</u>
10:20:00	0.191/0.137	0.67	<u>0.87</u>	0.0099/0.0130	0.0161	<u>0.61</u>	21.62/19.22	75.51	<u>0.67</u>
10:30:00	0.189/0.118	0.71	<u>0.89</u>	0.0118/0.0107	0.0169	<u>0.35</u>	22.44/19.02	81.14	<u>0.71</u>
10:40:00	0.213/0.137	0.79	<u>0.89</u>	0.0105/0.0096	0.0207	<u>0.58</u>	24.01/20.56	89.93	<u>0.72</u>
10:50:00	0.210/0.131	0.86	<u>0.99</u>	0.0132/0.0130	0.0207	<u>0.41</u>	25.41/21.73	94.74	<u>0.74</u>
11:00:00	0.213/0.125	0.91	<u>0.97</u>	0.0125/0.0134	0.0245	<u>0.58</u>	27.72/23.07	97.55	<u>0.70</u>
11:10:00	0.197/0.131	0.80	<u>0.98</u>	0.0114/0.0115	0.0276	<u>0.61</u>	26.99/22.93	88.15	<u>0.71</u>
11:20:00	0.214/0.147	0.88	<u>0.93</u>	0.0119/0.0111	0.0276	<u>0.60</u>	28.52/26.43	95.56	<u>0.68</u>
11:30:00	0.211/0.131	0.97	<u>1.03</u>	0.0144/0.0138	0.0376	<u>0.60</u>	27.04/26.16	99.82	<u>0.69</u>
11:40:00	0.226/0.150	1.00	<u>0.98</u>	0.0117/0.0111	0.0299	<u>0.56</u>	29.75/24.71	108.26	<u>0.68</u>
11:50:00	0.268/0.156	2.48	<u>1.41</u>	0.0225/0.0130	0.1434	<u>1.45</u>	31.21/27.67	106.00	<u>0.68</u>
12:00:00	0.247/0.162	1.00	<u>0.91</u>	0.0122/0.0130	0.0230	<u>0.50</u>	31.93/31.03	103.25	<u>0.65</u>
12:10:00	0.258/0.168	1.22	<u>0.99</u>	0.0134/0.0123	0.0268	<u>0.50</u>	33.56/29.59	126.32	<u>0.67</u>
12:20:00	0.240/0.159	1.13	<u>0.96</u>	0.0119/0.0107	0.0230	<u>0.51</u>	33.08/29.66	113.68	<u>0.64</u>
12:30:00	0.250/0.143	1.33	<u>0.97</u>	0.0111/0.0100	0.0238	<u>0.59</u>	31.99/29.83	134.83	<u>0.69</u>
12:40:00	0.220/0.156	1.01	<u>0.93</u>	0.0102/0.0092	0.0192	<u>0.55</u>	28.77/26.09	98.44	<u>0.66</u>
12:50:00	0.255/0.193	1.30	<u>0.92</u>	0.0115/0.0115	0.0199	<u>0.33</u>	28.87/26.02	137.37	<u>0.76</u>
13:00:00	0.230/0.181	1.16	<u>0.94</u>	0.0112/0.0115	0.0176	<u>0.35</u>	28.96/25.26	136.75	<u>0.75</u>
13:10:00	0.215/0.171	1.20	<u>0.98</u>	0.0086/0.0084	0.0184	<u>0.53</u>	27.58/24.71	130.09	<u>0.71</u>
13:20:00	0.229/0.162	1.18	<u>1.03</u>	0.0111/0.0084	0.0468	<u>0.91</u>	28.25/25.16	128.79	<u>0.73</u>
13:30:00	0.215/0.131	1.25	<u>1.10</u>	0.0110/0.0092	0.0353	<u>0.75</u>	26.37/22.93	125.29	<u>0.74</u>
13:40:00	0.217/0.137	1.12	<u>1.05</u>	0.0111/0.0088	0.0330	<u>0.86</u>	24.71/20.59	102.43	<u>0.78</u>
13:50:00	0.191/0.140	1.03	<u>1.00</u>	0.0081/0.0061	0.0299	<u>1.01</u>	21.94/19.63	82.79	<u>0.68</u>
14:00:00	0.188/0.131	0.91	<u>0.98</u>	0.0124/0.0096	0.0245	<u>0.66</u>	22.22/18.98	84.44	<u>0.71</u>
14:10:00	0.179/0.131	0.72	<u>0.89</u>	0.0107/0.0077	0.0222	<u>0.62</u>	22.11/17.47	83.27	<u>0.68</u>

14:20:00	0.173/0.125	0.75	<u>0.87</u>	0.0094/0.0054	0.0230	<u>0.95</u>	20.52/17.16	83.27	<u>0.69</u>
14:30:00	0.150/0.100	0.62	<u>0.96</u>	0.0106/0.0077	0.0215	<u>0.64</u>	19.15/16.24	80.46	<u>0.73</u>
14:40:00	0.163/0.106	0.60	<u>0.89</u>	0.0100/0.0092	0.0169	<u>0.45</u>	17.74/14.28	93.71	<u>0.82</u>
14:50:00	0.162/0.097	0.56	<u>0.96</u>	0.0105/0.0092	0.0184	<u>0.53</u>	17.01/12.91	89.45	<u>0.91</u>
15:00:00	0.148/0.094	0.52	<u>0.95</u>	0.0118/0.0138	0.0169	<u>0.41</u>	14.22/11.29	65.22	<u>0.84</u>
15:10:00	0.177/0.100	0.60	<u>0.92</u>	0.0157/0.0150	0.0245	<u>0.44</u>	13.59/10.81	73.66	<u>0.92</u>
15:20:00	0.155/0.112	0.51	<u>0.85</u>	0.0138/0.0134	0.0176	<u>0.24</u>	12.34/10.43	67.62	<u>0.86</u>
15:30:00	0.167/0.094	0.78	<u>1.09</u>	0.0159/0.0150	0.0307	<u>0.71</u>	11.29/9.61	68.65	<u>0.89</u>
15:40:00	0.118/0.106	0.29	<u>0.61</u>	0.0189/0.0038	0.0506	<u>1.45</u>	9.74/8.72	32.33	<u>0.71</u>
15:50:00	0.120/0.106	0.31	<u>0.71</u>	0.0337/0.0092	0.0828	<u>1.26</u>	9.55/8.34	42.77	<u>0.81</u>
16:00:00	0.119/0.112	0.36	<u>0.80</u>	0.0100/0.0100	0.0107	<u>0.11</u>	8.87/6.18	52.52	<u>1.00</u>
16:10:00	0.123/0.112	0.22	<u>0.37</u>	0.0268/0.0268	0.0498	<u>1.21</u>	7.88/5.97	49.43	<u>0.98</u>
16:20:00	0.134/0.118	0.33	<u>0.69</u>	0.0355/0.0138	0.0828	<u>1.15</u>	7.23/4.36	47.30	<u>1.19</u>
16:30:00	0.140/0.125	0.31	<u>0.60</u>	0.0230/0.0092	0.0529	<u>1.13</u>	6.32/3.43	45.10	<u>1.21</u>
16:40:00	0.128/0.106	0.28	<u>0.69</u>	0.0210/0.0115	0.0437	<u>0.94</u>	4.64/2.75	41.05	<u>1.29</u>
16:50:00	0.115/0.078	0.27	<u>0.91</u>	0.0166/0.0123	0.0337	<u>0.93</u>	3.72/2.37	38.24	<u>1.39</u>
17:00:00	0.256/0.150	0.69	<u>1.17</u>	0.0176/0.0176	0.0230	<u>0.43</u>	3.17/1.92	34.67	<u>1.51</u>
17:10:00	0.258/0.212	0.48	<u>0.79</u>	0.0127/0.0127	0.0138	<u>0.13</u>	2.90/1.65	31.10	<u>1.53</u>
17:20:00	0.200/0.193	0.34	<u>0.70</u>	0.0084/0.0084	0.0115	<u>0.51</u>	3.09/1.78	28.28	<u>1.45</u>
17:30:00	0.190/0.190	0.21	<u>0.12</u>	0.0092/0.0092	0.0092	-	3.19/1.44	25.54	<u>1.55</u>
17:40:00	0.106/0.106	0.15	<u>0.58</u>	-	-	-	3.11/1.58	21.83	<u>1.63</u>
17:50:00	0.150/0.150	0.15	-	-	-	-	3.29/2.20	20.32	<u>1.39</u>
18:00:00	0.118/0.118	0.12	-	-	-	-	2.65/1.65	14.97	<u>1.24</u>
18:10:00	0.094/0.094	0.09	-	-	-	-	1.94/1.58	7.55	<u>0.86</u>
18:20:00	0.019/0.020	0.02	-	-	-	-	1.87/1.24	5.90	<u>0.88</u>
18:30:00	-	-	-	-	-	-	1.58/1.10	5.29	<u>0.89</u>
18:40:00	-	-	-	-	-	-	1.84/1.37	4.94	<u>0.96</u>
18:50:00	-	-	-	-	-	-	2.04/1.17	4.12	<u>0.89</u>
19:00:00	-	-	-	-	-	-	2.03/2.03	3.09	<u>0.74</u>
19:10:00	-	-	-	-	-	-	1.13/1.13	1.92	<u>0.99</u>
19:20:00	-	-	-	-	-	-	0.89/0.89	0.89	-
19:30:00	-	-	-	-	-	-	-	-	-

CV: High-variance; Low-variance; **Coefficient of Variance during the monitoring period for the proposed time interval for *E. coli* inactivation.** Mean: Arithmetic mean; *Med*: Median; Max: Maximum; CV: Coefficient of variation.

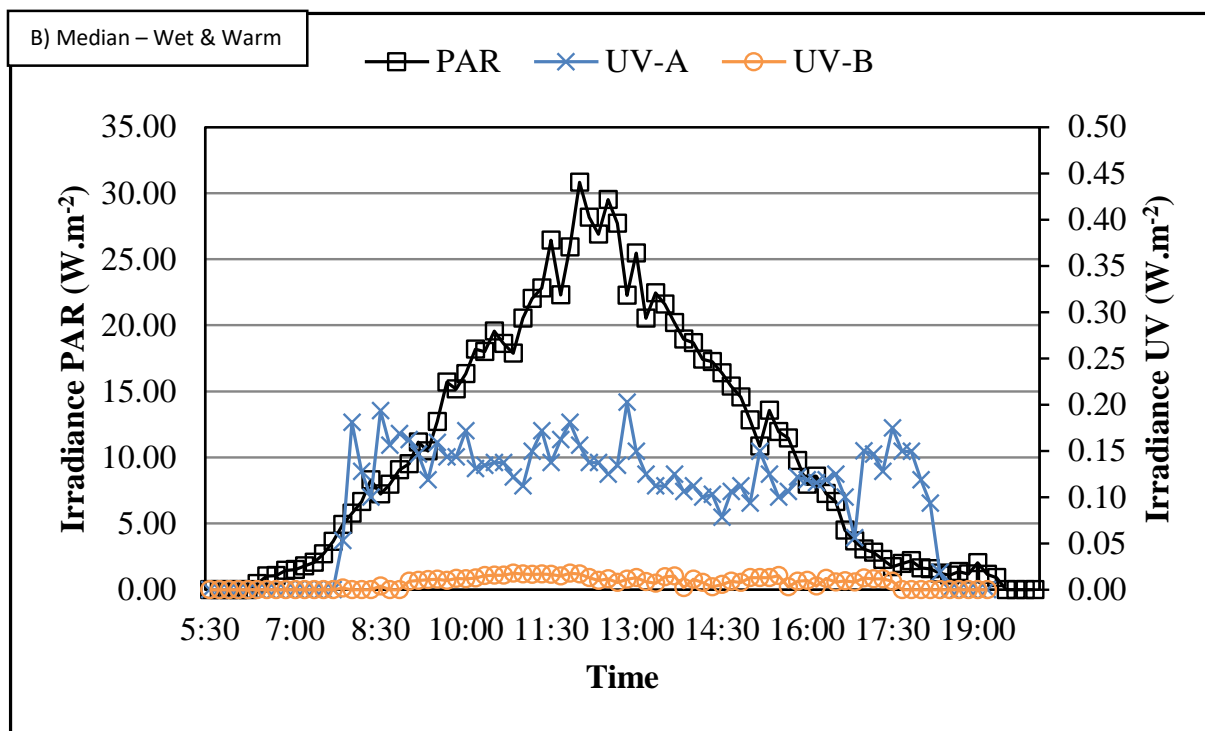
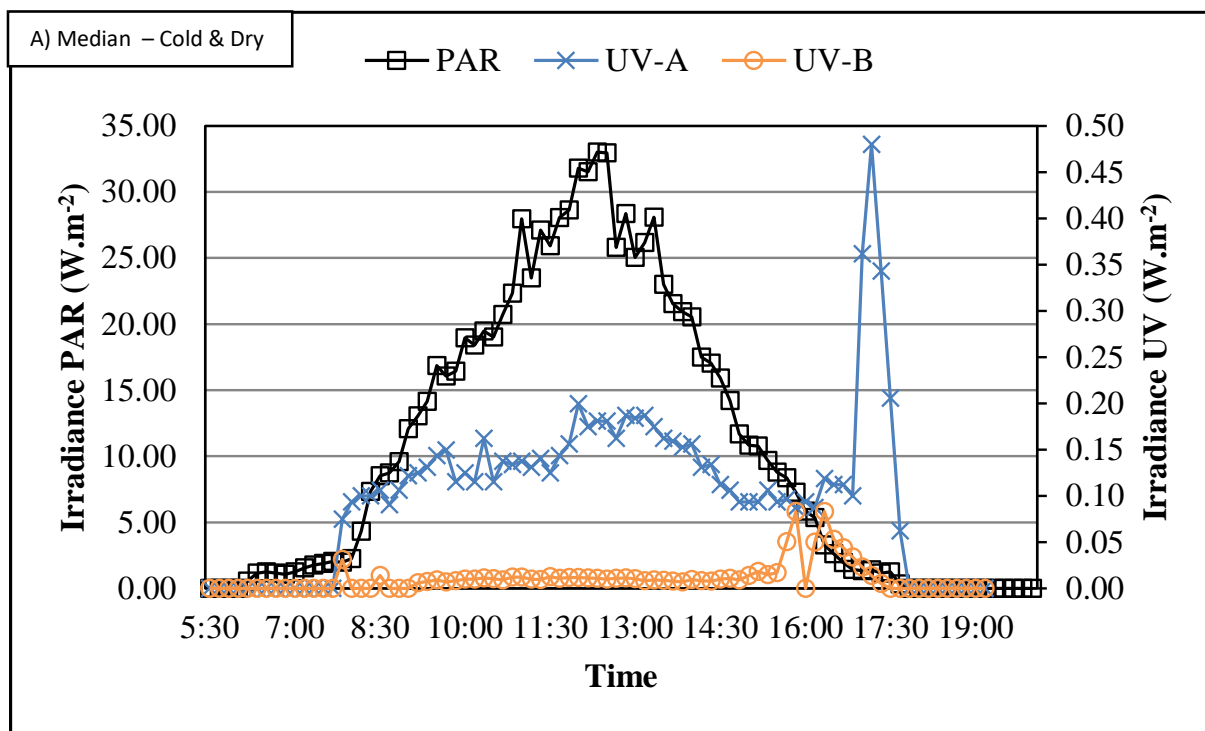
APPENDIX VIII

Descriptive statistical analysis of mean/median of UV-A, UV-B and PAR irradiance at 10 cm for cold and dry (C&D) and wet and warm (W&W) conditions.

Time	UV-A (10 cm)		UV-B (10 cm)		PAR (10 cm)	
	C&D – Mean/Med (W.m ⁻²)	W&W – Mean/Med (W.m ⁻²)	C&D – Mean/Med (W.m ⁻²)	W&W – Mean/Med (W.m ⁻²)	C&D – Mean/Med (W.m ⁻²)	W&W – Mean/Med (W.m ⁻²)
05:10:00	-	-	-	-	-	-
05:20:00	-	-	-	-	-	-
05:30:00	-	-	-	-	-	-
05:40:00	-	-	-	-	-	-
05:50:00	-	-	-	-	-	-
06:00:00	-	-	-	-	-	-
06:10:00	-	-	-	-	0.55/0.55	-
06:20:00	-	-	-	-	0.89/1.17	0.46/0.45
06:30:00	-	-	-	-	1.04/1.24	0.97/1.03
06:40:00	-	-	-	-	1.08/1.17	1.10/1.06
06:50:00	-	-	-	-	1.13/1.06	1.41/1.44
07:00:00	-	-	-	-	1.24/1.24	1.66/1.51
07:10:00	-	-	-	-	1.72/1.54	2.04/1.78
07:20:00	-	-	-	-	2.13/1.75	2.40/2.06
07:30:00	-	-	-	-	2.39/1.89	3.18/2.71
07:40:00	-	-	-	-	2.69/2.03	4.01/3.64
07:50:00	0.245/0.075	0.053/0.053	-	-	3.17/1.99	5.15/4.91
08:00:00	0.094/0.094	0.181/0.181	-	-	3.73/2.27	7.34/5.77
08:10:00	0.079/0.100	0.128/0.128	-	-	5.07/4.32	7.40/6.66
08:20:00	0.090/0.100	0.102/0.100	-	-	7.07/7.35	8.88/8.31
08:30:00	0.118/0.106	0.191/0.193	-	-	8.13/8.51	8.84/7.24
08:40:00	0.091/0.090	0.141/0.156	-	-	8.73/8.72	11.02/7.96
08:50:00	0.107/0.106	0.158/0.168	-	-	9.24/9.58	12.42/9.06
09:00:00	0.131/0.122	0.172/0.162	-	0.009/0.009	12.23/12.08	14.36/9.51
09:10:00	0.140/0.125	0.181/0.147	0.006/0.006	0.010/0.010	13.21/13.04	14.80/11.16
09:20:00	0.151/0.131	0.181/0.118	0.007/0.007	0.011/0.011	15.43/14.14	15.76/10.50
09:30:00	0.165/0.143	0.217/0.159	0.009/0.009	0.011/0.011	17.48/16.85	17.13/12.70
09:40:00	0.171/0.150	0.211/0.143	0.007/0.007	0.010/0.010	18.09/16.06	18.51/15.69
09:50:00	0.151/0.115	0.228/0.143	0.008/0.008	0.012/0.012	18.26/16.44	19.36/15.17
10:00:00	0.174/0.125	0.234/0.171	0.010/0.010	0.009/0.012	20.30/18.95	20.19/16.34
10:10:00	0.166/0.115	0.226/0.131	0.009/0.010	0.013/0.013	20.44/18.40	21.08/18.19
10:20:00	0.174/0.162	0.230/0.134	0.008/0.012	0.015/0.015	21.09/19.46	22.48/18.02
10:30:00	0.173/0.115	0.224/0.137	0.011/0.010	0.013/0.015	21.02/19.02	24.73/19.57
10:40:00	0.194/0.137	0.255/0.137	0.009/0.009	0.015/0.015	23.40/20.73	24.99/18.60
10:50:00	0.185/0.134	0.267/0.122	0.012/0.012	0.016/0.018	25.26/22.35	25.65/17.88
11:00:00	0.189/0.137	0.261/0.112	0.011/0.012	0.015/0.017	26.81/27.97	29.24/20.53
11:10:00	0.167/0.131	0.267/0.150	0.010/0.010	0.016/0.016	25.99/23.48	28.63/22.04
11:20:00	0.179/0.140	0.303/0.171	0.010/0.010	0.016/0.017	27.67/27.12	29.94/22.83
11:30:00	0.179/0.125	0.287/0.137	0.012/0.013	0.019/0.016	27.04/25.92	27.05/26.43
11:40:00	0.191/0.143	0.312/0.162	0.011/0.011	0.014/0.015	28.81/28.04	31.38/22.31
11:50:00	0.253/0.156	0.302/0.181	0.025/0.012	0.017/0.018	29.49/28.63	34.01/25.92
12:00:00	0.238/0.200	0.266/0.156	0.012/0.012	0.014/0.017	31.97/31.78	31.85/30.82
12:10:00	0.260/0.175	0.254/0.137	0.014/0.012	0.012/0.013	33.98/31.51	32.83/28.18
12:20:00	0.227/0.181	0.268/0.137	0.012/0.011	0.011/0.010	32.82/33.02	33.51/26.88
12:30:00	0.243/0.181	0.263/0.125	0.011/0.010	0.012/0.012	31.54/32.95	32.71/29.52
12:40:00	0.216/0.162	0.229/0.134	0.012/0.011	0.007/0.008	28.15/25.81	29.76/27.70
12:50:00	0.234/0.187	0.308/0.203	0.012/0.012	0.010/0.011	28.46/28.35	29.51/22.28

13:00:00	0.217/0.184	0.257/0.150	0.010/0.010	0.013/0.013	27.77/25.06	30.90/25.47
13:10:00	0.207/0.187	0.232/0.125	0.008/0.008	0.009/0.008	27.07/26.16	28.42/20.53
13:20:00	0.220/0.175	0.251/0.112	0.011/0.009	0.010/0.007	28.60/28.08	27.68/22.45
13:30:00	0.210/0.162	0.228/0.112	0.011/0.009	0.012/0.014	26.93/23.00	25.48/21.59
13:40:00	0.206/0.159	0.240/0.125	0.010/0.008	0.014/0.015	24.35/21.56	25.28/20.18
13:50:00	0.198/0.153	0.174/0.106	0.009/0.007	0.002/0.002	22.86/20.94	20.47/18.95
14:00:00	0.180/0.156	0.209/0.112	0.013/0.010	0.011/0.011	21.48/20.53	23.44/18.67
14:10:00	0.180/0.131	0.178/0.100	0.010/0.008	0.012/0.008	21.98/17.51	22.33/17.44
14:20:00	0.172/0.134	0.175/0.103	0.010/0.008	0.009/0.003	20.45/17.03	20.63/17.23
14:30:00	0.144/0.112	0.166/0.078	0.010/0.010	0.011/0.005	18.55/15.93	20.14/16.41
14:40:00	0.145/0.106	0.215/0.106	0.011/0.011	0.009/0.009	16.45/14.21	19.94/15.38
14:50:00	0.137/0.094	0.231/0.112	0.011/0.009	0.010/0.008	14.76/11.67	20.72/14.55
15:00:00	0.139/0.094	0.171/0.094	0.011/0.014	0.013/0.013	12.86/10.85	16.46/12.84
15:10:00	0.155/0.094	0.230/0.150	0.018/0.018	0.013/0.013	12.01/10.78	16.19/10.85
15:20:00	0.140/0.106	0.191/0.125	0.015/0.015	0.013/0.013	10.68/9.68	14.99/13.56
15:30:00	0.167/0.094	0.168/0.100	0.017/0.017	0.015/0.015	9.72/8.79	13.87/11.95
15:40:00	0.118/0.097	0.118/0.106	0.051/0.051	0.003/0.003	8.77/8.38	11.35/11.46
15:50:00	0.103/0.087	0.145/0.122	0.083/0.083	0.009/0.009	8.39/7.28	11.45/9.75
16:00:00	0.094/0.094	0.149/0.118	-	0.010/0.010	7.49/5.84	11.23/7.96
16:10:00	0.106/0.087	0.132/0.115	0.050/0.050	0.004/0.004	6.74/5.35	9.71/8.58
16:20:00	0.129/0.118	0.136/0.118	0.083/0.083	0.012/0.012	5.37/3.30	10.18/7.28
16:30:00	0.112/0.112	0.151/0.125	0.053/0.053	0.008/0.008	4.18/2.61	9.52/6.66
16:40:00	0.112/0.112	0.132/0.100	0.044/0.044	0.010/0.010	2.95/1.96	7.07/4.50
16:50:00	0.100/0.100	0.121/0.056	0.034/0.034	0.008/0.008	2.04/1.44	6.03/3.67
17:00:00	0.362/0.362	0.150/0.150	0.023/0.023	0.012/0.012	1.62/1.34	5.20/3.05
17:10:00	0.480/0.480	0.147/0.147	0.014/0.014	0.012/0.012	1.44/1.41	4.40/2.81
17:20:00	0.343/0.343	0.128/0.128	0.005/0.005	0.012/0.012	1.34/1.17	4.40/2.27
17:30:00	0.206/0.206	0.175/0.175	-	0.009/0.009	1.23/1.24	3.92/1.72
17:40:00	0.062/0.062	0.150/0.150	-	-	0.45/0.34	3.95/1.96
17:50:00	0.245/0.075	0.150/0.150	-	-	0.48/0.41	3.29/2.20
18:00:00	-	0.118/0.118	-	-	-	2.65/1.65
18:10:00	-	0.094/0.094	-	-	-	1.94/1.58
18:20:00	-	0.019/0.019	-	-	-	1.87/1.24
18:30:00	-	-	-	-	-	1.58/1.10
18:40:00	-	-	-	-	-	1.84/1.37
18:50:00	-	-	-	-	-	2.04/1.17
19:00:00	-	-	-	-	-	2.03/2.03
19:10:00	-	-	-	-	-	1.13/1.13
19:20:00	-	-	-	-	-	0.89/0.89
19:30:00	-	-	-	-	-	-

Median cold and dry (A) and wet and warm (B) for PAR and UV solar irradiance at 10 cm in depth over the length of the day.



APPENDIX IX

Descriptive statistical analysis of mean/median and maximum values of UV-A, UV-B and PAR irradiance at 15 cm, 20 cm and 30 cm, and respective CV values.

Time	PAR (15 cm): n= 1-24			PAR (20 cm): n= 1-42			PAR (30 cm): n= 2-74		
	Mean/Med (W/m ²)	Max. (W/m ²)	CV	Mean/Med (W/m ²)	Max. (W/m ²)	CV	Mean/Med (W/m ²)	Max. (W/m ²)	CV
05:40:00	-	-	-	-	-	-	-	-	-
05:50:00	-	-	-	-	-	-	-	-	-
06:00:00	-	-	-	-	-	-	-	-	-
06:10:00	0.34/0.34	0.34	-	-	-	-	-	-	-
06:20:00	0.96/0.96	0.96	-	-	-	-	-	-	-
06:30:00	0.93/0.93	1.24	<u>0.47</u>	-	-	-	-	-	-
06:40:00	1.00/1.03	1.58	<u>0.64</u>	1.44/1.44	1.44	-	-	-	-
06:50:00	1.26/1.17	1.85	<u>0.50</u>	1.44/1.44	2.27	<u>0.81</u>	-	-	-
07:00:00	1.29/1.30	2.33	<u>0.56</u>	0.87/0.58	2.61	1.03	-	-	-
07:10:00	1.35/1.34	3.50	<u>0.66</u>	1.04/0.93	2.88	<u>0.57</u>	0.72/0.72	0.76	<u>0.07</u>
07:20:00	1.54/1.30	3.71	<u>0.58</u>	1.21/1.10	3.98	<u>0.64</u>	1.00/1.00	1.03	<u>0.05</u>
07:30:00	1.77/1.44	5.35	<u>0.67</u>	1.20/1.13	3.78	<u>0.56</u>	1.06/1.17	1.58	<u>0.49</u>
07:40:00	2.01/1.54	5.42	<u>0.65</u>	1.26/1.17	3.98	<u>0.58</u>	1.38/1.13	2.20	<u>0.41</u>
07:50:00	2.30/1.78	6.80	<u>0.66</u>	1.38/1.30	2.54	<u>0.40</u>	0.95/0.69	2.33	<u>0.64</u>
08:00:00	2.55/1.75	7.62	<u>0.73</u>	1.62/1.58	2.81	<u>0.40</u>	0.87/0.89	1.72	<u>0.50</u>
08:10:00	2.83/1.72	9.34	<u>0.86</u>	2.34/2.20	5.90	<u>0.54</u>	1.03/0.96	3.30	<u>0.65</u>
08:20:00	3.14/1.82	9.82	<u>0.86</u>	2.38/1.54	7.55	<u>0.72</u>	1.18/1.03	3.09	<u>0.49</u>
08:30:00	3.28/2.30	9.75	<u>0.73</u>	2.68/1.85	8.79	<u>0.71</u>	1.24/1.24	2.54	<u>0.48</u>
08:40:00	3.50/2.27	12.29	<u>0.84</u>	2.94/2.23	10.43	<u>0.73</u>	1.42/1.34	2.95	<u>0.46</u>
08:50:00	4.08/3.16	8.92	<u>0.65</u>	3.55/3.23	11.53	<u>0.68</u>	1.52/1.41	4.12	<u>0.47</u>
09:00:00	4.48/3.47	14.35	<u>0.80</u>	4.36/3.95	12.70	<u>0.69</u>	1.43/1.37	4.19	<u>0.60</u>
09:10:00	4.54/3.64	14.97	<u>0.85</u>	4.71/4.32	14.28	<u>0.70</u>	1.68/1.58	5.22	<u>0.55</u>
09:20:00	4.79/2.95	15.86	<u>0.87</u>	5.30/4.87	14.83	<u>0.66</u>	1.63/1.51	5.08	<u>0.59</u>
09:30:00	4.92/3.16	17.44	<u>0.82</u>	5.95/5.22	15.79	<u>0.61</u>	1.75/1.44	4.39	<u>0.53</u>
09:40:00	5.63/3.84	20.87	<u>0.89</u>	5.85/5.05	15.58	<u>0.66</u>	1.72/1.44	5.08	<u>0.62</u>
09:50:00	6.01/4.39	22.17	<u>0.85</u>	5.74/5.01	17.44	<u>0.69</u>	1.81/1.54	6.11	<u>0.61</u>
10:00:00	6.47/3.91	25.81	<u>0.93</u>	6.26/5.22	17.92	<u>0.66</u>	1.83/1.68	5.01	<u>0.56</u>
10:10:00	6.84/4.67	33.36	<u>1.04</u>	6.63/5.49	15.45	<u>0.60</u>	1.87/1.78	5.15	<u>0.57</u>
10:20:00	8.36/5.63	35.77	<u>0.93</u>	6.46/5.70	18.60	<u>0.59</u>	1.90/1.78	5.49	<u>0.60</u>
10:30:00	9.77/6.73	36.73	<u>0.92</u>	6.96/5.63	16.54	<u>0.61</u>	1.99/1.82	5.49	<u>0.56</u>
10:40:00	8.46/5.49	38.99	<u>1.02</u>	7.32/6.32	16.20	<u>0.58</u>	2.15/1.96	6.18	<u>0.60</u>
10:50:00	8.29/5.15	42.01	<u>1.11</u>	7.65/6.59	18.12	<u>0.60</u>	2.26/1.99	7.00	<u>0.62</u>
11:00:00	8.30/5.29	27.87	<u>0.93</u>	8.40/7.28	19.29	<u>0.60</u>	2.16/1.89	5.90	<u>0.61</u>
11:10:00	7.40/5.15	21.97	<u>0.83</u>	8.59/7.48	20.53	<u>0.59</u>	2.18/1.92	6.73	<u>0.63</u>
11:20:00	9.61/5.49	33.36	<u>1.00</u>	8.43/7.28	19.91	<u>0.61</u>	2.18/1.89	6.25	<u>0.61</u>
11:30:00	10.43/5.46	44.69	<u>1.07</u>	8.86/7.41	22.17	<u>0.63</u>	2.40/2.03	6.45	<u>0.57</u>
11:40:00	9.32/5.29	25.54	<u>0.88</u>	9.01/8.20	20.11	<u>0.60</u>	2.39/2.06	7.07	<u>0.63</u>
11:50:00	10.83/5.22	51.56	<u>1.10</u>	8.94/8.10	21.56	<u>0.68</u>	2.31/1.96	7.48	<u>0.68</u>
12:00:00	11.52/5.49	50.73	<u>1.10</u>	9.04/8.14	22.17	<u>0.67</u>	2.39/2.09	7.69	<u>0.65</u>
12:10:00	11.06/5.35	46.27	<u>1.08</u>	9.34/7.76	22.52	<u>0.67</u>	2.46/1.99	8.03	<u>0.64</u>
12:20:00	11.44/5.01	54.51	<u>1.11</u>	8.72/7.35	19.57	<u>0.64</u>	2.40/2.13	7.28	<u>0.60</u>
12:30:00	10.20/4.81	54.10	<u>1.16</u>	8.73/6.62	22.65	<u>0.69</u>	2.36/2.23	8.10	<u>0.62</u>
12:40:00	9.08/4.46	52.31	<u>1.23</u>	8.63/7.28	23.14	<u>0.68</u>	2.43/2.06	7.35	<u>0.66</u>
12:50:00	9.08/4.53	50.39	<u>1.21</u>	8.86/6.21	24.85	<u>0.69</u>	2.37/2.03	7.35	<u>0.65</u>
13:00:00	8.39/4.74	45.17	<u>1.15</u>	8.70/7.07	22.45	<u>0.65</u>	2.40/2.20	7.76	<u>0.63</u>
13:10:00	8.64/4.53	47.09	<u>1.23</u>	8.26/7.14	19.77	<u>0.65</u>	2.25/1.99	6.38	<u>0.59</u>
13:20:00	9.13/4.74	46.89	<u>1.19</u>	8.29/8.10	22.31	<u>0.64</u>	2.24/1.92	7.55	<u>0.66</u>
13:30:00	7.59/4.60	26.70	<u>0.92</u>	9.17/7.96	25.19	<u>0.72</u>	2.12/1.85	6.73	<u>0.59</u>
13:40:00	9.34/3.98	43.94	<u>1.19</u>	8.34/6.38	26.02	<u>0.72</u>	1.94/1.58	6.93	<u>0.69</u>
13:50:00	9.08/4.19	36.80	<u>1.08</u>	7.71/6.38	26.98	<u>0.72</u>	2.08/1.85	7.14	<u>0.68</u>
14:00:00	8.42/4.08	41.53	<u>1.20</u>	6.94/5.05	21.56	<u>0.75</u>	2.19/1.99	7.00	<u>0.60</u>
14:10:00	8.29/3.50	51.90	<u>1.34</u>	6.85/5.29	20.11	<u>0.73</u>	1.97/1.72	6.86	<u>0.62</u>
14:20:00	7.25/3.16	29.45	<u>1.03</u>	7.04/5.63	23.68	<u>0.73</u>	1.90/1.72	7.00	<u>0.65</u>

14:30:00	7.70/4.05	43.73	1.23	6.57/5.15	18.95	<u>0.66</u>	1.87/1.65	6.38	<u>0.60</u>
14:40:00	7.06/4.22	34.53	1.12	6.02/4.87	17.03	<u>0.64</u>	1.77/1.58	6.52	<u>0.64</u>
14:50:00	6.98/3.36	34.81	1.21	5.42/4.12	15.93	<u>0.67</u>	1.70/1.58	5.90	<u>0.60</u>
15:00:00	6.90/3.09	30.34	1.14	4.58/3.71	13.94	<u>0.70</u>	1.58/1.58	5.49	<u>0.61</u>
15:10:00	5.90/2.68	20.46	1.12	4.03/3.02	12.84	<u>0.73</u>	1.56/1.44	4.87	<u>0.56</u>
15:20:00	6.48/2.54	31.78	1.20	3.87/3.33	11.60	<u>0.69</u>	1.57/1.51	4.39	<u>0.49</u>
15:30:00	4.88/2.13	15.03	1.01	3.51/2.88	9.89	<u>0.74</u>	1.32/1.27	3.98	<u>0.51</u>
15:40:00	4.12/1.92	12.15	1.00	3.44/2.88	8.99	<u>0.68</u>	1.24/1.24	3.50	<u>0.49</u>
15:50:00	4.07/2.06	14.83	1.07	3.05/2.33	8.17	<u>0.67</u>	1.12/1.17	2.95	<u>0.51</u>
16:00:00	4.07/1.85	21.90	1.27	3.08/2.68	8.24	<u>0.67</u>	1.07/1.03	2.47	<u>0.49</u>
16:10:00	4.50/2.54	24.78	1.34	2.74/2.03	8.10	<u>0.75</u>	0.95/0.96	2.27	<u>0.54</u>
16:20:00	4.18/2.57	20.87	1.19	2.09/1.58	6.86	<u>0.79</u>	0.98/0.96	2.54	<u>0.51</u>
16:30:00	4.20/2.81	10.37	<u>0.83</u>	1.82/1.34	5.49	<u>0.73</u>	0.88/0.82	2.54	<u>0.63</u>
16:40:00	4.32/3.98	9.82	<u>0.68</u>	1.69/1.37	4.53	<u>0.61</u>	0.72/0.55	1.85	<u>0.65</u>
16:50:00	4.55/3.88	13.11	<u>0.74</u>	1.16/1.03	2.06	<u>0.43</u>	0.75/0.62	1.30	<u>0.51</u>
17:00:00	3.52/2.37	10.30	<u>0.79</u>	1.15/1.24	1.65	<u>0.28</u>	0.77/0.89	1.03	<u>0.44</u>
17:10:00	3.09/2.20	9.82	<u>0.89</u>	0.95/1.03	1.37	<u>0.36</u>	1.39/0.79	3.64	1.10
17:20:00	2.62/2.23	6.38	<u>0.60</u>	0.93/0.89	1.24	<u>0.27</u>	-	-	-
17:30:00	2.67/1.82	5.84	<u>0.60</u>	0.84/0.72	1.37	<u>0.40</u>	-	-	-
17:40:00	2.00/1.75	4.74	<u>0.56</u>	0.89/1.03	1.17	<u>0.42</u>	-	-	-
17:50:00	2.11/1.58	4.26	<u>0.56</u>	0.69/0.69	0.76	<u>0.14</u>	-	-	-
18:00:00	1.31/1.44	2.20	<u>0.46</u>	-	-	-	-	-	-
18:10:00	1.24/1.30	1.78	<u>0.37</u>	-	-	-	-	-	-
18:20:00	1.22/1.30	1.72	<u>0.32</u>	-	-	-	-	-	-
18:30:00	1.06/0.96	1.85	<u>0.46</u>	-	-	-	-	-	-
18:40:00	1.17/0.89	1.92	<u>0.57</u>	-	-	-	-	-	-
18:50:00	1.17/1.17	1.65	<u>0.58</u>	-	-	-	-	-	-
19:00:00	0.62/0.62	0.62	-	-	-	-	-	-	-
19:10:00	-	-	-	-	-	-	-	-	-
19:20:00	-	-	-	-	-	-	-	-	-
19:30:00	-	-	-	-	-	-	-	-	-

CV: High-variance; Low-variance; **Coefficient of Variance during the monitoring period for the proposed time interval for *E. coli* inactivation.** Mean: Arithmetic mean; *Med*: Median; Max: Maximum; CV: Coefficient of variation.

APPENDIX X

Descriptive statistical analysis of mean/median of PAR irradiance at 15 cm, 20 cm and 30 cm for cold and dry (C&D) and wet and warm (W&W) conditions.

Time	PAR (15 cm)		PAR (20 cm)		PAR (30 cm)	
	C&D – Mean/Med (W.m ⁻²)	W&W – Mean/Med (W.m ⁻²)	C&D – Mean/Med (W.m ⁻²)	W&W – Mean/Med (W.m ⁻²)	C&D – Mean/Med (W.m ⁻²)	W&W – Mean/Med (W.m ⁻²)
05:10:00	-	-	-	-	-	-
05:20:00	-	-	-	-	-	-
05:30:00	-	-	-	-	-	-
05:40:00	-	-	-	-	-	-
05:50:00	-	-	-	-	-	-
06:00:00	-	-	-	-	-	-
06:10:00	-	0.34/0.34	-	-	-	-
06:20:00	-	0.96/0.96	-	-	-	-
06:30:00	1.10/1.10	0.93/0.93	-	-	-	-
06:40:00	1.58/1.58	1.00/1.03	1.44/1.44	-	-	-
06:50:00	1.92/1.92	1.26/1.17	1.44/1.44	-	-	-
07:00:00	2.13/2.13	1.29/1.30	0.87/0.58	-	-	-
07:10:00	1.05/0.89	1.35/1.34	1.04/0.93	-	-	0.72/0.72
07:20:00	1.26/0.96	1.54/1.30	1.21/1.10	-	-	1.00/1.00
07:30:00	1.40/1.30	1.77/1.44	1.23/1.17	0.62/0.62	-	1.06/1.17
07:40:00	1.53/1.51	2.01/1.54	1.25/1.17	1.37/1.37	0.89/0.89	1.48/1.17
07:50:00	2.17/1.99	2.30/1.78	1.38/1.27	1.33/1.51	0.72/0.72	1.08/0.69
08:00:00	2.45/2.44	2.55/1.75	1.61/1.58	1.69/1.72	0.85/0.89	0.90/0.89
08:10:00	1.53/1.37	2.83/1.72	2.36/2.13	2.15/2.47	0.90/0.89	1.33/1.03
08:20:00	2.32/1.44	3.14/1.82	2.54/1.61	1.56/1.30	1.07/1.00	1.47/1.17
08:30:00	2.37/1.54	3.28/2.30	2.77/1.92	2.10/1.72	1.20/1.27	1.36/1.17
08:40:00	2.71/2.03	3.50/2.27	3.06/2.27	2.17/1.72	1.39/1.30	1.51/1.44
08:50:00	2.69/1.85	4.08/3.16	4.06/3.91	1.56/1.41	1.51/1.44	1.54/1.41
09:00:00	2.92/2.16	4.48/3.47	4.99/4.22	1.87/1.51	1.31/1.27	1.80/1.51
09:10:00	3.00/1.68	4.54/3.64	5.33/4.53	1.83/1.44	1.66/1.58	1.72/1.30
09:20:00	2.95/1.96	4.79/2.95	5.99/5.18	2.15/2.20	1.53/1.51	1.91/1.30
09:30:00	3.30/2.57	4.92/3.16	6.59/5.97	2.64/2.13	1.72/1.44	1.85/1.85
09:40:00	3.48/2.64	5.63/3.84	6.63/5.56	2.39/2.27	1.71/1.51	1.77/1.17
09:50:00	3.57/2.75	6.01/4.39	6.38/5.08	2.80/2.81	1.75/1.58	1.97/1.30
10:00:00	3.74/2.33	6.47/3.91	7.09/6.42	2.93/2.23	1.91/1.78	1.66/1.34
10:10:00	4.02/2.47	6.84/4.67	7.49/6.80	3.27/2.78	1.96/1.85	1.67/1.48
10:20:00	3.64/2.37	8.36/5.63	7.25/5.97	3.40/3.19	2.08/1.89	1.54/1.17
10:30:00	4.39/3.54	9.77/6.73	7.87/6.93	3.46/2.85	2.13/2.13	1.67/1.37
10:40:00	4.36/3.54	8.46/5.49	8.24/7.21	3.78/3.12	2.23/2.20	1.95/1.72
10:50:00	4.94/3.74	8.29/5.15	8.60/7.14	3.45/3.02	2.27/2.13	2.24/1.89
11:00:00	4.46/3.81	8.30/5.29	9.45/8.24	4.07/3.02	2.37/2.27	1.76/1.37
11:10:00	4.45/4.22	7.40/5.15	9.70/9.23	4.16/2.95	2.40/2.06	1.74/1.58
11:20:00	6.54/6.11	9.61/5.49	9.30/9.41	4.83/3.02	2.36/2.06	1.81/1.72
11:30:00	5.26/5.49	10.43/5.46	9.93/9.06	4.98/4.05	2.52/2.06	2.16/1.89
11:40:00	3.87/4.19	9.32/5.29	10.39/10.57	4.19/3.78	2.54/2.33	2.11/1.58
11:50:00	5.17/5.84	10.83/5.22	10.20/10.43	4.69/3.30	2.39/2.20	2.16/1.58
12:00:00	4.81/4.81	11.52/5.49	9.79/8.72	5.92/5.08	2.39/2.20	2.39/1.58
12:10:00	5.61/5.08	11.06/5.35	10.38/9.75	4.76/5.29	2.53/2.30	2.33/1.37
12:20:00	4.90/4.19	11.44/5.01	9.53/9.27	5.69/5.29	2.47/2.20	2.27/1.65
12:30:00	4.72/4.22	10.20/4.81	9.79/8.44	5.06/3.16	2.51/2.47	2.10/1.37
12:40:00	5.08/4.87	9.08/4.46	9.51/7.59	5.49/5.22	2.51/2.37	2.26/1.58
12:50:00	5.11/3.71	9.08/4.53	9.92/8.92	5.23/4.94	2.53/2.27	2.07/1.65

13:00:00	4.79/3.57	8.39/4.74	9.52/8.17	5.31/4.77	2.45/2.23	2.28/1.99
13:10:00	4.05/4.26	8.64/4.53	9.08/7.76	4.90/4.19	2.32/2.27	2.09/1.58
13:20:00	3.78/4.12	9.13/4.74	8.98/8.24	5.47/4.63	2.28/2.06	2.15/1.65
13:30:00	2.68/3.02	7.59/4.60	10.09/9.06	4.86/4.67	2.19/1.92	1.99/1.72
13:40:00	2.18/2.27	9.34/3.98	9.36/7.69	4.16/3.57	2.07/1.72	1.65/1.44
13:50:00	2.49/2.20	9.08/4.19	8.64/7.07	3.91/3.43	2.02/1.78	2.21/1.96
14:00:00	3.79/1.78	8.42/4.08	7.95/6.93	3.24/2.81	2.14/1.92	2.33/2.09
14:10:00	3.72/2.06	8.29/3.50	7.70/6.45	3.36/3.02	1.99/1.72	1.94/1.65
14:20:00	3.02/1.92	7.25/3.16	7.73/5.77	3.78/3.84	1.91/1.75	1.90/1.58
14:30:00	2.24/1.37	7.70/4.05	7.11/5.46	4.06/3.64	1.84/1.58	1.93/1.85
14:40:00	2.22/1.44	7.06/4.22	6.37/5.05	4.30/4.05	1.74/1.44	1.85/1.89
14:50:00	1.80/1.58	6.98/3.36	5.65/4.39	4.33/3.91	1.69/1.58	1.74/1.65
15:00:00	1.36/1.58	6.90/3.09	4.88/3.84	3.36/3.12	1.55/1.58	1.65/1.48
15:10:00	1.40/1.58	5.90/2.68	4.34/3.02	2.85/2.78	1.49/1.44	1.70/1.44
15:20:00	2.06/1.99	6.48/2.54	4.35/3.78	2.23/1.92	1.50/1.51	1.71/1.44
15:30:00	2.38/2.33	4.88/2.13	3.83/3.12	2.20/2.27	1.27/1.24	1.41/1.37
15:40:00	2.04/1.92	4.12/1.92	3.67/2.95	2.40/2.47	1.17/1.24	1.37/1.51
15:50:00	2.11/1.85	4.07/2.06	3.25/2.47	2.17/1.92	1.06/1.03	1.22/1.30
16:00:00	1.74/1.92	4.07/1.85	3.25/2.81	2.32/2.33	0.91/0.93	1.35/1.44
16:10:00	1.21/1.58	4.50/2.54	2.89/2.06	2.11/1.99	0.84/0.76	1.08/1.17
16:20:00	1.21/1.44	4.18/2.57	2.16/1.54	1.80/1.58	0.76/0.69	1.09/1.00
16:30:00	1.61/1.61	4.20/2.81	1.89/1.24	1.55/1.58	0.58/0.58	0.99/0.89
16:40:00	1.68/1.68	4.32/3.98	1.75/1.20	1.49/1.58	0.76/0.76	0.72/0.55
16:50:00	1.61/1.61	4.55/3.88	1.11/1.03	1.27/1.44	-	0.75/0.62
17:00:00	1.20/1.20	3.52/2.37	1.08/1.13	1.28/1.30	-	0.77/0.89
17:10:00	0.69/0.69	3.09/2.20	0.84/0.86	1.13/1.03	-	1.39/0.79
17:20:00	0.76/0.76	2.62/2.23	0.76/0.76	1.00/0.89	-	-
17:30:00	-	2.67/1.82	0.55/0.55	0.89/0.82	-	-
17:40:00	-	2.00/1.75	-	0.89/1.03	-	-
17:50:00	-	2.11/1.58	-	0.69/0.69	-	-
18:00:00	-	1.31/1.44	-	0.62/0.62	-	-
18:10:00	-	1.24/1.30	-	-	-	-
18:20:00	-	1.22/1.30	-	-	-	-
18:30:00	-	1.06/0.96	-	-	-	-
18:40:00	-	1.17/0.89	-	-	-	-
18:50:00	-	1.17/1.17	-	-	-	-
19:00:00	-	0.62/0.62	-	-	-	-
19:10:00	-	-	-	-	-	-
19:20:00	-	-	-	-	-	-
19:30:00	-	-	-	-	-	-

APPENDIX XI

10 cm profile.

Time							
09:00:00	10:00:00	11:00:00	12:00:00	13:00:00	14:00:00	15:00:00	16:00:00
162	160	143	174	81.6	84.4	86.7	80
115	90.6	81.8	70.1	165	155	152	150
148	144	134	128	67.5	67	65.1	64.3
90.4	97.5	96.8	95.3	63.3	68.8	71.9	68.2
62.5	51	66.2	57	79.2	67.4	67.6	65.7
69.1	80.7	95.1	94	61	62.8	59.2	58.2
52.7	51.4	79.7	89	101	91.9	71	74.5
120	119	107	92.6	63.3	64.9	68.6	64.7
53.9	76	71.7	81.7	91.6	97.8	93.4	89.2
41.1	51.4	41.4	47	66.7	50.4	41.4	47.1
123	122	125	116	70.6	55.2	44.2	57.1
131	127	150	148	82.9	49.2	59.5	68.9
47.3	50	62.5	81.3	62.2	66.2	58.8	43.5
59.2	62.3	79.1	122	143	137	143	141
81.6	78	88.8	115	148	133	161	143

20 cm profile.

Time							
09:00:00	10:00:00	11:00:00	12:00:00	13:00:00	14:00:00	15:00:00	16:00:00
177	148	156	137	120	109	112	120
107	112	102	94.9	105	104	109	104
75.9	66.9	69.9	66.2	83.9	79.3	75.2	78.1
74.9	73.7	70.7	71.6	63.8	65.1	62.1	63.9
76.4	89.4	96.3	79.6	70.6	68.9	71.7	73.4
87.7	93.6	108	89.4	57.7	60.6	70.1	61.9
95.9	97.4	85.2	95.1	98.2	71.9	64.2	57.6
37.2	59.4	48.5	61.1	79.3	97.4	97.5	92.2
50.5	69.7	65.3	65	74.5	93	87.3	104
44.9	91	62.9	63.1	56.8	53.3	39.3	40.9
163	161	163	165	49.5	50.2	49.1	47.9
172	172	22.8	24.3	78.9	82.1	63.9	60.4
43.5	52	56.5	63	173	171	171	168
30	29.5	32.6	33.7	192	201	193	192
37.2	37.1	38.3	38.1	60.5	49.5	50.5	55.2

30 cm profile.

Time							
09:00:00	10:00:00	11:00:00	12:00:00	13:00:00	14:00:00	15:00:00	16:00:00
104	90.5	83.8	85.5	124	117	112	118
67.2	69.5	67.1	61.4	82.8	78.2	80.1	78
123	92.1	102	96.3	88.5	81.1	78.1	71.8
80.1	82.3	82.7	76.7	71.1	68.3	66.7	65.3
62.9	70.4	71.3	69.8	83	80.3	70.9	61
61.4	79	67.6	58.3	78.6	80.1	74.6	93.2
59.1	71.8	71.9	68.5	70.9	68.7	67	66.1
78.4	63.5	89	65.1	68.3	61.5	58.9	54
58.7	68.1	75.4	77.9	91.9	86.9	85.5	72.6
50.8	71.5	81.4	79.2	72.7	70.2	72.2	74.3
85.3	87	87.5	93.2	106	80.6	108	107
65.6	63.3	74.6	74.7	189	175	188	180
79	89.8	94	87.8	52.4	50.1	45.9	49.2
132	144	145	150	48.5	49.9	52.2	53
132	126	137	144	45.1	50.2	45.6	53

APPENDIX XII

Total solar irradiance (TSI – mean) measured from the meteorological (APPENDIX II) station multiplied by the percentages recommended by Shilton (2005) at noon for surface irradiance of UV-A (6% TSI), UV-B (0.2% TSI) and PAR (50% TSI).

Time/Wave	09:00:00	10:00:00	11:00:00	12:00:00	13:00:00	14:00:00	15:00:00	16:00:00
UV-A (6% TSI)	21.41	31.42	37.04	39.00	39.64	37.01	28.66	19.37
UV-B (0.2% TSI)	0.71	1.05	1.23	1.30	1.32	1.23	0.96	0.65
PAR (50% TSI)	178.41	261.80	308.70	325.03	330.34	308.42	238.87	161.44

K_a (mean) values calculated from TSI for each wave (UV-A, UV-B and PAR).

Time/Wave	09:00:00	10:00:00	11:00:00	12:00:00	13:00:00	14:00:00	15:00:00	16:00:00
K_aUV-A	94.3	95.7	96.5	96.8	96.3	95.7	94.1	92.2
K_aUV-B	80.8	82.2	83.1	83.3	82.9	82.3	80.9	79
K_aPAR	14.9	15.6	15.6	15.5	15.1	15.2	15.1	15

APPENDIX XIII

UV-A, UV-B and PAR surface irradiance predictions by the programme SMARTS.

Time/Wave	09:00:00	10:00:00	11:00:00	12:00:00	13:00:00	14:00:00	15:00:00	16:00:00
UV-A	45.96	54.47	58.46	57.46	51.60	41.49	28.61	15.16
UV-B	1.26	1.72	1.96	1.91	1.59	1.10	0.59	0.22
PAR	359.42	416.64	442.98	436.11	396.77	327.56	235.17	129.21

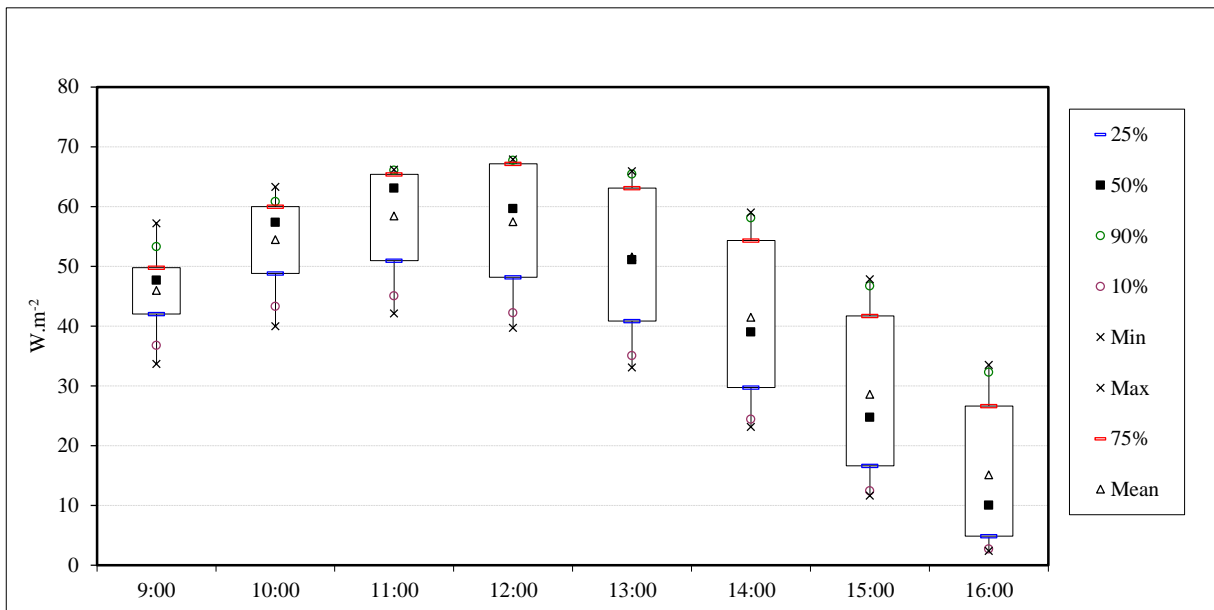
K_a (mean) values predicted from SMARTS for each wave (UV-A, UV-B and PAR).

Time/Wave	09:00:00	10:00:00	11:00:00	12:00:00	13:00:00	14:00:00	15:00:00	16:00:00
K_a UV-A	96	97	97.5	97.7	96.9	96	94.1	91.7
K_a UV-B	82.1	83.3	84.1	84.2	83.3	82.1	79.8	76.5
K_a PAR	16.5	16.7	16.4	16.1	15.5	15.3	15	14.5

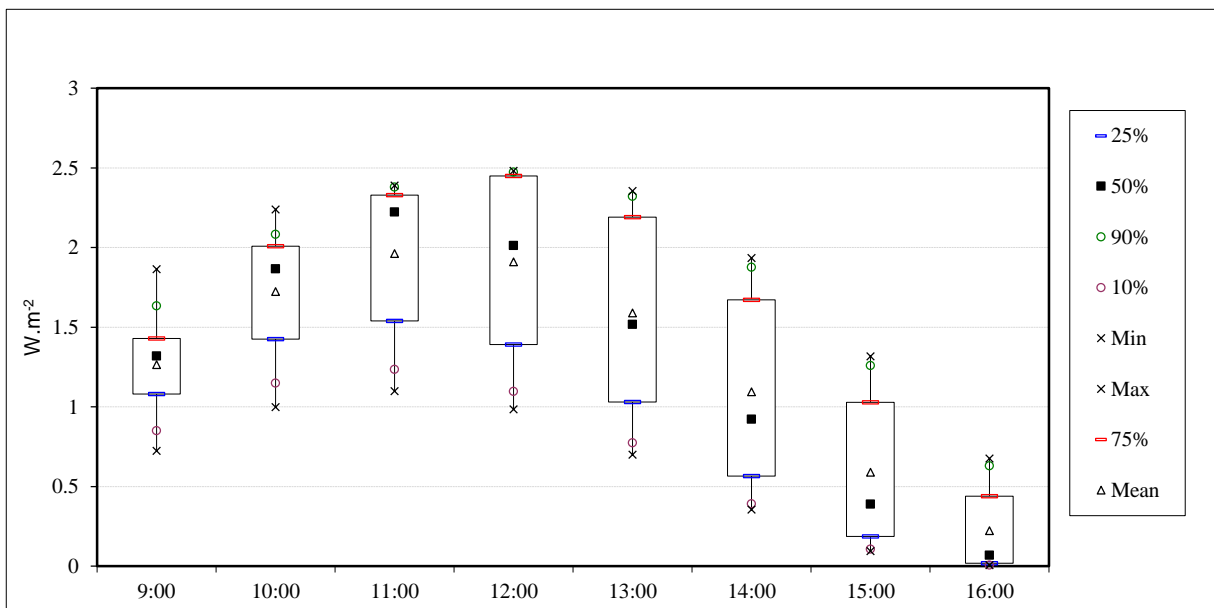
Irradiance values for UV-A, UV-B and PAR predicted by the SMARTS programme.

Time	n	UV-A Mean/median (W.m ⁻²)	CV	UV-B Mean/median (W.m ⁻²)	CV	PAR Mean/median (W.m ⁻²)	CV
09:00:00	264	45.96/47.71	0.13	1.26/1.32	0.23	359.42/372.02	0.12
10:00:00	263	54.47/57.38	0.13	1.72/1.87	0.21	416.64/436.42	0.11
11:00:00	262	58.46/63.09	0.14	1.96/2.22	0.23	442.98/473.93	0.13
12:00:00	260	57.46/59.68	0.17	1.91/2.01	0.28	436.11/451.44	0.15
13:00:00	260	51.60/51.10	0.22	1.59/1.52	0.37	396.77/394.22	0.19
14:00:00	259	41.49/39.05	0.30	1.10/0.92	0.51	327.56/312.29	0.27
15:00:00	259	28.61/24.78	0.45	0.59/0.39	0.75	235.17/210.44	0.40
16:00:00	256	15.16/10.10	0.75	0.22/0.07	1.10	129.21/92.49	0.72

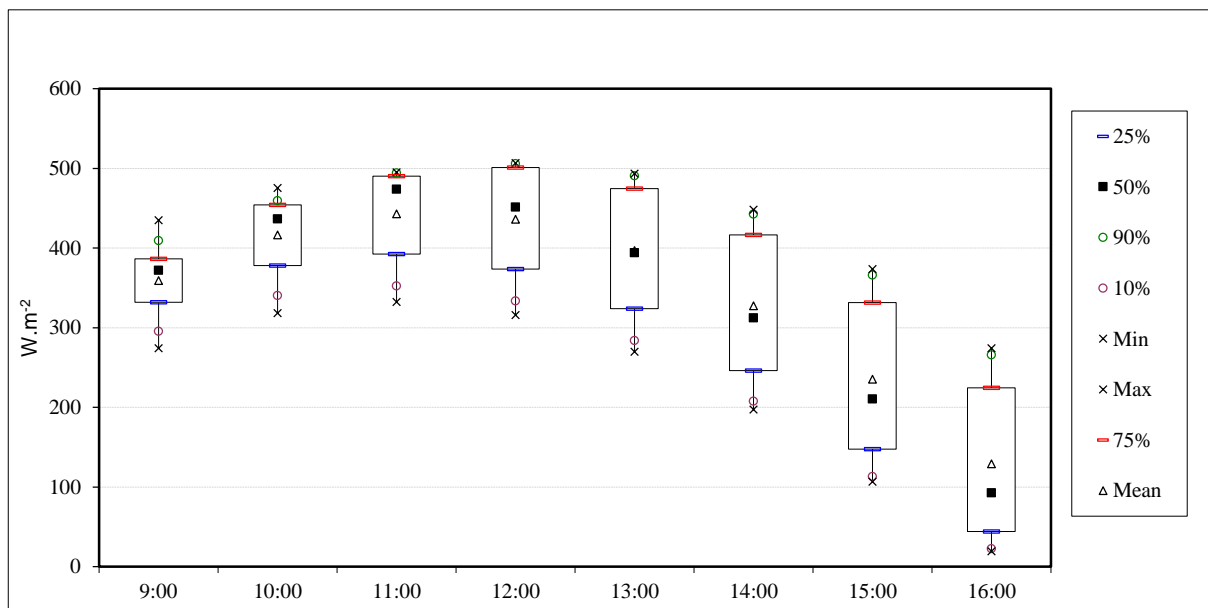
UV-A irradiance predicted by SMARTS.



UV-B irradiance predicted by SMARTS.



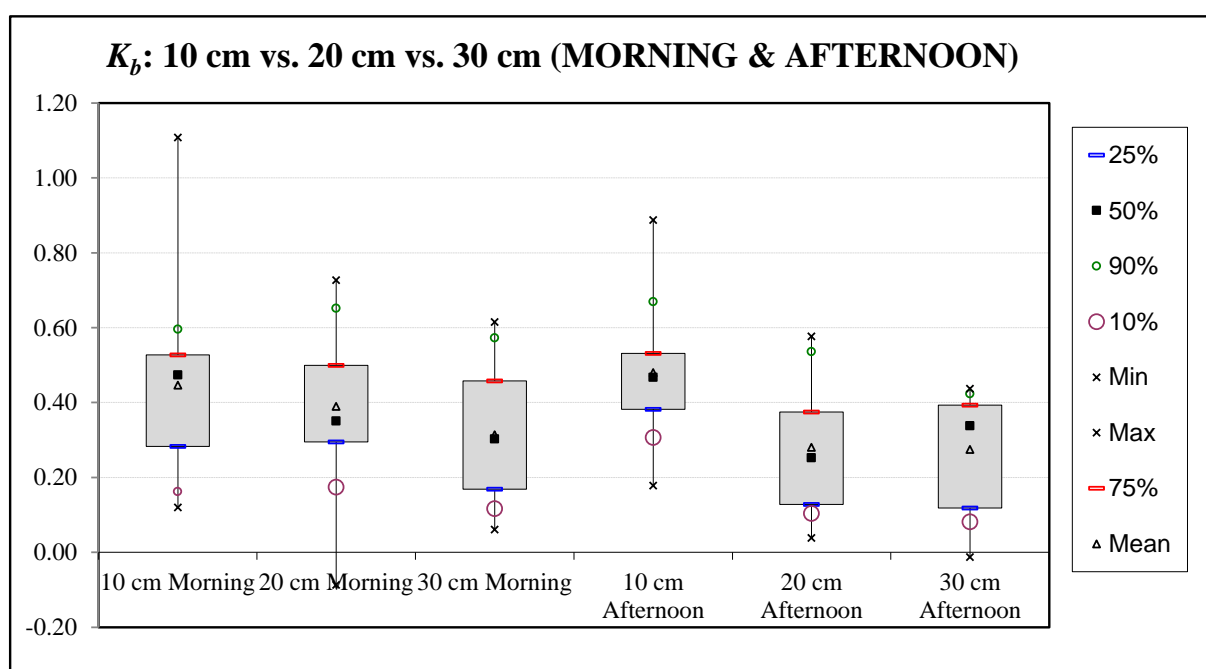
PAR irradiance predicted by SMARTS.



APPENDIX XIV

Calculated and boxplot of K_b values using batch flow regime for different depths and periods of the day.

n	K_b (h^{-1})					
	10 cm		20 cm		30 cm	
	Morning	Afternoon	Morning	Afternoon	Morning	Afternoon
In order of sampling						
1	0.58	0.89	0.56	0.38	0.42	0.11
2	0.47	0.36	0.35	0.29	0.20	0.43
3	0.49	0.60	-0.09	0.34	0.06	0.44
4	0.12	0.53	0.34	-	0.18	0.22
5	0.14	0.32	0.35	0.40	0.11	0.40
6	0.50	0.47	0.50	0.58	0.16	0.39
7	0.61	0.44	0.73	0.57	0.18	0.08
8	0.20	0.51	0.44	0.12	0.39	0.38
9	0.25	0.72	0.31	0.25	0.53	0.12
10	1.11	0.44	0.71	0.23	0.30	-
11	0.32	0.18	0.28	0.04	0.13	-0.01
12	0.47	0.53	0.25	0.10	0.50	-
13	0.40	0.40	0.12	0.13	0.60	0.33
14	0.49	0.30	0.49	-	0.62	0.35
15	0.55	0.52	0.50	0.23	0.34	0.34



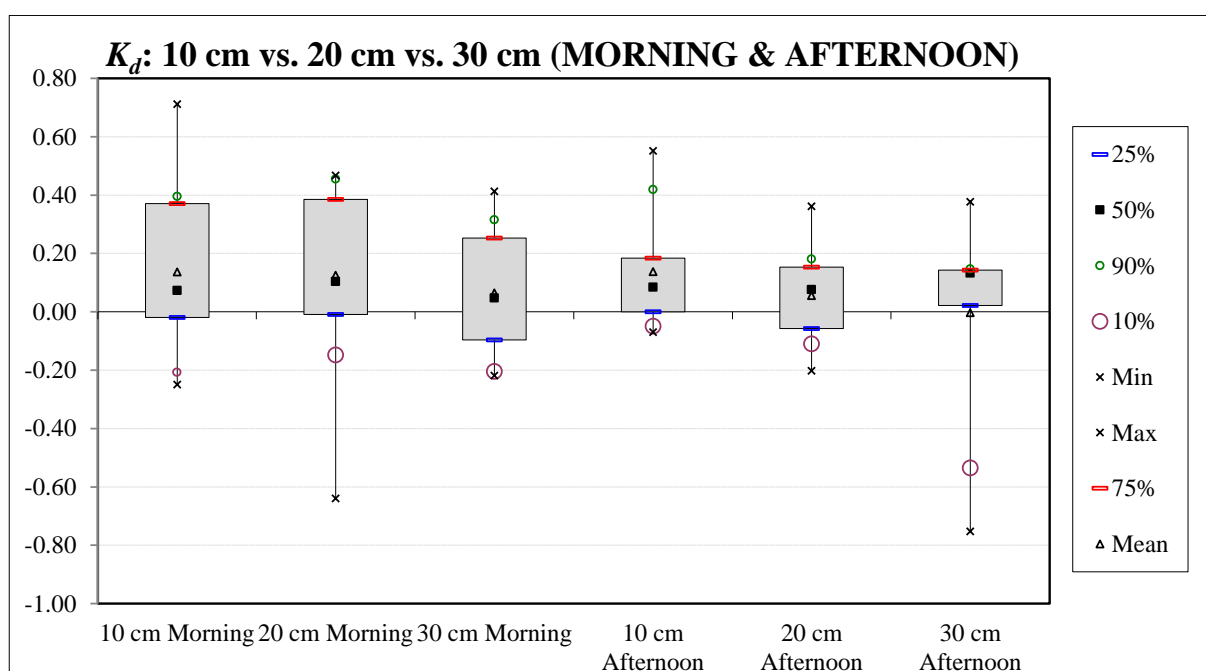
Calculated $K_{b20^{\circ}\text{C}}$ values using Equation 4.12 from the K_b values calculated above for the different depths and periods of the day.

$K_{b20^{\circ}\text{C}} \text{ (h}^{-1}\text{)}$						
n	10 cm		20 cm		30 cm	
In order of sampling	Morning	Afternoon	Morning	Afternoon	Morning	Afternoon
1	0.47	0.63	0.48	0.27	0.32	0.07
2	0.34	0.21	0.27	0.17	0.15	0.26
3	0.34	0.38	-0.08	0.23	0.05	0.32
4	0.10	0.34	0.35	-	0.15	0.17
5	0.12	0.25	0.35	0.37	0.08	0.40
6	0.56	0.35	0.53	0.50	0.15	0.38
7	0.61	0.36	0.77	0.50	0.17	0.07
8	0.22	0.47	0.42	0.11	0.42	0.35
9	0.26	0.67	0.28	0.23	0.56	0.10
10	1.10	0.38	0.61	0.15	0.33	-
11	0.29	0.17	0.21	0.03	0.13	-0.01
12	0.39	0.47	0.20	0.07	0.44	-
13	0.30	0.31	0.09	0.09	0.52	0.20
14	0.33	0.21	0.40	-	0.50	0.24
15	0.39	0.31	0.40	0.13	0.25	0.21

APPENDIX XV

Calculated and boxplot of K_d values using batch flow regime for different depths and periods of the day.

n	K_b (h^{-1})					
	10 cm		20 cm		30 cm	
	Morning	Afternoon	Morning	Afternoon	Morning	Afternoon
In order of sampling						
1	-	-	-	-	-	-
2	-	-	-	-	-	-
3	-	0.55	-0.64	0.12	-	0.10
4	0.00	0.08	0.08	0.00	-0.22	-0.06
5	0.04	0.02	-0.04	0.00	-0.09	0.14
6	0.19	0.45	0.10	0.08	-0.12	0.14
7	0.38	0.18	0.47	0.16	-0.21	-0.54
8	-0.22	0.10	0.38	-0.20	0.24	0.13
9	-0.25	0.07	0.37	-0.05	0.08	0.14
10	0.71	-0.06	0.44	0.18	0.32	0.23
11	0.11	0.00	0.07	0.14	-0.08	-0.75
12	0.40	0.18	-0.18	-0.07	0.01	0.36
13	0.00	0.00	-0.01	-0.11	0.30	0.13
14	0.37	-0.07	0.46	-0.03	0.41	0.38
15	-0.08	0.29	0.12	0.36	0.14	0.15



Calculated $K_{d20^{\circ}C}$ values using Equation 4.12 from the K_d values calculated above for the different depths and periods of the day.

$K_{b20^{\circ}C} (h^{-1})$						
n	10 cm		20 cm		30 cm	
In order of sampling	Morning	Afternoon	Morning	Afternoon	Morning	Afternoon
1	-	-	-	-	-	-
2	-	-	-	-	-	-
3	-	0.35	-0.61	0.08	-	0.08
4	0.00	0.05	0.08	0.00	-0.18	-0.05
5	0.03	0.01	-0.04	0.00	-0.07	0.14
6	0.21	0.34	0.11	0.07	-0.11	0.14
7	0.38	0.15	0.49	0.14	-0.20	-0.52
8	-0.24	0.09	0.36	-0.18	0.25	0.12
9	-0.26	0.06	0.34	-0.04	0.09	0.12
10	0.71	-0.05	0.37	0.12	0.35	0.18
11	0.10	0.00	0.05	0.11	-0.07	-0.51
12	0.33	0.17	-0.14	-0.04	0.01	0.23
13	0.00	0.00	-0.01	-0.07	0.26	0.08
14	0.25	-0.05	0.37	-0.02	0.33	0.26
15	-0.05	0.17	0.10	0.20	0.10	0.09

APPENDIX XVI

Calculated log unit removal efficiencies for different depths and periods of the day.

n	Log unit removed					
	10 cm		20 cm		30 cm	
	Morning	Afternoon	Morning	Afternoon	Morning	Afternoon
In order of sampling						
1	1.01	1.54	0.92	0.61	0.68	0.18
2	0.81	0.52	0.59	0.49	0.33	0.76
3	0.81	0.86	-0.15	0.60	0.10	0.76
4	0.21	0.93	0.59	-	0.31	0.38
5	0.23	0.55	0.61	0.69	0.18	0.71
6	0.87	0.81	0.87	1.02	0.26	0.68
7	1.01	0.77	1.26	1.03	0.32	0.13
8	0.35	0.91	0.77	0.21	0.68	0.67
9	0.43	1.25	0.53	0.44	0.93	0.21
10	1.93	0.76	1.18	0.38	0.53	-
11	0.55	0.31	0.49	0.07	0.23	-0.02
12	0.82	0.92	0.44	0.17	0.87	-
13	0.70	0.70	0.21	0.22	1.04	0.58
14	0.86	0.52	0.86	-	1.07	0.61
15	0.96	0.91	0.87	0.40	0.59	0.59

Dissolved oxygen concentrations for different depths and periods of the day.

n	DO (mg.L ⁻¹)					
	10 cm		20 cm		30 cm	
	Morning	Afternoon	Morning	Afternoon	Morning	Afternoon
In order of sampling						
1	2.04	9.45	10.97	14.49	2.72	8.95
2	2.23	11.32	4.01	11.44	4.76	14.13
3	5.59	13.56	6.98	13.93	5.68	13.61
4	5.2	11.67	3.59	-	8.18	13.91
5	5.06	8.27	2.71	9.16	4.87	8.61
6	4.29	9.22	2.58	6.13	6.98	9.5
7	4.95	8.31	2.09	6.19	5.32	13.4
8	1.47	12.62	2.95	4.51	4.56	8.19
9	4.53	2.94	2.01	7.44	4.18	8.79
10	2.13	14.32	4.81	11.84	3.28	-
11	4.62	10.05	6.35	9.12	2.82	15.68
12	3.77	8.67	6.29	7.99	4.41	-
13	4.96	9.34	3.08	10.34	6.04	12.13
14	5.04	9.84	2.18	-	4.55	10.42
15	3.82	8.14	2.48	8.01	3.77	11.13

pH concentrations for different depths and periods of the day.

pH (-)						
n	10 cm		20 cm		30 cm	
In order of sampling	Morning	Afternoon	Morning	Afternoon	Morning	Afternoon
1	7.81	8.17	8.12	8.36	7.74	8.18
2	7.73	8.09	7.66	8.08	7.86	8.23
3	7.88	8.26	7.78	8.36	7.78	8.19
4	7.83	8.13	7.74	-	7.83	7.91
5	7.77	8.07	7.74	7.71	7.73	8.05
6	7.83	7.78	7.64	7.82	7.81	7.77
7	7.72	7.87	7.57	7.91	7.69	8.5
8	7.78	8.41	7.6	7.68	8.07	7.72
9	7.69	7.71	7.67	8	8.14	7.73
10	7.57	7.88	7.69	7.98	7.66	-
11	7.84	7.87	7.81	7.81	7.69	7.99
12	8.04	7.65	7.59	7.69	8.44	-
13	7.88	7.80	7.6	8.75	7.8	7.66
14	7.71	8.16	7.58	-	7.66	8.05
15	7.53	8.01	7.64	7.63	7.63	8.34

Temperatures for different depths and periods of the day.

Temperature (°C)						
n	10 cm		20 cm		30 cm	
In order of sampling	Morning	Afternoon	Morning	Afternoon	Morning	Afternoon
1	23.1	25.10	22.3	25	23.9	25.4
2	25	27.70	24	28.1	23.9	27.2
3	25.2	26.70	20.8	26.2	23.4	24.6
4	23.4	26.60	19.7	-	22.5	23.6
5	22.4	23.40	19.9	21.2	23.7	20.1
6	18.4	24.10	19.1	22	20.6	20.5
7	19.9	22.90	19.2	21.9	20.8	20.5
8	19	21.10	20.9	21.7	18.9	21.6
9	19.6	21.10	21.3	21.5	19.3	21.9
10	20.1	22.30	22.3	26.2	18.6	-
11	21.5	20.50	24.8	24.4	20.7	25.8
12	22.7	21.60	23	26	22	-
13	24.5	23.90	25.2	25.9	22.2	27.6
14	25.9	25.30	23.2	-	23.1	25.5
15	25.3	27.90	23.3	29	24.5	27.1